PROVENANCE STUDY OF THE TORLESSE TERRANES – IMPLICATIONS FOR THE ORIGIN OF THE CONTINENTAL CRUST OF EASTERN NEW ZEALAND

A THESIS

SUBMITTED IN FULFILMENT

OF THE REQUIREMENT FOR THE DEGREE

OF

DOCTOR OF PHILOSOPHY IN GEOLOGICAL SCIENCES

AT THE

UNIVERSITY OF CANTERBURY

by

Marcel Charles Anekant Wandres

VOLUME ONE:

TEXT AND REFERENCES

University of Canterbury

July 2002

ABSTRACT

The Torlesse terranes – part of the New Zealand Eastern Province – are accretionary complexes that comprise an enormous volume of quartzofeldspathic sandstones and mudstones with subsidiary conglomerates plus minor oceanic assemblages. Two terranes are recognised in the South Island, the Permian to Late Triassic Rakaia terrane and the Late Jurassic to Early Cretaceous Pahau terrane. Recent studies in detrital petrology and geochemistry have been important in establishing the broad type of source for these two terranes. All studies point to a continental arc/cratonic provenance and various source areas have been proposed. This thesis provides the best evidence yet that the Pahau terrane is locally derived and that an Antarctic source for the Rakaia sediments must be (re)considered.

A detailed sampling program and geochronological, geochemical and Sr-Nd isotope analyses of igneous clasts from seven Torlesse terrane conglomerates, in conjunction with SHRIMP U-Pb detrital zircon ages from three Torlesse sandstones, have helped to broadly characterise the igneous protosources for the Pahau and Rakaia terranes. The conglomerate locations were chosen to represent the full stratigraphic range of both terranes, and the geographical distribution of the conglomerates mimics an approximate inboard to outboard transect of the two terranes with respect to the Panthalassan margin of Gondwana.

Igneous clasts from the Aptian (Mount Saul and Ethelton) and Albian (Kekerengu) Pahau terrane conglomerates are predominantly volcanic and hypersolvus, calc-alkaline, metaluminous to weakly peraluminous and display a general geochemical concordance that suggests a similar petrogenesis. SHRIMP U-Pb zircon ages of these clasts range from 128-123 Ma and from 147-135 Ma. These clasts are indistinguishable in age (except for the younger group), chemical composition, and petrogenesis from the felsic members of the calc-alkaline I-type granitoids of the Darran Suite, whereas alkaline rhyolitic clasts correlate best with the Electric Granite. The age range of all clasts overlaps with detrital zircon ages of the conglomerate matrix from Ethelton, indicating that Late Jurassic to Early Cretaceous magmatism was penecontemporaneous with the sedimentation of the Pahau terrane. The youngest detrital zircon from the Ethelton conglomerate matrix gives an age of 112±2 Ma that constrains the minimum age of magmatism in the source region.

An Early Jurassic calc-alkaline, weakly peraluminous rhyolite clast from Kekerengu (188±3 Ma) correlates with the calc-alkaline, weakly peraluminous to peraluminous Bounty Island Granite.

SHRIMP U-Pb zircon ages of Rakaia terrane igneous clasts define three distinct groups. The first group, Permian to Middle Triassic, ranges in age from 292-243 Ma with two subgroups recognisable, a minor one ranging in age from 292-277 Ma and a major one from 258-243 Ma. All these clasts are confined to the Kazanian Te Moana, the Dorashamian McKenzie Pass, and the Carnian Lake Hill conglomerates. The calc-alkaline to high-K calc-alkaline, metaluminous to peraluminous clasts range in composition from andesites to rhyolites and their intrusive equivalents. Adakitic, mylonitic and gneissic clasts are especially common at Lake Hill.

Carboniferous, calc-alkaline, metaluminous to weakly peraluminous clasts are confined to the (?)Permian Boundary Creek conglomerate, ranging in age from 356-325 Ma, constituting the second group. Pooled individual zircon ages from igneous clasts from the Boundary Creek

conglomerate point towards a possible presence of Carboniferous sediments within the Haast Schist.

The third group consists of two Cambrian clasts, a monzogranite from Te Moana (497±8 Ma) and a dacite from Lake Hill (c. 517 Ma). These two clasts indicate that Cambrian plutons and volcanics were a protosource that provided detritus to the Rakaia depocentres. Cambrian magmatism was confined to the New Zealand Western Province and its Australian and Antarctic correlatives as well as the Transantarctic Mountains and their Australian correlatives. The presence of the Cambrian clasts indicates an autochthonous setting of the Rakaia depocentres with respect to the Gondwana margin as early as the Kazanian.

Detrital zircon age distributions from the Anisian Kurow Hill and Balmacaan Stream Rakaia sandstones identify a Permian to Triassic arc source as the main contributor of detritus to the Rakaia sedimentary basin. Geochronology, geochemistry and Sr-Nd isotopes of Rakaia igneous clasts correlate broadly with those of Permian to Triassic plutons and volcanics from the Antarctic sector of the Panthalassan margin of Gondwana.

Sandstone clasts from two Rakaia and two Pahau conglomerates were collected to investigate the recycling of the older Rakaia rocks. Petrography and geochemistry of Pahau terrane clasts indicate that at the time of the Pahau sedimentation Permian to early Late Triassic Rakaia rocks were exposed and recycled into the Pahau basin. Recycling of the Rakaia sediments into the Pahau terrane is also supported by the detrital zircon age data from this and other studies. Furthermore, the similarities of petrographic and geochemical data between sandstone clasts from the Rakaia terrane and Rakaia sandstones suggest that clasts were derived by autocannibalistic reworking of older, consolidated, Rakaia sediments.

Geochronology, geochemistry and Sr-Nd isotopes of igneous clasts from the Pahau terrane identify the Median Tectonic Zone (Darran Suite and Electric Granite) as a detritus contributor to the Pahau depositional basin. Based on sandstone and sandstone clast geochronology, geochemistry and Sr-Nd isotopes, the recycling of the older inboard Rakaia and Caples terranes into the Pahau basin is demonstrated. A multi- source model is proposed in which the uplifted Rakaia and Caples terranes as well as an active volcanic arc contributed detritus to the Pahau sedimentary basin.

CONGLOMERATE PEBBLES

CONTENTS

Abstract

Index i

Figure Index vi

Table Index x

Appendix Index xi

CHAPTER 1 Introduction 1

1.1 Significance of Study 1

1.2 Background 1

1.3 Tectonostratigraphic Framework of New Zealand 4
1.3.1 Western Province 4
1.3.1.1 Buller Terrane 4
1.3.1.2 Takaka Terrane 6
1.3.2 Median Tectonic Zone 6
1.3.3 Eastern Province 8
1.3.3.1 Brook Street Terrane 9
1.3.3.2 Murihiku Terrane 9
1.3.3.3 The Dun Mountain - Maitai Terrane 10
1.3.3.4 Caples Terrane 11
1.3.3.5 Otago Schist 13
1.3.3.6 Torlesse Terranes 13
1.3.3.7 Waipapa Terrane 15
1.3.3.8 Cover Strata 16
1.3.4 Summary 16

1.4 Geographic and Stratigraphic Distribution of Torlesse Rocks 17

1.5 Conditions of Deposition 19

1.6 Torlesse Source 20

1.7 Sediment Provenance 21

1.8 Purpose of Study and Outline of Thesis 22

CHAPTER 2 Description of the Conglomerates 25

2.1 Pahau Terrane Conglomerate Locations 25
2.1.1 Mount Saul Conglomerate 25
2.1.1.1 Locality 25
2.1.1.2 Previous Work 26
2.1.1.3 Description 26
2.1.1.4 Age and Depositional Setting 27
2.1.1.5 Results from this Study 27
2.1.2 Ethelton Conglomerate 28
2.1.2.1 Locality 28
2.1.2.2 Previous Work 28
2.1.2.3 Description 28
2.1.2.4 Age and Depositional Setting 29
2.1.2.5 Results from this Study 29

2.1.3 Kekerengu Conglomerate 30
2.1.3.1 Locality 30
2.1.3.2 Previous Work 30
2.1.3.3 Description 30
2.1.3.4 Age and Depositional Setting 31
2.1.3.5 Results from this Study 31

2.2 Rakaia Terrane Conglomerate Locations 31
2.2.1 Boundary Creek Conglomerate 31
2.2.1.1 Locality 31
2.2.1.2 Description 32
2.2.1.3 Age and Depositional Setting 33
2.2.1.4 Results from this Study 33
2.2.2 Te Moana Conglomerate 34
2.2.2.1 Locality 34
2.2.2.2 Previous Work 34
2.2.2.3 Description 34
2.2.2.4 Age and Depositional Setting 35
2.2.2.5 Results from this Study 35
2.2.3 McKenzie Pass Conglomerate 35
2.2.3.1 Locality 35
2.2.3.2 Previous Work 36
2.2.3.3 Description 36
2.2.3.4 Age and Depositional Setting 36
2.2.3.5 Results from this Study 37
2.2.4 Lake Hill Conglomerate 37
2.2.4.1 Locality 37
2.2.4.2 Previous Work 37
2.2.4.3 Description 38
2.2.4.4 Age and Depositional Setting 38
2.2.4.5 Results from this Study 39

2.3 Sandstone Localities 39
2.3.1 Kurow Hill 39
2.3.1.1 Location and Depositional Age 39
2.3.2 Balmacaan Stream 39
2.3.2.1 Location and Depositional Age 39
2.3.3 Ethelton 40

2.4 Summary 40

CHAPTER 3 Geochronology **42**

3.1 Pahau Terrane Igneous Clasts 43
3.1.1 Late Jurassic to Early Cretaceous Clasts 43
3.1.1.1 Mount Saul 43
3.1.1.2 Ethelton 44
3.1.1.3 Kekerengu 46
3.1.2 Early Jurassic Clast 47
3.1.2.1 Kekerengu 47

3.2 Rakaia Terrane Igneous Clasts 47
3.2.1 Early Permian to Early Triassic Clasts 48
3.2.1.1 Te Moana 48
3.2.1.2 McKenzie Pass 49
3.2.1.3 Lake Hill 50
3.2.2 Carboniferous Clasts 51
3.2.2.1 Boundary Creek 51
3.2.3 Cambrian Clasts 52
3.2.3.1 Te Moana 52
3.2.3.2 Lake Hill 52

3.3 Detrital Zircons 53
3.3.1 Kurow 53
3.3.2 Balmacaan Stream 54
3.3.3 Ethelton 54
3.4 Summary of the U-Pb Zircon Data 55
3.5 Same Source Problem 57

CHAPTER 4 Rakaia and Pahau Terrane Sandstone Clasts 60

4.1 Petrography 61
4.1.1 Sandstone Components 61
4.1.2 Petrographic Procedures 61
4.1.3 Composition of Sandstone Clasts 62
4.1.4 Petrographic Comparison of Sandstone Clasts and Torlesse Sandstones 64
4.2 Geochemistry 65
4.2.1 Introduction 65
4.2.2 Major Elements 66
4.2.3 Trace Elements 69
4.3 Summary and Conclusions 71

CHAPTER 5 Pahau Terrane Igneous Clasts 74

5.1 Petrography 74
5.1.1 Petrographical Classification 74
5.1.1.1 Plutonic Clasts 74
5.1.1.2 Volcanic Clasts 75
5.1.2 Alteration 75
5.1.3 Mount Saul 76
5.1.3.1 Syenogranite 76
5.1.3.2 Monzogranite 77
5.1.3.3 Quartz Monzogranite 77
5.1.3.4 Granodiorite 78
5.1.3.5 Rhyolite 78
5.1.3.6 Dacite 79
5.1.3.7 Trachyte 79
5.1.4 Ethelton 80
5.1.4.1 Monzogranite 80
5.1.4.2 Granodiorite 81
5.1.4.3 Rhyolite 81
5.1.5 Kekerengu 82
5.1.5.1 Syenogranite 82
5.1.5.2 Monzogranite 82
5.1.5.3 Granodiorite 83
5.1.5.4 Rhyolite 83
5.1.5.5 Trachyte 84
5.2 Geochemistry 84
5.2.1 Introduction 84
5.2.2 Major and Trace Elements 85
5.2.3 Spider-diagrams 87
5.2.4 Rare Earth Elements 89
5.2.5 Discrimination of Tectonic Setting 89
5.2.6 Sr and Nd Isotopes 91
5.3 Summary and Conclusions 92
5.3.1 Petrography 92
5.3.2 Geochemistry 93

CHAPTER 6 Rakaia Terrane Igneous Clasts 95

6.1 Petrography 95
6.1.1 Boundary Creek 95
6.1.2 Te Moana 96
6.1.2.1 Monzogranite and Granodiorite 96
6.1.2.2 Rhyolite 97
6.1.3 McKenzie Pass 98
6.1.3.1 Monzogranite 98
6.1.3.2 Rhyolite 99
6.1.3.3 Andesite and Basalt 99
6.1.3.4 Dacite 100
6.1.4 Lake Hill 100
6.1.4.1 Monzogranite 100
6.1.4.2 Granodiorite and Tonalite 101
6.1.4.3 Rhyolite 102
6.1.4.4 Dacite 102

6.2 Geochemistry 103
6.2.1 Major and Trace Elements 104
6.2.2 Spider-diagrams 106
6.2.3 Rare Earth Elements 108
6.2.4 Discrimination of Tectonic Setting 108
6.2.5 Sr and Nd isotopes 108

6.3 Summary and Conclusions 109
6.3.1 Petrographical Interpretation 109
6.3.2 Geochemistry 111

CHAPTER 7 Provenance of Pahau Terrane Igneous Clasts 112

7.1 Overview of Jurassic to Cretaceous Magmatism Along the Panthalassan Margin 112
7.1.1 Introduction 112
7.1.2 Jurassic to Cretaceous Tectonic Regime in the SW Pacific 113
7.1.3 Calc-alkaline Magmatism 113
7.1.3.1 Australia 113
7.1.3.2 Western Province of New Zealand 114
7.1.3.3 Median Tectonic Zone and Amundsen Province 114
7.1.3.4 Antarctic Peninsula 114
7.1.4 Silicic and other Provinces Associated with the Gondwana Break-up 115
7.1.4.1 Australia 115
7.1.4.2 Antarctic Peninsula 115
7.1.4.3 East Antarctica 115
7.1.5 Post-subduction Magmatism in New Zealand and Antarctica 115
7.1.5.1 New Zealand Western Province 115
7.1.5.2 New Zealand Eastern Province 116
7.1.5.3 Antarctica 116

7.2 Potential Early Jurassic to Early Cretaceous Sources for the Igneous Clasts 116
7.2.1 Introduction 116
7.2.2 Eastern Australia 116
7.2.3 New Zealand 117
7.2.3.1 Median Tectonic Zone 117
7.2.3.2 Buller Terrane 118
7.2.3.3 Bounty Island 119
7.2.4 Antarctica 119
7.2.4.1 Marie Byrd Land 119
7.2.4.2 Thurston Island 120
7.2.4.3 Antarctic Peninsula 120

7.3 Comparison of Late Jurassic to Early Cretaceous Igneous Clasts with Potential Sources 121
7.3.1 Geochronology 122

7.3.2 Petrography 123
7.3.3 Major and Trace Elements 123
7.3.4 Spider Diagrams 125
7.3.5 REE Patterns 126
7.3.6 Discrimination of Tectonic Setting 126
7.3.7 Sr and Nd Isotopes 127
7.3.8 Summary and Conclusions 129

7.4 Comparison of Early - Middle Jurassic Igneous Clasts with Potential Sources 131
7.4.1 Geochronology 131
7.4.2 Major and Trace Elements 131
7.4.3 Spider Diagrams 132
7.4.4 Discrimination of Tectonic Setting 133
7.4.5 Isotopes 133
7.4.6 Summary and Conclusions 133

7.5 Comparison of Pahau Igneous Clasts with Pahau Terrane Sandstones 134
7.5.1 Introduction 134
7.5.2 Major Elements 134
7.5.3 Trace Elements 135
7.5.4 Sandstone and Sandstone Clast Sr-Nd Isotopes 136
7.5.5 Summary and Conclusions 137

CHAPTER 8 Provenance of Rakaia Terrane Igneous Clasts 138

8.1 Permian to Early Triassic Igneous Clasts 139
8.1.1 Introduction 139
8.1.2 Igneous Source Provinces 139
8.1.2.1 Eastern Australia 139
8.1.2.2 New Zealand 141
8.1.2.3 Antarctica 142
8.1.3 Comparison of Igneous Clasts with Source Provinces 143
8.1.3.1 Geochronology 143
8.1.3.2 Petrography 144
8.1.3.3 Major and Trace Element Geochemistry 144
8.1.3.4 Discrimination of Tectonic Setting 146
8.1.3.5 Isotopes 146
8.1.4 Summary and Conclusions 148

8.2 Carboniferous Igneous Clasts 150
8.2.1 Introduction 150
8.2.2 Igneous Source Provinces 151
8.2.2.1 Eastern Australia 151
8.2.2.2 New Zealand 151
8.2.2.3 Antarctica 152
8.2.3 Comparison of Igneous Clasts with Source Provinces 154
8.2.3.1 Geochronology 154
8.2.3.2 Petrography 155
8.2.3.3 Geochemistry 155
8.2.3.4 Discrimination of Tectonic Setting 156
8.2.3.5 Isotopes 156
8.2.4 Summary and Conclusions 158

8.3 Cambrian Igneous Clasts 159
8.3.1 Introduction 159
8.3.2 Igneous Source Provinces 160
8.3.2.1 Australia 160
8.3.2.2 New Zealand 161
8.3.2.3 Antarctica 161
8.3.3 Comparison of Igneous Clasts with Source Provinces 163
8.3.3.1 Geochronology 163
8.3.3.2 Petrography 164

8.3.3.3 Geochemistry 164
8.3.3.4 Discrimination of Tectonic Setting 165
8.3.3.5 Isotopes 165
8.3.4 Summary and Conclusions 166

8.4 Comparison of Igneous Rakaia Clasts with Rakaia Terrane Sandstones 167
8.4.1 Major Elements 168
8.4.2 Trace Elements 169
8.4.3 Isotopes 170
8.4.4 Summary and Conclusions 170

CHAPTER 9 Discussion and Conclusions **171**

9.1 Pahau Terrane Provenance 171
9.1.1 Median Tectonic Zone 172
9.1.1.1 Western Boundary 172
9.1.1.2 Eastern Boundary 175
9.1.2 Recycling of the Rakaia Terrane 176
9.1.3 Regional Tectonic Implications 178
9.1.4 Pahau Sandstone Provenance 181

9.2 Rakaia Terrane Provenance 185
9.2.1 Australian Source 188
9.2.2 New Zealand/Antarctica Source 191

9.3 Summary of Main Conclusions 196

Acknowledgements 199

References 201

Map of conglomerate locations back pocket Volume I

Terrane sequence chart of New Zealand back pocket Volume I

VOLUME 2

FIGURE INDEX

CHAPTER 1 INTRODUCTION

Figure 1.1 Igneous provinces of the southwest Pacific 1
Figure 1.2 Tectonostratigraphic terranes of New Zealand 2
Figure 1.3 New Zealand micro-continent 3
Figure 1.4 Geological map of NW Nelson 4
Figure 1.5 Geological map of Fiordland 5
Figure 1.6 Distribution of fossil localities and faunal zones 6
Figure 1.7 Conglomerate locations 7

CHAPTER 2 DESCRIPTION OF THE CONGLOMERATES

Figure 2.1 General view of Mount Saul conglomerate 9
Figure 2.2 Summit of Mount Saul with view of main conglomerate 9
Figure 2.3 Detail of Mount Saul conglomerate 10
Figure 2.4 Detail of Mount Saul conglomerate 10
Figure 2.5 View of Ethelton conglomerate with Kaiwara suspension bridge 11
Figure 2.6 Massive conglomerate bed at Lake Hill conglomerate 12
Figure 2.7 Detail of Lake Hill conglomerate 12
Figure 2.8 Steeply dipping conglomerate beds at Kekerengu 13
Figure 2.9 Detail of Kekerengu conglomerate 13
Figure 2.10 Core drilling of igneous clasts at Boundary Creek 14

Figure 2.11	Strongly deformed conglomerate clasts at Boundary Creek	14
Figure 2.12	Detail of Boundary Creek conglomerate with granitoid clast	15
Figure 2.13	Detail of deformed igneous clast from Boundary Creek	15
Figure 2.14	View of Te Moana conglomerate with Doughboy Saddle and Devils Peak	16
Figure 2.15	Te Moana conglomerate in Frasiers Stream	16
Figure 2.16	Detail of Te Moana conglomerate	17
Figure 2.17	View of McKenzie Pass conglomerate	18
Figure 2.18	Detail of McKenzie Pass conglomerate	19
Figure 2.19	View of Lake Hill conglomerate	20
Figure 2.20	Detail of Lake Hill conglomerate	21
Figure 2.21	Detail of Lake Hill conglomerate	21
Figure 2.22	Detail of Lake Hill conglomerate	22
Figure 2.23	Detail of Lake Hill conglomerate	22
Figure 2.24	Summary of clast compositions and distributions	23
Figure 2.25	Summary of depositional ages for conglomerate localities	24

CHAPTER 3 GEOCHRONOLOGY

Figure 3.1	U-Pb concordia plots for Jurassic-Cretaceous igneous clasts from Mount Saul	26
Figure 3.2	U-Pb concordia plots for Jurassic-Cretaceous igneous clasts from Ethelton	29
Figure 3.3	U-Pb concordia plots for Jurassic-Cretaceous igneous clasts from Kekerengu	32
Figure 3.4	U-Pb concordia plot for Jurassic igneous clast from Kekerengu	34
Figure 3.5	U-Pb concordia plots for Permian-Triassic Rakaia terrane igneous clasts	35
Figure 3.6	U-Pb concordia plots for Carboniferous igneous clasts from Boundary Creek	41
Figure 3.7	U-Pb concordia plots for Cambrian Rakaia terrane igneous clasts	43
Figure 3.8	U-Pb detrital age histogram for Kurow Hill sandstone	44
Figure 3.9	U-Pb detrital age histogram for Balmacaan Stream sandstone	45
Figure 3.10	U-Pb detrital age histogram for Ethelton conglomerate matrix sandstone	46
Figure 3.11	U-Pb ages of sandstones and igneous clasts	47
Figure 3.12	U-Pb ages of igneous clasts versus depositional ages of conglomerates	48
Figure 3.13	Comparative plots for igneous clast zircons and detrital zircons	49

CHAPTER 4 SANDSTONE CLASTS

Figure 4.1	Q-F-L diagrams for sandstone clasts	52
Figure 4.2	Petrographic data of sandstone clasts and Torlesse sandstones	53
Figure 4.3	Tectonic discrimination diagrams for sandstone clasts based on petrography	54
Figure 4.4	Major element data of sandstone clasts and Torlesse sandstones	57
Figure 4.5	Tectonic discrimination diagrams for sandstone clasts based on major elements	58
Figure 4.6	SAM plot for sandstone clasts and Torlesse sandstones	59
Figure 4.7	F2 vs. F1 plot for sandstone clasts and Torlesse sandstones	60
Figure 4.8	A-CN-K plot and CIA values for sandstone clasts and Torlesse sandstones	61
Figure 4.9	Tectonic discrimination diagrams for sandstone clasts based on trace elements	62
Figure 4.10	Trace element ratios of sandstone clasts and Torlesse sandstones	63
Figure 4.11	Th/Sc vs. SiO_2/Al_2O_3 for sandstone clasts and Torlesse sandstones	64
Figure 4.12	Th/Sc vs. Zr/Sc for sandstone clasts and Torlesse sandstones	65
Figure 4.13	Enlargement of Figure 4.12	66

CHAPTER 5 PAHAU TERRANE IGNEOUS CLASTS

Figure 5.1	Classification of plutonic and volcanic igneous clasts from Mount Saul	67
Figure 5.2	Photomicrograph of microcline	68
Figure 5.3	Photomicrograph of granophyric intergrowth	68
Figure 5.4	Photomicrograph of pseudomorphous biotite	69
Figure 5.5	Photomicrograph of granophyric intergrowth	69
Figure 5.6	Photomicrograph of lithic fragment	70
Figure 5.7	Classification of plutonic and volcanic igneous clasts from Ethelton	71
Figure 5.8	Photomicrograph of zircon in biotite	72
Figure 5.9	Photomicrograph of ductilely deformed quartz	72
Figure 5.10	Photomicrograph of pseudomorphous hornblende	73
Figure 5.11	Classification of plutonic and volcanic igneous clasts from Kekerengu	74
Figure 5.12	Photomicrograph of saussuritizised plagioclase	75
Figure 5.13	Photomicrograph of pseudomorphous mafic mineral	75

Figure 5.14	Distribution and proportion of igneous clasts	76
Figure 5.15	SiO_2 frequency plots	78
Figure 5.16	AFM diagrams	79
Figure 5.17	Peacock index diagrams	80
Figure 5.18	Alkali-Silica diagram	82
Figure 5.19	Diagram of shoshonite, high-K calc-alkaline, calc-alkaline, low-K tholeiite series	83
Figure 5.20	Aluminium saturation indices	84
Figure 5.21	Major element Harker diagrams	87
Figure 5.22	Trace element Harker diagrams	90
Figure 5.23	Multi-element diagrams of individual clast populations	92
Figure 5.24	Multi-element diagrams of individual lithotypes	98
Figure 5.25	Multi-element diagram of all lithotypes	100
Figure 5.26	Chondrite normalised REE diagram of alkaline clasts	101
Figure 5.27	Tectonic discrimination diagrams Rb vs. Nb+Y and Nb vs. Y	102
Figure 5.28	Discrimination diagrams Fe/Mg and $(K_20+Na_2O)/CaO$ vs. Zr+Nb+Ce+Y	103
Figure 5.29	Y and Nb vs. 10000*Ga/Al diagrams	104
Figure 5.30	Tectonic discrimination diagrams Nb-Y-Ce and Nb-Y-Ga*3	105
Figure 5.31	$\varepsilon Nd_{(i)}$ vs. $^{87/86}Sr_{(i)}$ diagram	108

CHAPTER 6 RAKAIA TERRANE IGNEOUS CLASTS

Figure 6.1	Photomicrograph of extensional deformation	109
Figure 6.2	Photomicrograph of ductilely deformed plagioclase	109
Figure 6.3	Photomicrograph of foliation	110
Figure 6.4	Photomicrograph of sericitised plagioclase	110
Figure 6.5	Classification of plutonic and volcanic igneous clasts from Te Moana	111
Figure 6.6	Photomicrograph of resorbed and embayed quartz	112
Figure 6.7	Photomicrograph of augite phenocryst	112
Figure 6.8	Photomicrograph of meta-sedimentary xenolith	113
Figure 6.9	Photomicrograph of spherulitic texture	113
Figure 6.10	Classification of plutonic and volcanic igneous clasts from McKenzie Pass	114
Figure 6.11	Photomicrograph of granophyric intergrowth	115
Figure 6.12	Photomicrograph of prehnite	115
Figure 6.13	Photomicrograph of biotite with reaction rims	116
Figure 6.14	Photomicrograph of hornblende	116
Figure 6.15	Classification of plutonic and volcanic igneous clasts from Lake Hill	117
Figure 6.16	Photomicrographs of prism-c slip with and without inserted tint plate	118
Figure 6.17	Photomicrograph of primary muscovite	119
Figure 6.18	Photomicrograph of saussuritizised plagioclase	119
Figure 6.19	Distribution and proportion of igneous clasts	120
Figure 6.20	SiO_2 frequency plots	122
Figure 6.21	AFM diagrams	123
Figure 6.22	Peacock index diagrams	124
Figure 6.23	Alkali-Silica diagram	126
Figure 6.24	Diagram of shoshonite, high-K calc-alkaline, calc-alkaline, low-K tholeiite series	127
Figure 6.25	Aluminium saturation indices	128
Figure 6.26	Major element Harker diagrams	130
Figure 6.27	Trace element Harker diagrams	133
Figure 6.28	Sr/Y vs. Y diagram	135
Figure 6.29	Multi-element diagrams for Boundary Creek	136
Figure 6.30	Multi-element diagrams for Te Moana	139
Figure 6.31	Multi-element diagrams for McKenzie Pass	141
Figure 6.32	Multi-element diagrams for Lake Hill	144
Figure 6.33	Chondrite normalised REE diagram of adakites from Lake Hill	147
Figure 6.34	Tectonic discrimination diagrams Rb vs. Nb+Y and Nb vs. Y	148
Figure 6.35	Discrimination diagrams Fe/Mg and $(K_20+Na_2O)/CaO$ vs. Zr+Nb+Ce+Y	149
Figure 6.36	Y and Nb vs. 10000*Ga/Al diagrams	150
Figure 6.37	$\varepsilon Nd_{(i)}$ vs. $^{87/86}Sr_{(i)}$ diagram	153

CHAPTER 7 PROVENANCE OF PAHAU TERRANE IGNEOUS CLASTS

Figure 7.1	Middle Jurassic Gondwana reconstruction	154

Figure 7.2	Crustal blocks of West Antarctica	155
Figure 7.3	Geochronology of Early Jurassic to Late Cretaceous igneous provinces	158
	LATE JURASSIC TO EARLY CRETACEOUS IGNEOUS CLASTS	
Figure 7.4	Alkali-Silica diagram	159
Figure 7.5	Diagram of shoshonite, high-K calc-alkaline, calc-alkaline, low-K tholeiite series	160
Figure 7.6	Aluminium saturation indices	161
Figure 7.7	Major element Harker diagrams	162
Figure 7.8	Trace element Harker diagrams	166
Figure 7.9	Comparison of Darran Suite and calc-alkaline igneous clast zircon compositions	168
Figure 7.10	Comparison of Electric Granite and alkaline igneous clast zircon compositions	170
Figure 7.11	Multi-element diagram for calc-alkaline igneous clasts and igneous provinces	172
Figure 7.12	Multi-element diagram for calc-alkaline igneous clasts and Largs Ignimbrite	173
Figure 7.13	Multi-element diagram for adakitic igneous clasts and Separation Point Suite	174
Figure 7.14	Multi-element diagram for alkaline igneous clasts and Electric Granite	175
Figure 7.15	Chondrite normalised REE diagram of alkaline igneous clasts and Electric Granite	176
Figure 7.16	Tectonic discrimination diagrams Rb vs. Nb+Y and Nb vs. Y	177
Figure 7.17	Discrimination diagrams Fe/Mg and $(K_20+Na_2O)/CaO$ vs. Zr+Nb+Ce+Y	178
Figure 7.18	Tectonic discrimination diagrams Nb-Y-Ce and Nb-Y-Ga*3	179
Figure 7.19	$\varepsilon Nd_{(137)}$ vs. $^{87/86}Sr_{(137)}$ diagram	180
Figure 7.20	$\varepsilon Nd_{(137)}$ vs. $^{147}Sm/^{144}Nd$ diagram	181
Figure 7.21	$\varepsilon Nd_{(137)}$ vs. depleted mantle model ages	182
Figure 7.22	Summary of geochemical and geochronological data	183
	EARLY JURASSIC IGNEOUS CLAST (KEKERENGU)	
Figure 7.23	Alkali-Silica diagram	184
Figure 7.24	Diagram of shoshonite, high-K calc-alkaline, calc-alkaline, low-K tholeiite series	185
Figure 7.25	Aluminium saturation indices	186
Figure 7.26	Major element Harker diagrams	187
Figure 7.27	Trace element Harker diagrams	190
Figure 7.28	Comparison of Bounty Island granite and Kekerengu clast	192
Figure 7.29	Multi-element diagram for igneous clast and igneous provinces	194
Figure 7.30	Tectonic discrimination diagrams Rb vs. Nb+Y and Nb vs. Y	195
Figure 7.31	$\varepsilon Nd_{(188)}$ vs. $^{87/86}Sr_{(188)}$ diagram	196
Figure 7.32	Summary of geochemical and geochronological data	197
	COMPARISON OF IGNEOUS CLASTS AND PAHAU TERRANE SANDSTONES	
Figure 7.33	F2 vs. F1 plot for igneous clasts and Pahau terrane sandstones	198
Figure 7.34	A-CN-K plot and CIA values for igneous clasts and Pahau terrane sandstones	199
Figure 7.35	Th/Sc vs. Zr/Sc for igneous clasts and Pahau terrane sandstones	200
Figure 7.36	La_N/Y_N vs. SiO_2/Al_2O_3 for igneous clasts and Pahau terrane sandstones	201
Figure 7.37	$\varepsilon Nd_{(137)}$ vs. $^{87/86}Sr_{(137)}$ diagram for igneous clasts and Pahau terrane sandstones	204
CHAPTER 8	**PROVENANCE OF RAKAIA TERRANE IGNEOUS CLASTS**	
Figure 8.1	Tasman Fold Belt System	205
Figure 8.2	Crustal blocks of West Antarctica and Transantarctic Mountains	206
Figure 8.3	Geochronology of Cambrian/Carboniferous/Permian-Triassic igneous provinces	207
	PERMIAN TO MIDDLE-TRIASSIC IGNEOUS CLASTS	
Figure 8.4	Aluminium saturation indices	210
Figure 8.5	Alkali-Silica diagram	211
Figure 8.6	Diagram of shoshonite, high-K calc-alkaline, calc-alkaline, low-K tholeiite series	212
Figure 8.7	Major element Harker diagrams	213
Figure 8.8	Trace element Harker diagrams	216
Figure 8.9	Sr/Y vs. Y diagram	217
Figure 8.10	Multi-element diagram for calc-alkaline igneous clasts and igneous provinces	218
Figure 8.11	Multi-element diagram for adakitic igneous clasts and adakitic source plutons	219
Figure 8.12	Tectonic discrimination diagrams Rb vs. Nb+Y and Nb vs. Y	220
Figure 8.13	$\varepsilon Nd_{(260)}$ vs. $^{87/86}Sr_{(260)}$ diagram	221
Figure 8.14	$\varepsilon Nd_{(260)}$ vs. $^{147}Sm/^{144}Nd$ diagram	222
Figure 8.15	$\varepsilon Nd_{(260)}$ vs. depleted mantle model ages	223
Figure 8.16	Summary of geochemical and geochronological data	224

CARBONIFEROUS IGNEOUS CLASTS

Figure 8.17 A-F-M diagram 227
Figure 8.18 Alkali-Silica diagram 228
Figure 8.19 Aluminium saturation indices 229
Figure 8.20 Major element Harker diagrams 230
Figure 8.21 Trace element Harker diagrams 232
Figure 8.22 Multi-element diagrams for calc-alkaline igneous clasts and igneous provinces 233
Figure 8.23 Tectonic discrimination diagram Nb vs. Y 234
Figure 8.24 Y and Nb vs. 10000*Ga/Al diagrams 235
Figure 8.25 $\varepsilon Nd_{(340)}$ vs. $^{87/86}Sr_{(340)}$ diagram 236
Figure 8.26 $\varepsilon Nd_{(340)}$ vs. $^{147}Sm/^{144}Nd$ diagram 237
Figure 8.27 $\varepsilon Nd_{(340)}$ vs. depleted mantle model ages 238
Figure 8.28 Summary of geochemical and geochronological data 239

CAMBRIAN IGNEOUS CLASTS

Figure 8.29 Diagram of shoshonite, high-K calc-alkaline, calc-alkaline, low-K tholeiite series 242
Figure 8.30 Aluminium saturation indices 243
Figure 8.31 Major element Harker diagrams 244
Figure 8.32 Trace element Harker diagrams 246
Figure 8.33 Tectonic discrimination diagram Nb vs. Y 247
Figure 8.34 $\varepsilon Nd_{(500)}$ vs. $^{87/86}Sr_{(500)}$ diagram 248
Figure 8.35 $\varepsilon Nd_{(500)}$ vs. $^{147}Sm/^{144}Nd$ diagram 249
Figure 8.36 $\varepsilon Nd_{(500)}$ vs. depleted mantle model ages 250
Figure 8.37 Summary of geochemical and geochronological data 251

COMPARISON OF IGNEOUS CLASTS AND RAKAIA TERRANE SANDSTONES

Figure 8.38 F2 vs. F1 plot for igneous clasts and Rakaia terrane sandstones 252
Figure 8.39 A-CN-K plot and CIA values for igneous clasts and Rakaia terrane sandstones 253
Figure 8.40 La_N/Y_N vs. SiO_2/Al_2O_3 for igneous clasts and Rakaia terrane sandstones 254
Figure 8.41 $\varepsilon Nd_{(220)}$ vs. $^{87/86}Sr_{(220)}$ diagram for igneous clasts and Rakaia terrane sandstones 255

CHAPTER 9 DISCUSSION AND CONCLUSIONS

Figure 9.1 Simple mixing curve between Darran Suite and Greenland Group 256
Figure 9.2 Comparison of igneous and detrital zircons 257
Figure 9.3 Comparison of igneous and detrital zircons 259
Figure 9.4 Early Cretaceous reconstruction of the Gondwana margin 261
Figure 9.5 $\varepsilon Nd_{(115)}$ vs. Th/Sc for Pahau terrane sandstone modelling 262
Figure 9.6 Paleoenvironmental reconstruction of the Early Cretaceous Gondwana margin 263

TABLE INDEX

CHAPTER 2 DESCRIPTION OF THE CONGLOMERATES

Table 2.1 Summary of conglomerate locations 8

CHAPTER 3 GEOCHRONOLOGY

Table 3.1 Summary of SHRIMP ages of igneous clasts 25

CHAPTER 4 SANDSTONE CLASTS

Table 4.1 Summary of compositions of Rakaia and Pahau terrane sandstone clasts 51
Table 4.2 Average compositions of sandstone clasts 55
Table 4.3 Average compositions of sandstones in the petrofacies suites 56

CHAPTER 5 PAHAU TERRANE IGNEOUS CLASTS

Table 5.1 Summary of geochemical analyses 77
Table 5.2 Sr isotope data for igneous clasts from the Pahau terrane 106
Table 5.3 Nd isotope data for igneous clasts from the Pahau terrane 107

CHAPTER 6 RAKAIA TERRANE IGNEOUS CLASTS

Table 6.1 Summary of geochemical analyses 121

Table 6.2 Sr isotope data for igneous clasts from the Rakaia terrane 151
Table 6.3 Nd isotope data for igneous clasts from the Rakaia terrane 152

CHAPTER 7 PROVENANCE OF PAHAU TERRANE IGNEOUS CLASTS

Table 7.1 Summary of Late Jurassic to Early Cretaceous igneous provinces 156
Table 7.2 Sr isotope and trace element data for sandstone clasts and sandstones 202
Table 7.3 Nd isotope data for sandstone clasts and sandstones 203

CHAPTER 8 PROVENANCE OF RAKAIA TERRANE IGNEOUS CLASTS

Table 8.1 Summary of Permian to Middle Triassic igneous provinces 208
Table 8.2 Summary of mainly Carboniferous igneous provinces 225
Table 8.3 Summary of Cambrian igneous provinces 240

APPENDIX INDEX

APPENDIX 1 SAMPLE TREATMENT

Igneous clasts from Mount Saul 264
Igneous clasts from Ethelton 265
Igneous clasts from Kekerengu 266
Igneous clasts from Boundary Creek 268
Igneous clasts from Te Moana 268
Igneous clasts from McKenzie Pass 268
Igneous clasts from Lake Hill 269
Sandstone clasts from Te Moana 271
Sandstone clasts from Lake Hill 271
Sandstone clasts from Mount Saul 271
Sandstone clasts from Ethelton 271
Sandstones for isotope analysis 272
Sandstones from Frost and Coombs (1989) 272

APPENDIX 2 METHODS AND PROCEDURES

Statistical counting 273
Thin section analysis 273
XRF analysis 274
INAA analysis 274
Sr and Nd isotopes 275
SHRIMP methodology 277
Table A2.1 Precision and detection limits 280
Table A2.2 International standards 281

APPENDIX 3 STATISTICAL COUNTS

Figure A3.1 Statistical counting 282
Statistical counts Mount Saul 283
Statistical counts Ethelton 284
Statistical count Kekerengu 285
Statistical count Te Moana 286
Statistical count McKenzie Pass 286
Statistical count Lake Hill 287

APPENDIX 4 SHRIMP U-PB DATA

Igneous clasts Ethelton 288
Igneous clasts Mount Saul 289
Igneous clasts Kekerengu 290
Igneous clasts Lake Hill 290
Igneous clasts McKenzie Pass 292
Igneous clasts Te Moana 293
Igneous clasts Boundary Creek 293
Detrital zircons Kurow Hill 295

Detrital zircons Balmacaan Stream 296
Detrital zircons Ethelton 297
Figure A4.1 Photomicrographs of zircons 298

APPENDIX 5 POINT COUNTS FOR SANDSTONE CLASTS

Te Moana 302
Lake Hill 303
Mount Saul 304
Ethelton 305

APPENDIX 6 PETROGRAPHIC DESCRIPTIONS

Abbreviations 306
Mount Saul volcanic clasts 308
Mount Saul A-type clasts 310
Mount Saul hypersolvus clasts 311
Mount Saul subsolvus clasts 312
Ethelton volcanic clasts 314
Ethelton hypersolvus clasts 316
Ethelton subsolvus clasts 317
Kekerengu volcanic clasts 319
Kekerengu A-type clast 322
Kekerengu hypersolvus clasts 322
Kekerengu subsolvus clasts 323
Lake Hill volcanic clasts 325
Lake Hill hypersolvus clasts 326
Lake Hill subsolvus clasts 326
Lake Hill adakitic clasts 329
McKenzie Pass volcanic clasts 331
McKenzie Pass hypersolvus clasts 333
McKenzie Pass subsolvus clasts 334
Te Moana volcanic clasts 336
Te Moana hypersolvus clasts 336
Te Moana subsolvus clasts 337
Boundary Creek meta-volcanic clasts 338
Boundary Creek meta-granitoid clasts 339

APPENDIX 7 XRF AND INAA DATA

Mount Saul volcanic clasts 340
Mount Saul A-type clasts 342
Mount Saul hypersolvus clasts 343
Mount Saul subsolvus clasts 345
Ethelton volcanic clasts 347
Ethelton hypersolvus clasts 350
Ethelton subsolvus clasts 351
Kekerengu volcanic clasts 353
Kekerengu hypersolvus clasts 356
Kekerengu subsolvus clasts 357
Lake Hill volcanic clasts 359
Lake Hill hypersolvus clasts 360
Lake Hill subsolvus clasts 361
Lake Hill adakitic clasts 364
McKenzie Pass volcanic clasts 365
McKenzie Pass hypersolvus clasts 368
McKenzie Pass subsolvus clasts 369
Te Moana volcanic clasts 370
Te Moana hypersolvus clasts 370
Te Moana subsolvus clasts 370
Boundary Creek meta-volcanic clasts 371
Boundary Creek meta-granitoid clasts 372

Te Moana sandstone clasts 373
Lake Hill sandstone clasts 374
Mount Saul sandstone clasts 375
Ethelton sandstone clasts 376
Sandstones used for isotope study 377

CHAPTER 1

INTRODUCTION

CHAPTER 1

INTRODUCTION

1.1 SIGNIFICANCE OF STUDY

Sandstone petrography, sedimentary geochemistry, detrital mineral geochronology and isotope geochemical studies of sediments have all been employed in provenance studies of Torlesse sedimentary rocks. These studies have broadly established the type of sedimentary source, but on their own are incapable of establishing a specific source. In this study igneous clasts in rare conglomerates within Torlesse strata are used to determine the Torlesse provenance. Using the tectonostratigraphic terrane concept of regional geology, the accumulated data provide tighter constraints on Torlesse provenance and a more accurate determination of the Mesozoic tectonic setting within the Southwest Pacific margin of Gondwana.

1.2 BACKGROUND

Gondwana's Panthalassan plate margin constituted one of the most extensive orogenic belts in Earth history. The margin was initiated during Neoproterozoic rifting followed by early Paleozoic convergent tectonism related to subduction of oceanic crust beneath the eastern Gondwana craton (Floettmann *et al.*, 1993). Subsequent accretion of arc-trench systems formed a series of eastward-migrating orogenic belts, the oldest of which are the formerly continuous Neoproterozoic-Ordovician Ross and Delamerian orogens (Stump *et al.*, 1986; Coney *et al.*, 1990; Floettmann *et al.*, 1993). Remnants of this orogenic belt are preserved in the formerly continuous Gondwana fragments of southeastern Australia, Antarctica and New Zealand (Gibson and Ireland, 1996, Figure 1.1).

Paleozoic-Mesozoic outboard terranes are characterised by vast volumes of monotonous sandstone and mudstone sequences that have been interpreted as massive accretionary prisms (MacKinnon, 1983; Veevers *et al.*, 1994b). A key question in understanding the Paleo-Pacific margin of Gondwana remains the provenance of these rocks. The source of the Torlesse terranes (part of the outboard Gondwana pre-break-up

margin, see Section 1.3.3 for nomenclature) has long been an outstanding problem in New Zealand geology (Coombs *et al.*, 1976; Howell, 1980; MacKinnon, 1983; Korsch and Wellman, 1988; Bradshaw, 1989; Mortimer, 1995; Roser and Korsch, 1999). A source along the Antarctic margin of Gondwana has been favoured in most of these studies. Recently, however, a possible Australian source for the Rakaia terrane has been proposed based on Ar-Ar ages of Torlesse detrital micas and SHRIMP detrital zircon ages (Adams, 1996; Adams *et al.*, 1998; Pickard *et al.*, 2000).

The present shape of the New Zealand micro-continent is mainly the result of Cretaceous-Cenozoic tectonics. The tectonic regime in the New Zealand region changed from subduction-related processes to extension in the period between 110-80 Ma, accompanied by widespread basin formation (Bradshaw, 1989; Luyendyk, 1995; Kamp, 1999), eventually culminating in the opening of the Tasman Sea and the Southern Ocean (Figure 1.1).

The basement geology of New Zealand can be described in terms of batholiths, suites and tectonostratigraphic terranes (Coombs *et al.*, 1976; Bishop *et al.*, 1983; Bradshaw, 1989), which can be grouped into three provinces: the Western Province, the Median Tectonic Zone and the Eastern Province (Figure 1.2). The Permian-Cretaceous stratified rocks of New Zealand are also divisible into four broad lithotectonic assemblages, which are, by definition, separated by major tectonic boundaries. These four assemblages, Parapara, Hokonui, Te Anau and Torlesse (Alpine) are further subdivided into tectonostratigraphic terranes or subterranes (Landis *et al.*, 1999).

The Western Province comprises two terranes and is largely made up of Lower Paleozoic metasedimentary rocks cut by Devonian, Carboniferous and Early Cretaceous granitoids (Muir *et al.*, 1994; Muir *et al.*, 1997), with minor volcanic and metamorphic rocks of Cambrian age (Cooper, 1989; Gibson and Ireland, 1996; Münker and Cooper, 1997). It had attained its continental thickness and its gross structure by the end of the Carboniferous and represents a fragment of the Gondwana Paleozoic margin. The terranes of the Eastern Province of New Zealand are believed to have formed along the eastern margin of Gondwana and amalgamated during the Mesozoic to form the basement of much of New Zealand. The Median Tectonic Zone separates the Western and Eastern Province rocks, and consists of suites of subduction-related calc-alkaline

plutons with subordinate volcanic and sedimentary rocks (Bradshaw, 1993; Kimbrough *et al.*, 1994a; Muir *et al.*, 1998; Mortimer *et al.*, 1999a).

The Torlesse terranes, as part of the Eastern Province, constitute approximately 60-70 % of the New Zealand land area and a large part of the micro-continent (Figure 1.3). The terranes underlie the eastern South Island and North Island. Two terranes are recognised in the South Island. The older part, the Rakaia terrane, was amalgamated to the Caples terrane by the Middle Jurassic (e.g., Adams *et al.*, 1985; Graham and Mortimer, 1992; Little *et al.*, 1999). Similar sedimentary rocks were deposited during the late Jurassic and early Cretaceous and form the related but younger Pahau terrane. The two terranes are separated by the Esk Head Mélange (Bradshaw, 1973; Silberling *et al.*, 1988).

Some 90 % of New Zealand continental crust lies beneath the sea. Direct sampling of offshore basement is limited to a few dozen dredge hauls and oil exploration wells. The major bathymetric feature of western New Zealand is the Lord Howe Rise, which is the continental extension of the Challenger Plateau (Figure 1.3). Median Tectonic Zone and Murihiku rocks underlie the Taranaki Basin and Torlesse and Waipapa rocks have been identified in the Wanganui Basin (Mortimer *et al.*, 1997).

The northern region from the Norfolk Ridge to the Kermadec Trench to the north of the North Island is dominated by Cenozoic tectonics associated with subduction and back-arc basin development (Mortimer *et al.*, 1998). The Norfolk Ridge is the continental link between New Zealand and New Caledonia (Eade, 1988), where correlatives of the Murihiku and possibly the Brook Street (Black, 1996a) and the Maitai terranes (Aitchison *et al.*, 1998) are found.

The prominent offshore features of eastern New Zealand are the Hikurangi Plateau, the Chatham Rise, the Bounty Trough and the Campbell Plateau. The Hikurangi Plateau lies mostly at depths of 2500-3500 m and is thought to be a Mesozoic igneous province similar to the Ontong Java Plateau and the Manihiki Plateau (Wood and Davy, 1994; Mortimer and Parkinson, 1996). The Chatham Rise and the Campbell Plateau are continental extensions of eastern New Zealand. Deformed and metamorphosed Torlesse basement rocks have been dredged from the crest of the Chatham Rise and are exposed on the Chatham Islands (Wood *et al.*, 1989; Ireland, 1992; Wood and Herzer, 1993).

1.3 TECTONOSTRATIGRAPHIC FRAMEWORK OF NEW ZEALAND

1.3.1 Western Province

The Western Province consists of two distinct, north-south trending, middle Cambrian to Lower Devonian tectonostratigraphic terranes - the Buller and Takaka terranes (Cooper, 1989). In northwest Nelson, where they are best developed, these two terranes are separated by the Anatoki Thrust. The two terranes have also been recognised in Dusky Sound, Fiordland, where they are separated by the Old Quarry Fault (Ward, 1986). These terranes are fragments of the now dispersed Gondwana continent. The Western Province is notable because it includes the oldest known rocks in New Zealand and is also host to extensive Paleozoic and Cretaceous igneous suites (Chart in back pocket).

1.3.1.1 Buller Terrane

The Buller terrane comprises a relatively uniform suite of latest Cambrian-Early Ordovician quartz-rich turbidites of the Greenland Group, derived from a passive continental margin (Roser *et al.*, 1996). Initial metamorphism and cleavage formation of the Greenland Group is dated at 438 Ma (Adams *et al.*, 1975). The Topfer Formation (Mortimer and Smale, 1996), a non-marine Triassic unit, is cut by the Kirwan Dolerite that has been correlated with the Ferrar magmatic province of Gondwana (Mortimer *et al.*, 1995). The Topfer formation and the Parapara Group have been included in the Parapara assemblage (Landis *et al.*, 1999).

Recent geochronological studies in the NW Nelson-Westland region have identified two periods of plutonism in the Paleozoic, with the bulk of the Karamea Suite being intruded in the Middle Devonian, and the Early Carboniferous Cape Foulwind and Windy Point granites representing a younger event (Figure 1.4, Muir *et al.*, 1994; Muir *et al.*, 1997). At least two periods of plutonism are identified in the Cretaceous, with most of the Separation Point Suite intruded around 118±2 Ma (Muir *et al.*, 1995). The Crow Granite, at 137±3 Ma is the oldest Cretaceous granite. The Hohonu Suite granitoids are slightly younger (109±3 to 114±2 Ma). Late Cretaceous magmatism is represented by the A-type French Creek Granite (81.7±2 Ma) and is broadly coincident with the opening of the Tasman Sea (Waight *et al.*, 1997).

The Paparoa Batholith forms the central region of a metamorphic core complex related to a major period of mid-Cretaceous crustal extension (Tulloch and Kimbrough, 1989; Spell *et al.*, 2000). The Buckland Granite of the Paparoa Batholith (110±2 Ma, Muir *et al.*, 1997) is similar in age and composition to the Hohonu Suite and is regarded as part of the Hohonu Suite (Waight *et al.*, 1997).

Three distinct geological regions are recognised in Fiordland (Figure 1.5); the western and eastern belts and the SW Fiordland block (Bradshaw, 1990). The latter comprises mainly low-grade metasedimentary rocks and granitoids that are generally regarded as an extension of the Lower Paleozoic Western Province terranes of SW Nelson-Westland (Cooper, 1989). The eastern belt comprises mainly Mesozoic plutonic rocks and occupies the structural position of the Median Tectonic Zone (see Section 1.3.2). The western belt has been interpreted as the deep crustal levels of a metamorphic core complex, collectively termed the Western Fiordland Orthogneiss, in which Early Cretaceous granulite-facies rocks (core) are structurally overlain by Paleozoic amphibolite-facies rocks (Gibson *et al.*, 1988). The magmatic emplacement of the granulite-facies rocks has been dated at c. 120-130 Ma (Mattinson *et al.*, 1986; Muir *et al.*, 1998). Enclaves in the Western Fiordland Orthogneiss have been dated at 380 Ma (Bradshaw and Kimbrough, 1991), which appears to correlate with the Karamea Suite rocks. The Kellard Point Orthogneiss, part of the basement, gives U-Pb zircon ages of 481 Ma (Gibson and Ireland, 1996). Two metasedimentary cover rocks, the Townly calc-silicate (502 Ma) and a quartzofeldspathic schist (334 Ma), have been regarded as the correlatives of the Australian Delamerian Fold Belt and the Lachlan Fold Belt, respectively (Gibson and Ireland, 1996).

Most of the strongly deformed orthogneisses and paragneisses in the Western Province are metamorphic core complexes (Gibson *et al.*, 1988; Kimbrough and Tulloch, 1989; Tulloch and Kimbrough, 1989; Kimbrough *et al.*, 1994b). The granulite-facies gneisses of the Western Fiordland Orthogneiss are considered to be the lower crustal equivalent of the Separation Point Suite (Muir *et al.*, 1995). Granitoids associated with convergent margin magmatism are involved in the core complexes (e.g., Buckland Granite) and have been overprinted by extensional deformation.

1.3.1.2 Takaka Terrane

The Takaka terrane contains a wide range of lithofacies and rock types, is structurally highly complex and spans a wide age range (Middle Cambrian to Devonian). A major fault, the Devil River Fault, separates the Central Belt from the Eastern Belt (Cooper, 1989). The Central Belt is of particular interest to this study. For a comprehensive review of the Takaka terrane geology the reader is referred to Cooper (1989).

The Central Belt is predominantly composed of Cambrian volcanics and volcaniclastic sediments (Münker and Cooper, 1999; Münker, 2000; Wombacher and Münker, 2000). Two assemblages are recognised. One comprises a Middle to Late Cambrian island arc (Devil River Volcanics Group) that is interbedded with the arc derived Haupiri Group sediments (Wombacher and Münker, 2000). The Devil River Volcanics Group consists of the Benson and Mataki Volcanic Formation and the Cobb Igneous Complex (Münker and Cooper, 1999). A U-Pb sensitive high resolution ion microprobe (SHRIMP) age of 515±7 Ma was obtained for zircons from a late stage plagiogranite intruding the Cobb Igneous Complex (Münker and Cooper, 1999).

The Triassic Parapara Group consists of black slates, quartzofeldspathic sandstones and mudstones and quartzose sandstones (Landis and Coombs, 1967; Smale *et al.*, 1996). They are compositionally distinct from correlative strata in the Eastern Province, but a geochronological study revealed that the sequence is dominated by a detrital zircon U-Pb age peak at about 240 Ma (Figure 3.12 this study, Wysoczanski *et al.*, 1997).

The Ordovician sequence is intruded by the Middle to Late Devonian Riwaka Complex (Muir *et al.*, 1996a). The Early Cretaceous Crow Granite is adjacent to the Anatoki Fault (Jongens, 1997). The Early Cretaceous Separation Point Suite of granitoids intrudes rocks of both the Buller terrane (e.g., Mt. Olympus Granite) and the Takaka terrane (e.g., Separation Point Batholith, Muir *et al.*, 1994; Muir *et al.*, 1997).

1.3.2 Median Tectonic Zone

The Median Tectonic Zone, also termed the Median Batholith (Mortimer *et al.*, 1999b), is a belt of deformed and undeformed mainly subduction-related I-type plutonic rocks with minor metasedimentary and metavolcanic units (Bradshaw, 1993;

Kimbrough *et al.*, 1994a; Mortimer *et al.*, 1999b). Geochronological studies using conventional U-Pb and SHRIMP methods show that magmatism extended from the Carboniferous to Early Cretaceous with two pronounced magmatic gaps occurring in the Permian and Early Jurassic (Kimbrough *et al.*, 1993; Kimbrough *et al.*, 1994a; Muir *et al.*, 1998; Mortimer *et al.*, 1999a).

Five volcanosedimentary units are recognised within the MTZ, the Drumduan terrane and Rainy River Conglomerate in Northwest Nelson, the Largs terrane and Lochburn Formation in Eastern Fiordland, and the Paterson Group on Stewart Island. There has been much debate on the significance of these terranes within the MTZ (Bradshaw, 1993). The volcanosedimentary rocks are of Jurassic or earliest Cretaceous age and most rest unconformably on, or contain clasts of, older plutonic rocks. A Tithonian – Berriasian depositional age is supported by a new 140±2 Ma U-Pb zircon date for the Largs Ignimbrite (Mortimer *et al.*, 1999a). All the volcanosedimentary units are intruded by younger plutons (Mortimer *et al.*, 1999b, and references therein).

The Rainy River Conglomerate forms a narrow belt in the east of the MTZ and comprises indurated conglomerates with minor sandstone-siltstone-mudstone and sparse coal seams. Based on ages and geochemistry of granitoid clasts the Rainy River Conglomerate has been tentatively correlated with the Barretts Formation of the Brook Street terrane (Tulloch *et al.*, 1999).

The bulk of the plutonic rocks in Eastern Fiordland range from Middle Jurassic to Early Cretaceous in age and are collectively referred to as the Darran Suite. The Darran Suite is cut by pegmatites (Wandres *et al.*, 1998) of the Separation Point Suite that give ages of c. 124 Ma (Muir *et al.*, 1998).

The Late Jurassic-Early Cretaceous plutonic rocks forming the Rotoroa Complex are probably equivalent to the voluminous Darran Suite rocks in Eastern Fiordland (Muir *et al.*, 1998). The Rotoroa Complex is stitched to the Lower Paleozoic rocks of the Takaka terrane by the Separation Point Batholith (Kimbrough *et al.*, 1994a). Carboniferous age granitoids occur in SW Fiordland (Pomona Diorite and Granite) at the western edge of, but within the Median Tectonic Zone. Carboniferous rocks also occur on Pepin Island in NW Nelson (Echinus Granite) (Kimbrough *et al.*, 1993). Triassic plutonic rocks are restricted to the eastern side of the zone (Kimbrough *et al.*, 1994a).

Modelling of K-feldspar Ar incremental heating ages indicate that most of the Longwood Range had cooled below 175° C by the Middle Jurassic (170 –180 Ma) and experienced no subsequent reheating (Mortimer *et al.*, 1999a). Significant younger thermotectonic activity in the MTZ in the Hollyford-Eglinton area is indicated by the emplacement of the Largs Ignimbrite and the Separation Point Suite rocks (Muir *et al.*, 1998).

Based on interpretations in the field, and geochronological and petrological relationships, Mortimer (1999b) suggested that the plutons of the Median Tectonic Zone constitute a Cordilleran batholith and are probably intruded into and/or alongside New Zealand's Western Province. This differs from the allochthonous island-arc setting for the MTZ proposed by Muir *et al.* (1995, 1998).

1.3.3 Eastern Province

The Eastern Province is an assemblage of accreted allochthonous terranes making up almost all of northern New Zealand and the eastern part in the South Island. There are two distinct groupings of terranes recognised in the South Island on the basis of gross composition. The first includes three terranes of island arc associations, dominated by volcaniclastic sediments. These are the Brook Street, Murihiku and Dun Mountain–Maitai terranes. They have been referred to as Central Arc Terranes (Campbell, 2000b) or Hokonui Assemblage (Landis *et al.*, 1999). The second grouping of the Eastern Province has been referred to as the Te Anau Assemblage (Caples-Rai-Pelorus terrane, Chrystalls Beach Complex and Croisilles-Greenstone) and Alpine Assemblage (Rakaia, Aspiring, Te Akatarawa, Kakahu and Pahau terranes and Esk Head Mélange) (Landis *et al.*, 1999). An alternative nomenclature has been proposed that groups the Caples and the Waipapa terranes with the terranes of the Alpine Assemblage into a Torlesse superterrane, and all previous Torlesse subterranes are accorded terrane status (Campbell, 2000b). In the South Island a subterrane nomenclature is in wide use (e.g., Bradshaw, 1989) and has also been adapted in more recent work on the North Island (Mortimer, 1995). In this study I assign a terrane status to the Rakaia and Pahau subterranes of the South Island based on results of this study.

1.3.3.1 Brook Street Terrane

The Brook Street terrane is an Early to Late Permian oceanic volcanic arc and includes a 14-16 km thick sequence of moderately metamorphosed submarine volcanics and volcaniclastics of mainly basaltic-andesitic composition with minor rhyolitic and dacitic lithologies. The terrane has been interpreted as the remnants of an Early Permian oceanic arc (Sivell and Rankin, 1983). A hornblende gabbronorite from the Brook Street terrane has yielded a U-Pb date of 265 Ma (Kimbrough *et al.*, 1992). The late Early Permian Caravan Formation, part of the Takitimu Group, consists of an over 1000 m thick-bedded volcanic breccia with minor limestone turbidities. The contact with the overlying late Early – early Late Permian Productus Creek Group, a limestone unit with minor tuffaceous and muddy horizons, is conformable. The Middle Jurassic Barretts Formation rests unconformably on the Productus Creek Group. The formation is up to 2000 m thick, is dominated by sandstones and distinctive conglomerates are widespread. Tuff, thin coal seams, and mudstone occur locally. The conglomerates include granitoid clasts of Triassic to Jurassic age (Tulloch *et al.*, 1999).

In eastern Fiordland and NW Nelson the Brook Street terrane - Median Tectonic Zone contact is marked by Cenozoic faulting (Mortimer *et al.*, 1999a), although the early Late Triassic Mistake Diorite (Eglinton Valley) has been interpreted as intruding the volcaniclastic rocks of the Brook Street terrane (Williams and Harper, 1978).

The Late Permian Pourakino Trondhjemite, the Hekeia Gabbro and the Colac Granite in the Longwood Range have been assigned, based on Sr and Nd initial ratios, to the Brook Street terrane (Mortimer *et al.*, 1999a). These plutons are intruded by more radiogenic diorite dikes and plutons of the Median Tectonic Zone (Mortimer *et al.*, 1999a). A Middle-Late Triassic accretion of the Brook Street terrane to the MTZ has been proposed (Mortimer *et al.*, 1999a).

1.3.3.2 Murihiku Terrane

The Murihiku terrane is the least structurally deformed and stratigraphically most coherent of the New Zealand basement terranes. It is weakly metamorphosed and includes a thick succession (up to 15 km) of mainly volcaniclastic sediments deposited from Triassic to late Early Cretaceous time (Campbell and Coombs, 1966). In Southland, the Permian to early Middle Triassic basal Malakoff Hill Group is marine in

origin with epiclastic andesitic sandstone and siltstone containing abundant interbedded tuff. Latest research suggests that the Kuriwao sequence is in gradational contact with the overlying Triassic strata, in which case it is best interpreted as a Permian 'basement' within the Murihiku (Campbell *et al.*, 2001). Petrographic and geochemical data, including Nd isotopes (Frost and Coombs, 1989), imply derivation from a nearby oceanic arc that lacked an older crystalline basement (Frost and Coombs, 1989; Landis *et al.*, 1999). In contrast, the overlaying Middle and Late Triassic Murihiku strata show compelling evidence for a more Andean type volcanic arc source (Boles, 1974; Frost and Coombs, 1989). The Murihiku rocks are generally considered to have formed parallel to and along the Gondwana margin in a forearc basin setting (e.g., Coombs *et al.*, 1976), although there is some evidence in favour of a backarc location (Coombs *et al.*, 1996). The southwest side of the basin is regarded as closest to the source, and the Brook Street terrane was believed to be the source of the detritus, but isotope data and paleomagnetic data suggest that the terranes are unrelated to each other (Grindley *et al.*, 1981; Ballance and Campbell, 1993; Bradshaw, 1994). However, based on compositional similarities, it is possible that the Barretts Formation (Brook Street) and Murihiku sediments shared closely related sources and might have been in close proximity in the Jurassic (Landis *et al.*, 1999). In addition, the Barretts Formation also received mafic material from a volcanic source.

Triassic-Jurassic granitic boulders, similar to the ones described from the Kawhia Syncline of the Late Triassic Murihiku strata (Moeatoa Conglomerate) in the North Island (Graham and Korsch, 1990), are very similar in composition to that of plutons from the MTZ (Mortimer, pers. comm.). A Rb-Sr whole-rock isochron for a suite of granitoid clasts from Moeatoa Conglomerate yields an age of 226±6 Ma and is similar to the U-Pb clast ages reported from the Barretts Formation. A reduction of vitric volcanic debris in the Middle to Late Jurassic Murihiku sediments has been reported by Ballance (1981) and Black (1993).

1.3.3.3 The Dun Mountain - Maitai Terrane

The Maitai Group, a 6 km thick, moderately metamorphosed volcaniclastic sedimentary succession, rests on the Early Permian Dun Mountain Ophiolite Belt (DMOB). The DMOB comprises a discontinuous exposure of up to 4 km thick mafic and ultramafic rocks which extends for a length of >1000 km. The northern and

southern sectors of the ophiolite belt are offset dextrally 450 km by the Alpine Fault. The DMOB is Early Permian and has been dated by the conventional U-Pb method at 285-275 Ma (Kimbrough *et al.*, 1992), and a similar Nd-isotope age of 278±4 Ma has been obtained from a plagiogranite (Sivell and McCulloch, 2000).

Sivell (2000) recognised three distinct suites in the DMOB based on petrological, geochemical and isotopic compositions. The data are strongly suggestive of a fore-arc setting for the DMOB suggesting that anomalous thin oceanic crust has been entrapped in an incipient subduction zone which may have been the precursor of eruptive activity in the Brook Street terrane.

The lower 1000-1500 m of the Maitai Group is of Late Permian age and consists of three units: Upukeroa Breccia, Wooded Peak Limestone and Tramway Formation. They comprise redeposited bioclastic sandstone and carbonate lithologies dominated by molluscan prismatic calcite shell debris attributed to unidentified atomodesmatinid bivalves. Thick lenses of polymictic breccia and bioclastic limestone of the basal Maitai Group locally rest in primary depositional contact on relatively intact ophiolite within the DMOB. The bulk (4500-5000 m) is now known to be of Early to Middle Triassic age (Campbell, 2000b). A granite clast from the Maitai Group has been dated by the conventional U-Pb method at 265 Ma (Kimbrough *et al.*, 1992).

A carbon isotope study by Krull (2000) on the marine organic matter of the Maitai Group strongly suggests a high-paleolatitude setting for the terrane and deposition at intermediate depth in the ocean (c. 400 m) within a volcanic arc-related basin.

The Livingstone Fault (Chart) marks the tectonic eastern margin of the Maitai terrane. The structures in the terranes south of the fault are relatively simple, whereas the deformation is more complex within the terranes on the northern side of the fault (Bradshaw, 1989).

1.3.3.4 Caples Terrane

The Caples terrane of Otago (Figure 1.2) crops out in an arcuate belt stretching from the East Otago coast to the Alpine Fault. The terrane includes a subdivided sequence (Caples Group) in the west and an undifferentiated sequence (Tuapeka Group) in the East. Similar rocks in the Nelson area, the Pelorus Group, have been offset along

the Alpine Fault. In Otago, the Caples terrane is metamorphosed, varying from prehnite-pumpellyite facies to lower greenschist facies (Bishop *et al.*, 1976). Previous petrographic studies of sandstones of the Caples rocks have established an arc provenance, and deposition is inferred to have been as fan deposits in structurally controlled lower trench-slope basins and on the trench floor adjacent to an active arc (Turnbull, 1979a; Turnbull, 1979b).

Geochemical analyses suggest that the sediments were derived from a relatively evolved calc-alkaline arc system (Roser and Korsch, 1986; Roser and Korsch, 1988) . Immobile trace element contents and ratios support these conclusions, with values intermediate between those typical of oceanic island arc and continental arc sediments (Roser and Cooper, 1990).

Comparison of the Caples samples with data from nearby terranes of similar age (Torlesse, Maitai, Murihiku and Brook Street) reveals consistent compositional differences, suggesting that provenance linkages are unlikely (Roser *et al.*, 1993b). The greater incidence of more mature sandstone in the east supports depositional models proposing eastward-increasing cratonic Gondwana influence and a westwards increasing arc-influence on the Caples sedimentary provenance (MacKinnon, 1983; Korsch and Wellman, 1988).

The Caples terrane is virtually unfossiliferous but contains allochthonous blocks of conodont-bearing Kungurian (Early Permian) micritic limestone with atomodesmatinid shell debris (Ford *et al.*, 1999).

The northern boundary of the Caples terrane is a cryptic suture that lies within the Otago Schist and has been defined on geochemical parameters (Mortimer and Roser, 1992). At the northern end of the Remarkables Range, Central Otago, psammitic schists of the Caples terrane pass downwards through a 300 m thick transitional zone into pelitic schists of the Aspiring lithologic association. Mortimer (1992) demonstrated that the Aspiring lithologic association is part of the Rakàia terrane. Structural geometry and shear criteria indicate that the Caples terrane overthrusts the Rakaia terrane from the south and west (Cox, 1991; Mortimer, 1993).

The Middle-Triassic (Ito *et al.*, 2000) Chrystalls Beach-Brighton coastal block south of Dunedin lies within the Caples terrane but is of distinctly different petrofacies

from that described for the Caples. On the basis of age, petrography and geochemical data the Chrystalls Beach–Brighton metasediments cannot be correlated with the known formations of the Caples terrane (Coombs *et al.*, 2000). The southern part of the complex contains Tethyan and non-Tethyan radiolarian faunas of possible Southern Hemisphere high-latitude origin (Ito *et al.*, 2000).

1.3.3.5 Otago Schist

The Otago Schist metamorphism overprints the Caples and the Rakaia terranes. Adams (1997) found that the Otago Schist north of Dunedin has $^{87}Sr/^{86}Sr$ initial ratios ranging from 0.7064 to 0.7092, similar to the Rakaia terrane. The Chrystalls Beach-Brighton metasediments have $^{87}Sr/^{86}Sr$ initial ratios that range from 0.7052 to 0.7064. These are lower than the Rakaia rocks yet higher than the Caples-type rocks elsewhere in Otago (0.7035 to 0.7055) (Graham and Mortimer, 1992).

Rb-Sr whole rock studies of the Otago Schist (Graham and Korsch, 1989; Graham and Mortimer, 1992) support K-Ar dating (Adams *et al.*, 1985) and indicate a Late Triassic – Early Jurassic age for schist metamorphism, with younger ages (to 115 Ma) representing either (1) long-continued uplift, or (2) a second stage of metamorphism (Adams and Graham, 1997). Interpretation of Ar-Ar dated white micas suggests that the peak metamorphism occurred in the Middle Jurassic (180-170 Ma), and a second younger peak (135±5 Ma) represents the onset of rapid unroofing and uplift (Little *et al.*, 1999). The metamorphism and deformation of the Otago Schist has been related to the juxtaposition of the Caples and the Rakaia terranes. A more detailed discussion of the Caples terrane and the Otago Schist can be found in Roser *et al.* (1993b) and Mortimer (1993).

1.3.3.6 Torlesse Terranes

The Torlesse terranes crop out over a large part of New Zealand (Figure 1.3) and consist of well-bedded but structurally complex felsarenites and mudstones. They are commonly inferred as representing accreted subduction complexes (MacKinnon, 1983). Oceanic associations of basalt, limestone and chert are preserved as regionally minor components and usually occur in fault or mélange zones (Silberling *et al.*, 1988; Mortimer, 1995). The rocks are poorly mapped and stratigraphic continuity may be difficult to establish for more than a few hundred metres. Although fossils are

uncommon in the Torlesse rocks, several fossil zones have been recognised (Campbell and Warren, 1965; Speden, 1974; Speden, 1976, see section 1.4). Fossil content of the Rakaia terrane indicates a depositional age range of Permian to Triassic, with the youngest Triassic fossil being Rhaetian radiolarians (Campbell, 2000b).

Geochemical (Roser and Korsch, 1999) and isotopic evidence shows distinct differences between the Caples and the Rakaia terranes, with initial $^{87}Sr/^{86}Sr$ ratios at the time of metamorphism higher (Adams and Graham, 1996) and εNd lower (Frost and Coombs, 1989) in the Rakaia terrane.

The Esk Head Mélange is mappable as a unit separating the Rakaia from the Pahau terrane. It has unclear boundaries but may be thought of as a zone of intense deformation between the two terranes. The sandstone and mudstone components of the mélange contain Jurassic fossils (Campbell and Warren, 1965), Jurassic chert and exotic blocks that are of a Pahau ocean floor and/or sea mount origin. Compositional studies show that the Esk Head matrix is essentially of Pahau origin (J. Bradshaw, pers. comm.). Allochthonous blocks include fossiliferous Triassic limestone, chert and siliceous hemipelagite (Silberling *et al.*, 1988). The clastic sequences of the Rakaia and the Pahau terranes differ in age by approximately 55 Ma (Rhaetian to Kimmeridgian; see Chart).

The Late Jurassic to Early Cretaceous Pahau terrane is similar in aspect to the Rakaia terrane and has been traditionally interpreted as an accretionary complex with a slightly more intermediate volcaniclastic input (MacKinnon, 1983). A detailed sedimentologic study of the Pahau type section gives support to a subaerial/marginal marine depositional environment based on beds containing numerous rootlets that have been found in both the conglomerate facies and in the mudstone facies in the Pahau River (Orlowski, 2001).

A link between the two terranes has been first proposed by (MacKinnon, 1983) and also, based on heavy minerals, by Smale (1997). However, Adams and Graham (1996) concluded that initial $^{87}Sr/^{86}Sr$ ratios of the younger Pahau terrane at the time of metamorphism are inconsistent with the Rakaia terrane being a dominant sediment source for the Pahau terrane.

In the North Island the volcaniclastic Waioeka petrofacies defines a new and provisional Late Jurassic to Early Cretaceous Waioeka terrane that is not present in the South (Mortimer, 1995). The Waioeka sandstones are compositionally similar to sandstones in the coeval eastern Waipapa terrane. On the basis of petrographic evidence and chemical composition, Mortimer (1995) subdivided the sandstones of the northern quarter of the Torlesse terrane into four new petrofacies: (1) Rakaia; (2) Pahau; (3) Waioeka and (4) Omaio petrofacies. A comparison of these petrofacies with existing South Island Torlesse classifications indicates continuation of the Triassic Rakaia subterrane and the Late Jurassic to Early Cretaceous Pahau subterrane into the central part of the North Island.

A SHRIMP U-Pb age of 99±2 Ma of a detrital zircon from the Omaio petrofacies approximates the age of deposition of these rocks (Cawood *et al.*, 1999), and this age is supported by a zircon fission track date of 108±6.3 Ma (Kamp, 1999).

1.3.3.7 Waipapa Terrane

The Waipapa terrane is a diverse assemblage of largely turbiditic terrigenous sediments west of the Torlesse terranes that extends over the central and northern North Island (Sporli, 1978). Nomenclature, internal subdivision, and external correlation of the Waipapa terrane are diverse and controversial. It is considered to be a superterrane divisible into the Omahuta, Bay of Island and Manaia Hill subterranes (Black, 1996b). The Manaia Hill subterrane consists of two contrasting facies. One of them, the Morrinsville facies, is compositionally similar to the coeval Waioeka terrane in the eastern North Island (Mortimer, 1995). Other authors consider the Bay of Island subterrane as the only Waipapa terrane and assign the other two subterranes to the Caples (Omahuta) and Waioeka (Manaia Hill) terranes (Campbell, 2000a). The depositional age of the Bay of Island subterrane ranges between late Early Permian to Late Triassic (Campbell, 2000b). The boundary between the Waipapa and Murihiku terranes in the North Island coincides with a magnetic anomaly (Stokes Magnetic Anomaly). Rare small serpentine outcrops suggest that the Dun Mountain Ophiolite Belt may be present although on a very reduced scale (Black, 1996a).

Based on petrographic and geochemical evidence Kear (2001) tentatively proposed a supergroup for the extensive Late Jurassic to probably Early Cretaceous

stratigraphic unit in the Central North Island that rests on older deformed and mutually amalgamated Murihiku, Waipapa and Rakaia terranes.

1.3.3.8 Cover Strata

Basement rocks on the South Island are separated by a regional unconformity from younger undeformed mainly non-marine cover-strata. A discussion of these strata is beyond the scope of this study. However, in the Eastern Province the Kyeburn Formation near Naseby (Bishop and Laird, 1976), Central Otago, and the Shag Point Group (Horse Range Formation) near Palmerston, eastern Otago (Paterson, 1941), contain interbedded silicic tuffs and ignimbrites. K-Ar biotite ages for the silicic tuffs (Kyeburn Formation) are 105±2 and 108±2.8 Ma and for the biotite-ignimbrite (Horserange Formation) 101±2 Ma and 103±2 Ma (Adams and Raine, 1988). The two localities thus give evidence of mid-Albian subaerial volcanism in Otago. In the Western Province the Stitts Tuff occurs within the region of the Paparoa core complex at the base of the Pororari Group in the Lower Buller Gorge (Bowen, 1964) and has been dated by the SHRIMP-method at 101±2 Ma and 102±3 Ma (Muir *et al.*, 1997). The source of the Albian silicic volcanism in the South Island region is unknown .

Offshore, the Great South Basin is also non-marine and unconformably overlays basement rocks of the Eastern Province (Beggs, 1993). Pollen from a drill hole (Tora 1) give Cenomanian ages (Raine *et al.*, 1993), but the seismic interpretation indicates that c. 1000 m of older sediments lie between the drill hole and the basement.

Marine dinoflagellates of Early Cretaceous (Neocomian to Aptian; 144-113 Ma) age from the bottom of the Waimamaku-2 exploration well in Northland have been interpreted as part of the Murihiku terrane basement (Isaac *et al.*, 1994).

1.3.4 Summary

Twenty five years of research has established the extent to which individual New Zealand terranes are distinct entities in terms of physical geometry and position in space and time. Terranes have been distinguished in terms of original sedimentary composition. Batholiths and suites have been identified and interpreted with respect to their petrogenesis.

A Middle-Late Triassic accretion of the Brook Street terrane to the rest of the MTZ (Batholith) is suggested by intrusive relationships of igneous rocks in the Longwood Range. The emplacement of the Separation Point Granite stitches the MTZ to the Western Province. Additionally, the age of the Crow Granite (137±3 Ma) is indistinguishable from the Darran Suite in Fiordland and suggests that the MTZ was autochthonous in the earliest Lower Cretaceous with respect to the Western Province.

Silicic volcanic rocks of similar age occur in Otago and in the Lower Buller Gorge suggesting a close proximity of Eastern and Western Provinces in Albian time.

The overlapping relationship of the Waipapa supergroup with the underlying basement terranes suggests a possible amalgamation of the North Island Eastern Province Terranes in the Late Jurassic. A Jurassic juxtaposition of the Brook Street terrane and the Murihiku terrane in the South Island has also been proposed. A Cenomanian minimum age of juxtaposition (and deformation) of the Eastern Terranes and the Median Tectonic Zone is suggested by the pollen ages from the Great South Basin. Sedimentation in the Murihiku terrane might have extended into the Lower Cretaceous.

Nd initial ratios, together with Rb-Sr isochron and detrital mineral age studies (U-Pb dating of zircons and Ar-Ar dating of muscovite) on the Eastern Province terrane sediments have provided 'isotopic finger prints' that are characteristic and distinctive of each terrane.

1.4 Geographic and Stratigraphic Distribution of Torlesse Rocks

Considering the total exposed area, on the order of 40 000 km^2 in the eastern South Island, the number of known fossil localities within the Torlesse terranes is very small (Figure 1.6). Most are isolated occurrences in flyschlike sequences, and many have been redeposited (Campbell and Warren, 1965). The fossil occurrences, although often isolated, are sufficiently consistent over large areas of the Torlesse terranes to enable some generalisations to be made and belts of rocks of the same age to be distinguished.

A number of faunal zones have been recognised by previous workers (Campbell and Warren, 1965; Landis and Bishop, 1972; Speden, 1974; Andrews *et al.*, 1976; MacKinnon, 1983). The zones range from the Carboniferous to the Early Cretaceous, although approximately one half of the international faunal stages during this time span are not represented by fossils. The gaps in the Permian-Jurassic Torlesse represent some 100 Ma of a total time span of 135 Ma: i.e. only 25 % of the time is represented (Fleming, 1970).

Most of the known fossils can be grouped into five major biostratigraphic units or zones (MacKinnon, 1983, Figure 2.1 this study): (1) a Permian *Atomodesma* zone, defined mainly by scattered and broken prisms of the Permian bivalve *Atomodesma;* (2) a Middle Triassic (Ladinian) zone, defined mainly by numerous species of bivalves and brachiopods (notably the bivalve *Daonella*) and also some distinctive plant material; (3) a lower Late Triassic (? Carnian) *Torlessia* zone, defined by the scattered occurrence of *Torlessia* and *Titahia*; (4) a Late Triassic (Norian) zone, defined by scattered and commonly broken shells of the world-wide Norian marker *Monotis*, a bivalve; and (5) a Late Jurassic – Early Cretaceous (Tithonian – Albian) zone defined by numerous fossils, mainly bivalves and some plant materials (MacKinnon, 1983). The faunas are considered to represent high-latitude coldwater depositional environments.

Most fossil occurrences fall within the five major zones but there are a few notable exceptions. Carboniferous conodonts, the oldest known fossils in the Torlesse terranes (Jenkins and Jenkins, 1971), are present in marble associated with volcanics in several locations in the small Kakahu terrane within the bounds of the *Atomodesma* zone (Figures 1.2 and 1.6) (Hitching, 1979). Other notable fossils which are known from one or just a few localities include the Late Permian fusulinids (Parafusulina cf. japonica, Hada and Landis, 1995) that have been found within the Akatarawa terrane (Figures 1.2 and 1.6) and in the Glenfalloch Stream, a north flowing tributary of the Rakaia River which drains the Palmer Range (Leven and Campbell, 1998). The fusulinids are taken as evidence for accumulation in an open oceanic environment at a low latitude setting (Hada and Landis, 1995). Van Dusschoten (2000) reported the first Anisian fauna from the Balmacaan Stream area.

1.5 CONDITIONS OF DEPOSITION

The stratigraphic relationships and geographic distributions of the faunal zones are of key importance in understanding the Torlesse terrane. Each major zone is clearly defined by numerous fossil localities with very few fossils falling outside their zones. These zones young generally towards the present ocean, whereas stratigraphic tops in major units face in the opposite direction, inboard and towards the more volcanogenic terranes against which the Torlesse terranes now occur (Landis and Bishop, 1972; Howell, 1980).

Although excellently preserved stratigraphic sections up to a few hundred metres thick are widespread (e.g., Hicks, 1981), there is a general lack of marker beds and a common occurrence of zones of pervasive tectonic disruption. In addition, Rangitata orogeny isoclinal and tight folding is pervasive throughout the Torlesse terrane and stratigraphic control is poor (e.g., Bradshaw, 1972; Andrews *et al.*, 1974; Force and Force, 1978; Bradshaw *et al.*, 1981). Sedimentological investigations are therefore mainly confined to describing the nature of well-exposed and undeformed sequences, and to interpreting the processes by which they were deposited. The interpretation of the environment of deposition is thus based primarily on disrupted facies associations.

The distribution of ecotypes has also been used to cast some light on the conditions of deposition of the Torlesse terranes, and the environmental significance of the Torlesse fossils has been summarised as follows (MacKinnon, 1983). (1) Some of the fossils (e.g., *Halobia, Monotis, Buchia*) clearly relate to the local shallowing of parts of the Rakaia terrane e.g., at Balmacaan Stream in the early Middle Triassic, in the Waitaki Valley in the Middle Triassic or the Otaki Valley in the Upper Triassic. A similar local shallowing in northern Canterbury (Hurunui, Cheviot) in the Late Jurassic – Early Cretaceous is probably reflected in the number and variety of fossils recorded for this area. A shallowing in the Hanmer area is supported by the appearance of rootlets and points to a subaerial/marginal marine depositional environment. (2) All other fossil occurrences are of uncertain environmental significance and offer no unequivocal criteria for depth. Thus pterioid bivalve occurrences (e.g., *Daonella*) are open to interpretation as benthic, nectoplanktonic and pseudoplanktonic. The tube worms *Torlessia* and *Titahia*, the most distinctive and abundant fossils, were soft-

bottom dwellers which may have inhabited either shallow or deep water (Andrews *et al.*, 1976; Stevens, 1978).

Paleoslope indications are contradictory (Beggs, 1980; Hicks, 1981) and there has been considerable debate in New Zealand concerning the depositional environments. A shallow depositional environment was proposed for the bulk of the Torlesse by Bradshaw (1972; 1973). Andrews (1976) noted that marginal and non-marine depositional environments, coarse detrital conglomerates, and vascular plant material are common in the eastern part and that they become less abundant towards the west, with conglomerates almost absent in the extreme west. MacKinnon (1983) and Hicks (1981) favoured the deposition of the clastic rocks by gravity-flow mechanisms in a deep-marine environment and noted that the few shallow marine and terrestrial deposits are of limited areal extent and are in fault contact with or overlie the Torlesse flysch unconformably.

Most Torlesse strata consist of alternating sandstone and mudstone. Many sandstone beds are graded, display solemarking, and contain all or parts of the Bouma sequence (Andrews *et al.*, 1976). This evidence indicates deposition by sediment gravity flow in a deep marine environment.

Although no single model for depositional environments of the Torlesse terranes has been agreed upon, the above features have led to the general acceptance of a submarine fan depositional model and accretionary wedge deformational model for at least the Rakaia terrane (Howell, 1980; MacKinnon, 1983; Roser and Korsch, 1999; Kamp, 2001).

1.6 TORLESSE SOURCE

Recent studies in detrital petrology (MacKinnon, 1983; Mortimer, 1995; Smale, 1997; Grapes *et al.*, 2001) and geochemistry (Roser and Korsch, 1986; Roser and Korsch, 1988; Mortimer, 1995; Roser and Korsch, 1999; Grapes *et al.*, 2001) have been important in establishing the broad type of source. Studies of igneous clasts, using petrology and geochemistry, have demonstrated that there is a wide range of lithologies within the source area and that the clasts exhibit trace element characteristics indicative of subduction-related magmatism (Barnes and Korsch, 1991; Dean, 1993; Mortimer, 1995). A Rb-Sr isotope study (Adams and Graham, 1996) confirms that initial $^{87}Sr/^{86}Sr$

ratios for the Rakaia terrane are consistent with the postulated continental arc/cratonic source. Detrital zircon age distribution (Ireland, 1992; Pickard *et al.*, 2000) in the Rakaia terrane rocks shows a distinct peak between c. 260-240 Ma suggestive of an active magmatic arc source of Permian age.

All these studies confirm a continental arc/cratonic provenance. Various source areas have been proposed for the Torlesse terranes, ranging from east of present day New Zealand (Andrews *et al.*, 1976), Marie Byrd Land (Bradshaw *et al.*, 1981; Korsch and Wellman, 1988) and the New England Fold Belt (Adams and Kelley, 1998; Pickard *et al.*, 2000). Recycling of the older Rakaia terrane has been suggested by MacKinnon (1983) Roser and Korsch (1999) and Smale (1997), and a possible Median Tectonic Zone source for the Pahau terrane was suggested by Mortimer (1995).

1.7 SEDIMENT PROVENANCE

Sedimentary provenance studies aim to determine the source areas of the clastic material in a sedimentary basin. The term provenance, when applied to sedimentary deposits, refers primarily to the source rocks from which the sediments have been derived. The terms 'ultimate' and 'proximate' source are commonly used to differentiate between older crystalline material and younger sedimentary deposits in sediment provenance studies (see Pettijohn *et al.*, 1987). The ultimate source of a quartz grain, for example, is defined as the igneous rock in which it originally crystallised. Its proximate source is the rock or environment from which the grain was most recently eroded. Pell *et al.* (1997) used the term protosource for the parent igneous rock and extended the definition further to include metamorphosed derivatives of those igneous parents but excluded metasedimentary deposits which may have been recycled from many different areas. This study uses the term protosource as proposed by Pell *et al.* (1997) and proximate source (for recycled sediments) used by Pettijohn *et al.* (1987).

Provenance data can play a critical role in assessing paleogeographic reconstructions, in constraining lateral displacement in orogens and in characterising crust that is no longer exposed. Although provenance analyses of sandstone detrital grains are a key to the definition of source terranes, petrographic analysis gives no indication of the age of those terranes. Different types of isotopic studies can be conducted on sedimentary and igneous rocks. Each of these methods provides different

types of information that can be used to distinguish potential source areas, provided the potential sources are geochemically, isotopically and geochronologically distinguishable on the basis of age formation and petrogenesis.

Over the last two decades the field of provenance analysis has undergone a revolution with the development of single-crystal isotope dating techniques. Many attempts were made to determine the provenance of sedimentary rocks using silt to sand sized single minerals (Ireland, 1992; Pell *et al.*, 1997; Adams *et al.*, 1998; Ireland *et al.*, 1998; Cawood *et al.*, 1999; Sircombe, 1999; Pickard *et al.*, 2000). However, small grain sized minerals are easily transported by fluvial and marine systems for thousands of kilometres (Moore *et al.*, 1982; Lewis, 1999; Bassett, 2000). Similar transportation has been reported by Sircombe (1999) from eastern Australian sediments and from the Australian Continental Dune Fields (Pell *et al.*, 1997). Pell *et al.* noted that there is only a limited amount of long-distance aeolian transport within the Australian Continental Dune Fields, with most sand material apparently reworked from older fluvial and marine deposits. These results reinforce the need for caution when interpreting provenance evidence from fine grained single heavy minerals.

Gravels are transported over 10s to 100s of kilometres rather than the 1000s of kilometres possible for finer grained sediments (Kodama, 1994a; Kodama, 1994b; Ferguson *et al.*, 1996). In addition, the pebble to boulder sized clasts provide a hand specimen of their source. Fingerprints such as petrography, geochemistry, isotopes and crystallisation age can be obtained.

Because a dated igneous clast has the age of the igneous source that it originally formed in, the date is in effect a direct measurement of the protosource it formed in and gives a time frame of the igneous activity in the clasts' source area. A major assumption is that the dated igneous clasts are representative of the protosource. A second assumption is that the igneous clasts represent the same source that provided the sedimentary detritus for the basin.

1.8 Purpose of Study and Outline of Thesis

Igneous clasts from 4 Rakaia and 3 Pahau terrane conglomerates within the South Island of New Zealand were collected in order to determine their provenance (Figure 1.7 and Location Map in back pocket). Clasts were analysed petrographically

and geochemically to identify petrological characteristics and types of magmas. Selected clasts of identified suites were dated and analysed for Sr and Nd to investigate the crustal contribution during petrogenesis and put further constraints on potential clast sources. Additionally, sandstone clasts from two Rakaia and two Pahau localities were collected to investigate the recycling of the older Rakaia rocks into the Pahau terrane.

The conglomerate locations were chosen to represent the full stratigraphic range of both terranes, and the geographical distribution of the conglomerates mimics an approximate inboard to outboard transect of the two terranes with respect to the Panthalassan margin of Gondwana.

The lower 'cut-off' size for collection of samples was an estimated intermediate axis of approximately 10 cm, considered to be the size necessary to produce a thin section (petrography) and powder for beads and pellets (X-ray fluorescence, XRF) for each clast. In addition, enough sample material had to be available for heavy mineral separation (zircons for U-Pb dating) and Sr/Nd isotope work (thermal ionisation mass-spectrometry, TIMS) if needed. A selective sampling method was chosen for this reason. In addition, approximately ten smaller igneous clasts were collected from all conglomerates except Te Moana and Boundary Creek, to investigate geochemically if smaller and bigger clasts are 'cogenetic' or represent different igneous suites.

Statistical counts were made to document the population of lithotypes in all the conglomerates, except Boundary Creek. The composition of a conglomerate was usually determined from river-worn or clean outcrop surfaces by counting all the clasts in a given surface area in which they could be clearly seen. All the clasts in the marked area were counted and grouped according to their size (intermediate axes estimated) and lithotype. No distinction was made between litharenites and felsarenites (Appendix 3).

Nearest fossil localities for each conglomerate are taken from publications or from the New Zealand Fossil Record (NZFR). The record file number is given in brackets and shown on the Location Map.

Sample numbers referred to in descriptions and figure captions throughout this thesis are listed with their relevant information (location, rock type etc.) in the tables of Appendix 1. Analytical methods and procedures used in this study are described in Appendix 2. Statistical counting and lithotype proportions of individual conglomerate

locations are presented in Appendix 3. U-Pb zircon age SHRIMP analyses of igneous clasts and detrital zircons of Rakaia and Pahau sandstones are given in Appendix 4. Petrological data obtained for this study consist of petrographic analyses of thin sections (including point counting of sandstone clasts), whole rock chemical analyses by XRF and rare earth elements by INAA. The data are presented in Appendix 5 to 7. Radiogenic isotope analyses (Sr, Nd) for selected igneous clasts are presented in Tables 5.2 and 5.3 (Pahau terrane) and Tables 6.2 and 6.3 (Rakaia terrane) and for sandstone clasts and sandstones in Table 7.2 and 7.3. The AGSO Phanerozoic Time Scale (Jones, 1995) is used in this study.

CHAPTER 2
DESCRIPTION OF THE CONGLOMERATES

CHAPTER 2

DESCRIPTION OF THE CONGLOMERATES

Introduction

In the following sections Pahau and Rakaia terrane conglomerates are described. Stratigraphic age based on the available fossil record, structure, texture and composition of each conglomerate are presented together with an interpretation of the environment of deposition for each conglomerate. Statistical counts of the clast population have been employed in order to evaluate the detrital contribution from various source (i.e., volcanic, plutonic, sedimentary) to the depositional basin of each conglomerate. In addition, the fossil record of the conglomerate locations are compared to the new U-Pb zircon ages from igneous clasts and detrital zircons (presented in Chapter 3) and a stratigraphic age has been assigned to each conglomerate (Table 2.1).

Sandstones from two Rakaia and one Pahau localities are briefly described, which have been collected for detrital zircon U-Pb zircon age analyses in order to get a better stratigraphic control on these two South Island terranes.

2.1 PAHAU TERRANE CONGLOMERATE LOCATIONS

2.1.1 Mount Saul Conglomerate

2.1.1.1 Locality

Extensive conglomerate outcrops occur on the southern side of the Hanmer Basin, North Canterbury (Location Map; NZMS 260, N33/127 149). The area is dominated by SW-NE oriented strike ridges which were identified as the western limb of a simple, upright, southwest plunging syncline with strata dipping 45-80° SSE (Bradshaw and Andrews, 1980) (Figure 2.1). Mount Saul (1020 m), which topographically dominates the area, is the centre of an approximately 600 m thick lens shaped body that comprises faulted slivers of predominantly clast supported conglomerate (Figure 2.2). The conglomerate is underlain by carbonaceous sandstone

and overlain by flysch sequences with abundant plant matter and occasional flute marks (Bradshaw and Andrews, 1980). The conglomerate is moderately indurated and whole clasts can be extracted easily from the matrix.

2.1.1.2 Previous Work

The Pahau River area was the subject of intermittent study since the 1970s, and general reference to the occurrence of conglomerates in this area was made by early reconnaissance geologists von Haast (1871) and Fyfe (1931). Freund (1971) attributed the morphology of the high country area to a lithological change in the Torlesse rocks. He noted conglomerate beds along the south side of the Hope Fault that extend towards the Pahau River to the south/southeast. The Pahau River area was briefly reviewed in a 1980 Geological Society conference field trip guide book and was proposed as the type area for the Pahau terrane (Bradshaw and Andrews, 1980). The Mount Saul conglomerate was remapped by Pescini (1997) and Orlowski (2001).

The petrographic and geochemical study by Dean (1993) showed that the source for the Mount Saul conglomerate igneous clasts was dominated by calc-alkaline and alkaline volcanism. The clasts preserve a record of at least three different magmatic phases that have a distinct chemical and mineralogical character that reflects different source rock features.

2.1.1.3 Description

The conglomerates are massive to thinly bedded, with thin beds of generally not less than 5 cm in thickness and massive beds poorly organised and chaotic in nature (Figures 2.3a and 2.3b). In a few beds clasts are imbricated and large scale cross-stratifications are present. Pescini (1997) describes large-scale cross-stratification structures with individual cross-beds that are either matrix or clast supported of up to 50 cm in thickness. The predominant clast size is between 2 and 10 cm, but individual igneous and sandstone clasts of boulder size are common. Concretions and sandstone rip-up clasts and flakes are common. In general the conglomerates are poorly sorted with only few beds displaying a moderate degree of sorting. The matrix of the conglomerate is a dark grey to grey and fine to medium grained sandstone. The clasts of the conglomerate are predominantly sub-rounded to well rounded. The larger rip-up

clasts are angular to sub-angular and the concretions display well rounded shapes (Figure 2.4).

Composition of the Mount Saul conglomerate is dominated by sandstones and an averaged statistical count for two areas shows that the clasts fit into four lithological groups: (1) arenites 42 %; (2) volcanics 23 %; (3) granitoids 13 %; and (4) lutites 8 %, and (5) others including quartz and chert 14 % (Appendix 3).

2.1.1.4 Age and Depositional Setting

The nearest fossil location outside the conglomerate area is approximately 7 km to the southeast of Mount Saul in the west bank of the Waiau River (NZFR S54/507) where pollen of uncertain age are reported. Prismatic shell fragments, *Buchia malayomaorica* and *Belemnopsis aucklandica* of Tithonian or slightly younger age were found 13 km to the west along Gorge Stream (New Zealand fossil record S54/513). Spores, pollen and rare dinoflagellates in the Pahau area indicate an upper Early Cretaceous (Valanginian – late Aptian) depositional age (Bradshaw and Andrews, 1980).

The area around Mount Saul is dominated by two facies, an alternating flysch facies interpreted to be of submarine origin and a massive sandstone-conglomerate association believed to be of alluvial-deltaic/marginal origin (Bradshaw and Andrews, 1980). Pescini (1997) interpreted the Mount Saul conglomerate as channelised mass flow deposits of entirely submarine origin. A detailed sedimentological study of the area gives support to a deltaic/marginal marine depositional environment for the conglomerate based on rootlets found in the conglomerate and fossils found in a shell bed just to the west of the conglomerate (Orlowski, 2001). Paleocurrent measurement obtained from cross bedding and imbrication indicate a northeast-southwest trending shoreline and suggest derivation from the northwest (Bradshaw and Andrews, 1980).

2.1.1.5 Results from this Study

The youngest U-Pb SHRIMP-dated clast gives an age of 141.4±2.9 Ma (UC30823; Table 3.1). This age is older than the Aptian stratigraphic minimum age (based on fossils) and for this study the **Aptian** age is considered to be the minimum age of the conglomerate (Fossil Zone 5; Figure 1.6).

2.1.2 Ethelton Conglomerate

2.1.2.1 Locality

The conglomerate is exposed in the banks of the Hurunui River, at the Kaiwara suspension bridge (Location Map; NZMS 260, N33/127149), about 3.5 km west of Ethelton, North Canterbury (Figure 2.5). The total thickness of about 150 m is exposed in an almost continuous section of about 350 m to the northeast and southwest on both sides of the river. The conglomerate fills scour channels in, and is interbedded with, massive and graded sandstones and mudstones that strike northeast and are steeply dipping towards the northwest. Beds above and below the conglomerate have the same attitude and the erosional breaks have probably no great time significance (Maxwell, 1964; Smale, 1978). Many clasts were sheared after deposition, though they still maintain their integrity. The conglomerate is indurated and individual whole clasts can be removed easily from the matrix for collection.

2.1.2.2 Previous Work

The conglomerate was described and included in the Kaiwara Bridge Formation by Hamilton (1950). In a general account of the Kaiwara area the conglomerate was described by Maxwell (1964) and named the Ethelton conglomerate. A detailed petrological and sedimentological account of the Ethelton conglomerate and its components was given by Smale (1978).

Dean's (1993) study of igneous conglomerate clasts showed that the clasts are predominantly metaluminous I-type and evolved I-type granitoids that relate mineralogically and geochemically to the rhyolitic and dacitic volcanic clasts present in the conglomerate.

2.1.2.3 Description

Two distinct types of conglomerates are present in the outcrop. One is characterised by a relatively low proportion of matrix of medium to coarse grained sandstone (15-35 % estimated), and contains thin beds of moderately sorted conglomerate interbedded with poorly sorted conglomerate (Figure 2.6). The other has a higher proportion of matrix (>50% estimated) and is virtually unbedded. Pebbles and

boulders in the conglomerate are usually rounded to well rounded, but large angular blocks of sandstones occur (Figure 2.7).

Statistical counts show that the clasts fit into four lithological groups: (1) arenites 60 %; (2) volcanics 11 %, (3) lutites 11 %, (4) granitoids 7 %, and (5) others including quartz and chert 12 % (Appendix 3). The lithotype distribution compares well with data published by Smale (1978, his Table 1), who did a systematic collection and counting of 300 pebbles.

2.1.2.4 Age and Depositional Setting

The conglomerate contains a mixed Late Jurassic - Early Cretaceous dinoflagellate assemblage (NZFR S62/644 – 648, Campbell and Warren, 1965). Some of the taxa are typically Cretaceous (*Odontochitina operculata* and *Spiniferites ramosus*) and it seems likely that the late Jurassic forms (e.g., *Belodinium dysculum*) are reworked (Smale, 1978). Other fossils of uncertain age include ammonites, brachiopods, belemnites (NZFR S62/512), and detrital plant fragments were reported by Maxwell (1964).

Smale (1978) concluded that the size distribution and pebble shape suggest that sorting and shaping took place in a fluvial environment and a source area to the southwest was proposed based on flute casts in the underlying sediments. The abundance of detrital plant fragments on bedding planes in sandstones underlying and overlying the conglomerate supports near-shore or terrestrial deposition, but the dinoflagellates suggest a solely marine environment (Smale, 1978).

2.1.2.5 Results from this Study

The youngest dated igneous clast from Ethelton is 125.1±2.1 Ma (UC30964) and a single zircon from the matrix of the conglomerate gives an age of 112±1.5 Ma (Figure 3.10; Appendix 4). These two ages are younger than the vaguely defined stratigraphic age based on fossils. For this study an **Aptian** age (Fossil Zone 5) is assigned as the youngest stratigraphic age for the Ethelton conglomerate based on the detrital zircon age.

2.1.3 Kekerengu Conglomerate

2.1.3.1 Locality

Several conglomerate beds up to 40 m thick are exposed in the banks and cliffs of the Kekerengu River near the Remuera homestead (Location Map; NZMS 260 P30/899 163). Prebble (1976) mapped the area and recognised three members within the Good Creek Formation: graded beds, massive sandstones and conglomerate. The steeply northwest dipping conglomerates are interbedded with massive sandstones, and some beds are laterally continuous and can be traced over several kilometres along their northeastern strike. A massive conglomerate, with up to boulder size clasts, is exposed approximately 400 m upstream from the Remuera homestead and most of the clasts for this study were collected from this location (Figure 2.8).

2.1.3.2 Previous Work

In the Marlborough region the Pahau terrane rocks are everywhere separated from younger strata by an intra-upper-Albian unconformity (Crampton and Laird, 1997). The Formation was included as part of the Pahau terrane by some workers and excluded by others. Ritchie (1986) included the formation in the Sawtooth Group, which is part of the Torlesse basement, but Prebble (1976) considered these rocks to be distinct from the Torlesse rocks and noted the possibility that they may relate to post-Torlesse units in the Clarence Valley. No major unconformity was mapped in the Kekerengu Valley between the Good Creek Formation and the basement rocks (Prebble, 1976). Structural deformation and fossil content in the Good Creek Formation are similar to Pahau rocks mapped elsewhere in the region, but differ significantly from strata post-dating the intra-Upper-Albian unconformity (M. Laird, pers. comm.). In this study the Good Creek Formation is considered to be part of the Pahau terrane.

2.1.3.3 Description

The sampled conglomerate is poorly to moderately sorted, matrix to clast supported and without obvious imbrication. The conglomerate fines upwards (upstream), some graded beds are recognisable and interbedded massive sandstone lenses occur. Fractured and unfractured clasts are rounded to well rounded and are embedded in a matrix of indurated dark grey mudstone (Figure 2.9). Sub-angular to angular sandstone clasts are present. Most of the clasts are pebble size but cobbles and

boulders up to 50 cm in diameter occur. An average clast size of 30 to 40 mm is estimated. Sandstones dominate the composition of the conglomerate and the clasts can be grouped into: (1) sandstones 59 %; (2) mudstones 18 %; (3) volcanics 10 %; (4) granitoids 6 %, and (5) others including quartz 5 %, and chert 2 % (Appendix 3).

2.1.3.4 Age and Depositional Setting

The Good Creek Formation is characterised by a paucity of fossils and only members of the genus *Inoceramus* were found and even these are rare (see Prebble, 1976, for a comprehensive list). Crampton (2000; pers. comm.) provided the following localities from the Kekerengu River area that have yielded macrofossils and are listed in the New Zealand Fossil Record: P30/f6124, f7408, f7409, f7999, f9001, f9043 and f9677. Most of these have Inoceramid bivalves related to *Inoceramus* sp.ex gr. *kapuus - ipuamus*. This is a poorly understood group, but indicates an Albian deposition age for the Pahau rocks in the Kekerengu area.

Prebble (1976) concluded that the lithological associations in the Kekerengu Valley are best explained with a shallow marine model suggested by the thick, abundant conglomerate and sandstone members and by cross bedding and the presence of carbonaceous material.

2.1.3.5 Results from this Study

An **Albian** depositional age (based on the published fossil record, Fossil Zone 5) is assigned as the youngest age for the Kekerengu conglomerate, which is younger than the youngest dated igneous clast (123.1±2.5 Ma; UC30743).

2.2 RAKAIA TERRANE CONGLOMERATE LOCATIONS

2.2.1 Boundary Creek Conglomerate

2.2.1.1 Locality

A conglomerate band of variable thickness, but averaging an estimated 6 m, is exposed at the lower western end of a cirque which forms part of the head waters of Boundary Creek (Location Map; NZMS 260 G39/131 469; 1500 m). The conglomerate is mapped on the new provisional Geological QMAP (N°18 213/647, Wakatipu Turnbull, 2000) within the TZ IIb (Bishop, 1972) semi-schist zone which is marked by

a weak, steeply to the east dipping foliation at the conglomerate location. The conglomerate is situated within the Haast Schist where the Rakaia terrane rocks are increasingly schistose toward the southwest, from TZ I sandstone east of the Ahuriri River to TZ IV schists on the Dunstan Range and in the Manuherikia Valley. Non-schistose and schistose Rakaia rocks are dominated by quartzofeldspathic sandstone, but large areas of mudstone are also mapped (Turnbull, 2000).

Access to the conglomerate is either by hiking and climbing along Boundary Creek from the shore of Lake Wanaka or by helicopter. Due to the remoteness of the location, the additional weight of the core drill equipment and the collected samples the helicopter option was used. Single and, when possible, multiple core samples (Figure 2.10; up to 13 cm long, ø 2.5 cm) of unfractured clasts were taken with the core drill. If a soft matrix surrounds the meta-conglomerate clasts these clasts were easily separated from the outcrop. Time schedule prevented a statistical count of the conglomerate.

2.2.1.2 Description

The conglomerate exposed in the creek bed and in the true right-hand cliff of Boundary Creek is mainly matrix supported and poorly sorted. No primary structures are recognisable within the conglomerate and the enclosing massive sandstones. Bedding is difficult to establish but sporadic exposures of the conglomerate at near right angles to the creek indicate a general north-northwest strike. Most clasts are strongly deformed (Figure 2.11) and clast elongation tends to be at moderate to low angle to a penetrative, anastomosing foliation that is defined by micas. Initial grain size is difficult to determine but average clast size is estimated at 40 to 50 mm, although larger clasts of up to 30 cm are present (Figures 2.12 and 2.13).

Clast lithologies include mainly a variety of sandstones and siltstones with lesser quantities of volcanic and granitoid clasts. Although no statistical counts were made visual estimates indicate that volcanic clasts are the predominant igneous lithotype. Siltstone and volcanic (intermediate and mafic) clasts tend to be more elongated than the other clasts. The matrix of the conglomerate is similar in colour and texture to the sandstone and siltstone clasts.

2.2.1.3 Age and Depositional Setting

A rare marble bed, cropping out about 200 m above the creek bed, was sampled but no fossils were obtained from it.

The nearest fossil location is west of Lake Ohau (Figure 1.6), approximately 45 km to the northeast of the Boundary Creek conglomerate, from which *Terebellina mackay* were reported (NZFR S99/501, Campbell and Warren, 1965). The presence of Torlessia indicates a probable lower Late Triassic age for the Lake Ohau Torlesse (Andrews *et al.*, 1976). Turnbull (2000) maps the Rakaia schist rocks as Permian to Triassic depositional age.

Hicks (1981) interpreted the association of bedded fine conglomerate, sandstone, siltstone and mudstone facies in the Ohau region as sub-aqueous mass flows deposited around the mid-fan region of a submarine fan-system. Paleo-current and paleoslope indicators suggest turbidity current transport down a northwest facing paleoslope.

2.2.1.4 Results from this Study

The youngest dated igneous clast returned a Namurian age of 325.2±4 Ma. Individual zircons from the four pooled igneous clast zircon populations give predominantly Carboniferous ages ranging from 318±11 Ma (σ1;UC31747) to 364±5 Ma (UC31775). These ages are distinctly older than the mapped Permian to Triassic (?) stratigraphic age for the Boundary Creek area (see Figure 3.12).

Interestingly, Figure 3.12 shows that in each conglomerate, apart from Boundary Creek, igneous clast zircon ages are very similar to the depositional age of the conglomerate (constraint by fossils). This strongly suggests that igneous source activity and deposition of the sediments was penecontemporaneous. Given this apparent trend, the question therefore arises whether there are older Carboniferous sediments located within the Haast Schist. However, until further research is undertaken in the Boundary Creek area (e.g., detrital zircon analysis) a tentative **Permian** depositional age is assigned to the conglomerate (Fossil Zone 1).

2.2.2 Te Moana Conglomerate

2.2.2.1 Locality

The Te Moana conglomerate is located near the headwaters of Frasers Stream, a tributary of the Hae Hae Te Moana River at the southern end of the Four Peak Range west of Geraldine (Location Map; NZMS 260 J37/488 880). The Four Peak Range and its surrounds consist mainly of alternating Torlesse sandstone and mudstone. The main outcrop is near a saddle, known locally as "Doughboy Saddle", at the head of the western branch of Frasers Stream (Figure 2.14). Stratigraphic thickness in this area is approximately 250 m and is the type area for the conglomerate (Smale, 1983). Other outcrops are exposed in the banks of the eastern branch of Frasers Stream (Figure 2.15). The conglomerate is well indurated and fractured, particularly near fault zones, although it is still possible to extract individual clasts. The matrix, a grey to dark grey and medium to coarse sandstone, is well indurated, and igneous and sandstone clasts had to be chiselled from the matrix for collection.

2.2.2.2 Previous Work

Wellman (1953) first described boulders in the middle reaches of the Hae Hae Te Moana River, presumably derived from the Frasers Stream or a similar conglomerate such as that nearer Waihi River 6.5 km further east. Smale (1983) traced the conglomerate boulders to the source and used the conglomerate in a provenance study to investigate if the Carboniferous Kakahu terrane rocks (Figure 1.2), cropping out approximately 14 km to the south, could represent the source area for the conglomerate clasts.

2.2.2.3 Description

In the main outcrop there are several conglomerate units up to 30 m thick, with alternating units of massive sandstone or interbedded sandstone and mudstone. Most of the conglomerate units are clast-supported, but matrix-supported units occur particularly in the adjacent sandstone units. Some of the conglomerate beds have filled in small channels about 10 cm deep and 20 cm across in the underlying sandstone. The conglomerate is clast to matrix supported, poorly to moderately sorted, and consists of mainly rounded to well rounded pebbles, but cobble and boulder size clasts occur (Figure 2.16).

The composition of the conglomerate was determined on an outcrop in the western bank along the eastern branch of Frasiers Stream. The estimated mean grain size is 35 to 45 mm and four lithotypes dominate: (1) volcanic clasts 41 %; (2) arenites 29 %; (3) lutites 15 %; (4) granitoids 8 %, and (5) others including quartz and chert 7 % (Appendix 3).

2.2.2.4 Age and Depositional Setting

The area of the Four Peak Range was assigned to the Permian by Andrews *et al.* (1976). The nearest Permian fossils (*Atomodesma*) are approximately 7 km to the east on a ridge above the northern branch of the Hae Hae Te Moana River (J37/559 890 Campbell and Warren, 1965). Fragments in limestone clasts in the Te Moana conglomerate contain Late Permian bryozoans and *Atomodesma,* and the depositional age cannot be older than Late Permian (Smale, 1983, and references therein).

The rocks at Kakahu consist dominantly of metasiltstone and metagreywacke with small amounts of conglomerate. Smale (1983) concluded that the Kakahu terrane cannot be the source for most of the clasts in the Te Moana conglomerate and that it is more likely that both the Kakahu and the Te Moana extrabasinal clasts come from the same as yet unknown source. Smale (1983) also noted a total absence of shallow-water features, the scarcity of grading or bedding in the conglomerate and the abundance of 'disorganised' conglomerates, and proposed a deposition by gravity flow in the upper part of a submarine fan. No conclusive paleocurrent indicators were found within the Four Peak Range area.

2.2.2.5 Results from this Study

A rhyolite clast returned an Artinskian age of 276.8±4.6 Ma (UC31813) that is older than the published fossil record. The **Kazanian** fossil age is used in this study as the youngest stratigraphic age for the Te Moana conglomerate (Fossil Zone 1).

2.2.3 McKenzie Pass Conglomerate

2.2.3.1 Locality

The conglomerate is well exposed along the ridge of the Dalgety Range (1320 m), approximately 2 km south-southeast of McKenzie Pass (Location Map; NZMS 260 I38/197 639). The McKenzie Pass conglomerate is immediately underlain and overlain

by massive, northwest striking and steeply to the southwest dipping sandstone units. Exposure of the conglomerate units along strike on both slopes of the range is poor and sporadic and is inadequate for determination of field relationships. The exposed conglomerate along the ridge of the range is an estimated 25 m thick (Figures 2.17a and 2.17b). The conglomerate is well indurated and individual clasts had to be chiselled and drilled from the matrix for collection.

2.2.3.2 Previous Work

The only published detailed bedrock mapping within 50 km is that along the northeastern shore of Lake Benmore (Haldon and Black Forest stations) by Force (1978), who mapped a Triassic outlier in an area previously mapped as Permian (Geological map S20, Mount Cook Sheet). The only previous work on the McKenzie Pass conglomerate was by Smale (1980b), who reported phosphorite intraclasts from various conglomerates and sandstone units in South Canterbury (see also Beggs, 1981).

2.2.3.3 Description

The conglomerate exposed on the ridge of the Dalgety Range is clast to matrix supported and generally poorly sorted. Clasts are rounded to well rounded and vary from pebbles to cobbles in size with an estimated average grain size of 40-50 mm, but a few clasts are up to 25 cm in size (Figure 2.18). Most of the conglomerate is structure-less, but rare sand lenses are present and in some areas pebbles display some stratification and grading. Irregular and deformed rip-up mudstone and sandstone rafts occur sparsely. The composition of the conglomerate is dominated by clasts of arenite 40 %; volcanic clasts 20 % are more abundant than granitoid clasts 14 % and lutite clasts 15 % (see Appendix 3).

2.2.3.4 Age and Depositional Setting

The nearest reported fossils are *Atomodesma* fragments from the gorge of the Dalgety Stream (I38/247 674) approximately 6.5 km to the northeast of the McKenzie Pass conglomerate (Campbell and Warren, 1965). Force (1978) reported a Middle Triassic faunal assemblage at Haldon (I39/947 443; I39/f1 & f3; 27 km from the conglomerate) containing the Middle Triassic *Daonella*. Rocks in the Haldon and Black Forest area are in part a stratigraphically upward-fining marine sequence and all the

primary sedimentary features are consistent with published descriptions of upper to middle fan deposits (Force and Force, 1978).

Ireland (1992) reported a U-Pb SHRIMP age of 211±5 Ma for a zircon rim spot analysis for a sample from the nearby Lake Aviemore in South Canterbury probably within the *Atomodesma* faunal zone.

2.2.3.5 Results from this Study

The youngest dated clast from McKenzie Pass returned an age of 253.4±4.2 Ma (UC30909). This **Dorashamian** age is in agreement with the proposed Permian depositional age (Atomodesma) for this area and is taken as the youngest stratigraphic age for this conglomerate (Fossil Zone 1; Figure 1.6).

2.2.4 Lake Hill Conglomerate

2.2.4.1 Locality

Lake Hill (709 m) is located along the shore at the eastern end of Lake Coleridge (Location Map, NZMS 260 K35/955 605) and is one of several basement islands surrounded by Upper Cretaceous coal measures and Pleistocene lake sediments and till, and recent gravel (Lauder, 1962). Outcrops are exposed on the northeastern face of Lake Hill and extend discontinuously to the northwest and southeast (Figure 2.19a and 2.19b). The conglomerate is interbedded with massive to well bedded coarse to fine sandstones that dip gently towards the northeast (Figure 2.20). Lake Hill is located close to the southwestern termination of a Porters Pass Fault strand (Elvy, 1999) and many clasts are fractured and sheared. The matrix is well indurated and clasts had to be separated from the matrix by chisel and core drill.

2.2.4.2 Previous Work

The components of the Lake Hill conglomerate were recorded by Lauder (1962), who estimated that the conglomerate contains about 15 % cobbles of gneissic granitoid clasts. The petrographic and geochemical pilot study by Dean (1993) of igneous conglomerate clasts showed that the clast population is dominated by clasts of granodioritic and monzogranitic compositions.

2.2.4.3 Description

The outcropping conglomerates are mainly well bedded to massive (20 cm up to 5 metre) and the contacts between the enclosing sandstone units and the conglomerates appear to be conformable. Intervening laminated siltstones are present and cross bedding is present in sandstone units (Figure 2.21). A quartzose sandstone matrix dominates the conglomerate but silt matrix occurs, especially in matrix supported conglomerate beds. The conglomerates are poorly to moderately sorted, clasts are rounded to well rounded and the conglomerates are clast supported, but can grade into matrix supported units (Figure 2.22). Clast sizes range from pebble to boulder size, with a variable average grain size ranging from 20 mm to 60 mm (Figure 2.23). The composition of the conglomerate is dominated by arenites and can be grouped into four distinct lithotypes: (1) arenites 49 %; (2) granitoids 23 %; (3) lutites 14 %; (4) volcanics 5 %, and (5) others including quartz and chert 9 % (Appendix 3).

2.2.4.4 Age and Depositional Setting

A boulder with *Terebellina mackayi* (NSFR S74/557) reported from the Acheron River represents the nearest fossil occurrence to the Lake Hill conglomerate (c. 4 km). Several specimens of *Terebellina mackayi* and one specimen of *Halobia sp.* were reported from the eastern slopes of Mount Hutt and the Rakaia River near the gorge (15-20 km) (Campbell and Warren, 1965). Campbell and Pringle (1982) reported a marine invertebrate assemblage of late Middle to early Late Triassic age from the Pudding Hill Stream that is associated with tubes of *Torlessia* (15-20 km). A Carnian age (Fossil Zone III, Figure 1.6) of deposition was assigned to the area near the Lake Hill conglomerate (Andrews *et al.*, 1976).

Kamp (2001) reported Early Jurassic (c. 189 Ma) zircon fission track ages for sand beds in the Rakaia valley (c. 20 km to the south). Kamp interpreted the fission track ages as cooling ages of the source, which would constrain the maximum deposition age of the Torlesse rocks in mid-Canterbury. Kamp (2001) proposed deposition of the Rakaia sediments in a deep sea fan environment between 185 to 150 Ma.

2.2.4.5 Results from this Study

The youngest dated clast from Lake Hill returned age of 244.1±3.8 Ma (UC30667) that is older than the Carnian fossils reported from the nearest location. For this study the **Carnian** fossil age is used as the depositional age of the Lake Hill conglomerate (Fossil Zone 4; Figure 1.6).

2.3 SANDSTONE LOCALITIES

In order to get a better stratigraphic control on the Torlesse terranes and to demonstrate the recycling of the Rakaia terrane rocks into the Pahau terrane depositional basins, three sandstones samples were collected for a detailed U-Pb detrital zircon age study (see discussions in Sections 3.3.1 to 3.3.3).

2.3.1 Kurow Hill

2.3.1.1 Location and Depositional Age

The sample is a dark grey, bedded, medium to coarse grained sandstone with a weak foliation and was collected from the slope of Kurow Hill (NZMS260 I40/093 060) just to the north of Kurow (Location Map and Figure 1.6). The outcrop is mapped within Fossil Zone I (Permian) and Atomodesma fragments were reported from the same hill by Campbell (1965).

2.3.2 Balmacaan Stream

2.3.2.1 Location and Depositional Age

The sample is a dark grey to grey and fine to medium grained sandstone and was collected from an exposure in the river bank of the Balmacaan Stream (NZ MS260 J36/518 283). The Balmacaan Stream is a tributary to the Ashburton River South Branch and drains part of the northern slopes of the Harper Range in south-Canterbury (Figure 1.6).

Van Dusschoten (2000) reported the first known Anisian fossils (NZFR J36/f99, *Trigonia balmae*, *Mellarium nodulosum, Parapopanoceras fraseri* and *Daonella jadii*) in the Rakaia terrane from the Balmacaan Stream area. He compared the Balmacaan fauna with the Anisian fauna of the Murihiku terrane and noted marked similarities at

species and genus level. The sample for this study was collected prior to the Van Dusschoten study and is not taken from the same stratigraphic horizon that contains the reported Anisian fossil assemblage.

2.3.3 Ethelton

The sample from the conglomerate matrix at Ethelton is from a massive, grey-brown, medium grained sandstone bed and was also analysed for U-Pb detrital zircon ages.

2.4 SUMMARY

- Sedimentary structures in Torlesse strata are indicative of an accretionary wedge depositional and deformational model, but stratigraphic control on the Torlesse terranes is poor and interpretation of the environment of deposition is primarily based on facies associations. The seven selected South Island conglomerates represent the stratigraphic range of both South Island terranes (Rakaia and Pahau) and provide an approximate inboard to outboard transect of the accretionary prisms (Table 2.1).

- Paleoslope indicator from the conglomerates at Mount Saul and Ethelton indicate the detrital material was supplied from a source located approximately west of the conglomarates.

- Paleoslope indications for the Rakaia terrane sandstones are few and contradictory and give no indication of the position of the source with respect to the depositional basins.

- Sedimentary clasts are predominant in all conglomerates (range 44-71 %) except Te Moana where volcanic clasts are the dominant lithotype. Volcanic clasts (range 5-41 %) dominate over granitoid clasts (range 5-22 %) in all conglomerates except at Lake Hill (Figure 2.24a). All the conglomerates are poorly sorted and their grain sizes are dominated by pebbles (Figure 2.24b).

- Depositional ages (fossil record) of the Pahau terrane conglomerates agree broadly with U-Pb ages from igneous clast and detrital zircons. The present fossil record indicates an Aptian stratigraphic age for the Mount Saul conglomerate, whereas an

Albian stratigraphic age is assigned to the Kekerengu conglomerate. An Aptian stratigraphic age is suggested by the youngest dated zircon from the Ethelton conglomerate matrix. The depositional age of each conglomerate location is shown in Figure 2.25.

- Published fossil records agree well with the dated igneous clasts of the Rakaia conglomerates at Te Moana, McKenzie Pass, and Lake Hill. A Kazanian depositional age is assigned to the Te Moana conglomerate, a Dorashamian depositional age to the McKenzie Pass conglomerate, and a Carnian depositional age to the Lake Hill conglomerate.

- A Permian depositional age is assigned to the Boundary Creek conglomerate. However, there are indications that there might be older Carboniferous sediments present within the Haast Schist.

CHAPTER 3

GEOCHRONOLOGY

CHAPTER 3

GEOCHRONOLOGY

Introduction

In this chapter, new ion microprobe (SHRIMP) U-Pb zircon ages for 33 igneous clasts from the Rakaia and Pahau conglomerate locations are presented. Also presented are new U-Pb zircon age data for two Rakaia terrane sandstone samples from Kurow and Balmacaan Stream and one sandstone sample from the Pahau terrane at Ethelton.

To determine and fingerprint the timing and trend of the igneous activity within the source area of the Torlesse terranes, as many igneous clasts as possible were analysed. For most of the samples a minimum of 6 analyses were made and this is considered to be an adequate number to determine unimodal or bimodal trends in a single clast data set. The disadvantage of such a small data set for an individual sample is the reproducibility, especially with respect to inherited zircons or zircons that have experienced lead loss.

Conclusions regarding inheritance patterns are further limited since the main purpose of this work was to determine the crystallisation ages of the igneous clasts and if possible pyramids of euhedral crystals, likely to give such ages, were specifically targeted.

Ion microprobe U-Pb zircon ages were determined at the Stanford University, California, and at the Australian National University, Canberra, using methods described by Muir (1998). A detailed discussion on SHRIMP methods is given in Appendix 2 and data are listed in Appendix 4.

3.1 PAHAU TERRANE IGNEOUS CLASTS

The new SHRIMP U-Pb ages for the 16 igneous clasts analysed from the Pahau terrane indicate that the igneous activity in the source area of the clasts was predominantly of upper Late Jurassic to Early Cretaceous age. One clast analysed from Kekerengu returned an Early Jurassic age. The samples dated are undeformed, metaluminous to weakly peraluminous I-type rocks of mainly volcanic origin, with most plutonic clasts displaying hypersolvus textures, but subsolvus clasts have also been analysed. Three rhyolite samples from Mount Saul were geochemically classified as peralkaline.

The new SHRIMP U-Pb data are summarised in Table 3.1 and Figure 3.11 and a short description of the individual igneous clasts is given below. Individual ages for each clast are shown on Tera & Wasserburg (1972) diagrams in Figures 3.1-3.4. These plots use the measured composition (e.g., not corrected for common Pb) and so an analysis must have no common Pb ($f206$) and have coincident $^{238}U/^{206}Pb$ and $^{207}Pb/^{206}Pb$ ages to be concordant in these representations. Common Pb is assessed through the $^{207}Pb/^{206}Pb$ ratios on the basis that any point is a mixture between common Pb and radiogenic Pb. The analyses are regressed from the estimated common Pb through the analysis to concordia (dashed line in the diagrams).

3.1.1 Late Jurassic to Early Cretaceous Clasts

3.1.1.1 Mount Saul

Rhyolite (UC30823) This weakly porphyritic rhyolite clast is classified as peralkaline (A-type). The 6 zircons analysed from this rhyolite have U concentrations ranging from 77-196 ppm, Th from 84-267 ppm, and Th/U from 0.91-1.40. Common Pb is low in all but one of the zircons (but $f206$ is still only 1.1 %). The weighted mean of all the 6 samples is 141.4±1.4 Ma ($1\sigma_m$; MSWD = 0.37). Including the error on the standard (0.4 %) gives a final age of 141.4±2.9 Ma ($2\sigma_m$).

Rhyolite (UC30867) This moderately porphyritic clast is geochemically classified as weakly peraluminous but has strong A-type affinities. 6 analyses were made from 6 zircons. U 111-279 ppm, Th 105-328 ppm, and Th/U 0.95-1.40; $f206$ is low in all samples. The weighted mean of all 6 analyses is 141.4±1.1 Ma ($1\sigma_m$; MSWD

= 1.14). Including the error on the standard (0.4 %) gives a final age of 141.4±2.6 Ma ($2\sigma_m$).

Rhyolite (UC30818) This weakly peraluminous I-type clast is weakly porphyritic and glomerophyric. 6 zircons were analysed from this sample. U concentrations range from 185-284 ppm, Th from 147-249 ppm, and Th/U ratios from 0.72-0.88. Common Pb ($f206$) is low in all the zircons. The weighted mean age of all zircons is 142.4±1.1 Ma ($1\sigma_m$; MSWD = 0.73). Including the error on the standard (0.34 %) gives a final age of 142.4±2.3 Ma ($2\sigma_m$).

Rhyolite (UC30854) The peralkaline rhyolite is moderately porphyritic and 6 zircons were analysed. The U concentrations are low, ranging from 52-103 ppm, Th from 51-164 ppm, and Th/U ratios from 0.95 to 1.72. Common Pb is variable and relatively high and ranges from 0.9-5.3 %. One single zircon returned an older age of 159 Ma that is 2.7σ above the weighted mean age. Excluding this inherited sample gives a weighted mean age of 145.2±1.5 Ma ($1\sigma_m$; MSWD = 0.91). Including the error on the standard (0.5 %) gives a final age of 145.2±3.4 Ma ($2\sigma_m$).

Monzogranite (UC30850) This metaluminous I-type clast crystallised initially under subsolvus conditions but the presence of granophyric rims around crystals is suggestive of a near surface final emplacement depth. 6 analyses were made on 6 zircons. U 101-224 ppm, Th 79-221 ppm, and Th/U 0.69-120; $f206$ 0.2-4.3 %. The MSWD of the weighted mean age of all the zircons is high at 4.0. The scatter is due to a single low analysis at 135 Ma (3.5σ below the mean). Rejecting this analysis gives a weighted mean age of 146.7±1.3 Ma ($1\sigma_m$; MSWD = 1.03). Including the error on the standard (0.42 %) gives a final age of 146.7±2.9 Ma ($2\sigma_m$).

3.1.1.2 Ethelton

Monzogranite (UC3964) This subsolvus granodiorite is a weakly peraluminous I-type rock. 6 analyses were made on 6 zircons. U 145-502 ppm, Th 109-290 ppm, and Th/U 0.47-0.82. Common Pb in all analyses is <1 %. The data are dispersed along a common Pb mixing line. Regression to concordia yields a single age population with a weighted mean age of 125.1±0.9 Ma ($1\sigma_m$; MSWD = 1.18). Including the error on the standard (0.42 %) gives a final age of 125.1±2.1 Ma ($2\sigma_m$).

Monzogranite (UC30944) This weakly peraluminous monzogranite displays a hypidiomorphic texture with granophyric intergrowth suggestive of a near surface emplacement. 6 analyses were made on 6 zircons. U concentrations range from 109-732 ppm, Th from 72-490 ppm and Th/U ratios from 0.55-0.70. Common lead ($f206$) is very low in all the zircons. The MSWD of the weighted mean is 2.2 with one crystal 2.6σ above the mean. Excluding this outlier at c. 134 Ma, the weighted mean for the remaining analyses is 128.2±1.0 Ma ($1\sigma_m$; MSWD = 0.54). Including the error on the standard (0.4 %) gives a final age of 128.2±2.2 Ma ($2\sigma_m$).

Rhyolite (UC30973) This weakly peraluminous A-type rock is strongly porphyritic. 6 zircons from this clast were analysed of which one is probably of inherited origin with an age of c. 152 Ma. U concentrations range from 428-1032 ppm, Th from 173-657 ppm, and Th/U from 0.36-0.67. With the exception of one analysis ($f206$ = 1.6 %) common lead is minor in all zircons. The MSWD of the weighted mean of all the zircons is high at 2.45 and is due to the 152 Ma zircon that is 2.56σ above the mean. Rejecting this analysis gives a mean age of 136.6±0.9 Ma ($1\sigma_m$; MSWD = 1.39). Including the error on the standard (0.4 %) gives a final age of 136.6±2.1 Ma ($2\sigma_m$).

Monzogranite (UC30952) Although this metaluminous I-type sample displays features typical of subsolvus granites the presence of a granophyric intergrowth suggests a rise of the granitic magma towards a shallower depth prior to the final emplacement. 6 analyses on 6 zircons were made. U ranges from 306-611 ppm, Th from 138-346 ppm and Th/U ratios from 0.38-0.57; $f206$ is very low in all but one of the zircons (but is still only 1 %). The weighted mean of the 6 U-Pb ages is 139.0±0.8 Ma ($1\sigma_m$; MSWD = 0.95). Including the error on the standard (0.34 %) gives a final age of 139.0±1.8 Ma ($2\sigma_m$).

Rhyolite (UC30954) This strongly porphyritic rhyolite is weakly peraluminous. 6 zircons were analysed from this volcanic clast. The U concentrations range over an order of magnitude from 189-1212 ppm, Th from 78-552 ppm and Th/U ratios from 0.41-0.63. Common Pb is variable for these zircons, but is largely (inversely) related to the range in U concentration; the analysis with the lowest U concentration has the highest common Pb component. The MSWD of the weighted mean of the 6 analyses is high at 2.2 and is due to a single zircon that is 2.75σ below the

mean. Rejecting this analysis gives a mean of 140.9±0.9 Ma ($1\sigma_m$; MSWD = 0.67). Including the error on the standard (0.34 %) gives a final age of 140.9±2.0 Ma ($2\sigma_m$).

Rhyolite (UC30925) Six zircons were analysed from this weakly porphyritic, weakly peraluminous rhyolite. U and Th concentrations are high and range from 3037-7046 ppm for U and 1011-4239 ppm for Th, with Th/U ratios from 0.33-0.60. Common Pb is very low but for one analysis (1.38 %). The MSWD of the weighted mean of all the analyses is high at 3.0 due to one older zircon that is removed 3σ from the mean. Rejecting this analysis gives a weighted mean age of 140.9±0.8 Ma ($1\sigma_m$; MSWD = 1.09). Including the error on the standard (0.45 %) gives a final age of 140.9±2.2 Ma ($2\sigma_m$).

3.1.1.3 Kekerengu

Monzogranite (UC30743) This weakly peraluminous sample has subsolvus petrographic characteristics, but minor interstitial granophyric intergrowth and rims on individual phenocrysts suggest a late stage rise of the cooling magma body to a final shallow emplacement depth. 6 analyses on 6 zircons were made. U 95-171 ppm, Th 69-154 ppm, and Th/U 0.47-1.10. Common lead in all the analyses is low. The weighted mean age of all the 6 zircons is 123.1±1.1 Ma ($1\sigma_m$; MSWD = 0.41). Including the error on the standard (0.5 %) gives a final age of 123.1±2.5 Ma ($2\sigma_m$).

Rhyolite (UC30731) This strongly porphyritic rhyolite is a weakly peraluminous I-type rock. 6 analyses were made on 6 zircons. U 471-800 ppm, Th 151-570 ppm, and Th/U 0.32-0.71. Common lead in all the analyses is very low. The weighted mean of all analyses is 134.7±0.8 Ma ($1\sigma_m$; MSWD = 1.52). Including the error on the standard (0.4 %) gives a final age of 134.7±2.0 Ma ($2\sigma_m$).

Monzogranite (UC30738) This weakly peraluminous, hypersolvus sample is weakly porphyritic and granophyric. 6 analyses were made from 6 zircons that have U concentrations in the range 199-284 ppm, Th from 96-145 ppm, and Th/U ratios from 0.46-0.54; $f206$ is very low in all analyses. The weighted mean age of all the analyses is 137.5±1.1 Ma ($1\sigma_m$; MSWD = 1.16). Including the error on the standard (0.45 %) gives a final age of 137.5±2.5 Ma ($2\sigma_m$).

Rhyolite (UC30730) This weakly peraluminous I-type rhyolite is strongly porphyritic. Seven zircons were analysed. U concentrations range from 552-911 ppm,

Th from 235-911 ppm, and Th/U ratios from 0.41-0.77. Common Pb is variable with $f206$ = 0.2-2.3 %. The MSWD of the weighted mean of all the samples is high at 4.53 with 2 zircons returning younger ages of 136 Ma and 133 Ma (2.16 and 3.18 below the mean). If the two outliers are rejected the weighted mean age of the remaining 5 analyses is 142.1±0.9 Ma ($1\sigma_m$; MSWD = 1.28). Including the error on the standard (0.42 %) gives a final age of 142.1±2.2 Ma ($2\sigma_m$).

3.1.2 Early Jurassic Clast

3.1.2.1 Kekerengu

Rhyolite (UC30732) This weakly peraluminous porphyritic rhyolite clast is the oldest sample of the dated clast population from the Pahau terrane. 6 zircons were analysed. The U concentrations range from 213-727 ppm, Th from 142-484 ppm, and Th/U ratios from 0.55-0.77. Common Pb is very low in all but one zircon (but is still low with only 1 %). One single zircon is 2.8σ above the weighted mean resulting in a high MSWD of the weighted mean (2.2). If the single analysis, which has also the highest $f206$ content, is rejected from the weighted mean age calculation the age of the 5 zircons is 188.3±1.2 Ma ($1\sigma_m$; MSWD = 0.27). Including the error on the standard (0.34 %) gives a final age of 188.3±2.6 Ma ($2\sigma_m$).

3.2 Rakaia Terrane Igneous Clasts

The 17 clasts analysed from the 4 Rakaia terrane conglomerates are dominated by weakly to strongly foliated rocks. Post-depositional deformation of the Boundary Creek samples took place under greenschist facies conditions and the clasts display a mylonitic to gneissic texture in hand specimen (see Chapter 6). Similar to the Pahau clasts the samples are mainly weakly peraluminous granitoids and rhyolites but peraluminous clasts have also been analysed. Rocks that are geochemically classified as adakites are unique to the Lake Hill conglomerate and two clasts were chosen to represent this clast population.

Three distinct age groups are recognised:

- Eleven Early Permian to Early Triassic plutonic and volcanic clasts from the Te Moana, McKenzie Pass and Lake Hill conglomerates.

- Four Carboniferous meta-volcanics and meta granitoids that are confined to the Boundary Creek conglomerate.
- Two Cambrian clasts: one monzogranite from Te Moana and one dacite from Lake Hill.

The new SHRIMP data is summarised in Table 3.1, and a short description of the individual igneous clasts follows below. Individual clast ages are plotted on Tera & Wasserburg (1972) diagrams in Figures 3.5 to 3.7 and are summarised in Figure 3.11.

3.2.1 Early Permian to Early Triassic Clasts

3.2.1.1 Te Moana

Rhyolite (UC31813) The fractionated rhyolite is moderately porphyritic and glomerophyric. 9 analyses were made from 9 zircons. U 97-618 ppm, Th 27-267 ppm, and Th/U 0.28-0.92. Common Pb in all the analyses is generally low with $f206$ <1 %. The U-Pb ages range from 265 Ma to 501 Ma with a bimodal distribution that results in a MSWD of the weighted mean of 221. The 3 samples with the lowest Th/U ratios return the highest ages and these 3 inherited zircons have a weighted mean age of 490±5 Ma (MSWD = 1.66). The weighted mean age for the remaining 6 analyses is 276.8±1.9 Ma ($1\sigma_m$; MSWD = 2.14). Including the error on the standard (0.5 %) gives a final age of 276.8±4.6 Ma ($2\sigma_m$).

Monzogranite (UC31818) Six zircons were analysed from this foliated, subsolvus hypidiomorphic monzogranite which is classified as weakly peraluminous. U concentrations are very high and range from 1102-3613 ppm, Th is high with a range of 400-2810 ppm, and Th/U ratios range from 0.35-0.87. Common Pb is variable and ranges from 0.1-4.2 %. The MSWD of the weighted mean is very high at 16.8 and reflects the wide spread of the data. Rejecting the oldest and the youngest analyses (6.3σ above and 6.0σ below the weighted mean), with the youngest zircon having the lowest U and Th concentrations, the MSWD of the weighted mean is still high with 2.6. If the analysis with the highest $f206$ (4.2 %) is also rejected the weighted mean age of the remaining 3 analyses is (?) 290±2 Ma. This age is inconclusive and more analyses are needed before an accurate result can be obtained.

3.2.1.2 McKenzie Pass

Trachydacite (UC30909) This weakly peraluminous trachydacite is moderately porphyritic. 8 zircons were analysed from this sample. U concentrations range from 108-523 ppm, Th from 83-718 ppm, and Th/U from 0.73-1.36. Common Pb is very low in all zircons. The MSWD of the weighted mean is high at 5.22. Rejecting the 2 oldest analyses the MSWD is still slightly high at 1.85 but no other outliers are obvious except the youngest analysis (2.07σ above the mean) and all the remaining analyses are considered. The weighted mean age is 253.4±1.9 Ma ($1\sigma_m$; MSWD = 1.85). Including the error on the standard (0.42 %) gives a final age of 253.4±4.2 Ma ($2\sigma_m$).

Monzogranite (UC30895) This metaluminous, hypersolvus monzogranite is weakly porphyritic and contains interstitial granophyric intergrowth suggestive of final crystallisation at shallow depth. 6 analyses were made from 6 zircons. U concentrations range from 113-625 ppm, Th from 98-921 ppm, and Th/U ratios from 0.62-2.37. Common Pb is very low in all but one analysis, which is still only 1 %. The MSWD of the weighted mean is slightly high at 1.67 but there is no clear outlier and all data were included. The weighted mean age is 254.3±1.6 Ma ($1\sigma_m$; MSWD = 1.67). Including the error on the standard (0.4 %) gives a final age of 254.3±3.8 Ma ($2\sigma_m$).

Rhyolite (UC30902) This moderately porphyritic, glomerophyric rhyolite is geochemically classified as metaluminous. 6 zircons were analysed. U 102-323 ppm, Th 72-534 ppm, and Th/U 0.71-1.72; $f206$ is very low in all analyses. The weighted mean age of all 6 zircons is 258.2±2.0 Ma ($1\sigma_m$; MSWD = 0.75). Including the error on the standard (0.4 %) gives a final age of 258.2±4.5 Ma ($2\sigma_m$).

Rhyolite (UC30901) Six zircons were analysed from this weakly peraluminous rhyolite. U concentrations are very high and range from 7012-10108 ppm, Th from 1323-2976 ppm, and Th/U ratios from 0.19-0.30. Common Pb in all but one zircon is low ($f206$ is still only 1.8 %). The MSWD of the weighted mean for all the analyses is high at 15.8 reflective of the bimodal age population. The weighted mean age of the older age component (3 zircons) is (?) 284.7 Ma and that of the younger age group is (?) 263±2 Ma. There is very little indication in the data set which is the magmatic age. In other data sets where such bimodality is seen the older age is assigned

to the inherited and the younger age to the magmatic component. More analyses are required before a conclusive answer can be obtained.

Rhyolite (UC30914) Six analyses of 6 zircons were made from this metaluminous weakly porphyritic rhyolite. U concentrations range from 138-392 ppm, Th from 76-241 ppm, and Th/U from 0.51-0.73; $f206$ is very low in all the analyses. The weighted mean age of all the analyses is 292.2±2.1 Ma ($1\sigma_m$; MSWD = 0.57). Including the error on the standard (0.45 %) gives a final age of 292.2±5.1 Ma ($2\sigma_m$).

3.2.1.3 Lake Hill

Monzogranite (UC30668) Seven zircons were analysed from this weakly peraluminous, foliated, subsolvus monzogranite. U concentrations range from 206-1465 ppm, Th from 63-413 ppm, and Th/U ratios from 0.11-0.82. Common Pb is very low in all the analyses. U-Pb ages range from 717-140 Ma with the weighted mean of all the samples having an MSWD of 904. If the 3 oldest analyses are treated as inherited and rejected the distribution becomes bimodal. The older peak still has a high MSWD of 2.93 due to one analysis that is 2.3 above the mean (and has the highest U concentration). Rejecting this analysis the weighted mean age for the older peak is (?) 243±2 Ma. One zircon returned a Late Jurassic age of 148±8 Ma. This youngest zircon most likely experienced some Pb loss and more analyses are needed before a conclusive result can be obtained.

Rhyolite (UC30667) Six analyses were made from this peraluminous, weakly porphyritic rhyolite. U 80-240 ppm, Th 52-289 ppm, and Th/U 0.43-1.20; $f206$ is low in all analyses (< 0.57 %). The weighted mean age for all the analyses is 244.1±1.7 Ma ($1\sigma_m$; MSWD = 0.14). Including the error on the standard (0.4 %) gives a final age of 244.1±3.8 Ma ($2\sigma_m$).

Granodiorite (UC30659) This weakly foliated subsolvus, peraluminous granodiorite is geochemically classified as an adakite, a rock believed to be derived from a source with garnet as a stable phase. Six zircons were analysed. U concentrations are variable and range from 119-1835 ppm, Th range from 41-220 ppm, and Th/U ratios range from 0.05-0.95. Common Pb is low and ranges from -0.51 to 0.28 %. The MSWD of the weighted mean is very high at 384 and reflects the wide spread of the data. Rejecting the oldest two analyses (24.3σ and 34.8σ above the weighted mean) the

weighted mean age of the remaining 4 analyses is 256.9±2.2 Ma ($1\sigma_m$; MSWD = 1.64). Including the error on the standard (0.5 %) gives a final age of 256.9±5.1 Ma ($2\sigma_m$).

Monzogranite (UC30673) The foliated, subsolvus monzogranite is classified as an adakite. 7 analyses were made. The U concentrations range over an order of magnitude from 97-1146 ppm, Th from 66-395 ppm, and Th/U ratios from 0.21-0.68. Common Pb in all but one analysis (18.6 %) is very low. The youngest analysis with the very high $f206$ concentration has been rejected but the MSWD of the weighted mean is still high at 5.9. Excluding the oldest analysis the MSWD remains still high at 3.1. One of the two younger zircons is 2.6σ below the mean and if rejected results in a weighted mean age of (?) 279±6 Ma. Also for this sample more analyses have to be made before a conclusive result can be obtained.

3.2.2 Carboniferous Clasts

3.2.2.1 Boundary Creek

Meta-rhyolite (UC31747) Six zircons were analysed from this metaluminous, mylonitic and glomerophyric meta-rhyolite. U concentrations range from 400-596 ppm, Th from 179-383 ppm, and Th/U ratios from 0.39-0.64. The weighted mean age of all 6 analyses is 325.2±1.7 Ma ($1\sigma_m$; MSWD = 0.82). Including the error on the standard (0.4 %) gives a final age of 325.2±4.4 Ma ($2\sigma_m$).

Meta-monzogranite (UC31775) Six analyses from 6 zircons were made from this metaluminous and mylonitic meta-monzogranite. U 256-871 ppm, Th 98-704 ppm, and Th/U 0.38-1.38. Common Pb in all the analyses is very low. The MSWD of the weighted mean age is high at 2.5 due to a single analysis that lies 2.08σ above the mean. Rejecting this analysis gives a mean age of 330.1±2.0 Ma ($1\sigma_m$; MSWD = 1.89). Including the error on the standard (0.4 %) gives a final age of 330.1±4.9 Ma ($2\sigma_m$).

Meta-granodiorite (UC31749) The 6 zircons analysed from this metaluminous and mylonitic meta-granodiorite give a weighted mean age of 334.9±2.1 Ma ($1\sigma_m$; MSWD = 1.52). U 82-184 ppm, Th 81-207 ppm, and Th/U 0.75-1.44. Common Pb in all the analyses is low with $f206$ <1 %. Including the error on the standard (0.34 %) gives a final age of 334.9±4.9 Ma ($2\sigma_m$).

Meta-dacite (UC31776) Six zircons were analysed from this metaluminous, mylonitic and glomerophyric meta-dacite. U concentrations range from 266-487 ppm, Th from 116-362 ppm, and Th/U from 0.44-0.78. Common Pb in all the analyses is very low. The 6 zircons return a weighted mean age of 355.6±2.0 Ma ($1\sigma_m$; MSWD = 1.55). Including the error on the standard (0.4 %) gives a final age of 355.6±5.0 Ma ($2\sigma_m$).

3.2.3 Cambrian Clasts

3.2.3.1 Te Moana

Monzogranite (UC31816) The foliated, subsolvus hypidiomorphic monzogranite is classified as a weakly peraluminous rock. Seven zircons were analysed. This U concentrations range from 206-1247 ppm, Th from 102-576 ppm, and Th/U ratios from -0.21-0.71. Common Pb is very low in all zircons. Two zircons are well above (5.2σ) and below (-6.2σ) the weighted mean resulting in a high MSWD of the weighted mean (12). The youngest zircon has the highest $f206$ content and Pb loss for this analysis is suggested. If this youngest zircon as well as the oldest (inherited) zircon are rejected from the weighted mean age calculation the age of the 5 zircons is 496.9±2.9 Ma ($1\sigma_m$; MSWD = 1.6). Including the error on the standard (0.5 %) gives a final age of 496.9±7.7 Ma ($2\sigma_m$).

3.2.3.2 Lake Hill

Dacite (UC30644) This dacite is moderately porphyritic and weakly peraluminous. U concentrations range from 123-364 ppm, Th from 59-111 ppm, and Th/U ratios from 0.37-0.53; $f206$ is very low in all the analyses. The U-Pb ages range from 478-602 Ma and are dispersed, with the weighted mean age for all analyses having an MSWD of 16.5. Removing the data with the oldest ages the MSWD is still slightly high at 1.9, with the youngest analysis 1.8σ below the mean. Rejecting this analysis would reduce the MSWD to 1.13 but would have little influence on the final age. Therefore the youngest zircon is included to give a weighted mean age of (?) 517±10 Ma. More analyses are needed to obtain a conclusive age.

3.3 DETRITAL ZIRCONS

Sandstones used in this study are all medium to coarse grain immature sandstones from turbidite beds. Zircons were separated from the rock samples at Stanford University using standard crushing and heavy liquid techniques. Approximately 150-200 grains were randomly handpicked and mounted in a 25 mm epoxy disc. The mounts then were polished to expose a cross-section of the grains. For analytical details and laboratory procedures the reader is referred to Appendix 2. Data are listed in Appendix 4.

Williams (1966) noted that the key to success is the analysis of a large number of individual crystals, particularly if several age populations are present. Only then are there sufficient analyses to give confidence that all significant populations were identified. To have a 95 % chance of sampling a population with 5 % relative abundance, 59 grains must be dated to make reasonable estimates of the relative numbers of grains in each of the principal age groups.

Data for the individual detrital samples are presented in Figures 3.8 to 3.10 as age histograms with a calculated interval of 20 Ma. Sample age distributions are summaries in terms of major age components (usually 5 %), but some minor groups are also identified when a peak is noted. The groups identified in each data set are defined by natural breaks in the data. The age histograms are overlain by cumulative probability curves to further highlight the principal age components. It is difficult to apply standard statistical analyses to define populations and sub-populations, especially for minor groups, as the data sets for individual groups are relatively small. Consequently, although the groups form distinct separate clusters, they probably rarely represent a single population. Little significance is placed upon single age determinations (but see below).

3.3.1 Kurow

Of the 60 analysed zircon grains, 70 % are represented by the age group with ages between 237 Ma and 349 Ma. The group is a complex cluster of 3 distinct peaks at c. 270 Ma, 300 Ma and 340 Ma with the main peak making up 28 % of the data. The group between 260-240 Ma (10 %) has a peak at c. 255 Ma and is regarded as the most reliable estimate of the maximum stratigraphic age limit. A minor Middle Devonian-

Silurian group (6 %) at 420-380 Ma has a peak at c. 420 Ma and an Ordovician-Early Cambrian group (540-480 Ma) makes up 12 % of the data with a broad peak at c. 510 Ma. The remaining 6 analyses range from 1499-630 Ma and make up 10 % of the data with a minor peak (6 %) at 640 Ma and insignificant peaks (3 %) at 966 Ma, 1050 Ma and 1500 Ma.

Cores of the two youngest zircons from this sandstone returned Middle Triassic (Anisian) 238±8 Ma and 239±6 Ma ages. There is no indication of lead loss from these two zircons, as they contain no cracks and inclusions. These two young ages are in disagreement with the Permian stratigraphic age based on fossils. An **Anisian** depositional age is proposed for the Kurow Hill area (Figure 2.25).

3.3.2 Balmacaan Stream

A total of 64 zircons were analysed from this sandstone sample. The major Late Triassic to Carboniferous (Namurian) group comprises 51 % of the whole data, with the main peak (16 %) between 280-260 Ma at c. 265 Ma and two minor younger peaks at c. 250 Ma (13 %) and 230 Ma (8 %). The youngest peak is regarded as the most reliable estimate of the maximum stratigraphic age. The group between 320-280 Ma make up 15 % of all the analyses and there are two possible peaks at 285 Ma (9 %) and 305 Ma (6 %). There are insignificant peaks (<5 %) between the Carboniferous and the Ordovician (480-320 Ma) and one minor group between 520-480 Ma (6 %) with a peak at 495 Ma. The remaining analyses (28 %) extend to 1848 Ma with minor groups at 929-870 Ma (5 %) and 1085-1004 Ma (9 %) with a peak at c. 1020 Ma.

The youngest zircon from this sandstone returned a Middle Triassic (Carnian) 223±5 Ma age that is in disagreement with the Anisian stratigraphic age based on fossils. There is no indication of lead loss from this single zircon. However, there is the possibility of the presence of a metamorphic rim. For this study no cathodoluminescent images have been obtained to detect such metamorphic rims. Given that the age of the Balmacaan Stream sediments is well constrained by the fossil record, the **Anisian** depositional age is retained (Figure 2.25).

3.3.3 Ethelton

This sample represents the matrix of the Ethelton conglomerate described in Chapter 2. A total of 60 zircons were analysed from this sample. Two distinct main

groups are recognised, one in the Cretaceous with an age range from 135-112 Ma and a second extending from the Late Triassic to the Early Permian (300-214 Ma). The main peak of the Cretaceous group is within the age range of 140-120 Ma (15 %) at c. 130 Ma. The two youngest analyses (3 %) show a minor peak at c. 112 Ma that suggests an Aptian maximum stratigraphic age. The second group (33 %) consists of a mixture of peaks with the main peak at c. 230 Ma (260-200 Ma; 25 %), a minor peak at c. 290 Ma (300-280 Ma; 5 %), and two possible minor peaks at c. 215 Ma (220-200 Ma; 7 %), and 247 Ma (260-240 Ma; 7 %). There is a minor Early Jurassic group (187-176 Ma; 5 %) with a peak at c. 185 Ma. A broad Silurian-Cambrian group (540-420 Ma; 15 %) has a peak at c. 470 Ma. There is a subdued Devonian peak at c. 385 Ma (400-360 Ma). The remaining 10 analyses make up 17 % of the data and extend into the Archean (2548 Ma) with a possible peak at 1627-1594 Ma.

3.4 Summary of the U-Pb Zircon Data

The detrital U-Pb zircon age distribution patterns of all 3 sandstones are shown as cumulative probability curves in Figure 3.11 together with individual igneous clast ages from all conglomerates from both terranes. Included in the diagram (grey box, legend on the left side) are the available published detrital U-Pb zircon age distribution patterns from Caples, Rakaia and Pahau terrane sandstones, and sandstones from the western Province of New Zealand (Ireland, 1992; Wysoczanski *et al.*, 1997; Cawood *et al.*, 1999; Pickard *et al.*, 2000).

The two Rakaia terrane samples analysed each contain a major age group in the range of 360-220 Ma (Middle Triassic-Devonian) that comprise 51 % and 70 % respectively of the data set. The major peak of the Permian Kurow sample is at c. 270 Ma indistinguishable from other published Permian Rakaia sandstones. The Middle Triassic (Anisian) Balmacaan Stream detrital zircon age distribution agrees well with a Middle Triassic sample analysed nearby (PUD1, Pickard *et al.* 2000) with a slightly older main peak at 265 Ma.

The major age group of the Lower Cretaceous (Aptian) Ethelton matrix sample makes up 38 % of the sample data set and this group is indistinguishable from major age groups recognised in Triassic Rakaia, Waipapa/Caples, and Western Province sandstones. The peak at c. 235 Ma strongly coincides with peaks recognised in these

samples. A second pronounced peak at c. 130 Ma in the Ethelton sample is reflected in sandstone samples from other Pahau localities.

Minor peaks at c. 300 Ma, 330 Ma and 500 Ma are apparent in all 3 sandstone samples and similar peaks are documented from other sandstones from all terranes shown in Figure 3.11. The minor peak at c. 180 Ma recognised in the Ethelton sample is also recognised as a minor peak in other Pahau samples from other localities.

All new igneous clast U-Pb zircon ages are plotted on the lower bars with the filled stars representing subsolvus clasts and open stars representing hypersolvus and volcanic clasts.

All but one analysed clast from the Pahau terrane are of a Late Jurassic to Lower Cretaceous age. Most of the clast ages from Ethelton and Kekerengu overlap with the Cretaceous detrital zircon age group (140-120 Ma) of the Ethelton sandstone. The remaining clasts from these two conglomerates and the samples from Mount Saul are just slightly older (c. 146-140 Ma) than the main detrital group. The Early Jurassic clast from Kekerengu is indistinguishable in age from the minor Early Jurassic peak in the Ethelton sandstone described above.

A similar pattern is observed in the Rakaia terrane. The majority of the igneous clasts from Lake Hill, McKenzie Pass and Te Moana define a narrow range of U-Pb ages (290-243 Ma). These ages are well within the peak range of the major detrital zircon age group identified in Rakaia sandstones from this and other studies (e.g., Pickard *et al.*, 2000). The 4 Carboniferous clasts from Boundary Creek conglomerate range in age from c. 355-325 Ma, which coincides with the c. 340 Ma peak recognised in the Anisian Kurow sandstone sample. The two Cambrian igneous clasts from Te Moana and Lake Hill are indistinguishable in age from the detrital peaks identified in Rakaia sandstones.

There is a distinct major age gap of c. 87 Ma in the new igneous U-Pb age record ranging from c. 243 Ma to 156 Ma that coincides with the recognised missing fossil record between the Rakaia and the Pahau terranes. The single Early Jurassic clast from this study and the Early Jurassic detrital zircons in the Ethelton matrix interrupt this pattern. Furthermore, the five Early Jurassic volcanosedimentary units within the MTZ (see section 1.3.2), together with other Early Jurassic igneous clasts from in the Brook

Street and Murihiku terranes (sections 1.3.3.1 and 1.3.3.2), suggest that the recognised missing sediments are not related to a break in source magmatism, but are more likely due to tectonic erosion. A similar, but minor, gap from c. 325-292 Ma (Upper Carboniferous) is recognised between the U-Pb ages from the Boundary Creek conglomerate and the other conglomerates within the Rakaia terrane.

In Figure 3.12 individual zircon U-Pb ages from the 3 sandstones and from igneous clasts from the Pahau and Rakaia terranes are pooled and plotted against the depositional age of each individual conglomerate.

All the igneous clast zircons from the Pahau terrane define a very narrow range of ages. The absence of individual zircons of Paleozoic age is conspicuous. The distribution pattern for the Pahau shows that timing of the igneous activity agrees well with the published depositional ages and that the deposition of the sandstone is essentially contemporaneous with the igneous activity.

The pooled U-Pb ages of igneous clasts from the Rakaia terrane display a crude inboard to outboard younging trend mimicking the trend displayed by stratigraphic ages of the conglomerates. In contrast to the igneous clasts analysed from the Pahau terrane the samples from the Rakaia terrane are noted for the presence of inherited zircons in various samples, and in some samples data is widely spread with a bimodal age population (Table 3.1 and Appendix 4). The observed younging trend suggests that igneous activity in the clast source area continued into the Carnian (Figure 3.12). A further pattern shows that in all the conglomerates (except Boundary Creek) igneous zircon ages and depositional ages of these conglomerates correlate. If sedimentation and igneous activity are assumed also to be penecontemporaneous for the Boundary Creek conglomerate then this might indicate that there are Carboniferous sediments present in the Haast Schist.

3.5 SAME SOURCE PROBLEM

One of the questions arising using coarse sized hand specimens for provenance analysis is: " Do the igneous clasts represent the same source that provided the sedimentary detritus for the basin?"

The similarity of individual clast ages from the Pahau terrane with the Cretaceous and Jurassic detrital age components of the Ethelton sample has been discussed above and is further emphasised by the cumulative distribution of individual igneous zircon ages in Figure 3.13 a.

The distribution shows that the zircon population from Mount Saul is slightly older than that of the Ethelton sandstone and the two populations from Ethelton and Kekerengu. The Cretaceous age components of the latter two conglomerates are indistinguishable from each other. The Ethelton and the Kekerengu igneous zircon ages overlap with most of the zircon ages from the sandstone sample. Furthermore, the minor age peak from the Ethelton igneous zircon population coincides with the main peak from the Ethelton matrix. The Early Jurassic igneous zircon age distribution from Kekerengu is identical to the distribution recognised in the sandstone.

On an Age - U comparative plot (Figure 3.13 b) the Ethelton and Kekerengu (Cretaceous = K1) igneous zircon populations display the widest range of values but are indistinguishable from each other. In contrast the igneous zircons from Mount Saul occupy a relatively small field that lies below the field for the other two igneous zircon populations with peralkaline clast zircons having the lowest values. Most of the detrital Ethelton zircons plot within the Ethelton and Kekerengu (K1) fields, with none of the detrital zircons showing Mount Saul affinities. Two zircons of the Jurassic detrital population plot within the field displayed by the single Early Jurassic clast from Kekerengu (K2).

A similar, but less clear trend is observed if Age - Th is compared (Figure 3.13 c). The Mount Saul population defines a narrow field of Th values but there is more overlap with the igneous zircon populations from Ethelton and Kekerengu (K1). The Mount Saul zircons with peralkaline affinities have generally the lowest values. Most of the Cretaceous detrital zircons plot well within the fields of Ethelton and Kekerengu (K1). The Jurassic Th composition of two detrital zircons is indistinguishable from that of the single igneous clast at Kekerengu (K2).

On the Age - Th/U diagram (Figure 3.13 d) the Ethelton igneous zircon population occupies a relatively narrow field and is indistinguishable from the Kekerengu (K1) field. In stark contrast, the Mount Saul zircon population displays the widest range with the highest values (peralkaline zircons) and there is only minor

overlap with the fields of the other two igneous zircon populations. Most of the Cretaceous detrital zircons have Th/U ratios similar to the Ethelton and Kekerengu (K1) igneous populations and plot within these fields.

Geochemical data from the Pahau terrane igneous clasts (Chapter 5) indicate that all the clasts have a general concordance that suggests a similar petrogenesis, and that they are derived from a single suite except for the peralkaline clasts from Mount Saul. The Jurassic detrital zircon ages and zircon compositions from the Ethelton matrix are similar to the zircon ages and compositions from the single Early Jurassic igneous clast at Kekerengu, lending further support to the above interpretation of the geochemical data.

The data presented in Figures 3.11 and 3.13 show that the predominantly volcanic igneous clasts are embedded in sandstones that contain zircons with U-Pb ages and compositions indistinguishable from that of the zircons in the igneous clasts. This strongly suggests that the igneous clasts represent the same source that provided the sedimentary detritus for the basin, and that igneous activity and sedimentation were penecontemporaneous.

CHAPTER 4

SANDSTONE CLASTS

CHAPTER 4

RAKAIA AND PAHAU TERRANE SANDSTONE CLASTS

Introduction

Only few authors have given detailed geologic and petrographic descriptions of sandstone clasts from Torlesse conglomerates (Andrews *et al.*, 1976; Smale, 1978; Smale, 1980a; MacKinnon, 1983; Smale, 1983; Barnes, 1990). They noted an abundance of Torlesse-like sandstone clasts which were inferred to have been reworked from older Torlesse rocks. MacKinnon (1980a) studied thin sections from 17 pebble-sized conglomerates and showed that most sandstone clasts are indistinguishable from coeval or older Torlesse sandstones. MacKinnon showed that sandstone clasts, together with mudstone clasts of similar composition, compose approximately 10 to 30 % of the clasts in Permian and some Middle Triassic Torlesse conglomerates, and 50 % or more in some Middle Triassic and most younger Torlesse conglomerates.

Smale (1983) described petrographic similarities between sandstone clasts, conglomerate matrix and interbedded sandstones in the Permian Te Moana conglomerate. He concluded that the conglomerate matrix was derived from the sandy substrate and that the sources of the sandstone and the sandstone clasts were the same.

MacKinnon (1980a) noted that the matrix of all the conglomerates is medium to coarse grained and that in pre-Jurassic conglomerates, the composition of matrix is different from that which would be produced by simple breakdown of conglomerate clasts, thus matrix and clasts were derived in part from different sources. In Upper Jurassic and Lower Cretaceous conglomerates, composition of matrix and clasts is compatible with the derivation from the same source. Older Torlesse rocks may have been the predominant source.

No previous study provides combined detailed information on petrography and geochemistry of Torlesse conglomerate sandstone clasts. In the current work, detrital composition of sandstone clasts was quantified by point counting grains from 50 clasts

each from 2 Rakaia terrane conglomerates (Te Moana and Lake Hill), and from 2 Pahau terrane conglomerates (Mount Saul and Ethelton). The lower cut-off size for collection was 10 cm (intermediate axis). Rip-up conglomerate clasts (derived from erosion of semi-consolidated sediments) and highly silicified clasts were excluded.

4.1 PETROGRAPHY

In order to compare the new data from this study with that of MacKinnon (1980a), his procedures and sandstone component categories were followed. The grain size of analysed samples was restricted to the range fine to medium (0.1 to 0.45 mm) sand. Classification of sandstone follows Pettijohn (1987).

4.1.1 Sandstone Components

A limited number of component categories were set up. Detrital categories include quartz, plagioclase, potassium feldspar, various rock fragments, mafic mineral categories and matrix (Table 4.1 and Appendix 5, also see MacKinnon 1980 for details of categories).

Accurate determination of the original detrital mineralogy of a sandstone can only be accomplished if the sample has little alteration, thus considerable care was taken to select samples which have experienced only minimal diagenetic and weathering modifications. Heavily veined samples were not counted. When point counting, incomplete alteration of grains or pseudomorphs, such as sericitized or albitized plagioclase or chloritized biotite, was ignored if it did not prevent recognition of original detrital grain composition. The remaining alteration or replacement components fall into the categories 'matrix' or 'others' which includes 'alterites' and 'cement'. The average and range of these, for the samples selected, are: matrix 9 % (4-14 %); others <1 % (0-1.4 %) (Table 4.1).

4.1.2 Petrographic Procedures

Sandstone composition was determined by point counting 500 grains from stained thin sections using a Swift automated point counter. Theoretical reliability of values obtained is within 5 % of true values at the 95 % confidence level (Van Der Plas and Tobi, 1965).

To assure a rapid and accurate identification of grain types thin sections were stained yellow with sodium cobaltnitrite in order to distinguish for potassium feldspar (see Appendix 2). Identification of quartz and plagioclase was based on interference figure, twinning and refractive index.

In this study quartz and feldspar crystals >0.0625 mm within microphaneritic lithic fragments are reapportioned to the quartz and feldspar categories. This was suggested by Dickinson (1970) and follows MacKinnon's procedures. In the same manner perthitic, granophyric and micrographic grains were also reapportioned. Hence there are no plutonic or gneissic lithic fragment categories. Polycrystalline quartz and sedimentary, metamorphic and volcanic fragments are categorised as lithic fragments. Contrary to Dickinson's (1970) suggestion, phenocrysts in aphanitic lithic fragments were counted as part of the lithic fragment (MacKinnon, 1980a).

Definitions of comparative parameters are as follows: Q = monocrystalline quartz and polycrystalline quartz, including chert; F = feldspar; L = sedimentary, metamorphic and volcanic aphanitic lithic fragments; P/F ratio = ratio of plagioclase and total feldspar; Lv/L ratio = ratio of volcanic lithics to total lithics; %M = mica as a percentage of all components except 'matrix' and 'others' (MacKinnon, 1980a).

A few sandstones contain mudstone rip-up clasts, which were clearly recognisable by their large size. They were not included in the point counts.

4.1.3 Composition of Sandstone Clasts

Sandstone clasts from each conglomerate were distinguished on the basis of compositional parameters determined in the point counts (Table 4.1).

Q-F-L are the major components and are shown in Figure 4.1 together with the 5 sandstone petrofacies (PF) defined by MacKinnon (1980a). The following are average framework compositions for the 4 Rakaia PFs: $Q_{24}F_{59}L_{26}$ (PF1, Permian), $Q_{29}F_{51}L_{20}$ (PF2, Middle Triassic), $Q_{31}F_{59}L_{10}$ (PF3, lower Upper Triassic), and $Q_{35}F_{42}L_{23}$ (PF4, Upper Triassic). The Pahau PF5 (Upper Jurassic-Lower Cretaceous) averages $Q_{27}F_{33}L_{40}$. The hexagon for each of these petrofacies and the sandstone clast populations is defined by one standard deviation around the mean. Also shown are the 5 point counted conglomerate clasts of MacKinnon (1980).

The Torlesse sandstone clasts are immature, moderately sorted, angular feldspathic arenites and have a restricted range of Q-F-L compositions averaging $Q_{30}F_{49}L_{21}$ (Figure 4.1a). The compositional change shown in the Q-F-L diagram from one location to the next is mainly due to the slight increase in framework %Q from the Permian Te Moana conglomerate to the Early Cretaceous (Aptian) Mount Saul conglomerate (Figure 4.1b). Framework lithic fragment content follows a general reversed trend with a slight decrease in volcanic lithics but no significant change in L/Lv ratios. Framework feldspar content shows no significant change with time but the ratio of plagioclase to potassium feldspar decreases slightly. The following paragraphs summarise the salient points of each sandstone clast population (SCP)[1].

The sandstone clast population from the Permian Rakaia terrane Te Moana conglomerate (SCP1) is the least mature with the lowest framework quartz content $Q_{26}F_{50}L_{24}$ and the highest P/F ratio compared with the other clast populations (Figure 4.2). Mean Q-F-L values for the Te Moana and Lake Hill clasts show that there is no modal difference between the two sandstone clasts populations. This is supported by P/F, Lv/L and %M ratios, which are statistically indistinguishable (Figure 4.2). The Carnian Lake Hill (SCP2) can be distinguished from the Te Moana SCP by a slightly higher framework %Q content and compared with all other SCP has the lowest framework feldspar and %M content.

The sandstone clast population from the Aptian Pahau terrane Ethelton conglomerate (SCP3) is similar to the Mount Saul sandstone clast population (SCP4) but can be distinguished by the lower framework %Q and %M mean content, higher lithic and P/F framework ratios, and a slightly higher Lv/L framework ratio. However, the Ethelton-Mount Saul differences are very slight and the standard deviations of framework values and ratios overlap. The wide range in framework %Q in the Ethelton conglomerate is mainly due to a couple of samples. One of these samples plots at the lithic poor end of the measured range. Q-F-L values show that the means of all the other SCP plot within the Ethelton SCP hexagon (Figure 4.1b) and that the Ethelton SCP is compositionally indistinguishable from the other 3 sandstone clast populations.

The Aptian Mount Saul sandstone clast population can be distinguished from all the other populations by the highest framework %Q and %M content and the lowest

[1] Sandstone clast populations are abbreviated as follows: SCP1 = Te Moana; SCP2 = Lake Hill; SCP3 =

lithic, P/F and Lv/L ratio. Mean Q-F-L parameters show that the Mount Saul SCP is statistically different from both Rakaia terrane sandstone clast populations.

Ternary compositional diagrams after Dickinson *et al.* (1983) and Ingersoll and Suczek (1979) are given in (Figure 4.3). The QFL diagram (Figure 4.3a) shows that the sandstones plot mainly in the dissected arc provenance field. The dominance of volcanic lithic fragments over sedimentary and metamorphic lithic fragments is demonstrated in (Figure 4.3b).

4.1.4 Petrographic Comparison of Sandstone Clasts and Torlesse Sandstones

Q-F-L data for all the sandstone clasts, except one quartz-rich clast from Ethelton, all fall within the range of Torlesse sandstone petrofacies compositions (Figure 4.1b). Values for other parameters (Lv/L, P/F and %M) are also compatible with the Torlesse sandstone composition as shown in Figure 4.2. The range and one standard deviation fields for the sandstone clast populations and the sandstone petrofacies 1-5 in Figure 4.1b show that the Rakaia terrane SCPs cluster around PF1 (Rakaia Permian) and PF2 (Rakaia Middle Triassic) and that the Pahau terrane SCPs cluster around PF2 and minimally overlap with PF3 (Rakaia Middle to early Late Triassic) and PF4 (Late Triassic).

Values for the Te Moana SCP show strong affinities with PF1 and only minor overlap with PF2. The P/F ratio compares well with the PF1 value. However Lv/L ratios are higher, and %M are slightly lower than PF1 values and are more compatible with PF2 to PF 4.

Q-F-L values for the Lake Hill SCP show an equal overlap with PF1 and PF2, and Lv/L and P/F ratio values fall within the range of the PF2-4 values.

Compared with the Torlesse sandstone petrofacies, the Ethelton SCP shows strong affinities with PF2 and some minor overlap with PF1 and PF3-4. The other parameters, P/F and Lv/L ratios, compare well with PF2-4.

Ethelton; SCP4 = Mount Saul

The Mount Saul SCP plots between PF3 and PF4 with some slight overlap with PF2-4. The Lv/L ratio falls within the range of PF2-4 but P/F is slightly lower than all PF values.

Based on the distinct QFL shift in PF4 to PF5 (Figure 4.1a), decrease in Lv/L, increase in sedimentary lithics of Torlesse derivation, and the presence of detrital pumpellyite in PF5, MacKinnon (1983) proposed that the compositions of these younger petrofacies were influenced by the reworking of indurated and metamorphosed sediments from PF1-3. The gradual and progressive change through time of Torlesse sandstone compositions relate to the evolution of the source and gradual unroofing of a continental margin volcano/plutonic arc that was still active during the deposition of PF1-3. Uplifted and metamorphosed older Rakaia rocks became the dominant supplier to the trench to form the younger Pahau terrane.

Petrographic observations made in the sandstone clast populations of this study lend support to MacKinnon's idea. Petrography of the 4 sandstone clast populations strongly suggests that:

- autocannibalistic reworking of PF1 sandstone is a major source for the Permian Te Moana conglomerate sandstone clasts;
- sandstone clasts in the Lake Hill conglomerate are derived by autocannibalistic recycling of PF1-3 sandstones;
- older rocks from PF1-3, with minor contribution of PF4 sandstones, are the main sandstone clast supplier to the younger Pahau conglomerates.

4.2 GEOCHEMISTRY

4.2.1 Introduction

To further support the petrographic data presented above, XRF whole-rock analyses of the 50 point counted samples were obtained. Whole-rock major and trace element compositions of all the sandstone clasts are listed in Appendix 7.

Studies of whole-rock geochemistry of sedimentary units have demonstrated that chemical data can be applied in studies of provenance, tectonic settings and terrane relationships (e.g., Bhatia and Crook, 1986; Roser and Korsch, 1986; Roser and Korsch,

1988; McLennan *et al.*, 1993; Roser and Korsch, 1999; Wombacher and Münker, 2000). Prior to 1980, few analyses of Torlesse rocks were available, and most were of major elements (e.g., Reed, 1957). Roser *et al.* (1995) presented XRF analyses of Torlesse terrane sandstones and argillites from the South Island and the southern part of the North Island. The authors analysed MacKinnon's (1980a) petrofacies sandstones, and Roser *et al.* (1993a) and Roser and Korsch (1999) used these data to confirm the geochemical validity of MacKinnon's (1980) South Island petrofacies scheme. All demonstrate that the sandstone chemistry compares well with the petrographic data. Roser and Korsch showed that small changes in elemental ratios in Rakaia terrane PF1 to PF3 parallel petrographic QFL trends, reflecting an initial source control. Local recycling into PF4, coupled with a small influx of volcanic detritus, lead to contrasts in provenance-linked indices e.g., SiO_2/Al_2O_3, K_2O/Na_2O, Th/Sc, La/Sc, Ce/Sc.

In this section the new geochemical data from the 4 sandstone clast populations (Table 4.2) are compared with the geochemical data from the 5 Torlesse petrofacies of Roser *et al.* (1995), and their average values are presented in Table 4.3. As already noted above (Table 4.1), matrix and diagenetic alteration in analysed sandstone clast samples is small (average <9 %) and the chemistry of the samples therefore largely reflects the abundance of the detrital constituents.

All geochemical data presented in the following sections and chapters were recalculated to a volatile free total of 100 %.

4.2.2 Major Elements

SiO_2 is relatively constant through sandstone clast populations 1 to 3 (70.8-71.2 wt%) but increases to 74.3 wt% in SCP4 with Al_2O_3 following a reverse trend. This causes a slight increase in SiO_2/Al_2O_3 ratios in SCP1-3 and a pronounced increase in SCP4 (Figure 4.4). Also shown in Figure 4.4 for comparison are mean values for Torlesse sandstone petrofacies from Roser *et al.* (1995). The SiO_2/Al_2O_3 ratio is used as an indicator of the maturity of detrital sediments, because this ratio increases as quartz is progressively concentrated at the expense of less resistant phases during weathering, transport or recycling (Roser and Korsch, 1988). The steady increase of SiO_2/Al_2O_3 ratios from SCP1-4 is consistent with the modal quartz content trends observed in clast petrography. At the same time there is a general decline for other components (TiO_2,

Fe_2O_3, MgO and CaO) which again is consistent with the increased quartz content of the sediments (Table 4.2).

Roser and Korsch (1986) have demonstrated that K_2O/Na_2O ratio is a good indicator for sandstone type and tectonic setting and should also increase with sedimentary maturation as feldspars are converted to K-rich clays. The K_2O/Na_2O ratios increase steadily from SCP1-4 and the K_2O/Na_2O - SiO_2 relationship in all clast populations indicates an active continental margin (Figure 4.5).

The values and the slight increase of SiO_2/Al_2O_3 and K_2O/Na_2O in SCP1-3 are similar to values from PF1-3, and the increase of values in SCP4 is similar to the rise in values in PF4.

On a SAM[2] diagram (Kroonenburg, 1994), which partly mimics a QFL plot, clasts from SCP1-2 lie generally along or just above the primary igneous compositional line (PCT), between granodiorite and granite (Figure 4.6). Clasts from SCP3 lie slightly higher in the distribution than those from SCP1-2 and are displaced slightly towards the SiO_2 apex. The wide extend of values for SCP4 reflects the petrographic range of this population. Clasts from all populations show a good correlation with Torlesse sandstone from PF1-4, with only a few clasts plotting within the field of PF5. Overall the observed trend in the SAM plot parallels the trend observed in the QFL diagram (Figure 4.1b).

A discriminant function plot[3] has been proposed by Roser and Korsch (1988) to distinguish between sediments whose provenance is either primarily mafic, intermediate or felsic igneous, or a quartzose sediment. The Rakaia PF1-PF4 petrofacies data occupy a relatively small field and are geochemically almost indistinguishable (Figure 4.7). However, PF4 shows a slightly different distribution from PF1-3, in plotting at the most felsic end and also extending down towards the PF3-PF4 boundary (consistent with maturation through cannibalistic recycling). Although there is some overlap with PF1-3, virtually all PF5 samples of MacKinnon (1980) plot below the line of igneous averages and also extend down towards the PF3-PF4 boundary but at a lower F2 than PF4. This reflects the minor mafic volcanogenic input inferred by Roser and Korsch (1999) and apparent in MacKinnon's modes. Most of the sandstone clasts plot within those fields

---

[2] SAM: $S = SiO_2/20$; $A = K_2O+Na_2O$; $M = TiO_2+MgO+FeO_t$ (wt%)

[3] $F1 = -1.773TiO_2 +0.607Al_2O_3 +0.76FeO_t -1.5MgO +0.616CaO +0.509Na_a2O -1.224K_2O -9.09$
$F2 = 0.445TiO_2 +0.07Al_2O_3 -0.25FeO_t -1.142MgO +0.438CaO +1.475Na_2O +1.426K_2O -6.861$

close to the rhyodacite composition (Figure 4.7). Mean values for the 4 sandstone clast populations are shown in Figure 4.7b and Table 4.2. The trends indicate a slight maturation from SCP1-4 with mean values for SCP1-3 confined to the PF1–PF3 fields and SCP4 falling within the fields of PF2-4. Almost none of the sandstone clast samples plot in the area in which only Pahau sandstones fall, giving major element support to the petrographic identification of the clasts as Rakaia.

A good measure of the degree of chemical weathering of the source rock can be obtained from the chemical index of alteration (CIA[4]) (Nesbitt and Young, 1982), and values for the clast populations are shown in Table 4.2. In addition weathering trends can be displayed on a $(CaO + Na_2O)$ - Al_2O_3 - K_2O triangular plot (Nesbitt and Young, 1984; Fedo *et al.*, 1995, Figure 4.8). On a diagram of this type the initial stages of weathering form a trend parallel to the $(CaO + Na_2O)$ - Al_2O_3 side of the diagram, whereas advanced weathering shows a marked loss in K_2O as compositions move towards the Al_2O_3 apex.

CIA values from the 4 clast populations show little variation (53.1-55.2) with a mean of 54 that is comparable to those of feldspar (CIA = 50) and unweathered felsic plutonic and volcanic rocks (45-55) (Fedo *et al.*, 1995). Thin section observations are consistent and show virtually unweathered and angular feldspar. The A-CN-K plot in Figure 4.8 shows that all the values are <60. Compositions trend away from the primary compositional line of average igneous rocks of near dacite composition. The average plagioclase to K-feldspar ratio of all the sandstone clasts is approx. 77:23 and is slightly higher than the ratio observed petrographically (P/F = 0.70), reflecting the small amount of K-rich matrix (Fedo *et al.*, 1995; Roser and Korsch, 1999). Comparison with Torlesse sandstone shows that the clasts from SCP1-3 plot mostly within the fields of PF1-3 sandstones and that clasts from SCP4 extend into PF4.

The CIA ratios and A-CN-K values indicate that the clast source has undergone very little chemical weathering prior to deposition, despite the indication that the source was a dissected arc (Figure 4.3), suggesting that uplift had to be fairly rapid, so fresh material was continuously exposed and eroded.

---

[4] CIA = $[Al_2O_3 / (Al_2O_3 + CaO^* + Na_2O + K_2O)$; molar proportions; * = corrected for apatite

4.2.3 Trace Elements

Trace element parameters and discriminatory plots are a useful tool to characterise the provenance and tectonic setting of clastic sediments (Bhatia and Crook, 1986; McLennan *et al.*, 1993). Although a large number of parameters can be used, the immobile trace elements (e.g., La, Th, Zr, Nb, Y, Sc, Co, and Ti) are the most useful.

Bhatia and Crook (1986) showed that sandstones from various tectonically influenced sources fall in discrete fields on trivariate plots. Most of the sandstone clasts of this study fall within the continental island arc field or straddle the active continental margin/passive margin fields (Figure 4.9). This is in agreement with K_2O/Na_2O - SiO_2 relationships of the sandstone clasts presented in Figure 4.3.

Elements typically enriched in evolved felsic rocks or concentrated in more resistant minerals (e.g., Ce, La, Nd, Th, and Y) show no significant variation in average trace element concentration from SCP1 (oldest conglomerate) to SCP4 (youngest conglomerate) (Table 4.2). Overall trends show a slight increase from SCP1-2 and a general slight decline in concentrations from SCP2-4. Elements enriched in basic igneous rocks and associated with mafic minerals (Cr, Cu, Ni, Sc, V, and Zn) display a slight increase in concentrations (Table 4.2). Although there are some anomalies, trace element concentrations for the sandstone clasts generally are similar to PF1-4 values published by Roser and Korsch (1999, Table 4.3), who ascribed the observed trace element variations to an initial source variability and the effect of partial recycling of earlier petrofacies. The observed pattern of enrichment of felsic-linked elements and the depletion of mafic-linked elements is expected both in residual melts during petrologic evolution and through the destruction of mafic minerals during weathering.

Several trace element ratios have been used by Roser and Korsch (1999) to emphasise the patterns observed based on average element concentrations. The use of ratios formed between felsic- and mafic-linked elements maximises the contrast between the elements. The authors state that average ratios of Th/Sc, La/Sc, Ce/Sc and La_N/Y_N should all increase in response to petrologic source evolution and/or maturation through recycling. Inverse ratios like V/La and Ti/Zr should decrease with evolution, as mafic constituents decrease in abundance through petrologic evolution.

Average ratios of trace element concentration for SCP1-4 and PF1-5 are given in Tables 4.2 and 4.3 and are plotted together in Figure 4.10.

Ratios for Th/Sc and La/Sc show a steady decline in concentration from SCP1-3 with a prominent increase between SCP3-4. Ce/Sc increases slightly from SCP1-3 with the biggest increase between SCP3-4. La_N/Y_N, which gives a measure of slope of rare earth (REE) patterns and has been normalised to the chondrite values of Taylor (1985), decreases steadily from SCP1-3 and increases from SCP3-4. Inverse ratios for V/La and Ti/Zr show a positive correlation with decreasing depositional age, with a steady increase from SCP1-3 and a distinct decline in concentration between SCP3-4. This pattern is consistent with the pattern displayed by the ratios for Th/Sc, La/Sc and La_N/Y_N.

Roser and Korsch (1999) used SiO_2/Al_2O_3 - Th/Sc ratios from the Torlesse petrofacies 1-4 together with data from the inboard terranes (Caples, Waipapa, Maitai and Brook Street) to model a possible recycling of these rocks to form the younger Pahau PF5 (their Figure 8b). The authors noted that SiO_2/Al_2O_3 ratios and Th/Sc ratios for PF1-PF3 lie within a narrow field. Both ratios increase in PF4, which is consistent with increase in quartz through recycling and heavy-mineral concentration. The ratios fall sharply in PF5, which the authors attributed to an influx of volcanogenic material, relatively enriched in Sc and depleted in Th.

When plotted on a SiO_2/Al_2O_3 - Th/Sc diagram (Figure 4.11a) the sandstone clasts from the two Rakaia conglomerates show a narrow range of SiO_2/Al_2O_3 ratios (4.5-5.8) and Th/Sc ratios (0.5-1.9). Values are confined to the field of PF1-3 with only one clast plotting in the field of PF5. Petrographically this clast has the highest quartz content, one of the highest mafic contents and one of the lowest total feldspar contents. The sandstone clast element ratios of almost all the Rakaia sandstone clasts are geochemically indistinguishable from PF1-3.

Pahau terrane clasts display a slightly wider range of SiO_2/Al_2O_3 ratios (3.8-6.5) but Th/Sc ratios (0.5-1.9) are similar to the ratios displayed by the Rakaia sandstone clasts (Figure 4.11b). However, clasts from the Mount Saul conglomerate plot within all the Torlesse petrofacies fields and are the only clasts that extend into PF4. Clasts from Ethelton generally plot within the PF1-3 field but extend into the volcanogenetic field.

In contrast to the maturation trend observed in SiO_2/Al_2O_3 - Th/Sc ratios from PF1-4 Torlesse sandstones as noted by Roser and Korsch, mean values for SCP1 to SCP3 display an inverse trend with a pronounced increase in PF4 (Figure 4.11c). This trend is consistent with trends observed in other trace element concentration ratios of the sandstone clasts.

McLennan *et al.* (1993, and references therein) pointed out that since a number of heavy minerals are dominated by elements that are trace elements in most sedimentary rocks (e.g., Zr in zircon, REE elements in monazite and allanite) it is important to assess the heavy mineral concentration during sedimentary sorting. One method of assessment is by examining zircon concentration via Th/Sc vs. Zr/Sc ratios since Zr is strongly enriched in zircon, whereas Sc is not enriched but generally preserves the signature of the provenance. In contrast, Th/Sc is a good overall indicator of igneous chemical differentiation processes since Th is typically an incompatible element, whereas Sc is typically compatible in igneous systems. Sandstone clasts straddle the typical arc volcanic compositional trend (VAT) and plot near the rhyolite composition average (Figure 4.12). There is a small inclined trend away from the VAT in the PF1-5 ratios that suggests minor heavy mineral concentration but in general the ratios of SCP1-4 and PF1-5 reflect the source material.

The Th/Sc vs. Zr/Sc ratios are indistinguishable from data reported by Roser and Korsch (1999) for PF1-5 Torlesse sandstones. All but two sandstone clasts from the Te Moana and Lake Hill conglomerates plot within the field of PF1-3 (Figure 4.13). The probable effect of recycling is also demonstrated by the data from the PF4 sandstones as they also plot mainly in the field of PF1-3. Clasts from Ethelton also show a predominantly PF1-3 association with only one clast plotting in the PF4 field. In contrast, the Mount Saul clasts have PF4 affinities with most of the clasts plotting close or within the field of PF4. Overall, the close association of PF4 with PF1-3 and PF5 with PF1-4 suggests that sedimentary processes have not greatly affected the PF1-3 bulk source composition.

4.3 SUMMARY AND CONCLUSIONS

- Sandstone clasts from SCP1-4 and PF1-5 sandstones are derived from a relatively unweathered source with an average composition similar to that of granodiorite.

- Sandstone clast major and trace element chemical data largely support petrographic observations derived from thin section analysis. Overall the slight increase in modal quartz content in SCP1-4 is consistent with the maturation trend displayed by the major element ratios SiO_2/Al_2O_3 and K_2O/Na_2O. At the same time elements associated with mafic minerals (e.g., TiO_2, Fe_2O_3, MgO, and CaO) display inverse trends. However, the maturation trend is not reflected in trace element concentrations, which vary only slightly between all the sandstone clast populations.

- Compared with Torlesse sandstones, the SCP1-4 clasts are petrographically and geochemically indistinguishable from PF1-3, and SCP4 clasts show some affinity with PF4 sandstones.

- The abrupt change in elemental abundance and indices between PF3 and PF4 is mirrored by the chemistry of the sandstone clasts from Ethelton and Mount Saul. The changes in SiO_2/Al_2O_3, K_2O/Na_2O, trace element ratios and elemental abundance between PF3 and PF4 are generally consistent with sedimentological maturation produced by the onset of recycling, as proposed by MacKinnon (1983) and Roser and Korsch (1999).

- Mean trace element ratios of SCP1-4 show that all sandstone clasts are geochemically indistinguishable from PF1-3. There is a negative correlation between Th/Sc, La/Sc and La_N/Y_N ratios with decreasing depositional age in SCP1-3. This negative trend is in agreement with the positive relationship between depositional age and V/La and Ti/Zr ratios. In other words, the trend observed in the SCP1-3 trace element ratios is toward slightly more primitive material as the depositional ages decrease. This trend contradicts the slight maturation trend for PF1-3 trace element concentration ratios reported by Roser and Korsch (1999).

- The trends observed in all trace element ratios in the sandstone clasts strongly suggest that the trace element ratios in SCP1-3 reflect the unroofing of older Rakaia terrane rocks. The Rakaia terrane collided with the Caples terrane by the latest Triassic and this marked the beginning of the uplift and erosion of the Rakaia rocks and possibly the inboard volcanogenetic terranes. As erosion of the source increases older sediments with less evolved trace elemental ratios are tapped and redeposited.

- The similarities of petrographic, chemical compositions and ratios between sandstone clasts from the Rakaia terrane conglomerates (SCP1-2) and Torlesse sandstones of PF1-3 suggest that clasts in the Te Moana and Lake Hill conglomerates have been derived mainly by autocannibalistic reworking of older Rakaia rocks. The reworking is illustrated by SiO_2/Al_2O_3 - Th/Sc ratios in Figure 4.11.

- Uplift of the Rakaia terrane into the Cretaceous (Adams and Graham, 1997; Little *et al.*, 1999) exposed older Rakaia rocks and at the same time rocks of PF4 affinities were exposed in the source area, at least for the Mount Saul conglomerate. This is shown in Figure 4.11 where only clasts from this conglomerate plot in the field of PF4.

- The exposure of volcanogenetic inboard rocks is suggested by the wide range of SiO_2/Al_2O_3 - Th/Sc ratios in the sandstone clasts from the Ethelton conglomerate. However, none of the sandstone clasts that plot in the VT (volcanic terrane) field show any petrographic similarities with sandstones from the Caples, Maitai, Murihiku or Brook Street terranes (i.e., high lithic content, Figure 4.1b). Petrographically the rocks with VT affinities have some of the highest %mafic content of all sandstone clasts and this is reflected in high Sc and low Th concentrations, indicating that sandstones of a more primitive nature (e.g., Caples terrane) were accessible for erosion.

CHAPTER 5
PAHAU TERRANE IGNEOUS CLASTS

CHAPTER 5

PAHAU TERRANE IGNEOUS CLASTS

Introduction

In this chapter petrography and chemistry of the igneous clasts from the Pahau terrane are documented in order to determine petrological characteristics and magma types for these clasts.

5.1 PETROGRAPHY

5.1.1 Petrographical Classification

5.1.1.1 Plutonic Clasts

Modal percent proportions were obtained from all granitoid samples except the granitic orthogneisses from the Boundary Creek location. All thin sections were first examined by transmitted light microscopy, and qualitative descriptions were made of all the major and accessory mineral phases, textural data and secondary modification features (Appendix 6). Plagioclase compositions were determined by the Michel-Lévy or the combined Carlsbad twin method outlined by Shelley (1985), or by comparison of refractive index where {010} could not be identified with confidence. Subsequently, all thin sections were stained for K-feldspar and each thin section was scanned using a high-resolution slide scanner. Quantitative analysis of each digitised image was made with 'Image Tool', an image analyser, and proportions of the major mineral phases quartz, alkali feldspar and plagioclase feldspar were obtained. Detailed description of feldspar staining techniques, scanning and image analysing procedures are given in Appendix 2.

Rock classification according to modal mineral content was made on the basis of the quartz–alkali feldspar–plagioclase feldspar ternary diagram (QAP) as described by Le Maitre (1989). Samples were grouped according to textural character at the final stage of crystallisation, i.e., hypersolvus or subsolvus. Hypersolvus granitoids are

defined as those which crystallise at low water pressure (<5 kbar), as indicated by the presence of a single alkali feldspar of intermediate composition, often unmixed to mesoperthite. Textural features such as granophyric intergrowth indicate a rapid quenching or freezing of the magma which may be related to loss of volatiles along fractures near the surface, or upward movement of magma which intersects the negative sloped of the water saturated-solidus for granite (Shelley, 1992). Subsolvus granitoids are defined as those that crystallised at higher water pressure and at greater depth as indicated by the presence of individual crystals of Or-rich alkali feldspar (orthoclase or microcline) and An-poor plagioclase.

Most granitoids collected range in crystal grain size from 1-5 mm and would traditionally be classified as medium grained (Hibbard, 1995). For the purpose of this study the break between medium and coarse grained is set at 2.5 mm to get a better resolution on the grain size variation between samples.

5.1.1.2 Volcanic Clasts

The fine grained nature of the matrix material in the volcanic samples precludes a classification using modal mineralogy determined by point counting or by digital image analysis. Samples were classified according to the Total-Alkali-Silica-diagram (TAS, Le Maitre *et al.*, 1989), and mineralogical and textural descriptions were made subsequent to the initial geochemical grouping (Appendix 6). Modal percent proportions for phenocrysts and matrix were estimated and the matrix is described using the terms 'glassy', 'felsitic' and 'spherulitic'.

5.1.2 Alteration

All the sequences in which the conglomerates occur have suffered low-grade metamorphism. The broad area of non-schistose Torlesse rocks (textural grade 1 as defined by Bishop (1972)) are zeolite and prehnite-pumpellyite facies, within which a few semi-schists and schists occur. MacKinnon (1980b) noted that the zeolite facies rocks are more common in eastern and northern exposures (Pahau terrane) and prehnite-pumpellyite facies rocks in the western and southern exposures (Rakaia terrane). The transition from non-schistose to semi-schistose rocks (textural grade 2) corresponds approximately to the transition from prehnite-pumpellyite- to pumpellyite-actinolite-facies rocks.

The conglomerate at Boundary Creek (Chapter 6) is located within the chlorite zone of the greenschist facies whereas all other Rakaia terrane conglomerates described in Chapter 6 are part of the prehnite-pumpellyite facies. The conglomerate locations of the Pahau terrane all fall within the zeolite facies.

Much of the alteration observed in the samples is the result of this metamorphism, and chlorite is the most widespread secondary mineral in all conglomerates, partly or completely replacing mafic silicate minerals – especially biotite, but also hornblende and clinopyroxene. Granular titanite often accompanies chlorite and epidote and also occurs marginally to opaque oxide mineral grains. Some epidote is associated with and replaces plagioclase and is sometimes accompanied by calcite. Crosscutting veins in some samples from the Rakaia terrane contain prehnite. However, it is not clear if the veins: (1) continue into the matrix and therefore post-date the deposition of the clast or (2) are confined to the clast and hence predate deposition of the clast. MacKinnon (1980b) observed that many of the clasts from at least the Middle Triassic onwards contain prehnite, pumpellyite or quartz veins, whereas the enclosing matrix does not, indicating that these clasts have been metamorphosed prior to deposition.

Brief petrographic descriptions of the Pahau terrane igneous clasts, concentrating on the primary minerals, and drawn mainly from the least altered rocks, are given below.

5.1.3 Mount Saul

Plutonic, holocrystalline and leucocratic samples plot predominantly within the monzogranite field with some scatter into the syenogranite, quartz monzogranite and granodiorite field (Figure 5.1a). Volcanic samples are dominated by rhyolites with minor dacites and trachytes as shown in (Figure 5.1b).

5.1.3.1 Syenogranite

The subsolvus syenogranite samples are coarse grained and hypidiomorphic. Euhedral to subhedral sodic oligoclase makes up 23 % of the rock, and laths measure up to 4 mm in size. Crystals are normally zoned, emphasised by the replacement of more calcic cores by sericite. The plagioclase is poikilitically overgrown by perthitic

orthoclase that constitutes 47-48 % of the samples. Quartz is interstitial, has sutured subgrain margins and sometimes exhibits an undulose extinction.

Dark brown biotite is a minor phase (1-2 %), is partially replaced by chlorite, and is often associated with titanite, epidote and subhedral Fe-Ti oxides. Accessory minerals include zircons that are enclosed in biotite.

5.1.3.2 Monzogranite

Both subsolvus and hypersolvus monzogranites are medium to coarse grained and leucocratic. Subsolvus samples are dominated by a hypidiomorphic texture but some samples display some interstitial granophyric intergrowth. Hypersolvus samples are moderately to weakly porphyritic and contain abundant granophyric intergrowth.

In subsolvus samples, subhedral sodic plagioclase makes up 31-47 % of the rock and calcic cores are sericitized. Some crystals display a poikilitic texture overgrowing small (0.5-1 mm) biotite grains. Orthoclase or microcline, displaying the distinct transformation twinning (Figure 5.2), is perthitic and constitutes 21-41 % of the samples. The interstitial, anhedral quartz displays undulose extinction, and in some samples forms an interstitial granophyric intergrowth that is mantling orthoclase and plagioclase grains (Figure 5.3).

1-5 % green brown/light brown pleochroic biotite is found in all the samples, and it usually shows replacement by chlorite and epidote (Figure 5.4). Other mafic minerals (possibly hornblende?) are represented by pseudomorphs made up of chlorite, epidote and Fe-Ti oxides. Accessory minerals include apatite and zircon.

Major minerals in hypersolvus monzogranite are similar in composition to those in the subsolvus monzogranites. However, orthoclase of intermediate Or-An composition is the alkali feldspar phase. In porphyritic samples the sodic plagioclase crystals are up to 5 mm in length. Biotite, partially replaced by chlorite and epidote, constitutes 1-5 % of the rock and in one sample (UC30822) 12 % of the rock.

5.1.3.3 Quartz Monzogranite

The medium to coarse grained quartz monzogranites display a moderate porphyritic texture. Quartz is interstitial and constitutes only 7-10 % of the rock. Sodic plagioclase (An_{15}) is normally zoned, and in sample UC30855 it is first mantled by

more sodic plagioclase or albite and subsequently by alkali feldspar, displaying a antirapakiwi texture. The alkali feldspar is orthoclase, exhibits patch perthite and in addition to its mantling plagioclase occurs interstitially. Alkali feldspar makes up 34-44 % and plagioclase 44-50 % of the samples.

Biotite, partially replaced by chlorite, is dark brown/light brown pleochroic and associated with opaque Fe-Ti oxides. Zircon is the only accessory mineral recognised.

5.1.3.4 Granodiorite

All samples are hypersolvus, medium to coarse grained, with a porphyritic texture and interstitial granophyric intergrowth (Figure 5.5).

Subhedral to euhedral, albite/pericline twinned sodic plagioclase (An_{15}) is rimmed with albite composition rims and cores are replaced by sericite. Crystals range in size from 1-4 mm and constitute 46-52 % of the rock. Small grains of alkali feldspar occur interstitially but are mainly intergrown with quartz to form a very pronounced granophyric texture, visible in hand specimen. Quartz also occurs as separate grains which display no obvious signs of strain..

Dark brown/light brown pleochroic, subhedral to euhedral biotite (1-5 %) is partially replaced by chlorite and often occurs together with anhedral opaque Fe-Ti oxides, epidote and titanite which have replaced other mafic minerals.

5.1.3.5 Rhyolite

These rocks are holocrystalline to hypocrystalline and dominate the volcanic sample population. Phenocrysts comprise 10-55 % of these rocks and include broken euhedral and/or deeply embayed bipyramidal quartz ranging in size from <1 mm up to 3.5 mm. Plagioclase (An_{15}-An_{20}) ranges in size from 1-4 mm. In some samples the subhedral to euhedral grains are rimmed with albite to sodic plagioclase (An_5-An_{15}) and cores are partially replaced by small epidote crystals during saussuritization. The alkali feldspar is perthitic, subhedral to euhedral orthoclase. The estimated phenocryst population consists of 1-25 % quartz, 4-15 % plagioclase, and 1-20 % orthoclase. In one sample quartz phenocrysts are absent. Phenocrysts are sometimes clustered to form a glomeroporphyritic texture. Volcanic lithic fragments constitute 1-10 % of the whole rock, displaying porphyritic, spherulitic and trachytic textures (Figure 5.6).

Accessory minerals include remnants of dark brown biotite, which in most samples has been replaced, together with other mafic minerals, by chlorite, epidote, calcite and Fe-Ti oxides. One sample (UC30854) contains small crystals (0.2-0.5 mm) of blue/green pleochroic amphibole, presumably riebeckite but difficult to determine optically.

The generally fine grained felsic matrix frequently displays flow layering, trachytic or spherulitic textures. The matrix is a mixture of quartz and alkali feldspar, altered biotite and Fe-Ti oxides.

5.1.3.6 Dacite

The samples are hypocrystalline and phenocrysts comprise 10-15 % of the rock. Quartz is present as small (0.5 mm) rounded and embayed crystals that make up <1% of the crystal population. Albite and Carlsbad twinned plagioclase is albite ($<An_5$), crystals range in size from 0.5-1.0 mm and phenocrysts display a glomeroporphyritic texture. Distinctive chlorite, epidote and calcite pseudomorphs after hornblende and biotite are common. Accessory minerals include minor primary euhedral epidote and titanite and subhedral Fe-Ti oxides.

Volcanic lithic fragments constitute 15-60 % of the rock. Very fine grained felsitic textures predominate but trachytic and minor spherulitic textures are recognised. Hypidiomorphic granodiorite xenoliths are present within some of the dacites.

The matrix is a felsitic combination of quartz and feldspar, with epidote, and chlorite also present. If glassy, the matrix usually displays a strong flow layering.

5.1.3.7 Trachyte

The samples are hypocrystalline and porphyritic with 20-45 % phenocrysts that are dominated by euhedral 0.2-3.5 mm large calcic oligoclase (An_{20}). Other phenocrysts include chloritized biotite and pseudomorphs now consisting of chlorite, Fe-Ti oxides and titanite.

The matrix is glassy or very fine grained crystalline felsite with flow layering and in some cases spherulitic texture.

5.1.4 Ethelton

The recalculated major mineral abundances for the leucocratic, holocrystalline granitoid samples from the Ethelton conglomerate have been plotted on the QAP ternary diagram (Figure 5.7a), and the classification of the volcanic samples based on the TAS diagram is shown in (Figure 5.7b).

5.1.4.1 Monzogranite

Subsolvus and hypersolvus monzogranites are generally medium to coarse grained. Subsolvus samples are hypidiomorphic or weakly to moderate porphyritic and some display a minor granophyric texture. The quartz, which forms 26-38 % of the rocks, occurs in equidimensional grains or in clusters of such grains and some show undulose extinction. In some samples quartz is recrystallised and displays a mosaic texture.

Subhedral plagioclase with normal zoning is albite to sodic oligoclase (An_5-An_{20}) and comprises between 30-49 % of the rocks, with a maximum crystal size of 5 mm. Rims of more sodic compositions mantle plagioclase in many rocks. The anhedral alkali feldspar (25-37 % of the rock) is perthitic oligoclase and occurs as large grains of up to 3.5 mm in size. In some samples euhedral to subhedral crystals are rimmed by granophyric intergrowth.

Hypersolvus monzogranites are undeformed, hypidiomorphic or porphyritic, and granophyric texture is common. Rocks consist of 23-44 % undeformed quartz. Albite, epidote, clinozoisite and sericite have replaced some sodic plagioclase (An_{10}-An_{20}). Alkali feldspar is perthitic orthoclase that is slightly kaolinitized in some samples.

Euhedral to subhedral green/brown biotite is the dominant mafic mineral and makes up 1-5% of the rock in all monzogranites. One sample (UC30956) contains subordinate muscovite and a dark brown biotite. Calcite, epidote and chlorite form pseudomorphs replacing previous mafic minerals that include biotite and hornblende. Opaque oxide minerals, apatite and zircons are widespread accessory minerals (Figure 5.8).

5.1.4.2 Granodiorite

The subsolvus granodiorites are medium to coarse grained and hypidiomorphic. Four samples are moderately to weakly porphyritic with one displaying minor interstitial granophyric intergrowth.

Quartz makes up 24-35 % of the rock and shows some undulose extinction. In one sample (UC30969), quartz has undergone grain size reduction as a result of dynamic recrystallisation and plastic deformation by basal a-slip, and ribbons are wrapped around more resistant feldspar (Figure 5.9).

The granodiorites contain 42-51 % subhedral to euhedral normally zoned plagioclase with slightly sericitized cores and rims of albite to sodic oligoclase (An_5-An_{15}). Crystal size is up to 5 mm in porphyritic samples. The alkali feldspar is interstitial, perthitic orthoclase, and it makes up 20-24 % of the rock. Myrmekite is commonly associated with alkali feldspar/plagioclase boundaries.

Minor green/brown subhedral to euhedral biotite is partially replaced by chlorite and makes up 1-5 % of the rock. Primary and secondary muscovite occurs in one sample but constitutes <1 % of the rock.

Accessory minerals include subhedral apatite and zircons. Epidote and chlorite replacement of mafic minerals is apparent. Calcite is common in crosscutting veins but is also associated with biotite.

5.1.4.3 Rhyolite

Samples are porphyritic or glomeroporphyritic and contain 10-70 % phenocrysts.

Phenocrysts include euhedral bipyramidal or deeply embayed quartz with slightly undulatory extinction; fractured grains are common. Quartz makes up 5-30 % of the phenocryst population. Euhedral to subhedral plagioclase (An_{10}-An_{20}) is normally zoned and cores are often replaced with sericite and in some cases replaced by epidote crystals during saussuritization. The euhedral to subhedral alkali feldspar is perthitic orthoclase ($2V_X \approx 60°$). Granitoid and volcanic xenoliths are also present and display granophyric, poikilomosaic and trachytic textures.

Light/dark brown pleochroic, euhedral to subhedral biotite is common, and some samples contain euhedral light green amphibole. Mafic pseudomorphs are associated

with opaque Fe-Ti oxides, epidote, titanite, and chlorite. Samples contain pseudomorphs of amphibole that are now represented by a symplectite of epidote and quartz, though the cleavages, intersecting at 120°/60° are still recognisable (Figure 5.10).

The hyalo- to hypocrystalline matrix in most samples displays generally a finely crystalline felsitic texture that comprises a mixture of feldspar and quartz with minor epidote, chlorite and opaques. In some samples the matrix is spherulitic.

5.1.5 Kekerengu

The majority of granitoid samples from Kekerengu plot within the monzogranite field with some minor scatter into the syenogranite and granodiorite fields (Figure 5.11a). All granitoid samples are medium to coarse grained and leucocratic. Rhyolites dominate the volcanic sample population (Figure 5.11b).

5.1.5.1 Syenogranite

The dominant mineral phase in the subsolvus, hypidiomorphic samples is perthitic orthoclase or microcline that makes up 53-58 % of the rock. Subhedral sodic oligoclase has albite twinning and normal zoning, and more calcic cores are replaced by sericite. Quartz is anhedral and undeformed. Minor phases include brown green biotite, partially replaced by chlorite, and pseudomorphs of green-blue amphibole. These phases are, together with plagioclase and quartz, poikilitically overgrown by alkali feldspar. Accessory minerals include Fe-Ti oxides and zircon.

5.1.5.2 Monzogranite

The subsolvus and hypersolvus samples differ in texture; the subsolvus are hypidiomorphic, the hypersolvus porphyritic and granophyric. In addition, the subhedral alkali feldspar in the subsolvus samples is perthitic Or-rich orthoclase or microcline that constitutes 24-39 % of the whole rock whereas in the hypersolvus samples the anhedral to subhedral, perthitic orthoclase is of intermediate Or-Ab composition and makes up 28-40 % of the rock.

In all the samples the plagioclase, often weakly sericitized and/or saussuritizised, is a sodic oligoclase (An_{10}-An_{15}), often rimmed by albite or more sodic oligoclase and constituting 29-37 % of the rock. The quartz in subsolvus samples forms large undeformed crystals whereas in hypersolvus samples most of the quartz is part of the

interstitial granophyric texture. In some samples myrmekite is present along the grain boundaries of alkali feldspar.

Dark brown/light pleochroic biotite constitutes 1-6 % of the rock, is often replaced by chlorite, and is often associated with minor epidote, calcite and Fe-Ti oxides. Primary muscovite is present as small (0.5-1.0 mm) crystals in a few samples only. Accessory minerals include euhedral apatite and zircon. Foliated samples are subordinate and most samples are undeformed.

5.1.5.3 Granodiorite

The granodiorite samples are dominantly undeformed and subsolvus. The subhedral to anhedral sodic oligoclase (An_{10}-An_{20}) is always strongly sericitized and is, at 44-52 %, dominant over the perthitic orthoclase which constitutes only 7-22 % of the samples. Interstitial quartz is anhedral with slight undulose extinction and varies in proportion from 22-48 %.

Biotite is fine grained dark brown/brown pleochroic and associated with opaques and, if strongly altered, replaced by chlorite and biotite. Titanite, apatite, Fe-Ti oxides and zircons are minor accessory phases.

5.1.5.4 Rhyolite

The samples are holo- to hypocrystalline and porphyritic, and phenocrysts comprise 10-60 % of the whole rock. Rounded or euhedral quartz is deeply embayed or skeletal and grains range in size from 0.2 mm up to 6.5 mm. Subhedral to euhedral oligoclase (An_{10}-An_{20}) is, at 6-35 %, the major phenocryst phase in most samples. The crystals range in size from 0.5-3 mm, and their cores are partially replaced by sericite or small epidote crystals as the result of saussuritization (Figure 5.12). The alkali feldspar is orthoclase, which is perthitic, subhedral to euhedral, and often Carlsbad twinned. Orthoclase crystals are smaller in size than the plagioclase, and make up 1-16 % of the whole rock. A glomeroporphyritic texture is common.

The rhyolites contain xenoliths with trachytic texture dominant. The xenoliths constitute c. 1-10 % of more than one third of rhyolite samples.

Minor minerals include remnants of dark brown biotite, which in many samples has been replaced by chlorite. Other mafic pseudomorphs are represented by amalgamations of chlorite, epidote, calcite, titanite and Fe-Ti oxides. (Figure 5.13).

The matrix, if not glassy, is felsitic, fine grained to microcrystalline, and frequently shows flow layering and/or a trachytic texture.

5.1.5.5 Trachyte

The trachytic samples are porphyritic and contain 15-30 % phenocrysts that are dominated by euhedral to subhedral 0.2-2.0 mm calcic oligoclase (An_{25}). Other minor phenocryst phases include quartz, perthitic orthoclase, brown and partially chlorite-replaced biotite and other, but minor, mafic pseudomorphs. Xenoliths constitute 3-40 % of the whole rock and are surrounded by a felsitic, trachytic matrix.

5.2 GEOCHEMISTRY

5.2.1 Introduction

Geochemistry, in association with petrographic characteristics has enabled subdivision of the igneous samples into the following groups: 'subsolvus', 'hypersolvus' and 'volcanic'. In addition, geochronological (Chapter 3) and isotope data (this chapter) strongly suggest that the main provenance for most of the samples from all 3 conglomerates is part of a single igneous suite. Thus all samples from the 3 conglomerate locations have been pooled and are discussed together. Some rhyolite samples from the Mount Saul conglomerate and one from Kekerengu have been chemically identified as peralkaline or 'A-type' and treated as a separate group.

Proportions and distributions of granitoid and volcanic samples analysed for this study, including samples from Dean (1993), are shown in Figure 5.14. As emphasised in Chapter 1 the collection of the analysed samples was biased towards larger samples (cut-off size approx. 10 cm). For this reason smaller samples from each conglomerate have been analysed as well to avoid an underrepresentation of this group. In discriminant diagrams chemical analyses of hypersolvus and subsolvus samples are plotted as granitoids and are combined with volcanic samples.

White and Chappell (1983) first recognised that the granitoids and related volcanic rocks of the Lachlan Fold Belt, southeastern Australia, could be grouped according to source rock features using petrography and geochemical data. Distinction is made between rocks derived from igneous (I-type) and sedimentary (S-type) sources. S-types chemically reflect a source that has undergone at least one weathering cycle at the Earth's surface. Late stage felsic anorogenic (A-type) granitoids and volcanics were identified as being derived from depleted crust formed as a result of previous I-type magma production (Collins *et al.*, 1982). Expansion of this classification has occurred with the recognition that further subdivisions could be made within these initial groupings (Whalen *et al.*, 1987; Eby, 1990; Chappell and White, 1992; Eby, 1992) and this is discussed in Section 5.2.5.

This alphabet-type classification of granitoid is only a useful way of emphasising unique geochemical characteristics and as a comparison between geochemically similar granitoids. However, highly fractionated granitoids approach minimum-melt compositions and the characteristic elements that define a granite type overlap with other granite types (e.g., Collins *et al.*, 1982; Whalen *et al.*, 1987; Weaver *et al.*, 1992).

5.2.2 Major and Trace Elements

The samples encompass a broad spectrum of compositions (Table 5.1 and Appendix 7), with SiO_2 values ranging from 64-81 % and with major concentrations between 74-78 % SiO_2 corresponding broadly to a monzogranitic composition (Figure 5.15).

On an AFM diagram (Figure 5.16) all the samples exhibit the fractionated end of a typical calc-alkaline trend. A modified Peacock diagram classifies the rocks more correctly (Figure 5.17) and shows a range of Peacock indices for all samples spreading between 56-66 with a Peacock index of 62 where the regression line crosses the zero value of $Log(CaO/Na_2O+K_2O)$. Samples from Ethelton define a narrow range (64-67; Peacock index of 66) and are classified as calcic whereas samples from Kekerengu are classified as calc-alkaline to calcic (57-66; Peacock index of 61). Samples from Mount Saul display a similar range of compositions (56-62) ranging from alkalic to calcic. This classification is also supported by the alkali-silica plot in Figure 5.18, which indicates a predominance of alkaline samples at Mount Saul and the presence of alkaline samples at Kekerengu. The majority of the samples lie within the high-K calc-alkaline series of

Peccerillo and Taylor (1976) and show a total overlap between the samples from all 3 locations (Figure 5.19).

Aluminium Saturation Indices (ASI) for all igneous samples (Appendix 7, Table 5.1 and Figure 5.20) show that a wide range of ASI occurs with a poorly defined trend of slightly increasing A/CNK and pronounced decreasing A/NK with increasing average SiO_2 content[5].

At Kekerengu 12 samples plot within the metaluminous field with an ASI <1.0 suggesting an igneous, or I-type character (White and Chappell, 1983; Chappell and White, 1992). Four samples have an ASI >1.1 suggesting a metasedimentary source, or S-type character (White and Chappell, 1983; Chappell and White, 1992). The remaining samples, and by far the dominant proportion, plot between ASI 1.0-1.1, within the peraluminous field, and as such provide ambiguous information in terms of the I- and S-type classification scheme, because evolved I-types can be weakly peraluminous (Zen, 1986).

At Ethelton 47 weakly peraluminous samples dominate the sample population with only 3 samples classifying as peraluminous granitoids. The remainder of the samples plot within the metaluminous field.

Of the 16 metaluminous samples at Mount Saul 10 are granitoids and 6 are volcanic samples with only 2 samples plotting as peraluminous. All 3 conglomerates are dominated by weakly peraluminous samples with A/CNK between 1 and 1.1. Several samples in the Mount Saul conglomerate are peralkaline with both A/CNK and A/NK <1.

Major element variations are illustrated on selected Harker diagrams in Figure 5.21. TiO_2, Al_2O_3, Fe_2O, MgO, CaO and P_2O_5 all show a negative correlation with SiO_2. Na_2O remains relatively constant with a slight decrease with increasing SiO_2. K_2O shows a crude increase with increasing SiO_2. On the major element Harker plots peralkaline samples are indistinguishable from the other samples. However, the FeO_T/MgO ratio versus SiO_2 is a more effective discriminant and most of the peralkaline samples have generally higher ratios than I- or S-type samples (Figure 5.28).

---

[5] A/CNK = ASI = molar(Al_2O_3/CaO+Na_2O+K_2O)
A/NK = molar(Al_2O_3/ Na_2O+K_2O)

Considerably greater scatter is observed for the trace elements compared to the major elements, however V, Cr, Ni, Zn, Ba, Zr, and Sr generally decrease and Rb increases with increasing SiO_2 (Figure 5.22). Peralkaline samples are characterised by generally lower contents of Cr, Ni, V and Sr, and higher Zr, Nb, Y and Ga which is typical of many A-type rocks (Whalen *et al.*, 1987; Eby, 1990; Eby, 1992). Particularly distinct are the elevated Zr and Nb concentrations in the peralkaline clasts and these clasts can be clearly distinguished from the other metaluminous and peraluminous clasts.

5.2.3 Spider-diagrams

The chemistry of igneous rocks can be illustrated using mantle normalised (McDonough *et al.*, 1992) multi-element diagrams or 'spider-grams'. Spider-diagrams can be used to illustrate any gross elemental differences between volcanic and granitoid rocks and to reflect source rock characteristics. Spider-diagrams of representative samples from each distinctive group of rocks from each conglomerate location are presented in Figure 5.23 and these groups are then compared with each other in Figure 5.24. Variation and scatter at the more mobile end of the spectrum (K, Th, Ba, Rb, Pb) partially reflects the solubility of these elements in aqueous fluids during alteration.

Selected hypersolvus and subsolvus igneous rocks from Ethelton display a distinct spiked pattern indicative of subduction-related magmas (Wilson, 1989; Saunders *et al.*, 1991). There is a general enrichment of large ion lithophile (LIL) elements (which have high ionic radius/charge ratios and include Rb, K, Sr, Ba, Th, Ce and La) and low abundance of high field strength (HFS) elements (which have low ionic radius/charge ratios and include Ti, Zr, Nb, and Y). There is a strong negative anomaly at Nb which is indicative of subduction-related magmas whereas negative anomalies at Ba, Sr and Ti are features that are generally considered characteristic of fractionated magmas (e.g., Saunders *et al.*, 1991). With increasing differentiation these anomalies increase as appropriate minerals (e.g., feldspar, apatite and Fe-Ti oxides) are crystallised. In contrast, relative incompatible elements such as Zr, REE and Y may increase with evolution as they become preferentially concentrated in the residual liquids.

The selected volcanic clasts from Ethelton display a similar inclined spider-pattern to that of the granitoid clasts, with similar negative anomalies at Ba, Nb, Sr and Ti suggestive of a similar source.

Hypersolvus and subsolvus rocks from the Mount Saul conglomerate display a similar multi-element pattern when compared to each other. The distinctive spiked pattern and the overall enrichment in LIL elements indicate that the magmas bear a distinctive crustal signature. The majority of the volcanic clasts mirror the trace element characteristics exhibited by the granitoid clasts and display a typical fractionated character.

Most samples designated A-type from Mount Saul, and one from Kekerengu, display large negative anomalies at Ba and Sr and Ti that are consistent with the removal of feldspar, apatite and Fe-Ti oxides phases. Negative Nb anomalies are minor or absent and together with the enrichment of HFS elements distinguishes these rocks from others of the Pahau terrane.

The multi-element diagrams for the hypersolvus and subsolvus rocks from Kekerengu exhibit similar evolved and subduction-related patterns. Considerable scatter is displayed by the Kekerengu subsolvus clasts with generally smaller negative Ba and Sr anomalies. However, some clasts display minor positive Sr and Ba anomalies that are associated with adakitic rocks (see adakites Chapter 6). Volcanic clasts and hypersolvus clasts display near identical patterns.

Calculated multi-element trend averages of selected rock groups from all 3 Pahau terrane locations are shown and compared in Figure 5.24. Hypersolvus and volcanic rocks from Ethelton, Mount Saul and Kekerengu display, if compared with each other, virtually identical spider-trends. Compared averages of all subsolvus clasts from the 3 conglomerates reflect the pattern displayed by hypersolvus and volcanic clasts from all 3 conglomerates, with minor scatter at Th and Rb. The subsolvus rocks from Kekerengu have a higher Sr content and a lower content in REE, Zr and Y. The averages of peralkaline rocks from this study and from Dean (1993) at Mount Saul are indistinguishable from the pattern displayed by the single clast at Kekerengu.

The metaluminous to weakly peraluminous subsolvus, hypersolvus and volcanic clasts from all conglomerates show a general concordance that suggests a similar petrogenesis for all the clasts described here (Figure 5.25).

5.2.4 Rare Earth Elements

Rare earth element data (REE; Appendix 7) have been obtained for 5 peralkaline rhyolites from Mount Saul and one rhyolite from Kekerengu and are presented in Figure 5.26 on a chondrite normalised diagram (Nakamura, 1974).

The clasts have characteristics typical of many peralkaline granitoids (Whalen *et al.*, 1987; Eby, 1990; Eby, 1992). The peralkaline clasts are LREE enriched (La_N/Yb_N = 2.83 - 8.08), have flat HREE (Gd_N/Yb_N = 0.81-1.52) and moderate to large negative Eu anomalies (Eu/Eu* = 0.17-0.57) indicative of significant feldspar fractionation, an interpretation which is supported by the depletion of Sr and Ba. Most of the samples are also enriched in total REE ($\sum$REE = 105-244), also typical of peralkaline granitoids. Flat HREE contents and relatively abundant Y suggest a source containing stable plagioclase.

The average REE abundance pattern from the Mount Saul peralkaline clasts mimics the pattern displayed by the peralkaline clasts from Kekerengu. Total REE content of the Mount Saul rocks ($\sum$REE = 244) is lower, LREE (La_N/Yb_N = 5.64) are slightly enriched and the Eu anomaly (Eu/Eu* = 0.35) is slightly larger if compared with the clasts from Kekerengu (La_N/Yb_N = 6.11; Eu/Eu* = 0.43), but both groups have near identical flat HREE distribution (Gd_N/Yb_N = 1.14 for Mount Saul; 1.04 for Kekerengu).

5.2.5 Discrimination of Tectonic Setting

Numerous geochemical discrimination diagrams have been published to distinguish the highly characteristic chemistries of peralkaline granitoids from more typical I-and S-type granitoids. Whalen *et al.* (1987) and more recently Eby (1990) and Eby (1992) have illustrate that fractionated, felsic I- and S-type granites can have major and trace element values that deviate from the fields used to distinguish average I- and S-type granites and overlap with those considered typical of A-type granites. The common discriminants used are the HFSE which include Zr, Ce, Nb, Y, and Ga, which have relatively low abundances in subduction-related magmas.

On plots Rb vs. Nb+Y and Nb vs. Y (Figure 5.27) most of the granitoids and most of the volcanic samples from all 3 conglomerates plot predominantly within the field of volcanic-arc-granite (Pearce *et al.*, 1984), with some clasts displaying some within-plate affinities. As expected, the peralkaline clasts from Mount Saul and the single peralkaline clast from Kekerengu all plot in the within-plate-granite field.

On major element vs. HFSE plots the granitoid and volcanic samples from all 3 conglomerate locations plot mainly in both I- and S-type granite fields, with some clasts spreading into the A-type field (Figure 5.28). Volcanic clasts generally exhibit a higher abundance of discriminatory HFS elements. The FeO_T/MgO ratios clearly indicate the evolved character of most of the samples analysed. The peralkaline rhyolite samples from Mount Saul and the one rhyolite sample from Kekerengu are distinctly enriched in the HFSE and are classified as A-type. In Figure 5.29 the peralkaline clasts plot around the average for A-type rocks (Whalen *et al.*, 1987).

Eby (1992) proposed two sub-types of A-type granitoids:

- A_1 sub-type granitoids have trace element compositions similar to ocean island basalts and are interpreted to be extreme crystal fractionates of mantle-derived melts, generally occurring in regions of continental rifting, or related to hotspots or mantle plumes.

- A_2 sub-type granitoids have element ratios intermediate between continental crust and island arc basalts, and are interpreted as being derived from continental crust, or crust that has been through a cycle of continent collision or island arc magmatism.

The identified A-type clasts from both conglomerates plot in the A_2 subtype field (Figure 5.30). Eby (1992) notes that the A_2 sub-type group contains granitoids emplaced in a variety of tectonic settings including post-collisional and what may be true anorogenic magmatism. However, at the present there seems to be no way to distinguish between these tectonic possibilities. Whalen *et al.* (1987) point to the fact that there is often a close spatial relationship and temporal association of peralkaline felsic igneous rocks with calc-alkaline magmatic arc systems.

5.2.6 Sr and Nd Isotopes

Sr and Nd isotopes for the igneous clasts from the Pahau terrane are listed in Table 5.2 and Table 5.3, with detailed analytical methods described in Appendix 2. Initial strontium ratios ($^{87}Sr/^{86}Sr_{(t)}$) and Epsilon Nd ($\varepsilon Nd_{(t)}$) for individual clasts have been calculated to their crystallisation age and are shown in Figure 5.31. Two peralkaline samples from Mount Saul (UC30823 = 0.69634; UC30854 = 0.69938) have very low Sr concentrations and high Rb/Sr ratios which makes them very sensitive to alteration. The unrealistically low $^{87}Sr/^{86}Sr_{(t)}$ values of these clasts have been omitted from the plot. Such low values can be produced by one or more of the following:

- The age used for the calculation of $^{87}Sr/^{86}Sr_{(t)}$ is too high. Recalculation to a common age has a big influence on samples with Rb/Sr ratios.
- The Rb-Sr systems have been disturbed, either Rb gain or ^{87}Sr loss or ^{86}Sr gain.

The accurate U-Pb zircon age determination (Table 3.1) suggests that the low $^{87}Sr/^{86}Sr_{(t)}$ values are mainly caused by the high Rb/Sr ratios of the samples but the disturbance of the Rb-Sr system of two clasts is a possibility.

On a broad scale all the clasts are constrained with $^{87}Sr/^{86}Sr_{(t)}$ between 0.70264 and 0.70622 and $\varepsilon Nd_{(i)}$ values between -1.9 and +3.9. Samples from the Mount Saul conglomerate have the most primitive isotopic compositions with $^{87}Sr/^{86}Sr_{(t)}$ between 0.70264 and 0.70398 and a narrow range of $\varepsilon Nd_{(i)}$ between +2.8 and +3.9. This suggests that the magmas of the clasts have undergone little or no interaction with continental crust.

Clasts from Ethelton have $^{87}Sr/^{86}Sr_{(t)}$ values between 0.70390 and 0.70622 that are similar to those displayed by the clasts from Kekerengu (0.70336 - 0.70592). Kekerengu clasts have the widest range of $\varepsilon Nd_{(i)}$ values ranging from -1.9 to +3.0. The isotopically most primitive clast from Kekerengu (UC30743) is indistinguishable in composition from the Mount Saul clasts whereas the other clasts from Kekerengu show strong similarities with the clasts from Ethelton (-1.7 to +1.3).

A model age is a measurement of the time elapsed since major Sm/Nd fractionation in a rock sample, or its protolith or parent reservoir from a defined mantle reservoir, took place. The basis of all model age calculations is an assumption about the

isotopic composition of the mantle source region from which the sample has been derived. Depleted mantle model ages (T_{DM}) are considered to be more appropriate than model ages calculated to the Chondritic Uniform Reservoir (CHUR, T_{CH}), due to the evidence of widespread existence of LREE depleted reservoirs contributing to the generation of continental crust (Goldstein *et al.*, 1984; Pickett and Wasserburg, 1989; Dickin, 1995). This is confirmed by several samples giving unrealistically low or negative T_{CH} ages (Table 5.3). T_{DM} ages for this study are calculated based on mantle depletion beginning at 4.5 Ga (Maas and McCulloch, 1991) and are presented in Table 5.3. This method of calculation results in T_{DM} ages 0.2 Ga older than those using the method of De Paolo (1981). Consequently all data from other sources used in this study have been recalculated to be consistent with the new data presented here.

T_{DM} values for the Kekerengu clasts range from 0.62 to 0.96 Ga, with one clast (Early Jurassic; UC30732) giving an older T_{DM} age of 1.57 Ga. Samples from Ethelton are slightly older with T_{DM} values ranging from 0.82 to 1.16 Ga, with a single sample giving an unrealistic result (T_{DM} = 6.19 Ga). Igneous clasts from the Mount Saul conglomerate define a narrow range with T_{DM} ranging from 0.6 to 0.9 Ga.

5.3 Summary and Conclusions

5.3.1 Petrography

Monzogranite and leucomonzogranite clasts dominate over granodiorite clasts in all three Pahau terrane conglomerates, but leucosyenogranites are present. Hypersolvus clasts are distinctly granophyric and can easily be distinguished from subsolvus clasts, which are generally undeformed. The volcanic clast population consists predominantly of rhyolites with minor dacites and trachytes. Spherulitic and felsic textures in the matrix of volcanic clasts indicate strong undercooling. However, no pyroclastic clasts were sampled and the source of these clasts is considered to be domes or flows. The alkaline nature of rhyolitic clasts from Mount Saul is petrographically shown by the occurrence of riebeckite, which typically occurs in alkaline plutonic and volcanic rocks (Shelley, 1985).

The evolved and fractionated igneous clasts lack the distinctive minerals that define I and S-type granitoids and if such minerals are present they are often strongly altered.

Petrographic evidence indicates that the source of the Pahau terrane igneous clasts was a volcano/plutonic arc. At the time of deposition of the conglomerates the mainly upper levels of the volcano/plutonic arc were exposed, eroded and subsequently transported to the place of final deposition.

As mentioned previously the collection of clasts was biased towards larger clast sizes. However, this does not preclude the possibility that more mafic samples (e.g., basalts) are represented in the conglomerate population. Basaltic clasts have been found in conglomerates exposed along the Clarence River north of Hanmer Springs (pers. comm. C. Mazengarb) Interestingly, sample collections by other workers (Smale, 1978; Dean, 1993; Mortimer, 1995) are also noted for the lack or rarity of mafic clasts. The preservation of dominance of rounded to well rounded mainly silicic clasts in the Pahau terrane conglomerates from all three locations may indicate that:

- siliceous magmatism dominated in the source area of all three conglomerates
- the catchment of all three conglomerates had no access to mafic rocks
- a selective process during transportation allowed only the more resistant silicic clasts to reach the deposition centre
- mafic clasts have disintegrated and are incorporated into the matrix
- a combination of two or more of these possibilities

5.3.2 Geochemistry

Chemical analyses of smaller sized samples from this study show that collected clasts of various sizes are geochemically indistinguishable from each other.

Two major geochemical groups have been identified within the igneous clast populations from the Pahau terrane: (1) a calc-alkaline group and (2) an alkaline group. A third, minor group consists of a few clasts from Kekerengu that have adakitic affinities. Although only a few clasts were identified, they are significant, as adakitic rocks were emplaced in the New Zealand region at the time of conglomerate deposition (Muir *et al.*, 1995).

Most of the clasts from all three conglomerate locations are part of the calc-alkaline to high-K calc-alkaline series. Weakly peraluminous clasts dominate over

metaluminous clasts and only a few peraluminous samples have been identified. A cogenetic relationship between the calc-alkaline clasts from all three conglomerates is indicated by coherent linear trends displayed in Harker diagrams and by near identical multi-element diagrams for various groups (volcanic, hypersolvus and subsolvus). A cogenetic relationship is also supported by the geochronological data presented in Chapter 4. All clasts display a typical subduction-related pattern and are enriched in incompatible large ion lithophile (LIL) elements with a strong negative Nb anomaly, indicating that the source for all the clasts has been through at least one subduction cycle.

Alkaline clasts and clasts with alkaline affinities from Mount Saul and Kekerengu are typically enriched in trace elements (Zr and Nb) and have rare earth element characteristics typical of A-type rocks, but overall retain a subduction-related signature, probably inherited from their source. The alkaline affinities of many clasts suggest a progression toward anorogenic intrusion during the waning stages of subduction. Trace element compositions do not conclusively differentiate between magmas emplaced at the waning stage of a subduction and magmas related to hotspots or mantle plumes.

Sr-Nd isotope data indicate that magmas of the Mount Saul clasts and one single clast from Kekerengu have undergone little or no interaction with continental crust whereas the magmas of the other Kekerengu clasts and the clasts from Ethelton have experienced some crustal contamination during their petrogenesis.

CHAPTER 6
RAKAIA TERRANE IGNEOUS CLASTS

CHAPTER 6

RAKAIA TERRANE IGNEOUS CLASTS

Introduction

Petrological and geochemical compositions of the igneous clasts from the four Rakaia terrane conglomerates are described in order to determine petrological characteristics and magma types for these clasts. The main feature of the igneous clasts from the Rakaia terrane that distinguishes them from the Pahau terrane igneous clasts is the presence of deformed clasts and the presence of some clasts with intermediate to mafic chemical compositions.

6.1 PETROGRAPHY

Petrographic procedures and classification are described in Section 5.1.1 and a detailed petrographic descriptions of selected clast is given in Appendix 6. A brief petrographic summary, concentrating on the primary minerals, and drawn mainly from the least altered rocks, is given below.

6.1.1 Boundary Creek

All clasts from the Boundary Creek conglomerate were affected by recrystallisation after deposition and display minor to intense deformation features that range from fractured crystals (Figure 6.1) to a mylonitic texture in which well developed solution seams are present.

However, in most samples layers and domains with original igneous crystals and texture are recognisable. Plagioclase (An_{10}-An_{45}) displays albite and pericline twinning, and Carlsbad twinning is present in some crystals. The relatively calcic cores are partially replaced by muscovite (sericite) or fine grained epidote and calcite during saussuritization. Crystals are often rimmed by albite or sodic plagioclase. Some plagioclase has been ductilely deformed (Figure 6.2), suggestive of pre-deposition

deformation. Alkali feldspar is a minor major mineral phase and, if present, is a perthitic orthoclase.

Primary mafic minerals are hornblende and biotite. The hornblende is green brown/light brown pleochroic often twinned hornblende, sometimes partially replaced by chlorite, epidote, titanite and Fe-Ti oxides. Crystals range in size from <0.2->4.0 mm. Dark brown/brown pleochroic biotite is subordinate to the amphibole and often chloritized. The additional secondary mafic mineral is colourless/light green pleochroic actinolite. Primary accessory minerals include euhedral to subhedral apatite, titanite and Fe-Ti oxides.

Dark solution seams are closely spaced and well developed in mylonitic granitoid samples and are wrapped around more resistant amphibole and feldspar porphyroclasts or sometimes around a cluster of igneous grains (Figure 6.3). Most of the quartz in all samples is recrystallised and has undergone grain size reduction. However, bigger grains with undulous extinction occur and are often associated with relic igneous domains. Recrystallised quartz occurs as ribbons with serrated grain boundaries or displays a mosaic texture with distinct dihedral angles of 120°. A weak lattice and/or shape preferred orientation (LPO and SPO) is exhibited by some ribbon quartz. When viewed with an inserted tint plate, subgrains have their c-axes oriented at a high angle to the incipient foliation, suggesting that intracrystalline basal <a> slip controlled the ductile deformation of the quartz.

Some samples display what resembles a glomeroporphyritic texture with clusters of igneous crystals and pseudomorphs of mafic minerals (Figure 6.4).

6.1.2 Te Moana

The recalculated major mineral phase data for the Te Moana granitoid samples are plotted in Figure 6.5a. Sampled volcanic clasts are exclusively rhyolites and are shown in Figure 6.5b.

6.1.2.1 Monzogranite and Granodiorite

The samples are medium to coarse grained and leucocratic. The two subsolvus monzogranite samples display a hypidiomorphic texture. The single granodiorite clast is slightly porphyritic with minor interstitial granophyric intergrowth.

The dominant mineral phase in all samples is subhedral sodic oligoclase (An_{10}–An_{15}) and constitutes 33-50 % of the whole rock. Normal zoning is present, with the more calcic cores replaced by sericite. The subhedral alkali feldspar in the foliated monzogranite samples is a perthitic K-rich orthoclase ($2V_x \approx 45°$), making up 30 % of the rock. It has poikilitically overgrown the plagioclase and some biotite. In the granodiorite sample the mesoperthitic orthoclase is of intermediate composition, is either subhedral or occurs interstitial and is intergrown with quartz to display a granophyric texture. Quartz is anhedral and interstitial and constitutes 28-31 % of the rock and sometime forms a foliation with distinct ribbons and a strong LPO and SPO.

Green brown/light brown euhedral to subhedral biotite is generally associated with opaque Fe-Ti oxides and has been partially altered to chlorite and epidote. Other mafic minerals are very minor and were replaced by chlorite, epidote and titanite. Accessory minerals include apatite, zircon and Fe-Ti oxides.

6.1.2.2 Rhyolite

The samples are porphyritic and hypocrystalline to holocrystalline. Phenocrysts comprise 5-35 % of the whole rock.

Phenocryst phases include undeformed embayed and/or bipyramidal quartz that makes up 2-10 % of the crystal population (Figure 6.6). The crystals are dominated by euhedral to subhedral albite ($<An_{10}$) or sodic oligoclase (An_{10}–An_{20}) that often has cores sericitized or saussuritized. The alkali feldspar is perthitic orthoclase. Plagioclase comprises 3-30 % of the phenocryst population, whereas orthoclase is a minor phase with 1-6 %. Phenocrysts often display a glomeroporphyritic texture.

Partially chlorite-replaced, euhedral to subhedral dark brown/light brown pleochroic biotite is often associated with primary epidote and titanite. Other mafic minerals include euhedral, colourless augite (Figure 6.7), and green/yellow brown hornblende partially replaced by chlorite, epidote and titanite. Accessory minerals include apatite, zircon and Fe-Ti oxides.

Xenoliths constitute 2-5 % of the rock and include volcanic lithics that generally display a trachytic texture but also a rare fine grained, partially recrystallised sandstone fragment (Figure 6.8).

The felsitic matrix comprises a mixture of quartz and alkali feldspar together with minor chlorite, epidote and Fe-Ti oxides that have replaced mafic minerals. Glassy matrix, flow layering and spherulitic textures were observed (Figure 6.9).

6.1.3 McKenzie Pass

The recalculated major mineral phase compositions are plotted on a QAP diagram. The majority of granitoid samples plot within the monzogranite field (Figure 6.10a). All granitoid samples are holocrystalline, medium to coarse grained and leucocratic. Rhyolites dominate the volcanic clast population but minor more basic samples are present and unique to this location and are plotted in Figure 6.10b. Selected lithotypes are described here.

6.1.3.1 Monzogranite

The monzogranite samples are leucocratic. Subsolvus samples are coarse grained and display some deformation whereas hypersolvus samples are generally undeformed.

The hypersolvus differ from subsolvus samples in texture, the hypersolvus being porphyritic and granophyric, the subsolvus hypidiomorphic. In addition, the anhedral alkali feldspar in hypersolvus samples is mesoperthitic orthoclase of intermediate Or-Ab composition that constitutes 23-41 % of the whole rock. In subsolvus samples the anhedral to subhedral alkali feldspar is K-rich orthoclase ($2V_x \approx 45^\circ$) that displays some poikilitic texture and makes up 23-45 % of the rock. An interstitial, fine granophyric intergrowth is observed in one subsolvus sample (UC30900; Figure 6.11).

Weakly to strongly sericitized and/or saussuritized sodic oligoclase (An_{10}–An_{20}) is present in subsolvus and hypersolvus samples and constitutes 28-34 % of the whole rock in the subsolvus and 27-46 % in the hypersolvus samples. Albite twinned crystals are often rimmed by albite or more sodic oligoclase. Crystal sizes range between 0.2-<2 mm, but in porphyritic samples can be >5 mm.

Quartz in subsolvus samples forms large undeformed crystals and constitutes 27-39 % of the whole rock. In foliated samples the quartz has undergone a grain size reduction, forms ribbons with serrated subgrain boundaries and displays a strong lattice and/or shape preferred orientation. In hypersolvus porphyritic samples, quartz can form large euhedral and/or rounded phenocrysts. However, most of the quartz is part of the

interstitial granophyric texture. Myrmekite, when present, is confined to grain boundaries of alkali feldspar.

Dark brown/light brown pleochroic biotite is formed in all samples and is often partially chloritized. Primary muscovite is observed in one sample and is subordinate to red/brown biotite. Epidote, chlorite and titanite form pseudomorphs after mafic minerals. All accessory minerals include subhedral apatite, euhedral to subhedral Fe-Ti oxides and zircon. Prehnite has been observed in crosscutting veins (UC30913; Figure 6.12).

6.1.3.2 Rhyolite

The rhyolite samples are hypocrystalline porphyritic. Phenocrysts constitute 5-25 % of the samples, with 2-15 % quartz, 2-15 % plagioclase and <1-6 % alkali feldspar. Plagioclase phenocrysts are euhedral to subhedral albite or sodic oligoclase (An_5-An_{20}) that range in size from <1-4 mm. In some samples the subhedral to euhedral grains are rimmed with albite to sodic plagioclase (An_5-An_{15}) and cores are sericitized or partially replaced by small epidote crystals as a result of saussuritization. The alkali feldspar is perthitic, subhedral to euhedral orthoclase. Quartz is euhedral or corroded and/or deeply embayed, and grains range in size from <0.2->4.0 mm. Phenocrysts are sometimes clustered to form a glomeroporphyritic texture.

Volcanic xenoliths within the rhyolites constitute 2-10 % of the whole rock and generally display a trachytic texture, but porphyritic and felsitic textures occur.

Accessory minerals include remnants of dark red brown/light brown biotite, which in many cases has been replaced, together with other mafic minerals, by chlorite, epidote, calcite, titanite and Fe-Ti oxides. Mafic minerals make up 1-5 % of the whole rock. One clast (UC30889) contains small crystals (0.2-1.0 mm) of garnet.

The matrix, occasionally glassy, is generally fine grained felsitic and frequently displays flow layering, trachytic or spherulitic textures. The matrix is a mixture of quartz and alkali feldspar, altered biotite, epidote and Fe-Ti oxides.

6.1.3.3 Andesite and Basalt

These samples are hypocrystalline and porphyritic. Plagioclase constitutes 15-35 % of the samples and has been strongly sericitized. In one sample, chemically classified

as an andesite, an andesine composition (An_{45}) has been determined for the plagioclase. Crystal sizes range from groundmass microlath to crystals >4.0 mm. In two samples, twinned, light green/blue green strongly pleochroic hornblende constitutes 10-50 % of the crystal population and is dominant over clinopyroxene, which constitutes only 2-5 % of the rock.

Accessory minerals include dark brown biotite, titanite, epidote, and euhedral Fe-Ti oxides. The matrix exhibits a predominantly trachytic texture, but in one clast a felsitic texture is observed.

6.1.3.4 Dacite

The dacite samples are hyalocrystalline and porphyritic. Phenocrysts comprise 40-55 % of the whole rock and are mainly euhedral to subhedral, albite twinned calcic oligoclase (An_{20}-An_{25}) that range in size from <0.2->3.0 mm and often have strongly sericitized and/or saussuritized cores. Mafic minerals constitute 8-10% of the whole rock and include red brown/light brown strongly pleochroic biotite that shows pronounced opaque peppered reaction rims and partial replacement by chlorite (Figure 6.13). Unaltered hornblende is green brown/light brown pleochroic (Figure 6.14) but mainly, together with other mafic minerals, it is totally altered to chlorite, epidote, titanite and opaque Fe-Ti oxides. Other accessory minerals include euhedral titanite, apatite and Fe-Ti oxides. The matrix is felsitic or glassy with flow texture in places.

6.1.4 Lake Hill

The recalculated major mineral phases for the leucocratic, medium to coarse grained granitoid samples are plotted on a QAP ternary diagram (Figure 6.15a). Subsolvus samples dominate and are described below. Volcanic clast compositions are shown on the TAS classification diagram in Figure 6.15b.

6.1.4.1 Monzogranite

All subsolvus samples are hypidiomorphic. Interstitial granophyric intergrowth has been observed in one clast only. Approximately 70 % of the samples display foliations that range from weakly to strongly developed, and recrystallisation is evident. Strain partitioning is obvious in some samples.

Euhedral to subhedral, albite twinned albite to sodic oligoclase (An_5–An_{15}) constitutes up to 45 % of the rock. Crystals are rimmed with albite or sodic oligoclase and normal zoning is emphasised by the sericitization of the cores. In some samples epidote partially replaced the more calcic cores during saussuritization. Some crystals display a rounded form and were ductilely deformed. The alkali feldspar is subhedral to anhedral perthitic orthoclase or microcline which often poikilitically encloses plagioclase, biotite and/or muscovite. Alkali feldspar crystals range in size from <0.2->5 mm and make up 20-42 % of the whole rock.

Anhedral quartz is in most samples interstitial, has sutured subgrains and comprises 23-48 % of the rock. In foliated gneissic samples, quartz displays a strong lattice and/or mineral preferred orientation. Quartz ribbons are deflected around more resistant porphyroclasts and, if viewed with an inserted tint plate, have their c-axes oriented either at a high angle to the foliation or parallel to the foliation. The first suggests that the chief parameter controlling MPO of quartz is intracrystalline basal <a> slip; the latter suggests intracrystalline prism <c> slip (Figure 6.16).

Subhedral, brown-green and, if associated with muscovite, red-brown biotite, is present in all samples and constitutes 1-5 % of the rock. Crystal sizes range from <0.2->2.5 mm. Alteration is minor and if present, crystals are partially replaced by chlorite, epidote and Fe-Ti oxides. Primary muscovite is encountered in more than a third of all the samples (Figure 6.17). Muscovite is equally proportioned to, or subordinate to, biotite. Accessory minerals include Fe-Ti oxides, apatite, zircon and often euhedral garnet.

6.1.4.2 Granodiorite and Tonalite

The majority of the rocks chemically identified as adakites (see below) are part of this group. In these hypidiomorphic rock samples the dominant major mineral phase is euhedral to subhedral sodic to calcic oligoclase (An_{10}–An_{25}) that makes up 41-57 % of the granodioritic rock, and 53-68 % of the tonalitic rock. Core replacement is by sericitization or saussuritization with associated secondary muscovite and epidote. The alkali feldspar in granodiorite samples is subhedral to anhedral perthitic microcline or orthoclase and constitutes 7-23 % of the rock. Microcline is common in the majority of the samples. Perthitic orthoclase is the minor alkali feldspar phase in tonalite samples and makes up only 1-5 % of the whole rock.

Anhedral quartz in both granodiorite and tonalite constitutes 21-40 % of the rock, is interstitial and, if associated with a foliation, displays a strong LPO and/or SPO.

In both lithotypes the dark brown/light brown pleochroic biotite is euhedral to subhedral, ranges in grain size from <0.2->1.5 mm and constitutes 1-7 % of the rocks. Primary euhedral to subhedral muscovite of similar grain size is common, but is always subordinate in abundance to biotite. In the granodiorite samples the muscovite and biotite are often poikilitically overgrown by alkali feldspar.

Very few other mafic minerals are present, but if present, they were replaced by chlorite, epidote and opaque Fe-Ti oxides. Accessory minerals include euhedral garnet, apatite and zircon.

6.1.4.3 Rhyolite

The porphyritic rhyolite samples are hyalo- to holocrystalline and contain 10-65 % phenocrysts. Phenocrysts include euhedral and/or well-rounded, often fractured, deeply embayed and skeletal quartz with slightly undulatory extinction. Quartz makes up 2-25 % of the phenocryst population. Euhedral to subhedral albite (An_5-An_7) constitutes 4-25 % of the samples and is normal zoned and cores are replaced with sericite and/or fine epidote crystals (Figure 6.18). The euhedral to subhedral alkali feldspar is perthitic orthoclase, is subordinate, and together with plagioclase often displays a glomeroporphyritic texture. Volcanic lithic fragments are found in most samples, but with 2-5 % are minor constituents of the whole rock. Most of the xenoliths display a trachytic texture.

Green brown/light brown pleochroic biotite and other mafic minerals are partially or totally replaced by chlorite, epidote, titanite and opaque Fe-Ti oxides.

A mixture of feldspar and quartz with minor epidote, chlorite and Fe-Ti oxides makes up the matrix of most of the samples and displays a finely crystalline felsitic texture. In some samples the matrix exhibits a trachytic texture with a prominent flow layering.

6.1.4.4 Dacite

Phenocrysts comprise 25-40 % of the dacite samples. Sodic oligoclase (An_{10}-An_{15}) constitutes c. 15-20 % of the whole rock. In all three samples the oligoclase has

been strongly sericitized. Undeformed euhedral or rounded quartz makes up c. 5-25 % of the rock. Quartz and oligoclase phenocrysts display a glomeroporphyritic texture in one sample.

Distinctive, opaque peppered chlorite and calcite pseudomorphs after hornblende are recognisable. Other mafic minerals include partially chloritized green brown biotite, green/yellow brown hornblende, titanite, epidote and Fe-Ti oxides. The matrix is either a felsitic combination of quartz and feldspar together with titanite, epidote, chlorite and Fe-Ti oxides, or is glassy with flow layering.

6.2 GEOCHEMISTRY

Petrographic characteristics have enabled subdivision of the igneous samples into the following groups: 'subsolvus', 'hypersolvus' and 'volcanic'. In discriminant diagrams chemical analyses of hypersolvus and subsolvus samples are pooled and plotted together as granitoids. In addition, granodiorite and monzogranite samples from the Lake Hill conglomerate were chemically identified as adakites (Defant and Drummond, 1990; Drummond and Defant, 1990; Atherton and Petford, 1993) and are treated as a separate group.

Geochronological data from Chapter 3 show that the main provenance for most of the samples from the Te Moana, McKenzie Pass and Lake Hill conglomerates is of Permian to Early Triassic age. The main provenance for the Boundary Creek conglomerate samples is of Carboniferous age. However, isotope data presented in Section 6.2.5 show that samples from all four conglomerate locations have a similar petrogenetic signature. In this chapter they are therefore plotted and described together.

Proportions and distributions of granitoid and volcanic samples analysed for this study, including samples from Lake Hill by Dean (1993), are shown in Figure 6.19. As emphasised in Chapter 5 the collection of the analysed samples was biased towards larger samples and for this reason smaller samples from two conglomerates were analysed to avoid an underrepresentation of this group.

Rakaia terrane conglomerates described here are part of the prehnite-pumpellyite facies whereas the conglomerate at Boundary Creek is located within the chlorite zone of the greenschist facies. Hence, all the conglomerate clasts have suffered regional

metamorphism. In addition, some of the clasts from all four conglomerate locations display mylonitic (mainly at Boundary Creek) to gneissic (mainly at Lake Hill) textures and some clasts are crosscut by calcite and/or quartz veins. The deformation of clasts, if present, took place prior to their deposition, with the exception of Boundary Creek clasts, which have undergone recrystallisation and/or deformation mainly after their deposition. Tobisch *et al.* (1991) noted that mylonitised rocks show significant enrichments in SiO_2, CaO, Fe_2O_3 and Sr, and depletion in Na_2O, K_2O, MgO, Ba and Rb with increasing stages of deformation. Element mobility, enrichment and depletion may contribute to and enhance data dispersion in graphical chemistry presentations resulting in outliers.

Mobility of alkalis, and Ca in particular, may be expected given the widespread albitisation of plagioclase observed in Section 6.1. Elements considered to be essentially immobile during alteration are Ti, Zr, Y, Nb, and in particular the rare earth elements (REE); also generally useful are FeO_{total} and Mg (Crawford *et al.*, 1992, and references therein). For example, major element mobility is displayed by many of the adakitic granitoids from Lake Hill. Some lasts display high K_2O values for adakitic rocks, which is probably compensated for by anomalous Na_2O values, whereas the immobile REE elements (Figure 6.33) attest to their adakitic nature.

6.2.1 Major and Trace Elements

The samples encompass a broad spectrum of compositions (Table 6.1 and Appendix 7), with SiO_2 values ranging from 51-81 %. Granodiorite samples are present and form a minor peak. However, the major concentration for all four conglomerates is between 73-79 % SiO_2, with the main peak corresponding broadly to a monzogranitic composition (Figure 6.20).

All the samples exhibit a typical calc-alkaline trend when plotted on an AFM diagram (Figure 6.21). A modified Peacock diagram (Brown, 1982) classifies the rocks more correctly (Figure 6.22) and shows a range of Peacock indices for clasts from individual conglomerates. Samples from Boundary Creek display a wide spread between 55-72, classifying the samples as alkali-calcic to calcic.

Samples from Te Moana define a narrow range (59-67) with an approximate Peacock index of 62, where the regression line crosses the zero value of

Log(CaO/Na_2O+K_2O), and are classified as calcic. Peacock indices for the McKenzie Pass samples range from calc-alkaline to calcic (58-66), with a mean Peacock index of 61 (calc-alkaline). Samples from Lake Hill display a similar range of compositions (58-68), ranging from calc-alkaline to calcic (Peacock index 62). The Peacock classification is, to some extent, supported by the alkali-silica plot in Figure 6.23. The Boundary Creek, Te Moana and Lake Hill clast populations are dominated by calc-alkaline samples (Figure 6.24), with the majority of these samples plotting within the high-K calc-alkaline series of Peccerillo and Taylor (1976). The majority of the Boundary Creek samples and some samples from Lake Hill display low-K tholeitic affinities. Although the whole compositional spectrum of rocks is represented in this classification, the data dispersion may be attributed in part to element mobility.

Aluminium Saturation Indices (ASI) for all igneous samples are shown in Table 6.1 and Figure 6.25.

At Boundary Creek the majority of the clasts plot within the metaluminous field with an ASI <1.0 suggesting an igneous, or I-type character (White and Chappell, 1983; Chappell and White, 1992). One sample is classified as peraluminous (S-type). The remaining five samples have an ASI between 1.0 and 1.1 and as such provide ambiguous information in terms of the I- and S-type classification scheme.

All the clasts from Te Moana have ASI indices >1.0 and are classified as weakly peraluminous or peraluminous.

At McKenzie Pass, 25 clasts have an ASI of <1.0 and are classified as metaluminous or I-type, 25 clasts have A/CNK between 1.0 and 1.1, and 3 clasts have an ASI >1.1 suggesting crustal involvement during petrogenesis.

With the exception of two clasts, all samples from the Lake Hill location have A/CNK >1.0. The majority of the clasts plot between 1.0 and 1.1 giving ambiguous information according to the classification scheme. A significant proportion of the Lake Hill clast population however has an ASI >1.1 suggesting a metasedimentary source, or S-type character (White and Chappell, 1983; Chappell and White, 1992).

Selected Harker diagrams in Figure 6.26 illustrate that TiO_2, Al_2O_3, Fe_2O, MgO and CaO all show a negative correlation with increasing SiO_2. Na_2O increases slightly with increasing SiO_2 content but displays a wide spread between 70-80 % SiO_2. On the

major element Harker plots the adakitic samples from Lake Hill generally have higher Al_2O_3 and Na_2O content but no clear distinction can be made from the other samples.

Some minor scatter is observed within the trace elements, however V, Cr, Ni, Zn, Ba, Zr and Sr generally decrease and Rb increases with increasing SiO_2 (Figure 6.27). Adakite samples from Lake Hill can be distinguished from other samples by their generally lower Y and higher Sr contents. This is further emphasised on a plot of Sr/Y vs. Y (Figure 6.28) used by Defant and Drummond (1990) to distinguish slab-derived from mantle-wedge-derived magmas. All the adakitic samples plot within the adakite field and other plutonic clasts from Lake Hill and one rhyolite sample from McKenzie Pass also show adakitic affinities.

6.2.2 Spider-diagrams

Spider-diagrams of representative samples from each distinctive group of rocks from each conglomerate location are presented in Figures 6.29 to 6.32. The samples are plotted and listed according to their SiO_2 (wt%) content, with the highest SiO_2 content at the bottom of the legend.

Selected volcanic and granitoid clasts from Boundary Creek are divided into four groups according to their SiO_2 content (Figures 6.29a to 6.29d) All groups display a considerable scatter at the mobile element end of the spectrum but are overall enriched in LIL elements. The distinct spiked pattern together with negative anomalies at Nb for most of the samples in all four groups is indicative of subduction-related magmas. Most volcanic and granitoid samples with SiO_2 content >70 % display negative Ba, Sr and Ti anomalies reflecting their more fractionated nature, whereas the same elements in the more mafic clasts display less pronounced peaks. These anomalies increase with increasing differentiation, which is emphasised if calculated averages of all the groups are compared in Figure 6.29e.

With the exception of one clast, the plutonic clasts from Te Moana are strongly enriched in LIL elements (Figure 6.30a). The majority of the volcanic clasts generally mirror the trace element characteristics exhibited by the granitoid clasts and display typical fractionated, subduction-related characteristics (Figure 6.30b). Calculated multi-element trend averages (Figure 6.30c) of the two selected rock groups show that the volcanic and granitoid clasts from Te Moana have similar petrogenetic origins.

Hypersolvus and subsolvus clasts from the McKenzie Pass conglomerate exhibit evolved and subduction-related spider patterns (Figures 6.31a and 6.31b). A single hypersolvus clast (UC30898) contains, if compared to other samples from this group, the highest Rb, Nb, Zr and the lowest Ba and Sr content, resulting in distinct negative anomalies at Ba, Sr and Ti and a weak negative anomaly at Nb, features associated with A-type rocks. Selected volcanic clasts from McKenzie Pass with <70 % SiO_2 content have generally higher Ba, Sr and Ti content if compared to volcanic clasts with >70 % SiO_2 content, reflective of their less fractionated nature (Figures 6.31c and 6.31d). However, comparison of calculated averaged trends (excluding the A-type clast) of all four groups from McKenzie Pass indicates that all the clasts have a similar subduction-related origin (Figure 6.31e).

The multi-element diagrams for selected weakly peraluminous plutonic rocks from the Lake Hill conglomerate exhibit similar evolved and subduction-related patterns with a distinct negative Nb anomaly (Figure 6.32a). Overall, a considerable scatter is displayed by these clasts, with generally negative Ba and Sr anomalies. However, some clasts display minor positive Sr and Ba anomalies that are associated with adakitic rocks. A similar fractionated trend and data dispersion is observed for peraluminous clasts from the same conglomerate (Figure 6.32b). The less inclined trends displayed by selected volcanic clasts with <70 % SiO_2 content are reflective of their more primitive nature and contrast with the more evolved trends displayed by volcanic clasts with a SiO_2 content of >70 %. However, all the volcanic clasts have strong subduction-related characteristics (Figures 6.32c and 6.32d).

All but two adakitic samples from Lake Hill display a positive Ba anomaly (Figure 6.32e). All samples have a positive Sr peak and are strongly depleted in Y, characteristic of adakites. The contrast between the individual groups from Lake Hill is emphasised in Figure 6.32f. The calculated multi-element trend averages of the selected rock groups from Lake Hill indicate that the adakitic rocks have a different petrogenetic origin than the other rock groups. These other rock groups show strong similarities with each other. The generally wide spread of LIL elements in all the groups from Lake Hill can probably be related to source heterogeneity or various degrees of crustal involvement during petrogenesis.

6.2.3 Rare Earth Elements

Rare earth element data were obtained for adakitic samples from the Lake Hill conglomerate and are presented in Figure 6.33 on a chondrite normalised diagram (Nakamura, 1974).

The adakitic samples are light to strongly fractionated (La_N/Yb_N = 4.47-15.44; mean = 9.32), have a generally flat HREE (Gd_N/Yb_N = 1.23-2.10; mean = 1.65) and have no or strongly positive Eu anomalies (Eu/Eu* = 1.00-2.16; mean = 1.47). The absence of strong negative Eu anomalies suggests that no major feldspar retention took place in the source. Garnet has high partition coefficients for the HREE (Wilson, 1989; Rollinson, 1993), and retention of garnet as a residual phase during partial melting is commonly attributed to the formation of HREE depletion such as observed in the adakitic clasts from Lake Hill. The low partition coefficients for Sr and Ba in garnet may also contribute to the high abundance of these elements in the adakitic samples.

6.2.4 Discrimination of Tectonic Setting

On plots Rb vs. Nb+Y and Nb vs. Y (Figure 6.34) the majority of the granitoid and volcanic clasts from all 4 conglomerates plot within the field of volcanic-arc-granite (Pearce *et al.*, 1984), with some clasts from McKenzie Pass and from Lake Hill displaying some within-plate affinities. The low-K nature displayed by clasts from Lake Hill and Boundary Creek is reflected in the low Rb content of clasts but might be, as mentioned above, a function of element mobility during pre-depositional and/or post-depositional metamorphism of individual clasts.

If major elements are plotted against high field strength elements (HFSE) the majority of the granitoid and volcanic samples from all 4 conglomerates fall into both the I- and S-type granite fields and volcanic clasts generally exhibit a higher HFSE content (Figure 6.35). Some clasts are enriched in HFSE and spread into the A-type field, plotting around the average for A-type rocks (Figure 6.38, Whalen *et al.*, 1987).

6.2.5 Sr and Nd isotopes

Sr and Nd isotope data for the igneous clasts from the Rakaia terrane are presented in Table 6.2 and Table 6.3. Initial strontium ratios and $\varepsilon Nd_{(t)}$ for individual clasts were calculated to their crystallisation age presented in Chapter 3 and are shown in Figure 6.37. With the exception of two samples from Lake Hill (UC30667 and

UC30668), the clasts from all four conglomerates define a narrow field with isotopic compositions similar to that of Bulk Earth. Fields for individual conglomerate locations show good overlap with each other and many clasts are indistinguishable from each other. The clasts (except the two Lake Hill samples) define a narrow field with $^{87}Sr/^{86}Sr_{(t)}$ ranging from 0.70320 to 0.70685 and $\varepsilon Nd_{(i)}$ from -2.1 to +1.6. The two Lake Hill samples are slightly more radiogenic with values for $^{87}Sr/^{86}Sr_{(t)}$ between 0.70722 and 0.70768 and $\varepsilon Nd_{(i)}$ between -4.5 and -3.7.

Permian to Early Triassic samples define a narrow range of T_{DM} values ranging from 0.82 Ga to 1.16 Ga, with one clast from Lake Hill giving a T_{DM} age of 1.48 Ga. T_{DM} values for the Carboniferous clasts are of similar age and range from 0.99 Ga to 1.13 Ga. The Cambrian samples give T_{DM} ages of 1.16 Ga and 1.59 Ga.

6.3 Summary and Conclusions

6.3.1 Petrographical Interpretation

All igneous clasts from the Rakaia terrane have undergone regional metamorphism, and igneous and metamorphic recrystallisation is encountered in all thin sections. Chlorite is the most widespread secondary mineral and, together with epidote and titanite, partly or completely replaces mafic silicate minerals.

Granitoid clasts at Boundary Creek range in modal composition from meta-diorite to meta-leucomonzogranite, and the volcanic clasts from meta-dacite to meta-rhyolite. All clasts were affected by post-depositional recrystallisation and deformation, and thereby overprinting of original igneous textures. In most samples layers and domains with original igneous crystals and texture are recognisable and meta-volcanic clasts still display a glomerophyric texture. Interpretation of textural features in the granitoid sample population with respect to the emplacement depth is however not conclusive. The presence of ductilely deformed plagioclase suggests that some clasts have undergone pre-depositional deformation under subsolvus conditions. Overall, the sampled clasts suggest that they were derived by erosion of the upper levels of a volcano/plutonic arc in a continental margin setting.

The igneous clast population from the Te Moana conglomerate is dominated by volcanic clasts of rhyolitic composition. The spherulitic and felsitic textures in the

matrix of these clasts indicate a high degree of undercooling. No evidence of a pyroclastic origin has been recognised and all clasts are assumed to have been derived from rhyolitic domes or flows. Subsolvus monzogranites and a hypersolvus granodiorite are present. Although the lithological-type distribution within the clast population at Te Moana is inconclusive (small number of samples) the analysed samples suggest that, similar to the Boundary Creek conglomerate, they are predominantly derived from the upper levels of a continental volcanic arc. The bias towards volcanic clasts might also be due to the fact that medium to coarse grained granitoids break down and disintegrate more easily than volcanic rocks and therefore fewer granitoid clasts get transported to the final place of deposition.

At McKenzie Pass the clast population consists of predominantly volcanic clasts of rhyolitic composition, but clasts of intermediate and mafic compositions are present. Hypersolvus (subvolcanic) clasts, dominant over weakly foliated subsolvus clasts, are typified by granophyric intergrowth that often surrounds subsolvus discrete minerals, indicating a change in crystallisation pressure prior to final consolidation. Similar to the conglomerates described above the clasts from McKenzie Pass are mainly derived from the upper levels of a continental volcanic arc, but the presence of a single basaltic clast suggests that oceanic island arc volcanism might have contributed detritus to the conglomerate.

Subsolvus clasts at Lake Hill range in modal composition from tonalite to leucomonzogranite and are dominated by two-mica granitoids. The clasts display a full range of deformational features from undeformed to mylonitic and gneissic. Shape and mineral preferred orientations and recrystallisation indicate post-intrusive deformation. If intracrystalline prism <c> slip controls the deformation of quartz, a temperature of >650°C is indicated and suggests emplacement depths of >12 km (Mainprice *et al.*, 1986; Garbutt and Teyssier, 1991; Wandres *et al.*, 1998). Volcanic clasts are not common within the Lake Hill conglomerate and exhibit no pyroclastic or ignimbrite characteristics. The predominantly subsolvus and deformed nature of the clasts, and the abundance of two-mica granitoids indicates that the clast source was a continental arc system emplaced in a mature continental crust and that lower levels of this source were exposed at the time of the conglomerate deposition.

6.3.2 Geochemistry

Igneous clasts from all 4 Rakaia conglomerate localities are generally silica-rich and display a wide degree of scatter if plotted on Harker diagrams, emphasising the mixture of granitoid and volcanic types each conglomerate contains. Clasts are predominantly calc-alkaline to high calc-alkaline. The tholeiitic character displayed by mylonitised and strongly deformed clasts, mainly from Boundary Creek and Lake Hill, is ascribed to the mobility and removal of major elements during mylonitisation. Multi-element diagrams, compiled for groups of clasts from each conglomerate, display significant similarities and differences. The enrichment in incompatible large ion lithophile (LIL) elements (with respect to a primitive mantle source) is, together with a strong negative Nb anomaly, common to all groups and indicates that the source for all the clasts has been through at least one subduction cycle.

Adakites and rocks with adakitic affinities from Lake Hill have generally strong positive Sr and Ba anomalies and are depleted in Y, characteristics typical of adakites. The distinct geochemical features of these rocks, including high SiO_2, Al_2O_3 and Na_2O, and low Y content with high Sr/Y ratios, suggest that these rocks were derived from partial melting of a mafic source with residual garnet and amphibole (Defant and Drummond, 1990). The weakly negative to strongly positive Eu anomalies indicate that feldspar was not a stable phase. Defant & Drummond (1990) proposed a model in which the adakitic magma was derived from the partial melting of a hot, young (<25Ma) subducted slab of eclogite or garnet amphibolite mineralogy. Atherton and Petford (1993) have pointed out that Na-rich magmas similar to adakites can be produced by partial melting of newly underplated mafic crust beneath a thickened continental arc (>40km).

CHAPTER 7
PROVENANCE OF PAHAU TERRANE IGNEOUS CLASTS

CHAPTER 7

PROVENANCE OF PAHAU TERRANE IGNEOUS CLASTS

Introduction

In this chapter the igneous provinces of the now dispersed Gondwana margin (Figure 1.1) are described in order to compare and correlate their petrography, geochemistry and geochronology with those of the Jurassic to Early Cretaceous Pahau terrane igneous clasts. After an overview of magmatism along the Panthalassan margin of Gondwana in Section 7.1 the potential sources for the Pahau terrane igneous clasts are briefly described in Section 7.2. Based on geochronological data (Table 3.1) the igneous clast population is divided into two groups (Late Jurassic to Early Cretaceous, and Early Jurassic), which are compared to penecontemporaneous potential source provinces in Sections 7.3 and 7.4 respectively.

In addition, new Sr-Nd isotope data for Pahau and Rakaia sandstones and sandstone clasts are presented in Section 7.5 in order to compare the chemistry of these sandstones to that of the igneous clasts, thus investigating if simple erosion of the igneous clast source can provide detritus of suitable Pahau sandstone composition.

7.1 OVERVIEW OF JURASSIC TO CRETACEOUS MAGMATISM ALONG THE PANTHALASSAN MARGIN

7.1.1 Introduction

A summary of the Jurassic to Cretaceous tectonic regime of the SW Pacific is given first followed by a brief overview of Jurassic to Cretaceous igneous provinces from the SW Pacific (Figure 1.1).

Correlation of Paleozoic to Mesozoic terranes and magmatism along the pre-break-up SW Pacific margin of Gondwana (Figure 7.1) has been summarised by various authors (Bradshaw *et al.*, 1996; Weaver *et al.*, 1996; Storey and Kyle, 1997; Pankhurst *et al.*, 1998b; Millar *et al.*, 2001) and only salient points are given below. For a

comprehensive tectonostratigraphic review of the Panthalassan margin of Gondwana the reader is referred to Veevers *et al.* (2000a).

7.1.2 Jurassic to Cretaceous Tectonic Regime in the SW Pacific

From the Jurassic to Early Cretaceous the SW Pacific margin of Gondwana was dominated by oblique subduction (Bradshaw, 1989; Luyendyk, 1995), large scale strike-slip faulting (DiVenere *et al.*, 1995), diachronous magmatic events, and significant compositional variation in magma production. Calc-alkaline magmatism, related to subduction, is characteristic of terranes recognised in New Zealand and Antarctica (Pankhurst *et al.*, 1993; Kimbrough *et al.*, 1994a; Muir *et al.*, 1994; Weaver *et al.*, 1994a; Muir *et al.*, 1998; Pankhurst *et al.*, 1998b). In New Zealand and Antarctica, a rapid change to extensional tectonics in the mid-Cretaceous was recognised by the formation of metamorphic core complexes (Gibson *et al.*, 1989; Tulloch and Kimbrough, 1989; Luyendyk *et al.*, 1996; Spell *et al.*, 2000). SHRIMP U-Pb ages between 114 to 129 Ma on detrital zircons from a Marlborough Pahau terrane siltstone-sandstone sequence (sample HUN4, Pickard *et al.*, 2000) and one detrital zircon age from the Ethelton matrix (111.7±1.4 Ma, Figure 3.10) indicate that deposition of the South Island Pahau terrane sandstone continued at least into the Aptian. A detrital zircon SHRIMP U-Pb age of 99±2 Ma from the Omaio petrofacies (Cawood *et al.*, 1999) approximates the age of deposition of the youngest Pahau terrane sandstones in the North Island. These depositional ages broadly coincide with the formation of the Western Province core complexes and the proposed subduction termination in the New Zealand region (Bradshaw, 1989), with subduction continuing longer in the North Island (Cawood *et al.*, 1999; Kamp, 1999). Subduction cessation was accompanied by rift-bounded sedimentary basins in the Western Province, and in Western Marie Byrd Land by voluminous A-type and associated mafic magmatism (Weaver *et al.*, 1996; Storey *et al.*, 1999). This was followed by rifting of the Campbell Plateau from Marie Byrd Land, and of the Western Province from Australia.

7.1.3 Calc-alkaline Magmatism

7.1.3.1 Australia

The closest probable correlatives of MTZ rocks in Australia are in the New England Fold Belt (Aitchison, 1993; Mortimer *et al.*, 1999a; Sutherland, 1999), which

experienced a pulse of Carboniferous to Permian calc-alkaline magmatism (Shaw and Flood, 1981; Gust *et al.*, 1993; Kent, 1994; Veevers *et al.*, 1994a; Williams and Korsch, 1996). However, these rocks are too old to present a suitable source for the Pahau terrane igneous clasts and are not further considered here (but see Chapter 8).

7.1.3.2 Western Province of New Zealand

The Early Cretaceous Separation Point Suite intruded rocks of the Takaka terrane and the MTZ, stitching the two terranes at the c. 118 Ma time of emplacement (Muir *et al.*, 1995). The mid-Cretaceous granitoids of the Hohonu Batholith (c. 114 - 110 Ma) and associated rocks were generated during a period of rapid tectonic transition from crustal thickening during collision to crustal thinning and core complex formation during extension (Waight *et al.*, 1998b).

7.1.3.3 Median Tectonic Zone and Amundsen Province

Recent research has documented close similarities in geological history between the MTZ found in New Zealand (Figures 1.4 and 1.5) and rocks found in Marie Byrd Land and Thurston Island (Weaver *et al.*, 1996; Bradshaw *et al.*, 1997; Pankhurst *et al.*, 1998b). Marie Byrd Land comprises two geological provinces, a western Ross Province and an eastern Amundsen Province (Pankhurst *et al.*, 1998b, Figure 7.2). The MTZ has been correlated with the Amundsen Province (Pankhurst *et al.*, 1998b). Distinct pulses of late Paleozoic – Early Cretaceous intrusive activity are recognised in both regions (Pankhurst *et al.*, 1993; Kimbrough *et al.*, 1994a; Muir *et al.*, 1994; Weaver *et al.*, 1994a; Muir *et al.*, 1998; Pankhurst *et al.*, 1998b). Jurassic to Early Cretaceous plutons in the Median Tectonic Zone and Amundsen Province are considered to be part of a continental margin magmatic arc (Kimbrough *et al.*, 1994a; Muir *et al.*, 1998; Mortimer *et al.*, 1999b) and are termed Median Tectonic Zone/Amundsen Province (MAVB) in this study.

7.1.3.4 Antarctic Peninsula

Plutonic rocks which form the Antarctic Peninsula Batholith were emplaced between c. 240 Ma and 10 Ma (Millar *et al.*, 2001, and references therein; Riley *et al.*, 2001), with the majority of Triassic to Early Jurassic plutons emplaced along the paleo-Pacific margin of Gondwana prior to the break-up of the supercontinent. Unequivocal

subduction-related magmatism was initiated by c. 140 Ma, and was most voluminous and widespread between 125 Ma and 100 Ma.

7.1.4 Silicic and other Provinces Associated with the Gondwana Break-up

7.1.4.1 Australia

A large volume of silicic magmatism has been reported from Queensland, which has many features of continental margin volcanism, but has been attributed to continental rifting during the break-up of Gondwana in the Cretaceous between 125 to 95 Ma (Bryan *et al.*, 1997; Bryan *et al.*, 2000).

7.1.4.2 Antarctic Peninsula

Magmatism associated with the Jurassic break-up of Gondwana is represented by extensive silicic volcanism and associated sub-volcanic plutonism that extended from Patagonia to the Antarctic Peninsula and as far as Thurston Island (Pankhurst *et al.*, 1998a; Pankhurst *et al.*, 2000, their Figure 10). The term Chon Aike Province has been proposed for these rocks by Pankhurst *et al.* (1998a).

7.1.4.3 East Antarctica

The Ferrar magmatic province is an Early to Middle Jurassic intra-Gondwana continental flood-basalt and dolerite province (Hergt *et al.*, 1989) and extends in pre-Gondwana break-up reconstruction from the Theron Mountains (East Antarctica) to southeastern Australia (Veevers, 2000c) and New Zealand (Mortimer *et al.*, 1995).

7.1.5 Post-subduction Magmatism in New Zealand and Antarctica

7.1.5.1 New Zealand Western Province

In the Late Cretaceous magmatic activity is represented by the emplacement of the peralkaline A-type French Creek Granite at 83 Ma and coincides with the appearance of oceanic crust in the Tasman Sea (Waight *et al.*, 1998a) (Tulloch *et al.*, 1994). These rocks are post-subduction and are not further considered in this study.

7.1.5.2 New Zealand Eastern Province

In contrast with the western Province and MTZ magmatic rocks of Cretaceous age are scarce in the Eastern Province. Alkaline complexes (Tapuaenuku, Mandamus etc.) are spread throughout the middle and upper part of the South Island and they are thought to have been emplaced during crustal extension in the Torlesse accretionary wedge (Weaver *et al.*, 1989, and references therein). These rocks are therefore clearly post-Pahau deposition and are not further considered in this study.

7.1.5.3 Antarctica

Diverse suites of A-type granitoids and mafic dike swarms were emplaced at about 105-95 Ma along the Ruppert-Hobbs Coast (Storey *et al.*, 1999), in the Ford Ranges and Edward the VII Peninsula of Marie Byrd Land (Weaver *et al.*, 1994b), and were accompanied by metamorphic complexes (Richard *et al.*, 1994; Luyendyk *et al.*, 1996). These rocks are deemed to be unsuitable as a source for the igneous clasts based mainly on their younger ages and their differing chemistry.

7.2 Potential Early Jurassic to Early Cretaceous Sources for the Igneous Clasts

7.2.1 Introduction

Only penecontemporaneous igneous suites and plutons with geochemistry and isotopic compositions similar to that of the Pahau terrane igneous clasts are considered for comparison (Figure 7.3 and Table 7.1).

7.2.2 Eastern Australia

The Whitsunday Volcanic Province (WVP, Figure 1.1), interpreted as a rift-related large silicic igneous province, extends along the central and southern Queensland coast (Ewart *et al.*, 1992; Bryan *et al.*, 1997; Bryan *et al.*, 2000). Evidence of volcanic and intrusive activity shows a broad range of ages from 132 to 95 Ma, with a major volcanic episode between c. 120 to 105 Ma (Ewart *et al.*, 1992; Bryan *et al.*, 1997). Recent K/Ar data from the west of the WVP suggests that precursory magmatic activity may have begun as early as 145 Ma (Allen *et al.*, 1998). However, Bryan *et al.*

(2000) argue that these Jurassic to lower Early Cretaceous ages might have been reset by the major thermal event associated with the emplacement of the LIP.

The volcanism in the WVP occurred in a low relief, multiple volcanic vent environment, dominated by several large caldera-type centres (Bryan *et al.*, 2000). The volcanic and intrusive rocks show a broad range of compositions from basalt to rhyolite, although intermediate-silicic compositions volumetrically dominate. The volcanics show calc-alkaline affinities and resemble modern destructive-plate-margin volcanics rather than alkalic volcanism associated with continental rifts. Based on trace element and isotope studies Ewart *et al.* (1992) concluded that the wide variety of igneous compositions was generated by two-component mixing, with the two magma sources identified as: (1) a large volume, partial melt of relative young, non-radiogenic, calc-alkaline crust, and (2) a within-plate tholeiitic basalt. Initial $^{87}Sr/^{86}Sr_{(i)}$ ratios range from 0.70312 to 0.70429 and $\varepsilon Nd_{(i)}$ values are all positive (+2.6 to +6.4).

Bryan *et al.* (2000) suggested a causal relationship between volcanism in WVP and volcanoclastic sedimentation in the Otaway/Gipsland and Great Artesian Basin, and that volcanism occurred along the length of the present Australian margin (>2000 Km). The continuation of the WVP into the New Zealand region prior to the Gondwana break-up has been tentatively suggested (Ewart *et al.*, 1992; Bryan *et al.*, 2000).

7.2.3 New Zealand

7.2.3.1 Median Tectonic Zone

A detailed description of age and spatial distribution of the Jurassic to Lower Cretaceous igneous rocks of the Buller terrane and MTZ is given in Sections 1.3.1.1 and 1.3.2 (see also Chart, and Figures 1.4 and 1.5) and salient points are summarised here.

The bulk of the plutonic rocks of the Median Tectonic Zone south of the Alpine Fault (SW Fiordland) range in age from 168 to 137 Ma and have been referred to as the Darran Suite (Muir *et al.*, 1998). The Suite contains two distinct compositional groups: (1) mafic (gabbros and diorites), and (2) felsic (granodiorites and monzogranites). The rocks are classified as metaluminous to weakly peraluminous (ASI < 1.1) and have mantle-normalised multi-element patterns generally considered characteristic of subduction related magmas. Initial $^{87}Sr/^{86}Sr_{(i)}$ ratios range from 0.70345 to 0.70392 and $\varepsilon Nd_{(i)}$ values are all positive (+3.4 to +4.5).

The peralkaline Electric Granite (137±2 Ma) contains alkali-rich amphiboles and is characterised by high SiO_2, high alkalis, high Ga, Y, Zn, Zr, Nb, and high REE (except Eu) and Sr. On a tectonic discriminant diagram (Pearce *et al.*, 1984) the granites plot in the Within-Plate Granite field (Muir *et al.*, 1998). The initial $^{87}Sr/^{86}Sr_{(i)}$ ratio is unrealistically high due to a very high and poorly determined Rb/Sr ratio (Sr 3 ppm) and $\varepsilon Nd_{(i)}$ value is +2.2.

The Darran Suite is cut by Early Cretaceous Separation Point-type granites (c. 124 Ma) that are slightly older than the equivalent Separation Point Batholith in NW Nelson (117±2 Ma, Muir *et al.*, 1997) but similar in age to the Western Fiordland Orthogneiss (WFO) of Fiordland. The adakitic Separation Point-type plutons (NW Nelson and SW Fiordland) are metaluminous to weakly peraluminous and are characterised by high SiO_2, high Al_2O_3, Na_2O/K_2O ratios, high Sr and Ba, and low Y concentrations. Chondrite-normalised REE and mantle-normalised multi-element patterns suggest that garnet was present in the source region (Muir *et al.*, 1995; Muir *et al.*, 1998). For SW Fiordland the initial $^{87}Sr/^{86}Sr_{(i)}$ ratios range from 0.70375 to 0.70384 and $\varepsilon Nd_{(i)}$ values are +3, for NW Nelson the initial $^{87}Sr/^{86}Sr_{(i)}$ ratios range from 0.70414 to 0.70498 and $\varepsilon Nd_{(i)}$ values are –3.2 to +1.8.

The dioritic WFO is considered to be the lower crustal equivalent of the Separation Point plutons (Muir *et al.*, 1995; Muir *et al.*, 1998), and it has similar adakitic characteristics. Initial $^{87}Sr/^{86}Sr_{(i)}$ ratios range from 0.70379 to 0.70388 and $\varepsilon Nd_{(i)}$ values range from +2.2 to +2.5.

A U-Pb age of 140±2 Ma on a metaluminous Largs Ignimbrite has been reported by Mortimer *et al.* (1999a), indicating that volcanic activity accompanied plutonism in the MTZ in the Late Jurassic - Early Cretaceous. Mortimer *et al.* correlated the ignimbrite tentatively with the Glade Suite of the Darran Complex. The Paterson Group of Stewart Island has a range of volcanic rock types of a similar age to that of the Largs Ignimbrite (Kimbrough *et al.*, 1994a).

7.2.3.2 Buller Terrane

The low-Ti tholeiitic Kirwans dolerites are the only Jurassic intrusions within the Buller terrane. Whole rock K-Ar ages range from 172-151 Ma. The dolerites have been correlated with the Ferrar magmatic province (Mortimer *et al.*, 1995). Initial $^{87}Sr/^{86}Sr_{(i)}$

ratios range from 0.71030 to 0.71081 and $\varepsilon Nd_{(i)}$ values range from -5.2 to -5.6. However, the distinct tholeiitic geochemistry and the highly radiogenic isotope composition make these rocks an unlikely source for the Early Jurassic igneous clast found in the Kekerengu conglomerate.

The metaluminous, calc-alkaline Crow Granite at 137±3 Ma is similar in age and geochemistry to plutons from the MTZ (Muir *et al.*, 1997).

Waight (1998b) recognised two distinct but related suites (Te Kinga and Deutgam) in the Hohonu Batholith, with the bulk of the plutons emplaced in the mid Cretaceous (114 to 109 Ma). The relatively mafic, metaluminous, I-type Deutgam Suite and the peraluminous, high silica Te Kinga Suite are characterised by restricted radiogenic isotopic compositions ($^{87}Sr/^{86}Sr_{(i)}$ = 0.7062 to 0.7085; $\varepsilon Nd_{(i)}$ -6.1 to -4.4). The Te Kinga Suite is weakly adakitic and similar in chemistry to the Separation Point Suite rocks.

7.2.3.3 Bounty Island

The Bounty Islands, located on the Campbell Plateau (Figure 1.1), are a group of nine small islets and isolated rocks that comprise biotite (± muscovite) granite (Speight and Finlayson, 1909; Tulloch, 1983). The absence of basement exposure on the Bounty Islands does not allow them to be placed in any terranes with confidence. However, Cook *et al.* (1999) placed the Bounty Islands within the Median Tectonic Zone. The Bounty Island subduction related, calc-alkaline granites are dominated by peraluminous (ASI 1.0 to 1.15) samples with S-type affinities. A single sample has given a U-Pb age on zircons (SHRIMP) of 194±5 Ma (Ireland, pers. comm.). If the MTZ allocation of the Bounty Islands by Cook *et al.* (1999) is correct, then Lower Jurassic magmatism occurred in the MTZ.

7.2.4 Antarctica

7.2.4.1 Marie Byrd Land

Weaver *et al.* (1994b) described a mid-Cretaceous (124-108 Ma) calc-alkalic, metaluminous suite from the Ruppert-Hobbs Coast that ranges in composition from diorite to monzogranite (Figure 7.2). The calc-alkalic I-type granitoids have $^{87}Sr/^{86}Sr_{(i)}$ ratios from 0.7054 to 0.7056; $\varepsilon Nd_{(i)}$ 0 to -2. In Pine Island Bay granitoids range in age

from 125-114 Ma but have a slightly more primitive isotopic composition, with $^{87}Sr/^{86}Sr_{(i)}$ ranging from 0.7044 to 0.7048 and $\varepsilon Nd_{(i)}$ from 0 to +2 (Weaver *et al.*, 1996, Weaver et al. pers. comm., Pankhurst et al. pers. comm.).

Granodiorites from the Kohler Range and Pine Island Bay yield ages between 105-95 Ma but are too young to be considered as a clast source.

Unpublished Sr/Nd isotope data (Pankhurst, pers. comm.) from Pine Island Bay contain 6 samples of Lower to Middle Jurassic age (c. 178 Ma). No major and trace element data are available for these rocks and only the isotope data ($^{87}Sr/^{86}Sr_{(i)}$ 0.70473 to 0.70644; $\varepsilon Nd_{(i)}$ -3.4 to +0.6) will be used for comparison with the single Lower Jurassic clast from the Kekerengu conglomerate.

7.2.4.2 Thurston Island

Pankhurst *et al.* (1993) and Leat *et al.* (1993) recognised two major periods of magmatism on Thurston Island and the adjacent Eight Coast, one in the Late Jurassic (152-142 Ma; Rb-Sr method) and the second in the Early Cretaceous (125-110 Ma; Figure 7.2). The rocks range in composition from gabbro to fractionated granites that form a uniformly calc-alkaline, predominantly metaluminous suite (Leat *et al.*, 1993). Most of the rocks have $^{87}Sr/^{86}Sr_{(i)}$ ratios from 0.705 to 0.706 and $\varepsilon Nd_{(i)}$ ranging from +2 to -4. Early Jurassic (c. 200 Ma) granitoids have been reported from the Jones Mountains ($^{87}Sr/^{86}Sr_{(i)}$ ratios 0.70958 to 0.70979; $\varepsilon Nd_{(i)}$ -6.3 to -5.1), and volcanic and volcanogenic rocks from the central Thurston Island (Mount Dowling c. 180 Ma; $^{87}Sr/^{86}Sr_{(i)}$ 0.70835; $\varepsilon Nd_{(i)}$ -4.4). Granitoids from the Jones Mountains (100 Ma and 90 Ma) are too young to be considered as a source for the Pahau terrane igneous clasts.

7.2.4.3 Antarctic Peninsula

Early-Middle Jurassic magmatism in the Antarctic Peninsula has been summarised by Pankhurst *et al.* (2000) and Riley *et al.* (2001, their Figure 1), who recognised that the magmatism spanned c. 35 m.y. with three distinct episodes termed V1 (188-178Ma), V2 (172-162 Ma) and V3 (157-153 Ma). Pankhurst *et al.* (2001) assigned an average age of 185 Ma for the V1 magmatism and 168 Ma for the V2 magmatism. V1 and V2 are both confined to the Antarctic Peninsula and possibly Thurston Island (Pankhurst *et al.*, 2000, their Figure 10). V1 magmatism is of rhyolitic composition, and coincides in age with the single dated clast of Jurassic age of the

present study. A high-Ti and a low-Ti group have been identified within the V1 rhyolites exhibiting a slight within-plate geochemical signature, i.e., a tendency to high Nb and Zr content (Pankhurst *et al.*, 1998a). In addition they also have strong negative $\varepsilon Nd_{(i)}$ values (-9 to -4) (Riley *et al.*, 2001). Only V1 rhyolites are considered here as a potential source for early Jurassic igneous clasts ($^{87}Sr/^{86}Sr_{(i)}$ 0.71062 to 0.72057; $\varepsilon Nd_{(i)}$ -7.8 to -2.4).

Millar *et al.* (2001, their Figure 2) reported on the granitoids of the Antarctic Peninsula, but most of the granitoids described are either too old or too young, or too radiogenic, to be contenders for the Pahau igneous clast sources. In addition, following a Jurassic pre-break-up configuration of the Gondwana margin (e.g., Pankhurst *et al.*, 2000; Millar *et al.*, 2001; Riley *et al.*, 2001), granitoids from the Antarctic Peninsula may be considered to be too distal with respect to the Pahau depositional basins to be major detritus contributors. Similarly, the Middle-Jurassic (c. 175 Ma) peraluminous granitoids within the Ellsworth-Whitmore Mountains (Storey *et al.*, 1988) differ too much geochemically and radiogenically to represent a suitable source.

7.3 Comparison of Late Jurassic to Early Cretaceous Igneous Clasts with Potential Sources

The very fact that the igneous clasts are now found in conglomerates means that only their deeper level equivalents are now preserved in the source area (e.g., all present plutonic igneous rock exposures within the Western Province of New Zealand are mid to upper crust, implying significant erosion).

Brown *et al.* (1998) demonstrated that granitoid lithic fragments from the Taupo Volcanic Zone (TVZ) are geochemically and isotopically identical to penecontemporaneous rhyolite lavas and pyroclastic rocks erupted from the central TVZ. Petrographic features of the granitoid lithics are characteristic of high middle level intrusions, with textures indicating hypersolvus and subsolvus crystallisation conditions (see Section 5.1.1.1). REE data and Sr, Nd, Pb and O isotope ratios for granitoids are comparable to published data from the TVZ rhyolites, and consequently the granitoids are considered by Brown *et al.* (1998) to represent crystallised portions of the magma chamber. These findings thus show a linkage between the volcanic and plutonic systems.

In view of the observations made by Brown *et al.* (1998) it is therefore reasonable to compare the chemistry and isotopic composition of predominantly volcanic and hypersolvus igneous clasts with that of penecontemporaneous source provinces that are now dominated by upper to middle crust exposures.

Based on age, major and trace element chemistry, REE distribution and isotopic compositions, the calc-alkaline plutons and suites from the Median Tectonic Zone and the Amundsen Province (including Thurston Island) are deemed to be suitable sources for the Late Jurassic to Early Cretaceous Pahau terrane igneous clasts.

The Electric granite appears to be the most likely source for the peralkaline clasts. The Separation Point type granitoids (including the Western Fiordland Orthogneisses) from the Median Tectonic Zone and the Te Kinga Suite of the Hohonu Batholith are compared with clasts with adakitic affinities.

The Largs Ignimbrite is rare evidence for Late Jurassic - Early Cretaceous silicic volcanism within the Median Tectonic Zone and is used here to demonstrate the similarities between the ignimbrite and the analysed clasts.

Although interpreted as rift-related magmatism, the Whitsunday Volcanics display calc-alkaline affinities and are used for comparison based on their geochemistry and the proposed large regional extent.

7.3.1 Geochronology

The 15 calc-alkaline, metaluminous and minor alkaline igneous clasts dated from the Pahau terrane range in age from c. 147-123 Ma (plus one Early Jurassic clast, Table 3.1 and Figure 7.3, discussed below). Only a small fraction of the total analysed igneous clast population has been dated and younger igneous clasts might be present as indicated by the youngest dated detrital zircon (Chapter 3). It is assumed that the SHRIMP-dated igneous clasts broadly represent the age distribution within the total igneous clast population.

The majority of the dated igneous clasts, 11 samples ranging in age from 147-134 Ma (termed Group 1 in Figure 7.9), show a good correlation in age with rocks from the Darran Suite of the MTZ, Crow Granite of the Western Province and rocks from

Thurston Island. The 140±2 Ma age of the Largs Ignimbrite is also indistinguishable from dated rhyolitic clasts mainly from Mount Saul.

The three slightly younger clasts (128-123 Ma; termed Group 2 in Figure 7.9) show a strong overlap in age with the oldest dated Whitsunday Volcanics. They are also similar in age to the Separation Point Suite of the MTZ, the Western Fiordland Orthogneiss, and the granitoids exposed on the Ruppert-Hobbs Coast, the Pine Island Bay and Thurston Island.

7.3.2 Petrography

A summary of petrographic observations has been given in Section 5.3.1, and the predominance of volcanic and hypersolvus clasts (Figure 5.14) indicates that volcanism was active in the source area at the time of the Pahau terrane sedimentation. However, with the exception of the Whitsunday Volcanics, plutonic rocks predominate the above-described SW Pacific igneous provinces. As mentioned above it is of course reasonable to assume that all the plutonic source rocks had volcanic equivalents that are not preserved.

7.3.3 Major and Trace Elements

Selected geochemical plots comparing major and trace elements of igneous clasts with the various potential source provinces are presented here. For simplicity the total population of the igneous clasts is referred to as 'the clasts', the calc-alkaline igneous clasts and igneous clasts with calc-alkaline affinities are referred to as 'calc-alkaline clasts' and the A-Type clasts are referred to as 'alkaline clasts'. The felsic members (SiO_2 c. >65 %) of the Darran Suite, Separation Point Suite, Thurston Island, Marie Byrd Land, Te Kinga Suite and Whitsunday Volcanics are termed the 'Felsic Source'. Their mafic members (SiO_2 c. <65 %), if present, are referred to as 'Mafic Source'. Data used for comparison are from Ewart *et al.* (1992, Whitsunday Volcanics), Muir *et al.*(1998, Median Tectonic Zone, including Darran and Separation Point Suites, WFO and Electric Granite), Muir *et al.* (1995, Separation Point Batholith), Pankhurst *et al.* (1993, Thurston Island), Waight *et al.* (1998b, Te Kinga Suite), Weaver *et al.* (1994b, Marie Byrd Land), Weaver (pers. comm., Marie Byrd Land) and Mortimer (pers. comm., Largs Ignimbrite).

Due to the distinctive high SiO_2 content of most of the clasts, which has been discussed above, the clasts correlate well with the Felsic Source compositions (Figures 7.4 to 7.18). The wide spread in alkalinity (Figure 7.4) displayed by the calc-alkaline clast population is mirrored by the Felsic Source rocks and generally emphasises the predominant calc-alkaline nature of clasts and Felsic Source. Most of the alkaline igneous clasts are indistinguishable or very similar in composition from the Electric Granite. The tholeiitic affinity of the Largs Ignimbrite might be due to the very low Na_2O content (Figure 7.7). The majority of the clasts and Felsic Source rocks lie within the high-K calc-alkaline series of Peccerillo and Taylor (1976) and show a strong overlap (Figure 7.5).

The Felsic Source is dominated by weakly peraluminous (ASI between 1.0 and 1.1) and metaluminous plutons (Figure 7.6). Minor peraluminous rocks are confined to the Te Kinga Suite and the Separation Point Suite. The majority of the calc-alkaline igneous clasts are statistically indistinguishable from the Felsic Source and the Largs Ignimbrite, whereas the peralkaline clasts show a strong affinity with the Electric Granite.

Major and trace element variations are shown on Harker diagrams in Figures 7.7 and 7.8. TiO_2, Al_2O_3, Fe_2O, MgO, CaO and P_2O_5 of the source suites all show a negative correlation with SiO_2 and their felsic members (including the Largs Ignimbrite) correlate well with the calc-alkaline igneous clast population. The Electric granite has slightly higher TiO_2 and Fe_2O, and a lower Al_2O_3 content than the Felsic Source and this is also reflected by the alkaline igneous clasts. Na_2O remains relatively constant and shows a strong overlap between the compared rocks.

Trace element distributions show considerably greater scatter within the source rocks (Figure 7.8). Sr content generally decreases with increasing SiO_2 content whereas Rb increases. The higher Sr content of some members of the Felsic Source (in particular the Separation Point Suite and the Te Kinga Suite) is characteristic of adakitic rocks and is also found in some igneous clasts from Kekerengu. Overall the calc-alkaline clasts overlap with the data plotted from the other members of the Felsic Source. The low Sr and the high Zr and Nb content separates the Electric Granite and the alkaline clasts from the other source rocks.

The SHRIMP-dating method involved measurement of U and Th (ppm) concentrations in individual zircons. Trace element data for individual zircons from calc-alkaline clasts and alkaline clasts are plotted against their igneous age (Figures 7.9 and 7.10). The zircon compositions from this study are compared with individual zircons from the Median Tectonic Zone (Muir *et al.*, 1998).

The U and Th content of selected zircons from Group 1 (age range 147-134 Ma; see Section 7.3.1) and their igneous ages are indistinguishable from the felsic and the mafic members of the Darran Suite, and also display some overlap with zircon compositions from rocks of to the Separation Point Suite. The younger igneous zircons (Group 2, 128-125 Ma) are mainly confined to the Separation Point Suite field with a minor overlap with the felsic member of the Darran Suite. The igneous zircons display a narrow range if Th/U ratios are plotted. Although the source zircons display a wide range of composition in all the plots their mean values lie close to or within the fields for the igneous clast zircons.

Th concentrations of peralkaline clast zircons (all are from rhyolites) are indistinguishable from that of the Electric Granite (Figure 7.10). However, the rhyolites display a strong U depletion compared with the granite resulting in higher Th/U ratios for the rhyolites. Given the good correlation of geochronological, geochemical and isotopic parameters between the peralkaline clasts and the Electric granite the low U content might be the effect of volcanic processes.

7.3.4 Spider Diagrams

Calculated averages of calc-alkaline igneous clasts (see Figure 5.25), plotted on a mantle-normalised multi-element diagram, correlate well with average trends for selected Felsic Source rocks from the SW Pacific (Figure 7.11). All the rocks, including the Whitsunday Volcanics, are enriched in LIL elements and display a distinct spiked pattern with a strong negative anomaly at Nb, all characteristic of subduction-related magmas.

The multi-element trend for the calc-alkaline Largs Ignimbrite is compared with rhyolites from the Mount Saul conglomerate since three dated rhyolites from this conglomerate are indistinguishable in age from the ignimbrite (Figure 7.12). The Largs Ignimbrite exhibits an evolved and subduction-related trend and follows closely the

trend displayed by a typical calc-alkaline rhyolite (UC30818) from Mount Saul, but clearly differs from the averaged alkaline clast trend with its pronounced troughs at Ba, Sr and Ti.

Samples with adakitic affinities from the Kekerengu conglomerate follow a trend similar to the averaged Separation Point Suite granites and are strongly depleted in Y with a pronounced positive Sr anomaly and negative anomalies at Th, Nb and Ti (Figure 7.13).

The calculated multi-element trend of all the A-type designated clasts from Mount Saul and Kekerengu and that of the Electric Granite are nearly identical with marked negative anomalies at Ba, Sr and Ti, minor negative anomalies at Nb, and enrichment in HFS elements (Figure 7.14).

7.3.5 REE Patterns

Rare earth element data (REE) from the alkaline clasts at Mount Saul (averaged) and the single clast from Kekerengu are compared with the REE pattern from the Electric Granite and are presented in Figure 7.15 on a chondrite normalised diagram (Nakamura, 1974).

The Electric Granite is slightly enriched in all the elements ($\sum$REE = 286; LREE La_N/Yb_N = 4.33), but has a near identical Eu anomaly (Eu/Eu* = 0.37) and flat HREE distribution (Gd_N/Yb_N = 0.93) if compared with the alkaline clasts (Mount Saul $\sum$REE = 160, La_N/Yb_N = 5.64, Eu/Eu* = 0.35, Gd_N/Yb_N = 1.14; Kekerengu $\sum$REE = 224, La_N/Yb_N = 6.11, Eu/Eu* = 0.43, Gd_N/Yb_N = 1.01).

7.3.6 Discrimination of Tectonic Setting

On tectonic discrimination plots, Rb vs. Nb+Y and Nb vs. Y (Pearce *et al.*, 1984), calc-alkaline clasts are indistinguishable from source rocks that plot predominantly within the field of volcanic-arc-granite with some minor spread into the within-plate (Thurston Island and Marie Byrd Land, Whitsunday Volcanics) and ocean-ridge fields (Whitsunday Volcanics). The peralkaline clasts from Mount Saul and the single peralkaline clast from Kekerengu cluster around the Electric Granite and all plot in the within-plate-granite field (Figure 7.16).

A-type affinities of some of the source rocks, similar to those displayed by the calc-alkaline clasts, are shown on major element vs. HFSE plots (Whalen *et al.*, 1987) in which the alkaline clasts and the Electric Granite can be clearly differentiated from all the other rocks. The FeO_t/MgO ratios emphasise the evolved character of many of the clasts if compared with the source rocks (Figure 7.17).

On a triangular discriminant plot after Eby (1992) all alkaline clasts plot within the subduction-related A2 field and are very similar in trace element composition to the Electric Granite (Figure 7.18).

7.3.7 Sr and Nd Isotopes

To compare the radiogenic isotope chemistry of the Late Jurassic - Early Cretaceous igneous clasts with published data from SW Pacific igneous provinces, the initial $^{87}Sr/^{86}Sr_{(i)}$ and $\varepsilon Nd_{(t)}$ values have been recalculated to the mean age of the clasts (see Table 5.3). $^{87}Sr/^{86}Sr_{(137)}$ and $\varepsilon Nd_{(137)}$ for the igneous clasts from the three Pahau localities are plotted again in Figure 7.19. The two youngest samples from the Pahau terrane (UC30743 Kekerengu; UC30964 Ethelton) give unrealistically low recalculated $^{87}Sr/^{86}Sr_{(137)}$ values and their initial $^{87}Sr/^{86}Sr_{(i)}$ values are plotted. The two alkaline clasts (UC30823 and UC30854) with high Rb/Sr ratios have been omitted from the plot. Source province plutons with high Rb/Sr ratios and igneous ages younger or older than the 137 Ma average age of the clasts have been excluded from the comparison.

Sr and Nd isotope values for the Late Jurassic to Early Cretaceous source rocks from the Whitsunday Volcanics (Ewart *et al.*, 1992), Median Tectonic Zone and Western Fiordland Orthogneiss (Muir *et al.*, 1998), Separation Point Batholith (Muir *et al.*, 1995), Hohonu Batholith (Waight *et al.*, 1998b), Ruppert-Hobbs Coast and Pine Island (Pankhurst, pers. comm.), and Thurston Island (Pankhurst *et al.*, 1993) have been added in Figure 7.19 for comparison. The Paleozoic Karamea Batholith (Muir *et al.*, 1996b) and Lachlan Fold Belt (McCulloch and Chappell, 1982) have been added to demonstrate that these igneous provinces are not only too old but also too radiogenic to be source contenders. The Permian New England Fold Belt (Hensel *et al.*, 1985) has been proposed as a source for the Triassic/Jurassic Rakaia sandstone (Pickard *et al.*, 2000) and is added for comparison. Mortimer *et al.* (1999b) proposed an in situ development of the Median Tectonic Zone adjacent to the Western Province of New Zealand. The Greenland Group (Buller Terrane) could therefore be a possible basement

to the Median Tectonic Zone and has been added for this reason (see Section 9.1.1.1). Values for the potential source provinces have been recalculated so that they include the range of isotopic compositions calculated from the clast ages (146-123 Ma).

The New England Fold Belt shows good overlap with most of the igneous clasts (Figure 7.19a), however the Permian age precludes it from being a source (but see Section 8.1.3.5). The Hohonu Batholith (Deutgam and Te Kinga suites) is compositionally distinct and too radiogenic, and the isotope data preclude these granites from being a possible source for the igneous clasts.

Two groups can be recognised within the Felsic Source (Figure 7.19b). The first group consists of the Whitsunday Volcanics, the Darran and Separation Point suites and the Western Fiordland Orthogneiss (WFO) of Fiordland, and the Separation Point Batholith of NW Nelson. The second, slightly more radiogenic group consists of the Antarctic sector granitoids from the Ruppert-Hobbs Coast, Pine Island Bay and Thurston Island. The Mount Saul clasts have isotopic characteristics similar to that of the Group 1 granitoids with some minor overlap with Group 2 granitoids. The isotopic compositions of the Ethelton and Kekerengu clasts show good correlation with the fields for the granitoids of Group 2, with one clast from Kekerengu showing good correlation with group 1 source provinces.

A similar pattern is observed on the $\varepsilon Nd_{(137)}$ vs. $^{147}Sm/^{144}Nd$ plot in Figure 7.20. Sm and Nd are not significantly fractionated within the continental crust by metamorphic and sedimentary processes, and are immobile during hydrothermal conditions, thus preserving the parent/daughter ratios (unlike the Rb/Sr system) of the source region. Although $^{147}Sm/^{144}Nd$ ratios change with time (getting lower as Sm decays away) this change is imperceptible at the precision at which the ratios are measured (0.1-0.2 %) and the present day ratios are also a very good estimate of the initial $^{147}Sm/^{144}Nd$ ratios. The Electric Granite has a $^{147}Sm/^{144}Nd$ ratio that is very similar to that of a single alkaline clast from Mount Saul but is just slightly more radiogenic than this clast. The distinct isotopic composition of the Hohonu Batholith excludes this batholith as a source for the analysed clasts.

Depleted mantle model ages (T_{DM}) were calculated for all igneous sources and igneous clasts (see Table 5.3), assuming that the Sm/Nd ratios of all these rocks have not been modified by crystal fractionation after their separation from the mantle and that

material for each sample came from the mantle in a single event. T_{DM} ages are not easy to interpret, and Waight (1995) noted that if the granitoids are considered to be entirely crust derived then the T_{DM} ages represent the time since the source was originally derived from the mantle. If granitoids represent mixing between crustal and mantle components then the model ages can only give a minimum age for the ultimate mantle derivation of the crustal source, and represent an intermediate age between that of the mantle and crustal members (see also Dickin, 1995).

A $\varepsilon Nd_{(137)}$ vs. T_{DM} plot (Figure 7.21) indicates that the source rocks from the Darran Suite (felsic members), the Separation Point Suite and Batholith, and the WFO, together with the Whitsunday Volcanics, are composed of material of similar age to that of the majority of the clasts from Mount Saul and a single clast from Kekerengu. The mafic members of the Darran Suite, and most of the plutons from the Antarctic sector of Gondwana, were derived from material too old to be a viable source for most of the Mount Saul clasts. These source plutons have T_{DM} ages similar to those shown by most of the clasts from Ethelton and Kekerengu. However, the mafic members of the Darran Suite are less radiogenic than the Ethelton/Kekerengu clast population, but they have primitive εNd values similar to a single clast from Mount Saul. The plutons of the Hohonu Batholith are not only too radiogenic, but most of them are composed of material too old to be a source for the igneous clasts.

7.3.8 Summary and Conclusions

- Geochronological, major and trace element, and Sr-Nd isotope data presented above define the subduction-related MTZ/Amundsen Province volcanic belt (MAVB) as the major Late Jurassic to Early Cretaceous source of the Pahau terrane igneous clasts (Figure 7.22).

- Calc-alkaline clasts are geochemically indistinguishable from the Whitsunday Volcanics and Sr-Nd analysed clasts from Mount Saul and Kekerengu show petrogenetic similarities with this volcanic province. The main period of volcanic activity occurred between c. 120 and 95 Ma, coinciding with the youngest detrital zircon from the Ethelton matrix (111.7±1.4 Ma) and approximately with the youngest dated igneous clasts and A-type magmatism along the Marie Byrd Land margin. The low relief, caldera dominated Whitsunday Volcanic Province is generally too young in age to be a major clast source, although older volcanics might

occur on the submerged Lord Howe Rise. However, the extension of the volcanic province into the New Zealand region is still a strong possibility. For example the Stitts Tuff, the ignimbrites from the Kyeburn formation (Section 1.3.3.8) and the Mount Somers volcanics could be considered representatives of the Whitsunday Volcanic Province.

- The majority of the calc-alkaline clasts from all three conglomerates are indistinguishable in age, chemical composition and petrogenesis from the calc-alkaline I-type granitoids of the Darran Suite and the Thurston Island granitoids. The calc-alkaline clasts correlate well with the granitoids from Marie Byrd Land.

- Calc-alkaline clasts with adakitic affinities from Kekerengu can geochemically best be correlated with the Separation Point Suite, and these rocks are deemed to be the adakitic source. The Hohonu Batholith is generally too young in age and isotopically too radiogenic relative to the clasts.

- Many of the A-type clasts from Mount Saul and Kekerengu are indistinguishable in age, geochemistry and petrogenesis from the Electric Granite of the MTZ. The Electric Granite (or a source similar in composition) is therefore proposed as the clast source.

- The presence of both Darran Suite and Separation Point-type derived clasts at Kekerengu and of the Electric Granite derived clasts at Mount Saul is distinctive. The similar petrogenesis of A-type clasts from Kekerengu and Mount Saul and of I-type clasts from all three conglomerate locations is noteworthy. If the close proximity (todays's geography) of the three conglomerate locations is considered, then this might suggest that all three conglomerate locations have been sourced from a relatively narrow sector of MAVB where the Darran Suite, the Separation Point-type rocks and the Electric Granite are in close proximity. The granitoids of the Darran Suite are proposed as the main source of calc-alkaline clasts. The geographic separation between the Thurston Island crustal block and the New Zealand sector of an Early Cretaceous (Aptian) MAVB configuration (Figure 9.4) indicates that the granitoids of Thurston Island are too distal with respect to the depositional basins of the Pahau terrane sandstone.

- Collected clasts from all three conglomerates are dominated by silicic and highly fractionated volcanic and granophyric, hypersolvus clasts. The paucity of volcanic rocks in present day source areas and the ubiquitous presence of predominantly rhyolitic volcanic and hypersolvus granitoid clasts in the conglomerates is distinctive. It points strongly to a causal relationship between the stripping and erosion of the upper levels of MAVB and the subsequent transportation to the place of final deposition.

7.4 Comparison of Early - Middle Jurassic Igneous Clasts with Potential Sources

The scarcity of Early Jurassic source rocks from the Australian sector that can be correlated with detrital zircons analysed from the Pahau and Waipapa terrane sandstones has been highlighted by Pickard *et al.* (2000). These authors proposed an extensive volcanic centre offshore of eastern Australia on the northern Lord Howe Rise or West Norfolk Ridge. No adequate data are available from this region. However, Lower Jurassic to Middle Jurassic volcanism is extensive in Antarctica (see above). The Lower to Middle Jurassic V1 rhyolites from Palmerland (Riley *et al.*, 2001, high-Ti and low-Ti group are plotted separately), granitoids from Pine Island Bay (Pankhurst, pers. comm.), Eights Coast (Jones Mountains) and central Thurston Island (Pankhurst *et al.*, 1993, Mount Dowling), and the samples from Bounty Island (Dean, 1993) are used for comparison with the Lower Jurassic rhyolite clast from Kekerengu (UC30732).

7.4.1 Geochronology

The single Lower Jurassic rhyolitic clast (188±3 Ma) is indistinguishable in age from the dated monzogranite from the Bounty Islands (Figure 7.3). The Pine Island Bay granitoids are generally younger, but rocks of ages similar to that of the clast occur (c. 188-165 Ma). The volcanic rocks from Mount Dowling and the V1 rhyolites from Palmerland, part of the Chon Aike province, are of similar age, whereas the two-mica granites from the Jones Mountains are slightly older than the clast.

7.4.2 Major and Trace Elements

Selected major elements indicate that all the source rocks considered here are calc-alkaline except for the low-Ti V1 volcanics that show tholeiitic affinities (Figure

7.23). All the source rocks are part of the high-K calc-alkaline series and are slightly peraluminous, with some of the high-Ti V1 volcanics and one of the low-Ti V1 volcanics being strongly peraluminous (Figures 7.24 and 7.25).

The negative correlation of TiO_2, Al_2O_3, Fe_2O, MgO, CaO and P_2O_5 with increasing SiO_2 for all the source rocks is shown on Harker diagrams, with Na_2O showing a wide scatter (Figure 7.26). On these plots the Bounty Island granites and granites from the Jones Mountains are indistinguishable from the Kekerengu clast, whereas the low-Ti volcanics show some affinities with the clast.

Trace element distributions show a considerably greater scatter between the source rocks, and only the Bounty Island granites display characteristics similar to those of the igneous clast (Figure 7.27). The Jones Mountains granites are highly evolved, displaying characteristics similar to the igneous clast but they have noticeably higher Rb and Nb, and lower Zr concentrations, indicative of their mixed characteristics as noted by Leat *et al.* (1993). All rocks from Palmerland have relatively high Zr and Nb concentrations indicative of their suggested plume related petrogenesis (Riley *et al.*, 2001).

U and Th concentrations are plotted for the Kekerengu clast and the Bounty Island Granite (Figure 7.28) and show that zircons from both rocks have overall near identical compositions, with the Kekerengu clast having generally higher Th/U ratios.

7.4.3 Spider Diagrams

Multi-element plots for all the source rocks are shown in Figure 7.29 and are compared with the igneous clast from Kekerengu (normalised to primitive mantle; McDonough, 1992). Considerable discrepancies between all source rocks occur, but all, except the Mount Dowling andesites, have distinct negative anomalies in Sr and Ti that are consistent with extensive crystal fractionation of plagioclase and Fe-Ti oxides. Adakitic characteristics are displayed by the Mount Dowling rocks, which have positive anomalies in Sr and Ba. All source rocks (except Jones Mountains) have a pronounced negative anomaly in Nb indicative of a subduction-related petrogenesis. A clear difference between the Kekerengu clast and the source rocks is apparent, with the clast characterised by a slight relative depletion in almost all elements except some LIL-elements.

7.4.4 Discrimination of Tectonic Setting

On tectonic discrimination plots Rb vs. Nb+Y and Nb vs. Y (Pearce *et al.*, 1984) the silicic volcanics from Palmerland plot mainly across the boundary between within-plate and volcanic-arc-granite fields, whereas the Jones Mountains granites display characteristics typical of within-plate or syn-collision granites (Figure 7.30). The calc-alkaline igneous clast from Kekerengu is indistinguishable from the Bounty Island granites and similar to the rocks from Mount Dowling, which all plot within the field of volcanic-arc-granite.

7.4.5 Isotopes

Sr and Nd isotope values of source rocks used for comparison are plotted in Figure 7.31. All data have been recalculated to the crystallisation age of the igneous clast from Kekerengu. No isotope data are available for the Bounty Island granites.

Source rocks from Palmerland, the Jones Mountains and from Mount Dowling are characterised by more radiogenic $^{87}Sr/^{86}Sr_{(188)}$ and $\varepsilon Nd_{(188)}$ values than the clast from Kekerengu. These isotopic ratios clearly suggest a significant crustal component in the petrogenesis of these rocks. The Pine Island Bay granites have the same isotopic signature as the igneous clast and overall have the least radiogenic $^{87}Sr/^{86}Sr_{(188)}$ and the least negative $\varepsilon Nd_{(188)}$ values, indicating lower levels of crustal contamination.

7.4.6 Summary and Conclusions

- Based on available geochronological and geochemical data presented above the Early Jurassic calc-alkaline I-type clast from Kekerengu is best correlated with granitoids exposed on the Bounty Islands and in Pine Island Bay (Figure 7.32).
- If the allocation of the Bounty Islands to the Median Tectonic Zone proves to be correct then the new age would fall within the "magmatic gap" recognised in the MTZ (see Chart).
- Although the geochemical data record of the Bounty Islands and Pine Island Bay granitoids is incomplete, the available data show that the age and petrogenesis of the Pine Island Bay granites and the age and geochemistry of the Bounty Island granites are indistinguishable from that of the single clast.

- The similarities between the Bounty Island Granite and the penecontemporaneous Pine Island granites indicate that they share a similar petrogenetic history and suggests that the Campbell Plateau was a part of Marie Byrd Land in the Early Jurassic.

- The calc-alkaline Mount Dowling andesites are geochemically too mafic and isotopically too radiogenic to be a viable source for the clast.

- The penecontemporaneous Jones Mountains calc-alkaline S-type granitoids and the volcanics from Palmerland are isotopically too radiogenic relative to the clast and display mixed geochemical signatures consistent with the emplacement into an intra-plate environment.

7.5 Comparison of Pahau Igneous Clasts with Pahau Terrane Sandstones

7.5.1 Introduction

In this section the geochemistry of the Pahau terrane igneous clasts is compared with published sandstone geochemistry (Roser *et al.*, 1995) and new sandstone Sr-Nd isotope data from this study, to demonstrate that the collected clasts, representing the igneous source of the Pahau sandstone, are not the sole provider of detritus to the depositional basins.

7.5.2 Major Elements

Roser and Korsch (1988; 1999) demonstrated that the major element chemistry of sandstones can be compared using discriminant functions. The Pahau sandstones (PF5) lie on the average igneous rock trend indicating rhyodacitic composition and its plutonic equivalent (Figure 7.33).

On this diagram the clasts from Ethelton define a narrow field and plot, with one exception, within the field typical of evolved rocks, close to a rhyolitic (or granitic) composition. The clast population from Mount Saul is dominated by felsic clasts of rhyolitic composition, but clasts of chemically intermediate rocks occur, with one clast of distinct dacitic composition. At Kekerengu the intermediate clasts are dominated by

granodiorites, but similar to the other conglomerates the majority of the clasts are evolved rhyolites and dacites.

Following Roser and Korsch (1999) an average source composition can also be assessed using the A-CN-K of Fedo *et al.* (1995). The clasts from all three Pahau conglomerate locations plot near the plagioclase - K-feldspar join with a chemical index of alteration (CIA) of around 50, along a primary source line defined by average igneous rocks (Figure 7.34). The PF5 sandstone field is defined by a narrow range of K-feldspar - plagioclase ratios and CIA values, with a trend from an average dacitic composition towards illite and muscovite (see also Roser and Korsch, 1999). Most of the clasts plot to the right of the PF5 field with higher K-feldspar - plagioclase ratios, with only few clasts plotting within the sandstone field. The observation that nearly all the clasts plot close to the line of primary igneous source compositions indicates: (1) that the igneous clast source has undergone very little weathering, and (2) that the clasts are first cycle (apparent from hand specimen). It further supports the conclusion that igneous activity and sedimentation were penecontemporaneous (Sections 3.4 and 3.5).

7.5.3 Trace Elements

The more felsic nature of the igneous clasts as compared to the PF5 sandstones can also be demonstrated using trace elements (Figure 7.35). Ethelton clasts predominantly plot near or above the rhyolitic composition, with some more mafic clasts plotting near the PF5 field. Similar distribution patterns are observed in the Mount Saul and the Kekerengu samples, which are also dominated by evolved to highly evolved clasts. More mafic clasts with PF5 affinities are also present. The generally higher Th/Sc ratio of the igneous clasts is mainly due to the higher Th content of these clasts, in the range of 1-30 ppm with an average content of 15 ppm. In contrast, the sandstones have a Th range of 6-13 ppm with an average content of 10 ppm. Sc ranges from 2-25 ppm in igneous clasts and from 5-11 ppm in PF5 sandstones, with averages of 3 ppm in the igneous clasts and 8 ppm in the sandstones respectively.

Most samples presented here classify as weakly peraluminous or metaluminous I-type clasts. However, peralkaline clasts or clasts that have A-type affinities differ with a higher Zr ppm content, and this is reflected in the clasts plotting to the right of the volcanic arc trend line (VAT).

Chondrite normalised La_N/Y_N ratios have been used by Roser and Korsch (1999) to investigate bulk source compositions, to demonstrate High Field Strength (HFS) element enrichment trends and to show how fractionated different rocks are. Igneous clasts and sandstones are plotted against SiO_2/Al_2O_3 as a measure of maturity and sorting (Figure 7.36). Igneous clasts from all three locations clearly plot across the field of PF5 with the majority of the clasts plotting either above (more fractionated) or below the field. However, many clasts are indistinguishable from the PF5 sandstones and a mix of these clasts could well represent the source of the sandstones. There is no clear distinction between metaluminous and peraluminous clasts due to the fact that most of the clasts are weakly peraluminous and are ambiguous with respect to the I/S-type classification scheme.

7.5.4 Sandstone and Sandstone Clast Sr-Nd Isotopes

Sr-Nd isotopic data of ten new sandstone samples are presented in Tables 7.2 and 7.3 (for sample locations see Appendix 1). Four sandstone samples from the Pahau terrane (Petrofacies-5: Ethelton, Mount Saul area) have been analysed for Sr-Nd isotopes in order to compare these samples with isotopic compositions of the igneous clasts of the Pahau terrane. In addition, three sample from the Rakaia Petrofacies-4 (Late Triassic: Ashly Gorge,Lake Coleridge, Waimakariri Gorge), one sample from Petrofacies-3 (Lower Late Triassic: Mount Hutt) and two sandstone clasts from Petrofacies-1 (Permian: Te Moana) were analysed. These last two clasts were cannibalistically recycled (Chapter 4) and are at least of Permian age. Stratigraphic ages were described in Chapter 2 (Table 2.1) and are based on zircon ages from this study or on the nearest fossil location to the sample analysed. To compare the various rocks of different ages all isotopes have been recalculated to the mean age of the igneous clasts (137 Ma), which broadly coincides with the depositional age of the Pahau sandstone, and they are described with respect to this age.

The Pahau sandstones from Mount Saul and the Hanmer basin are tightly constrained with $^{87}Sr/^{86}Sr_{(137)}$ between 0.70661 and 0.70698 and $\varepsilon Nd_{(137)}$ values between -2.6 and -2.9, whereas the Ethelton sample is more radiogenic and displays with $^{87}Sr/^{86}Sr_{(137)}$ of 0.70812 and $\varepsilon Nd_{(137)}$ -4.1 strong Rakaia sandstone affinities (Figure 7.37). All the sandstones and sandstone clasts from the Rakaia terrane define a narrow field and range in $^{87}Sr/^{86}Sr_{(137)}$ from 0.70784 to 0.70817 and $\varepsilon Nd_{(137)}$ values from -4.4 to -5.5.

Model ages (T_{DM}) for the Pahau igneous clasts have been discussed previously (Sections 5.2.6 and 7.3.7) and these ages are an estimate of the time at which the protolith separated from a mantle reservoir. Because a sediment sample may be a mixture of components of different source areas, the model age for sediments represents an average, weighted according to the amount of Nd contributed from each source.

Pahau sandstones (Mount Saul and Hanmer basin) have a T_{DM} of 1.1 Ga whereas the sample from Ethelton has a T_{DM} of 1.2 Ga that is indistinguishable from the youngest Rakaia sandstones, which range in T_{DM} from 1.2 to 1.3 Ga.

7.5.5 Summary and Conclusions

Geochemical comparison of igneous clasts with published data from Pahau terrane sandstones indicates that the igneous clast source cannot be the sole source of the Pahau sandstones. On all the comparative plots presented here some of the igneous clasts lie in positions which are indistinguishable from Pahau sandstone compositions. Parent plutons of these clasts could provide the bulk source composition for the sandstones. However, in all but one comparative plot (Figure 7.36) most clasts are distinctly different in composition from the sandstones and are generally more felsic with greater Th/Sc and Th. The comparison of alteration indices (Figure 7.34) shows that sandstones and igneous clast sources have undergone little or no weathering, suggesting that the deposition of sediments and magmatism in the source area was contemporaneous.

$^{87}Sr/^{86}Sr_{(137)}$ and $\varepsilon Nd_{(137)}$ data for all but one Pahau sandstone clearly fall between the fields defined by the igneous clasts and the Rakaia sandstones. This indicates that: (1) the igneous clast source is isotopically too primitive with respect to the Pahau sandstone to produce the sandstones by simple erosion of this source, (2) the Rakaia sandstones are generally too radiogenic with respect to the Pahau sandstone at the time of the Pahau sandstone deposition. The implications of these observations with regard to the provenance of the Pahau terrane in particular, and the configuration of the pre-break-up Gondwana margin in general, are discussed in Chapter 9.

CHAPTER 8
PROVENANCE OF RAKAIA TERRANE IGNEOUS CLASTS

CHAPTER 8

PROVENANCE OF RAKAIA TERRANE IGNEOUS CLASTS

Introduction

In this chapter the geochemistry and geochronology of the igneous clasts from the Rakaia conglomerates are compared and correlated with selected penecontemporaneous Cambrian to Middle Triassic igneous provinces from the dispersed Gondwana margin (Figures 1.1 and 8.2) in order to constrain the provenance of the Rakaia igneous clasts. In addition, the chemistry of the igneous clasts is compared with published South Island sandstone geochemistry in order to evaluate whether the igneous clast source is the sole source providing detritus to the Rakaia terrane sedimentary basins.

Only a small fraction of the Rakaia terrane clast population was dated by the U-Pb SHRIMP-method and younger/older clasts might be present. Nevertheless, the dated clasts are deemed to represent the age distribution within the collected clast population. In conjunction with major and trace element geochemistry (Chapter 6), the Rakaia terrane igneous clasts are separated into three groups: (1) Triassic to Permian, (2) Carboniferous, and (3) Cambrian. The three age groups are discussed in this order. Igneous provinces are described in terms of the I and S-type classification scheme of Chappell and White (1974).

The igneous provinces selected for comparison are considered to broadly represent the magmatic activity at a particular time in that area (Tables 8.1 to 8.3). A more detailed comparison is hampered by the scarcity of published age data, as well as major, trace, and isotope geochemical data for many of these provinces.

8.1 PERMIAN TO EARLY TRIASSIC IGNEOUS CLASTS

8.1.1 Introduction

Extensive Permian-Early Triassic igneous complexes are exposed in the New England Orogen of eastern Queensland (Shaw and Flood, 1981; Gust *et al.*, 1993; Bryant *et al.*, 1997; Allen *et al.*, 1998; Sivell and McCulloch, 2001) and northeastern New South Wales, Australia (Hensel *et al.*, 1985; Chappell, 1994; Caprarelli and Leitch, 1998) (Figure 8.1). Permian to Middle Triassic magmatism in New Zealand has been reported from the Median Tectonic Zone (Kimbrough *et al.*, 1994a; Muir *et al.*, 1998) and the Brook Street and Maitai terrane (Mortimer *et al.*, 1999a; Sivell and McCulloch, 2000) (Figures 1.4 and 1.5). In Antarctica penecontemporaneous magmatism in Marie Byrd Land is confined to the Amundsen Province (Pankhurst *et al.*, 1993; Pankhurst *et al.*, 1998b) (Figure 8.2).

Geochronological, selected major-, trace- and rare earth element, and radiogenic isotope data for these provinces are presented in Figures 8.3 to 8.16 and summarised in Table 8.1.

8.1.2 Igneous Source Provinces

8.1.2.1 Eastern Australia

Pickard *et al.* (2000) proposed that the sedimentary depocentres of the Permian to Triassic (predominantly) Rakaia terrane sandstones formed at the eastern margin of Australia, adjacent to the New England Orogen, which extends from northeastern Queensland to northern New South Wales (Figure 8.1). These authors proposed that the igneous provinces of the New England Fold Belt (NEFB) were the main source of the Rakaia detritus. In this study, the igneous suites of the NEFB are considered to represent the Australian sector of the Panthalassan Gondwana margin and are used for comparison.

The granitoids of the NEFB, collectively forming the New England Batholith, have been divided into five suites (Shaw and Flood, 1981; Hensel *et al.*, 1985): the S-type Bundarra and Hillgrove (Hillgrove is Carboniferous, see Section 8.2), and the younger I-type Nundle, New England Supersuite and Clarence River Suite.

The Early Permian peraluminous Bundarra Suite granitoids are characterised by LREE enrichment (Shaw and Flood, 1981) and have $^{87}Sr/^{86}Sr_{(i)}$ ratios between 0.70574 and 0.70612. The corresponding $\varepsilon Nd_{(i)}$ values range from -0.2 to -0.9. An emplacement age of c. 290 Ma has been assigned to these granitoids (Hensel *et al.*, 1985).

The Early Permian Volcanics within the NEFB are characterised by a variety of rocks with tholeiitic to calc-alkaline affinities ranging from basalt to rhyolites. No major and only a few trace element data are available for the volcanic rocks. A few Nd and Sr isotope measurements have been made, with $^{87}Sr/^{86}Sr_{(i)}$ ratios ranging from 0.70241 to 0.70404 (mean = 0.70348) and $\varepsilon Nd_{(i)}$ values ranging from +2 to +8, using an emplacement age of 280 (Caprarelli and Leitch, 1998).

The Late Permian calc-alkaline I-type New England Supersuite (NESS) (Hensel *et al.*, 1985) constitutes the core of the NEFB and is characterised by much greater mineralogical and geochemical variation than any of the other suites of the NEFB. It embraces a number of distinct, individual suites in its 400 km extent (e.g., Uralla, Moonbi) and spans the whole compositional range (from diorites to monzogranites). Rb-Sr total-rock ages for the Supersuite fall into a narrow range of c. 265 Ma with $^{87}Sr/^{86}Sr_{(i)}$ ratios ranging from 0.70382 to 0.70624 and $\varepsilon Nd_{(i)}$ values from -1.7 to +4.6 (Hensel *et al.*, 1985).

Late Permian calc-alkaline I-type Nundle Suite plutons of about 250 Ma age (Shaw, 1994) include mainly fine-medium grained granodiorites and tonalites, with $^{87}Sr/^{86}Sr_{(i)}$ ratios ranging from 0.70357 to 0.70396 and corresponding $\varepsilon Nd_{(i)}$ values from +3.3 to +6.1 (Hensel *et al.*, 1985). Apart from the Early Permian volcanic rocks the Nundle suite has significantly lower $^{87}Sr/^{86}Sr$ initial ratios and higher $\varepsilon Nd_{(i)}$ values than any other suite within the NEFB.

The calc-alkaline Clarence River Suite or Supersuite (Bryant *et al.*, 1997) intrusions are compositionally diverse and range from gabbro to monzogranite but are dominated by tonalites, granodiorites and diorites. Similarly to the Nundle Suite they are amongst the most isotopically primitive plutonic rocks, typically having $^{87}Sr/^{86}Sr$ initial ratios between 0.70314 to 0.70402 and corresponding $\varepsilon Nd_{(i)}$ values from +0.4 to +6.1 (using a 260 Ma crystallisation age for all the plutons, Bryant *et al.*, 1997). Most intrusions are characterised by LREE enrichment and moderate negative Eu anomalies. In contrast, the Duncans Creek Trondhjemite has a steep REE pattern and a small

positive Eu anomaly, indicating stabilisation of garnet at depth >26km (Bryant *et al.*, 1997). No Sr and Nd isotope data are available for these adakites.

Post-orogenic granitoids are all of Triassic age (235-220 Ma, Shaw, 1994) and are very similar to the Late Permian I-type granitoids described above. Two samples analysed by Hensel *et al.* (1985) gave $\varepsilon Nd_{(i)}$ values ranging from +1.0 to +4.5 and corresponding $^{87}Sr/^{86}Sr_{(i)}$ ratios from 0.70427 to 0.70458.

For comparison with igneous clasts from the Rakaia terrane and for simplicity (overcrowding of diagrams) the igneous provinces described here are grouped as follows: Bundarra Suite, Early Permian Volcanics, New England Supersuite (including the Nundle Suite and the post-orogenic granitoids), and Clarence River Supersuite. The adakitic plutons from the Clarence River Supersuite are grouped together with other adakites described below.

8.1.2.2 New Zealand

Permian to Triassic plutonic rocks in Fiordland occur in the Median Tectonic Zone and along its eastern side where they are in intrusive contact with the Brook Street terrane (Muir *et al.*, 1998; Mortimer *et al.*, 1999a, Kimbrough, 1994 #39) (Figure 1.5). Triassic ages have also been reported from the Buller Diorite in the Speargrass Creek area in Northwest Nelson (Figure 1.4, Kimbrough *et al.*, 1994a; Mortimer *et al.*, 1999a) (Figure 1.4).

Mortimer *et al.* (1999a) identified two metaluminous calc-alkaline suites in the Longwood Range area that are part of the MTZ. The non-radiogenic Permian Hekeia Gabbro (c. 250 Ma, Kimbrough *et al.*, 1994a) and the Pourakino Trondhjemite plutons (c. 290 Ma and 261±2 Ma, Mortimer *et al.*, 1999a; Tulloch *et al.*, 1999) intrude the Brook Street terrane and have $^{87}Sr/^{86}Sr$ initial ratios ranging from 0.70265 to 0.70306 and corresponding $\varepsilon Nd_{(i)}$ values ranging from +6.8 to +8.1. The Pourakino plutons have characteristics typical of adakites, and Tulloch *et al.* (1999) reported a 262±2 Ma crystallisation age for them, with an $^{87}Sr/^{86}Sr_{(i)}$ ratio of 0.70274 and a $\varepsilon Nd_{(i)}$ value of +6.8.

The Triassic metaluminous calc-alkaline Holly Burn Intrusives (c. 230 Ma, Kimbrough *et al.*, 1994a) range in composition from diorite to monzogranite and are isotopically more evolved than the Permian Pourakino and Hekeia plutons, with

$^{87}Sr/^{86}Sr$ initial ratios in the range of 0.70309 to 0.70352 and $\varepsilon Nd_{(i)}$ values from +3.9 to +4.8. Rock compositions indistinguishable from the inland Holly Burn Intrusives have been reported from the Longwood Range coast. Only the Colac Granite (c. 247 Ma, Kimbrough *et al.*, 1994a) is clearly different with radiogenic isotope characteristics similar to those of the Pourakino and Hekeia plutons.

The two suites defined by Mortimer (1999a) are used for comparison with the Rakaia igneous clasts. The Pomona Island granite sheet, the Manapouri Granite (296.6±4.4 Ma) and the Mistake Diorite (226.4±3.3 Ma, Muir *et al.*, 1998) are grouped with the Holly Burn Intrusives and termed MTZ Intrusives. The adakitic Pourakino Trondhjemite is grouped with the other adakites from Australia and Antarctica.

8.1.2.3 Antarctica

Permian intrusions are exposed in the Kohler Range in Marie Byrd Land (Mt. Isherwood, Mt. Strange, Ferri Ridge and Mt. Wilbanks, Figure 8.3) and are compositionally dominated by granodiorites and monzogranites but also include diorites (Mt. Wilbanks). The suite is overall low to moderate in K, calc-alkaline, metaluminous and I-type, with the Wilbanks diorites displaying characteristics typical of adakites. Samples analysed from the Kohler Range lie on a single Rb-Sr isochron defining an age of 276±2 Ma and $^{87}Sr/^{86}Sr_{(i)}$ ratios ranging from 0.70490 to 0.70606 and corresponding $\varepsilon Nd_{(i)}$ values of -1 (Pankhurst *et al.*, 1998b).

The Kinsey Ridge Granite (Ruppert and Hobbs Coast), is a calc-alkaline, metaluminous I-type biotite-hornblende monzogranite of Middle Triassic age (239±4 Ma, Pankhurst *et al.*, 1998b) with a $^{87}Sr/^{86}Sr_{(i)}$ ratio of 0.7035 and a $\varepsilon Nd_{(i)}$ value of +4.6.

The Middle Triassic two-mica syenogranite from the Mt. Murphy Massif gave a Rb-Sr age of 229±10 Ma, a $^{87}Sr/^{86}Sr_{(i)}$ ratio of 0.7058 and a corresponding $\varepsilon Nd_{(i)}$ value of -2.3 (Pankhurst *et al.*, 1998b). It is isotopically more radiogenic than the Kinsey Ridge Granite but is still in the range of most of the calc-alkaline granitoids of Marie Byrd Land.

On Thurston Island Permian to Triassic magmatism gave rise to mafic to intermediate plutonic rocks ranging in compositions from hornblende (Morgan Inlet) to olivine gabbros (Mt. Fleury) and diorites (Mt. Bramhall and Guy Peak). Igneous ages range from earliest Permian (286±8 Ma, Morgan Inlet) to late Early Permian (c. 270

Ma, Guy Peak) to Middle-to-Late Triassic (c. 230 Ma, Mt. Bramhall), and $^{87}Sr/^{86}Sr$ initial ratios vary between 0.70407 and 0.70658 with corresponding $\varepsilon Nd_{(i)}$ values of -3.5 to +0.9 (Pankhurst *et al.*, 1993).

For simplicity the Thurston Island plutons are treated as a single group. Similarly, the granitoids from the Kohler Range (except the adakites), the Kinsey Ridge Granite and the Mt. Murphy granitoids are plotted as a group. The Wilbanks Diorite is grouped with the other described adakites.

8.1.3 Comparison of Igneous Clasts with Source Provinces

8.1.3.1 Geochronology

Given the small number of zircons analysed from each igneous clast and the bimodal U-Pb zircon age distribution in a few Rakaia terrane clasts only imprecise ages can be assigned to four of these clasts (Table 3.1). The geochronological record of the igneous provinces considered for comparison consists of ages mainly determined by the Rb/Sr-, conventional U-Pb, or SHRIMP U-Pb-method (e.g., Kimbrough *et al.*, 1994a; Muir *et al.*, 1998; Pankhurst *et al.*, 1998b; Scheibner and Veevers, 2000). However, no significant age differences have been observed between the various dating methods (e.g., Kimbrough *et al.*, 1994a; Muir *et al.*, 1998; Pankhurst *et al.*, 1998b; Mukasa and Dalziel, 2000), and for this study no distinction is made between ages determined by the various methods. The dated clasts are considered to represent the age range of all the sampled igneous clasts from the conglomerates at Lake Hill, McKenzie Pass and Te Moana and are plotted together with igneous provinces in Figure 8.3.

Ten dated calc-alkaline igneous clasts from the Rakaia conglomerates give ages from c. 292-243 Ma, with two minor groups recognisable, one ranging in age from 258-243 Ma (Group 1) and the second from 292-277 Ma (Group 2).

The Group 1 igneous clasts broadly correlate with plutons from the Median Tectonic Zone (Hekeia Gabbro and Pourakino Trondhjemite) and calc-alkaline granitoids from the New England Fold Belt (NEFB), namely the New England Supersuite and the Clarence River Supersuite. The single adakite granodiorite (UC30659) is similar in age to the Pourakino and Duncan Creek trondhjemites. In Marie Byrd Land the Kinsey Ridge granites are similar in age to the youngest dated clasts from Group 1 whereas the Triassic Intrusives from Thurston Island are considered

to be too young to be a source. The two-mica Mount Murphy Syenogranite is also too young to be considered as a source for the single dated S-type clast from Group 1 (UC30667).

Two of the Early Permian clasts from Group 2 (UC30914 and 31818) correlate well with plutons from the Western Province (Pomona Island and Manapouri granites), and plutons and volcanics from the NEFB (Bundarra Suite and Early Permian Volcanics), and are also similar in age to the mafic to intermediate intrusives from Thurston Island (Morgan Inlet). A second adakitic monzogranite (UC30673) is similar in age to adakitic Wilbanks diorites reported from the Kohler Range in Marie Byrd Land. The Bundarra Suite is too old to be a suitable source for the S-type clast from Te Moana (UC31813).

The 'age-gap' in the Late Permian between Group 1 and 2 igneous clasts is also reflected in the age record of the igneous provinces from Australia and New Zealand. However, the Kohler Range granitoids overlap in age with both clast groups, and their ages coincide strongly with the main peaks of the detrital zircon age distribution of the Rakaia sandstones (Figures 3.8 and 3.9).

8.1.3.2 Petrography

The predominantly evolved and fractionated igneous clasts lack the distinctive minerals that define a granite type. If these minerals are observed in clasts they usually are altered or present in a pseudomorphous state, inhibiting a rigorous and conclusive petrographical comparison with source provinces.

8.1.3.3 Major and Trace Element Geochemistry

Most of the igneous clasts studied have undergone some degree of mineralogical readjustment (Chapter 6), similar to many of the igneous source provinces, and geochemical data must therefore be interpreted with caution before drawing petrogenetic or tectonic conclusions.

Although intermediate compositions occur, the Permian - Middle Triassic igneous clast population is dominated by evolved granitoids and rhyolites. The clast population is also dominated by slightly peraluminous clasts (68.7 %; referred to as I/S-type), which are ambiguous to classify using the alphabet classification scheme of

Chappell and White (1974). Minor groups of I-type (11.9 %), S-type (12.7 %) and adakitic (6.7 %) clasts also occur (Figure 6.25). The clast population is grouped and plotted according to aluminium saturation indices and compared to that of the source rocks, which display a similarly wide range of compositions (Figure 8.4). As previously noted, metaluminous granitoids can become weakly peraluminous to peraluminous with extended fractionation and the alphabet classification scheme should therefore be used with caution. For example, a fractionated rhyolitic clast from Te Moana (UC31813) classifies as peraluminous (ASI = 1.17), but has Sr-Nd isotope characteristics of a typical I-type rock (Chappell and White, 1992). This rhyolite is grouped with the other I/S-type clasts.

The calc-alkaline nature of all the igneous clasts is shown on an AFM-diagram (Figure 6.21) and in Figure 8.5. All the source rocks lie within the calc-alkaline and high-K calc-alkaline series of Peccerillo and Taylor (1976), a trend mirrored by the igneous clast population (Figure 8.6), which shows strong affinities with felsic members of most source provinces. If compared with the source-adakites, the Lake Hill adakites have a higher SiO_2 content and are generally enriched in K_2O, with only a few clasts plotting close to the source-adakite field. Low-K clasts are all weakly to strongly foliated and element mobility may account for the seemingly tholeiitic characteristics.

Major and trace element variations are shown in selected Harker diagrams in Figures 8.7 and 8.8. TiO_2, Al_2O_3, Fe_2O_3, MgO, CaO, and P_2O_5 of the source provinces and igneous clasts all show a negative correlation with SiO_2. Na_2O remains relatively constant and shows a strong overlap between the compared rocks. Major element concentrations of igneous clasts correlate well with the felsic members of all the igneous provinces. Adakitic clasts broadly correlate with the source-adakites but are depleted in CaO.

A similar correlation trend between clasts and source rocks is displayed by trace elements (Figure 8.8). Sr content generally decreases with increasing SiO_2 content whereas Rb increases. The characteristic high Sr content of adakites separates these clasts from most other rocks. On a Sr/Y vs. Y plot, used by Defant and Drummond (1990) to distinguish slab-derived from mantle-wedge-derived magmas, virtually all the source and Lake Hill adakites plot within the adakitic field. No REE element data are

available for the source adakites, limiting a more detailed comparison of these rocks (Figure 8.9).

On a multi-element variation diagram the calc-alkaline I-type igneous clasts (>70 wt% SiO_2) correlate well with averaged trends of selected source provinces (Figure 8.10). All the rocks are enriched in LIL elements and display a distinct spiked pattern with pronounced negative anomalies at Nb, all characteristics of subduction-derived magmas.

The multi-element trends of the calc-alkaline source-adakites broadly mimic the trend displayed by the adakites from Lake Hill. All plotted samples are enriched in LIL elements, have positive Ba and Sr anomalies and are strongly depleted in Y, confirming their adakitic characteristics (Figure 8.11).

8.1.3.4 Discrimination of Tectonic Setting

On tectonic discrimination plots (Figure 8.12, Pearce *et al.*, 1984) virtually all calc-alkaline, metaluminous to peraluminous igneous clasts and the source province rocks plot within the field of volcanic-arc-granite with some minor spread into the within-plate and ocean-ridge fields (Early Permian Volcanics). The clasts display a strong affinity with plutons from the Clarence River Supersuite, the Median Tectonic Zone and the Amundsen Province. Half of the adakitic clast population is indistinguishable in composition from that of the source-adakites.

8.1.3.5 Isotopes

Isotope data from the New England Fold Belt include samples from the New England and Clarence River supersuites, the Bundarra Suite and the Early Permian Volcanics (Hensel *et al.*, 1985; Bryant *et al.*, 1997; Caprarelli and Leitch, 1998). Median Tectonic Zone data are from Fiordland (Muir *et al.*, 1998; Mortimer *et al.*, 1999a; Tulloch *et al.*, 1999) and those for Antarctica are from Marie Byrd Land (Pankhurst *et al.*, 1998b, and pers. comm.) and Thurston Island (Pankhurst *et al.*, 1993, and pers. comm.). For comparison Silurian to Devonian rocks from the Lachlan Fold Belt (McCulloch and Chappell, 1982) and Karamea Batholith (Muir *et al.*, 1996b) are shown as well.

To compare the isotopes of this study with the various igneous source rocks all the initial $^{87}Sr/^{86}Sr_{(t)}$ and $\varepsilon Nd_{(t)}$ values have been recalculated to the approximate mean age (c. 260±20 Ma) of the dated Permian to Early Triassic clast population (Figure 8.13). This age broadly corresponds to the crystallisation age of most of the penecontemporaneous source rocks. The initial $^{87}Sr/^{86}Sr_{(t)}$ values for an igneous clast with a high Rb/Sr ratio (>2; UC31813) and source plutons with high Rb/Sr ratios have been excluded from the comparison, as they give unrealistic recalculated $^{87}Sr/^{86}Sr_{(260)}$ values. Values for the potential source provinces have been recalculated so that they include the range of isotopic compositions calculated from the clasts (c. 260±20 Ma). Similar procedures are applied when comparing the Carboniferous (Section 8.2.3.5) and the Cambrian (Section 8.3.3.5) clasts with source provinces.

On a broad scale all the Early Triassic to Permian clasts are constrained with $^{87}Sr/^{86}Sr_{(260)}$ between 0.70320 to 0.70750 and $\varepsilon Nd_{(260)}$ values between -4.3 and +0.8 (Figure 8.13a). Figure 8.13b is an enlargement of Figure 8.13a and shows in detail that I-type clasts range in $^{87}Sr/^{86}Sr_{(260)}$ from 0.70393 to 0.70638 and in $\varepsilon Nd_{(260)}$ concentrations from -1.1 to +0.8. The clasts designated I/S-type have $^{87}Sr/^{86}Sr_{(260)}$ ratios ranging from 0.70320 to 0.70707 and $\varepsilon Nd_{(260)}$ values from -4.3 to +0.1. The adakitic clast has a $^{87}Sr/^{86}Sr_{(260)}$ ratio of 0.70583 and a corresponding $\varepsilon Nd_{(260)}$ value of -0.9, whereas the single analysed S-type clast from Lake Hill has a $^{87}Sr/^{86}Sr_{(260)}$ ratio of 0.70750 and a $\varepsilon Nd_{(260)}$ value of -3.5.

Although some clasts show isotopic similarities with the Lachlan Fold Belt and the Karamea granitoids, the Silurian to Devonian age of the granitoids precludes them from being a source. The Nundle Suite and the Early Permian Volcanics of the New England Fold Belt, as well as rocks from the Median Tectonic Zone (Hekeia Gabbro) and from Marie Byrd Land (Kinsey Ridge) are isotopically more primitive than all the igneous clasts. Isotope compositions of the I-type and the I/S-type clasts broadly correlate with radiogenically evolved endmembers of the New England Supersuite, the Clarence River Supersuite, and the Median Tectonic Zone. These clasts also show good correlation with plutons from the Bundarra Suite, Amundsen Province and Thurston Island. The adakitic clast is indistinguishable from the compositions displayed by plutons from the Antarctic margin and the Bundarra Suite but strongly differs in isotopic composition from the isotopically primitive Pourakino Trondhjemite. The most radiogenic clasts (UC30668 and 30667) have affinities with the most radiogenic

members of Thurston Island and point to the involvement of a crustal component during petrogenesis.

On a $\varepsilon Nd_{(260)}$ vs. $^{147}Sm/^{144}Nd$ plot (Figure 8.14) all igneous clasts display $^{147}Sm/^{144}Nd$ ratios similar to the crustal average (0.11, Goldstein *et al.*, 1984).

Isotope compositions of the majority of the source rocks plot well above the field of the igneous clasts. The more radiogenic igneous clasts correlate not only with source plutons from Marie Byrd Land, Thurston Island, the New England Supersuite and the Bundarra Suite, but they are also very similar in composition to the Rakaia sandstones (Table 7.2 this study and data from Frost and Coombs, 1989). The sandstones display uniform continental characteristics suggesting derivation from a single source or a mixture of sources whose weighted isotopic average is similar to that of the sandstones.

Depleted mantle model ages (T_{DM}) for the Permian to Early Triassic clasts range from 0.82 to 1.16 Ga, with one clast from Lake Hill (UC30668) giving a T_{DM} age of 1.48 Ga. Also plotted are data for the Rakaia sandstones (Table 7.2 this study and data from Frost and Coombs, 1989).

A $\varepsilon Nd_{(260)}$ vs. T_{DM} plot (Figure 8.15) indicates that the source rocks from the Median Tectonic Zone, the Kinsey Ridge, Nundle Suite, and the Early Permian Volcanics of the NEFB are not only isotopically too primitive but are also composed of materials on average too young to be a valid source for the Rakaia igneous clasts. The Clarence River Supersuite includes some plutons with T_{DM} ages similar to those of the clasts, but in general they have more primitive isotope compositions.

The more radiogenic plutons of the New England Supersuite and the Amundsen Province granitoids (Kohler Range, T_{DM} 0.99 to 1.48 Ga) were derived from sources similar in age to that of the igneous clasts, whereas plutons from Thurston Island are composed of material generally too old. The compositions of the most radiogenic clasts with the older T_{DM} ages are very similar to the Rakaia sandstones.

8.1.4 Summary and Conclusions

Geochronological, Sr-Nd isotope, and major and trace element data presented in this section are incapable of defining a distinct source province for the Permian to Early Triassic igneous clasts (Figure 8.16). However, the following conclusions can be drawn:

- The tholeiitic to calc-alkaline Early Permian Volcanics from the New England Fold Belt are indistinguishable in age from the Permian clasts, however their overall primitive Sr-Nd isotope composition precludes them from being a clast source.

- The Hekeia Gabbro is geochemically and isotopically too primitive to be the source for the clasts. In addition, model ages indicate that the gabbros are derived from material too young to be a viable source.

- Sr-Nd isotopic compositions from the few sampled plutonic rocks from Thurston Island correlate broadly with the more radiogenic clasts, but geochronology, geochemistry, and model ages of these plutons display a poor correlation with most igneous clasts.

- Felsic and intermediate igneous clasts broadly correlate with penecontemporaneous intermediate to felsic members of the Clarence River Supersuite, and the Nundle and Bundarra suites, but all these suites from the Australian sector of pre-break-up Gondwana are overall isotopically more primitive than the igneous clasts.

- The geochemistry and the isotopic compositions of the igneous clasts correlate well with those of the penecontemporaneous felsic members of the Median Tectonic Intrusives. However, the intrusives are derived from material on average too young compared with the igneous clasts.

- Crystallisation ages, geochemistry, Sr-Nd isotope compositions and model ages of most of the igneous clasts correlate well with felsic members of the New England Supersuite and felsic plutons from the Amundsen Province. Based on the available data presented here these two provinces are considered to be possible sources for the Permian to Early Triassic igneous clasts.

- Although penecontemporaneous adakites occur within the Australian to Antarctic sectors of Gondwana their geochemistry and isotopic compositions correlate poorly with those displayed by the adakitic clasts from the Lake Hill conglomerate.

- Nd isotope compositions of the more radiogenic igneous clasts ($\varepsilon Nd_{(i)}$ -4.3 to -0.5) and the Amundsen Province and Thurston Island plutons are indistinguishable from the Nd isotope compositions of the Rakaia terrane sandstones.

8.2 CARBONIFEROUS IGNEOUS CLASTS

8.2.1 Introduction

Dated igneous clasts of Carboniferous age from this study are unique to the Boundary Creek conglomerate, which is dominated by calc-alkaline, metaluminous I-type clasts.

Carboniferous magmatism in Australia occurred mainly in the New England Fold Belt contemporaneous with minor intrusions in the Lachlan Fold Belt (Shaw and Flood, 1981; Hensel *et al.*, 1985; Shaw and Flood, 1993; Chappell, 1994; Bryant *et al.*, 1997; Caprarelli and Leitch, 1998). In New Zealand Carboniferous magmatism is confined to the Western Province (Cooper and Tulloch, 1992; Muir *et al.*, 1994) (Mortimer *et al.*, 1997; Malloch, 1999) and the Median Tectonic Zone (Kimbrough *et al.*, 1993; Kimbrough *et al.*, 1994a; Beresford *et al.*, 1996; Muir *et al.*, 1998). In Antarctica Carboniferous plutons were emplaced in Northern Victoria Land (Laird *et al.*, 1974; Stump, 1995) and Ross and Amundsen Province (Adams, 1987; Pankhurst *et al.*, 1993; Pankhurst *et al.*, 1998b).

Extensive Silurian to Devonian magmatism occurs in the Lachlan Fold Belt (Richards and Singleton, 1981; Chappell, 1994), Tasmania (Brooks and Compston, 1965; McDougall and Leggo, 1965; Cocker, 1982; McClenaghan, 1984; Sawka *et al.*, 1990), Western Province of New Zealand (e.g. Karamea Batholith, Muir *et al.*, 1994), Northern Victoria Land (e.g. Admiralty Intrusives, Borg *et al.*, 1987) and Ross Province (e.g. Ford Range, Weaver *et al.*, 1991). Many of these, based on U-Pb SHRIMP ages and radiogenic isotope compositions, are generally too old to be a suitable source for the igneous clasts from the Boundary Creek conglomerate. However, the Middle-Late Devonian Karamea Batholith, the Admiralty Intrusives and the Ford Range granodiorites are used here for comparison. Geochronological, selected major, trace and rare earth element, and radiogenic isotope data for the selected igneous provinces are presented in Figures 8.3 and 8.17 to 8.28 and summarised in Table 8.2.

8.2.2 Igneous Source Provinces

8.2.2.1 Eastern Australia

The Hillgrove Suite from the New England Fold Belt consists of peraluminous, foliated biotite (± garnet) granodiorites and granites (Figure 8.1, Shaw and Flood, 1981). A U-Pb zircon SHRIMP age of 303±3 Ma (Kent, 1994) obtained for the suite is in good agreement with previous Rb/Sr ages (Flood and Shaw, 1977; Hensel *et al.*, 1985). $^{87}Sr/^{86}Sr_{(i)}$ ratios range from 0.70364 to 0.70481 and corresponding $\varepsilon Nd_{(i)}$ values from -0.1 to +1.8.

Minor granitoids in the southern portion of the northern New England Fold Belt are also Carboniferous in age, e.g., the S-type Claddagh Granodiorite with an $^{40}Ar/^{39}Ar$ age of c. 306 Ma (Little *et al.*, 1992). U-Pb zircon SHRIMP dating of the granitoids from the northern New England Fold Belt gives ages of 304.3±5.8 and 308.2±7.1 Ma for the Urannah Suite (Allen *et al.*, 1998). Minor Carboniferous granitoids with similar geochemistry to that of the New England Fold Belt are exposed in the northeastern part of the Lachlan Fold Belt and may be related to the NEFB (Shaw and Flood, 1993).

8.2.2.2 New Zealand

The megacrystic Cape Foulwind and Windy Point granites (327.3±6.2 Ma and 328.6±4.4 Ma, Muir *et al.*, 1994) outcrop as isolated plutons within the Buller terrane (Figure 1.4) and are both weakly peraluminous, high-K calc-alkaline, unfractionated and fractionated A-type monzogranites (Muir *et al.*, 1996b). The Cape Foulwind Suite has $^{87}Sr/^{86}Sr_{(i)}$ ratios ranging from 0.70509 to 0.71238 and $\varepsilon Nd_{(i)}$ values from -2.0 to +3.2, whereas Windy Point is slightly more radiogenic with $^{87}Sr/^{86}Sr_{(i)}$ ratios ranging from 0.71869 to 0.72705 and corresponding $\varepsilon Nd_{(i)}$ values from -8.3 to +0.5 (Waight, pers. comm.).

The highly fractionated metaluminous to weakly peraluminous, high-K, calc-alkaline Toropuihi Granite, occurring as cuttings in the Toropuihi-1 drillhole (c. 310 Ma, Cooper and Tulloch, 1992; Mortimer *et al.*, 1997) and the I-type Paringa Tonalite (c.300-330 Ma, Hurley *et al.*, 1962; Aronson, 1965; Cooper and Tulloch, 1992) show no mineralogical, geochemical and geochronological relationship with the Cape Foulwind Supersuite of Malloch (1999). For simplicity these rocks are grouped together with the calc-alkaline, metaluminous I-type Kakapo and Hauroko granites (c. 340 Ma

and 358.5±5.3 Ma, Muir *et al.*, 1998) exposed in the Western Province in Fiordland (Figure 1.5). The $^{87}Sr/^{86}Sr_{(i)}$ ratio for the Kakapo Granite is 0.70537 and the $\varepsilon Nd_{(i)}$ value is -2.2 (Muir *et al.*, 1998). A 334±5 Ma U-Pb SHRIMP zircon age on a quartzofeldspathic schist in Fiordland (Gibson and Ireland, 1996) also supports Carboniferous magmatism in the New Zealand region.

Carboniferous granitoids also occur in the Median Tectonic Zone. The leucocratic I-type Echinus Granite (310±3 Ma, Kimbrough *et al.*, 1993; Beresford *et al.*, 1996) outcrops on Pepin Island in northwest Nelson. In Fiordland the Pomona Island Granite and Diorite (305±4 Ma and 345±4 Ma, Muir *et al.*, 1998) and Poteriteri Granite (c. 330 Ma, Muir *et al.*, 1998), together with the Lake Roxburgh Tonalite (344±4 Ma, Muir *et al.*, 1998), are the main Carboniferous intrusions within the Median Tectonic Zone (Kimbrough *et al.*, 1994a; Muir *et al.*, 1998). These Median Tectonic Zone plutons are metaluminous to weakly peraluminous, I-type, calc-alkaline rocks and have $^{87}Sr/^{86}Sr_{(i)}$ ratios in the range of 0.70400 to 0.70422 and corresponding $\varepsilon Nd_{(i)}$ values from +1.4 to +4.9 (Muir *et al.*, 1998).

The Devonian Karamea Batholith (375±5 Ma, Muir *et al.*, 1994; Muir *et al.*, 1996a) consists of high-K, calc-alkaline, biotite, and two-mica granites. $^{87}Sr/^{86}Sr_{(i)}$ ratios range from 0.70485 to 0.72098 and corresponding $\varepsilon Nd_{(i)}$ values range from -9.3 to -0.3 (Muir *et al.*, 1996b). Many Karamea plutons are characterised by a megacrystic texture. The penecontemporaneous Riwaka complex of the Takaka terrane is thought to represent the mantle component of the Karamea Suite with a $\varepsilon Nd_{(i)}$ value of +1.9 and a $^{87}Sr/^{86}Sr_{(i)}$ ratio of 0.70439 (Muir *et al.*, 1996b).

8.2.2.3 Antarctica

The Carboniferous Salamander Granite Complex outcrops in the Salamander Range in northern Victoria Land (Vetter and Tessensohn, 1987; Stump, 1995). Based on geochronology, mineralogy and geochemistry Borg (1986) considered the Salamander Granite Complex a separate intrusive phase, distinct from the Devonian Admiralty Intrusives. A Rb-Sr whole rock/mineral isochron yields a 319±5 Ma emplacement age for the Salamander Granite (Stump, 1995) (Borg *et al.*, 1987).

The metaluminous I-type Devonian Admiralty Intrusives have Rb/Sr whole rock ages that range from c. 390-360 Ma (K/Ar mineral ages 370-350 Ma) and range in

composition from monzogranites to tonalites but are predominantly granodiorites with calc-alkaline affinities (Kreuzer *et al.*, 1981) (Vetter *et al.*, 1983; Stump, 1995). $^{87}Sr/^{86}Sr_{(i)}$ ratios range from 0.70592 to 0.71744 and corresponding $\varepsilon Nd_{(i)}$ values range from -7.1 to -2 (Borg *et al.*, 1987).

Carboniferous plutons in the Ross Province were first recognised at Mount McCoy by Palais *et al.* (1993), with more extensive work being undertaken by Pankhurst *et al.* (1998b). Along the Ruppert coastline the Bruner Hill Granite outcrops as a leucogranite which is cut by micro-syenogranite sheets. U-Pb SHRIMP dating gives an age of 330±5 Ma for the Bruner Hill Granite which is comparable to the Rb/Sr age of 335±20 Ma (Pankhurst *et al.*, 1998b). Muscovite-bearing aplites and pegmatites that cut the 360±84 Ma Chester Granodiorite in the Chester Mountains also record the c. 330 Ma intrusion phase. A Rb/Sr isochron for the aplites and pegmatites gives an age of 338±3 Ma with an initial $^{87}Sr/^{86}Sr_{(i)}$ ratio of 0.7210±0.002 (Pankhurst *et al.*, 1998b).

Granodiorites from the Gutenko and Hermann Nunataks yield c. 375 Ma U-Pb SHRIMP dates and a c. 330 Ma age from a Rb/Sr isochron with an initial $^{87}Sr/^{86}Sr_{(i)}$ ratio of 0.7053 (Pankhurst *et al.*, 1998b). This Rb/Sr age is thought to be related to the emplacement of granitoids, such as the aplites from the Chester Mountains and the Bruner Hill Granite (Pankhurst *et al.*, 1998b).

A slightly younger Carboniferous intrusion age is recorded at Mount McCoy in the titanite-biotite-hornblende granodiorite (U-Pb age 322±9 Ma, Palais *et al.*, 1993), giving a $^{87}Sr/^{86}Sr_{(i)}$ ratio of 0.7042 and a $\varepsilon Nd_{(i)}$ value of +3 and indicating a primitive source region (Pankhurst *et al.*, 1998b). The similarities of the Carboniferous intrusive ages suggests a regional felsic igneous event along the Ruppert coastline and in the Ford Ranges at c. 340-335 Ma (Pankhurst *et al.*, 1998b).

The Devonian to earliest Carboniferous (380-350 Ma) Ford, Chester and Herman Nunatak granodiorites, outcropping in the Ford Ranges, intrude Cambrian-Ordovician metasedimentary rocks of the Swanson Formation in the Ross Province (Adams, 1987). The calc-alkaline, metaluminous to peraluminous rocks of the Ford Granodiorite range in composition from tonalites to monzogranites, with granodiorites that are biotite rich and hornblende-bearing predominant (Weaver *et al.*, 1991). On the basis of trace element tectonic discrimination diagrams, Weaver *et al.* (1991) suggested that the granitoids were emplaced into an active continental margin environment. $^{87}Sr/^{86}Sr_{(i)}$

ratios for the granodiorites range from 0.7051 to 0.70575 with corresponding $\varepsilon Nd_{(i)}$ values from -1.0 to -3.3 (Pankhurst *et al.*, 1998b). The Ford Granodiorite is geochemically and mineralogically similar to the Devonian, calc-alkaline I-type Admiralty Intrusives of Northern Victoria Land.

Carboniferous granitoids also outcrop in the Amundsen Province. Calc-alkaline, medium-K granitoids outcropping at Bear Peninsula (Jeffrey Head and Mt. Bodziony) are intruded by gabbro-diorite intrusions. Combination of data for both rock types yields a Rb-Sr age of 312±10 Ma with $^{87}Sr/^{86}Sr_{(i)}$ ratios for the gabbro and granodiorite from 0.70369 to 0.70376 and corresponding $\varepsilon Nd_{(i)}$ values from +4.1 to +3.2 (Pankhurst *et al.*, 1998b).

Orthogneisses exposed on Thurston Island (Morgan Inlet and Cape Menzel) range in composition from meta-diorite to meta-leucogranite (Leat *et al.*, 1993), with a Rb-Sr age of 309±5 Ma and $^{87}Sr/^{86}Sr_{(i)}$ ratios ranging from 0.70359 to 0.70403 and $\varepsilon Nd_{(i)}$ values from +0.5 to +2.6 (Pankhurst *et al.*, 1993). The Late Carboniferous age, the radiogenic isotope values, and the geochemistry are comparable to that of the Amundsen Province. For this study the Thurston Island and the Amundsen Province data are combined and plotted together.

8.2.3 Comparison of Igneous Clasts with Source Provinces

8.2.3.1 Geochronology

The four dated calc-alkaline metaluminous igneous clasts from the Boundary Creek conglomerate range in age from 325±5 to 356±5 Ma (Figure 8.3). They correlate well with calc-alkaline plutons from the Western Province of New Zealand (Cape Foulwind Supersuite, Paringa Tonalite) and plutons from the Fiordland section of the Median Tectonic Zone (Pomona Island Diorite, Roxburgh Tonalite, Poteriteri Granite). The Salamander Intrusives of northern Victoria Land are similar in age to the youngest dated clast. The Bruner Hill Syenogranite and the Mount McCoy Granodiorite (Ross Province) are indistinguishable in age from the younger igneous clasts from Boundary Creek. The Chester Mountain and Ford granitoids are, together with the Admiralty Intrusives and the Karamea Batholith, too old, whereas the calc-alkaline, peraluminous Hillgrove Suite, the Bear Peninsula granites (Amundsen Province) and Morgan Inlet

orthogneisses (Thurston Island) are too young to be a source for the dated clasts (Figure 8.3).

8.2.3.2 Petrography

The strongly deformed and partially recrystallised and altered nature of all the clasts from the Boundary Creek conglomerate preclude petrographic comparison with potential source rocks. No clasts with megacrystic texture, charcteristic of many plutons of the Karamea Batholith and the Cape Foulwind Suite, have been found.

8.2.3.3 Geochemistry

The selected igneous provinces and the igneous clasts from Boundary Creek all display a calc-alkaline trend (Figures 8.17 and 8.18). Classification by aluminium saturation index of Zen (1986) indicates that the Foulwind Supersuite, Hillgrove Suite and Karamea Batholith are entirely peraluminous, whereas the remaining source provinces contain plutons of both metaluminous and peraluminous character, a trend displayed also by the igneous clasts (Figure 8.19).

On selected Harker diagrams (Figure 8.20) major and trace element variations show that TiO_2, Al_2O_3, Fe_2O_3, MgO, CaO, and P_2O_5 of the source provinces and igneous clasts all show a negative correlation with SiO_2. The predominantly felsic Boundary Creek clasts (>70 wt% SiO_2) correlate well with felsic members of the igneous provinces, but the clasts are slightly enriched in CaO, and have distinctly higher Na_2O concentrations than the potential sources. Apart from two samples, the igneous clasts of intermediate compositions (<70 wt% SiO_2) show chemical affinities similar to those displayed by source province plutons of similar SiO_2 content.

Trace element variation plots (Figure 8.21) show that the Sr content of the igneous clasts is indistinguishable from that displayed by most of the source provinces. Most of the clasts are depleted in Rb compared to the source rocks but show some affinities with rocks from the Western Province granitoids, Median Tectonic Zone and Amundsen Province.

Rb and K mobility is also shown on a multi-element variation diagram for the calc-alkaline I-type igneous clasts (>70 wt% SiO_2), which display characteristics of subduction-derived magmas with negative anomalies at Nb and an overall enrichment

in LIL elements (Figure 8.22). Selected plutons from the source provinces display similar calc-alkaline trends. The A-type Cape Foulwind Granite has pronounced negative Ba, Sr, and Ti anomalies reflecting its fractionated nature. The pronounced negative Nb anomaly suggests either a subduction-related tectonic setting or a source inheritance. LIL element mobility is less pronounced in igneous clasts, with SiO_2 content ranging from 60 to 70 wt%, and the trend of these clasts is broadly mirrored by trends of selected source plutons.

8.2.3.4 Discrimination of Tectonic Setting

Using a tectonic discrimination diagram of Pearce (1984) all calc-alkaline, metaluminous to peraluminous igneous clasts from Boundary Creek plot well within the field for volcanic-arc-granite and show good correlation with a similar pattern displayed by Median Tectonic Zone, Western Province, Amundsen and Ross Province plutons. The Cape Foulwind Supersuite, the Toropuihi Granite, the Karamea Batholith, and the Ford Range intrusives spread well into the within-plate field which is thought to equate with A-type granitoids (Figure 8.23). A similar trend is displayed on a diagram of Whalen (1987), with all the igneous clasts plotting within the field for I and S-type granitoids and showing compositional similarities mainly with rocks from the Median Tectonic Zone and the Western Province granitoids. A-type affinities are displayed by the Cape Foulwind Supersuite, the Toropuihi Granite, the Karamea Batholith, and the Ford Range plutons (Figure 8.24).

Such discriminant diagrams should be interpreted with caution as they do not take into account the fractionation of the discriminating elements. For example, the calc-alkaline, metaluminous to peraluminous I-/S-type Karamea Batholith plots in both the A-type (least fractionated) and I-/S-type fields (most fractionated) despite its clearly subduction-derived origin (see Muir *et al.*, 1996b).

8.2.3.5 Isotopes

Radiogenic Sr and Nd isotope compositions of the Carboniferous igneous clasts and selected Devonian to Carboniferous igneous source provinces are compared in Figures 8.25 to 8.27.

Australian data are for the Hillgrove Suite (Hensel *et al.*, 1985), and those for New Zealand include rocks from the Median Tectonic Zone (Muir *et al.*, 1998), the

Western Province granites (Muir *et al.*, 1998), Cape Foulwind Supersuite (Waight pers. comm.) and the Karamea Batholith (Muir *et al.*, 1996b). The Admiralty Intrusives (Borg *et al.*, 1987) and plutons from Marie Byrd Land (Pankhurst *et al.*, 1993; Pankhurst *et al.*, 1998b, and Pankhurst pers. comm.) represent the Antarctic sector of the pre-break-up Gondwana margin. Comparison data for the Silurian Lachlan Fold Belt (McCulloch and Chappell, 1982) are shown as well (Figure 8.25).

Initial $^{87}Sr/^{86}Sr_{(t)}$ and $\varepsilon Nd_{(t)}$ values for igneous clasts and selected source provinces have been recalculated to the approximate mean age (340±15 Ma) of the dated Carboniferous clast population.

The Carboniferous calc-alkaline, metaluminous Boundary Creek clasts have $^{87}Sr/^{86}Sr_{(340)}$ ratios between 0.70488 and 0.70673 and $\varepsilon Nd_{(340)}$ values from -2 to +1.5, radiogenic isotope compositions typical of subduction-related magmas. These compositions are similar to those of most of the plotted provinces, with three of the clasts correlating well with rocks from the Ross Province. The isotopically most primitive clast correlates also with the Hillgrove Suite, whereas the isotopically most evolved clast plots in the field defined by the Ford granitoids and overlaps with the isotopically most primitive endmembers of the Admiralty Intrusives. Compared to the igneous clasts, the Cape Foulwind granitoids have $\varepsilon Nd_{(340)}$ values (-1.9 to 3.3) indistinguishable from those of the clasts but have more radiogenic $^{87}Sr/^{86}Sr_{(340)}$ ratios (0.70700 to 0.71073 with Rb/Sr ratios ranging from 0.8 to 6.7; Windy Point Suite 0.71774 to 0.72546 and Rb/Sr between 2 and 3), most likely caused by the disturbance of their Rb/Sr system during Early Cretaceous tectonic events in the Western Province of New Zealand (Waight, pers. comm.).

A similar correlation pattern is observed when $\varepsilon Nd_{(340)}$ vs. $^{147}Sm/^{144}Nd$ are plotted (Figure 8.26). Isotopic compositions of two clasts correspond broadly with those displayed by plutons from the Ross Province. One clast is indistinguishable from the compositional ranges displayed by the Amundsen Province and Cape Foulwind plutons whereas the most radiogenic clast has compositional affinities similar to the Ford granitoids.

Depleted mantle model ages for the igneous clasts range from 0.99 to 1.13 Ga and are compared with the selected source provinces in Figure 8.27. Granitoids from the Karamea Batholith, Admiralty Intrusives, and part of the Ford Range granitoids are

composed of materials on average too old to be a source for the clasts. Rocks from the Hillgrove Suite, the Cape Foulwind Supersuite, the Ross and Amundsen Provinces were derived from material similar in age to that of the igneous clasts, whereas plutons from the Median Tectonic Zone are composed of material generally too young to be a viable source for the clasts.

8.2.4 Summary and Conclusions

No distinct source for the Carboniferous clasts can be determined (Figure 8.28). However, certain igneous provinces can be excluded as provenance contenders and the following conclusions can be drawn from the available data presented in this section:

- The peraluminous, S-type Hillgrove Suite from the Australian sector is too young in age and overall isotopically too primitive to be a source for the Carboniferous clasts from the Boundary Creek conglomerate.
- The Cape Foulwind Supersuite and the Toropuihi Granite correlate well in age with the igneous clasts, however, their distinct weakly peraluminous to peraluminous A-type chemistry excludes these plutons as a source.
- The Western Province granites (Paringa, Kakapo, and Hauroko) are of similar age and display similar geochemical major and trace element characteristics as the igneous clasts. Isotope data are available for the Kakapo Granite only and show that this pluton is more radiogenic than the igneous clasts.
- The high-K, calc-alkaline plutons of the Devonian Karamea Batholith (and rocks of the Riwaka Complex) are too old and isotopically too radiogenic (or too primitive, Riwaka) to be a clast source.
- Major and trace elements of penecontemporaneous plutons exposed in the Median Tectonic Zone broadly correlate with those of the clasts, but the plutons are isotopically too primitive and are derived from material too young to be a source for the clasts.
- The Admiralty Intrusives exposed in northern Victoria Land are too old in age, are overall isotopically too radiogenic, and model ages indicate that they are composed of material too old. They are thus excluded as a source.

- The oldest members of the Salamander Intrusives broadly correlate in age with the youngest Carboniferous clast, but the lack of geochemical data for this province precludes a more rigorous comparison.

- Felsic plutons from the Amundsen Province (Bear Peninsula granites) and Thurston Island (Morgan Inlet Orthogneiss) broadly correlate in major and trace element chemistry with the igneous clasts, but these plutons are too young and are overall isotopically too primitive to be a clast source.

- The Devonian to earliest Carboniferous granitoids exposed in the Ross Province (Ford, Chester, Hermann Nunatak granitoids) are similar in age to the oldest Carboniferous clast, but they are too radiogenic and composed of material overall too old to be a viable clast source.

- The younger Carboniferous (Visean) plutons from the Ross Province (Bruner Hill Granite, Mount McCoy Granodiorite) correlate well in geochronology and isotopic composition with the younger Carboniferous igneous clasts. Based on the available data presented in this section these Ross Province plutons are the most likely source for the younger Carboniferous (Visean) igneous clasts.

8.3 Cambrian Igneous Clasts

8.3.1 Introduction

Two calc-alkaline, weakly peraluminous igneous clasts of Cambrian age have been collected from the Lake Hill (dacite) and Te Moana (monzogranite) conglomerate.

Cambrian magmatism in eastern Australia occurred in northeastern Queensland in the Charters Tower area (Henderson, 1986; Withnall *et al.*, 1991; Draper and Bain, 1997), in central Queensland at the western side of the New England Fold Belt (Aitchison *et al.*, 1992), Adelaide and Kanmatoo Fold Belt (e.g. Turner *et al.*, 1993) and Tasmania (e.g., Crawford and Berry, 1992; Whitford and Crawford, 1993). The Cambrian igneous rocks of the Takaka terrane, New Zealand (Cooper, 1989; Münker and Cooper, 1999) have correlatives in the Bowers terrane in northern Victoria Land (Weaver *et al.*, 1984; Bradshaw *et al.*, 1985; Münker and Cooper, 1995; Fioretti *et al.*, 2002). Gibson and Ireland (1996) suggest that the c. 500 Ma old granitoids in Fiordland (see Section 1.3.1.1) may represent Delamerian/Ross orogen rocks in New Zealand.

Other Late Proterozoic to Early Paleozoic rocks are exposed in southern Victoria Land (Encarnacion and Grunow, 1996; Cox *et al.*, 2000), the Central Transantarctic Mountains (Borg *et al.*, 1990), and the Queen Maud Mountains (Wareham *et al.*, 2001). Geochronological, selected major and trace element, and radiogenic isotope data are presented in Figures 8.3 and 8.29 to 8.37 and summarised in Table 8.3.

8.3.2 Igneous Source Provinces

8.3.2.1 Australia

Late Cambrian - Ordovician magmatism in northeastern Queensland is extensive and has been summarised by various authors (Figure 8.1, Hutton *et al.*, 1997; Withnall *et al.*, 1997). The volcanics and intrusives of the Mount Windsor Subprovince, part of the Seventy Mile Range Group, are similar in age to the Balcooma meta-volcanics, which range in age from 507±22 Ma to 471±4 Ma. Withnall *et al.* (1991) correlated the Cambrian age of the Balcooma meta-volcanics with the Mount Windsor volcanics. The calc-alkaline rocks comprise a cosanguineous series ranging from basaltic andesite to rhyolite, with the silicic variety volumetrically predominant. The Mount Windsor igneous rocks are believed to be the remnant of an active arc terrane which might have extended the whole length of eastern Australia (Henderson, 1986; Withnall *et al.*, 1991).

The Upper Bingara Plagiogranite, a minor component of the Weraerai ophiolite, is the oldest rock within the New England orogen with an age of 530±6 Ma. These rocks have geochemical affinities with Ti-poor supra-subduction-zone ophiolite sequences and are considered to represent an end product of differentiation during the development of oceanic crust (Aitchison *et al.*, 1992, and references therein).

Two Lower Cambrian (c. 510 to 490 Ma, Scheibner and Veevers, 2000) medium to high-K calc-alkaline suites from the Mount Read Volcanics in western Tasmania are used for comparison. The Volcanics include intrusive and extrusive rocks ranging in composition from basalt to monzogranites. The two suites are part of five recognised suites within the Read Volcanics that together indicate a magmatic evolution from transitional medium to high-K to strongly enriched shoshonitic rocks (Crawford and Berry, 1992; Crawford *et al.*, 1992). The only published isotope data available for the Read Volcanics are from Whitford *et al.* (1990, their Figure 9, no raw data available) and are shown in Figure 8.36. Penecontemporaneous correlatives of the Read volcanics

occur in Western Victoria (Stavely Greenstone Belt; Crawford, pers. comm.) but are not considered in this study.

8.3.2.2 New Zealand

The Cambrian Devil River arc system consists of calc-alkaline low to high-K arc rocks (Benson Volcanics), bonninites and back-arc tholeiites (Figure 1.4). The Benson Volcanics have been divided into 9 suites, of which eight are predominantly of basaltic-andesitic composition (low to medium-K) while the one high-K Heath Suite (including other felsic Benson Volcanics) is dominated by an andesitic-rhyolitic composition (Münker, 2000). U-Pb SHRIMP zircon ages and amphibole $^{40}Ar/^{39}Ar$ for the Devil River Volcanics vary from 515-490 Ma (Münker, 2000). $^{87}Sr/^{86}Sr_{(i)}$ ratios at 500 Ma for the high-K Heath Suite range from 0.70333 to 0.70616 and $\varepsilon Nd_{(i)}$ values range from +2.0 to +4.1. $^{87}Sr/^{86}Sr_{(i)}$ ratios for the low to medium-K Benson Volcanics range from 0.70385 to 0.70735 with corresponding $\varepsilon Nd_{(i)}$ values from -1.2 to +3.5.

8.3.2.3 Antarctica

Late Proterozoic to Cambrian magmatism in Antarctica is widespread, and only key igneous provinces that are penecontemporaneous with the igneous clasts are considered here (Figure 8.2). A more comprehensive overview and description of Antarctic igneous provinces is given in Stump (1995).

The calc-alkaline Granite Harbour Intrusives are confined to the Wilson terrane of northern Victoria Land and consist of various lithologies which are exclusively I-type in the east and predominantly S-type in the west (Borg *et al.*, 1986; Stump, 1995). Rb-Sr mineral/whole rock isochron ages for the Granite Harbour Intrusives range from c. 535-490 Ma (Borg *et al.*, 1987) with $^{87}Sr/^{86}Sr_{(i)}$ ratios ranging from 0.70945 to 0.71693 and $\varepsilon Nd_{(i)}$ values from -9.3 to -6.2 (Borg *et al.*, 1987).

The Middle Cambrian Glasgow Volcanics are confined to the Bowers terrane and consist of pillow lavas and breccias of basalt and andesite, with subordinate dacites and rhyolites (Laird *et al.*, 1976; Weaver *et al.*, 1984). No radiogenic isotope data are available for these rocks. Fioretti et al. (2002) report a 511.6±2.9 Ma crystallisation age for the Surgeon Island Granite, but no geochemistry is available for these rocks.

Encarnacion and Grunow (1996) concluded that the main subduction-related magmatism in southern Victoria Land and the central Transantarctic Mountains (Scott Glacier) took place between c. 530-485 Ma. In the Dry Valleys region in southern Victoria Land two major calc-alkaline and adakitic suites have been identified. The U-Pb dating of the Bonney Pluton, the largest of the calc-alkaline intrusions, indicates emplacement of this regional-scale body at 505±2 Ma. The Valhalla pluton age of 488±5 Ma records the major pulse of adakitic plutonism (Cox *et al.*, 2000). The calc-alkaline suite consists of monzodiorite-granodiorite intrusions, whereas the adakitic suite is dominated by granodiorite and monzogranite intrusions. $^{87}Sr/^{86}Sr_{(i)}$ ratios for the calc-alkaline suite range from 0.70710 to 0.7080 and $\varepsilon Nd_{(i)}$ values range from -4.2 to -6.1. The adakitic suite rocks have a wider range of $\varepsilon Nd_{(i)}$ values from -1.9 to -7.2 with corresponding $^{87}Sr/^{86}Sr_{(i)}$ ratios from 0.7065 to 0.7097 (Cox *et al.*, 2000).

In the central Transantarctic Mountains the c. 500 Ma old intrusive rocks range in composition from gabbro to granite and are calc-alkaline, with peraluminous granodiorites and monzogranites dominating in the Miller Range. Metaluminous to weakly peraluminous granodiorites and monzogranites occur east of the March Glacier, whereas gabbros, diorites, tonalites, and granodiorites dominate at Gabbro Hill, southeast of the Shackleton Glacier (Borg *et al.*, 1990, and references therein, their Figure 4). $^{87}Sr/^{86}Sr_{(i)}$ ratios for the Miller Range rocks (calculated at 500 Ma) are high and range from 0.73243 - 0.74174, with near uniform $\varepsilon Nd_{(i)}$ values from -10.5 to -11.8. Granitoids east of the March Glacier have $^{87}Sr/^{86}Sr_{(i)}$ ratios ranging from 0.70684 to 0.71906 and corresponding $\varepsilon Nd_{(i)}$ values from -1.6 to -8.2. Gabbro Hill plutons are the least radiogenic rocks described here with $^{87}Sr/^{86}Sr_{(i)}$ ratios ranging from 0.70446 to 0.70589 and $\varepsilon Nd_{(i)}$ values from +0.4 to +1.7 (Borg *et al.*, 1990).

The Cambrian volcanic Liv Group occurs in the Queen Maud Mountains and consists of dacitic flows (Wyatt and Ackermann formations) that were erupted at c. 525 Ma, as well as a bimodal assemblage of basalts and rhyolites (Taylor, Fairweather and Leverett formations) that were erupted at c. 515 Ma (Wareham *et al.*, 2001). The dacites are the most radiogenic rocks of the Liv Volcanics with $^{87}Sr/^{86}Sr_{(i)}$ ratios ranging from 0.71222 to 0.71445 and εNd values from -1.8 to -3.1. They are interpreted as partial melts of continental crust. The basalts have $^{87}Sr/^{86}Sr_{(i)}$ ratios from 0.70504 to 0.70750 and $\varepsilon Nd_{(i)}$ values from -1.1 to +5.7, whereas the rhyolites have $\varepsilon Nd_{(i)}$ values from -2.8 to +2.1 and $^{87}Sr/^{86}Sr_{(i)}$ ratios from 0.70436 to 0.70759 (Wareham *et al.*, 2001). The basalts

are interpreted by Wareham *et al.* (2001) as asthenospheric melts, whereas the rhyolites are interpreted as mixture of fractionated mafic magmas and crustal partial melt. The tectonic setting of the Liv Volcanics is not conclusively defined by the chemistry of the rocks. However, Wareham *et al.* (2001) favour an extensional rift setting behind an active subducting margin.

A granodioritic orthogneiss from Kay Peak at Mount Murphy (Ross province) gave a U-Pb SHRIMP zircon age of 505±5 Ma which is mirrored by detrital zircon age distribution patterns from a paragneiss from the same area (Pankhurst *et al.*, 1998a). The gneisses have $^{87}Sr/^{86}Sr_{(i)}$ from 0.70419 to 0.71128 and $\varepsilon Nd_{(i)}$ values from -3.8 to +0.3 (Pankhurst *et al.*, 1998a). In comparative plots the two orthogneiss provinces are, if not otherwise stated, plotted together and termed Marie Byrd Land.

Orthogneisses and mylonites are also exposed along the Wallgreen Coast in Marie Byrd Land, and Pankhurst *et al.* (1998a) assigned a 500 Ma crystallisation age to the gneisses at Gerrish Peak, which gave $\varepsilon Nd_{(i)}$ values from +2.0 to +5.7 and corresponding $^{87}Sr/^{86}Sr_{(i)}$ ratios from 0.70476 to 0.70528 (Pankhurst *et al.*, 1998a).

8.3.3 Comparison of Igneous Clasts with Source Provinces

8.3.3.1 Geochronology

The two dated igneous clasts from the Te Moana and Lake Hill conglomerates returned imprecise ages of c. 496 Ma and 517 Ma respectively (Figure 8.3; Table 3.1). Nevertheless, these ages are considered to broadly represent the crystallisation ages of these clasts and are used for comparison.

The monzogranitic clast from Te Moana correlates well in age with rocks from the Mount Windsor Province and rocks now exposed in northern Victoria Land (Granite Harbour Intrusives), southern Victoria Land and the central Transantarctic Mountains. It is also similar in age to the orthogneisses in Marie Byrd Land (Ross and Amundsen provinces).

The volcanic clast from Lake Hill is indistinguishable in age from the Read, Devil River and Glasgow volcanics, from the Granite Harbour Intrusives and the granitoids in southern Victoria Land. The clast broadly correlates with the Liv

Volcanics and the Marie Byrd Land orthogneisses, whereas the Upper Bingara Plagiogranite is considered to be too old to be a viable clast source.

8.3.3.2 Petrography

The alteration of the Lake Hill dacite and the fractionated nature of the leucocratic monzogranite from Te Moana, lacking the characteristic minerals that define a granite type, preclude a petrographic comparison with the selected source provinces.

8.3.3.3 Geochemistry

The igneous provinces contain a wide range of rock compositions, ranging from gabbro/basalt to granitoids/rhyolites. These potential source rocks are dominated by calc-alkaline to high-K calc-alkaline volcanics, but tholeiitic volcanic members are present (Figure 8.29). The calc-alkaline dacite from Lake Hill correlates with the Mount Windsor, Read, Devil River (Heath) and Liv volcanics, whereas the monzogranitic clast shows affinities with the Granite Harbour Intrusives and the orthogneisses from Marie Byrd Land. Classification using the aluminium saturation index of Zen (1986) (Figure 8.30) shows that the weakly peraluminous dacite correlates with weakly peraluminous members of the Liv and Read volcanics, whereas the weakly peraluminous monzogranite correlates with the Granite Harbour Intrusives and the orthogneisses of Marie Byrd Land.

Major element Harker diagrams (Figure 8.31) illustrate that TiO_2, Al_2O_3, Fe_2O, MgO, CaO, and P_2O_5 of the selected source provinces show a general negative correlation with SiO_2, whereas Na_2O defines no clear trend. The dacitic clast has a slightly higher Al_2O_3 content than most of the volcanic source rocks apart from the adakites in southern Victoria Land, but overall is indistinguishable from volcanic province members that have similar intermediate SiO_2 contents. The monzogranite shows compositional affinities with the most felsic plutons from the Mount Windsor Province, the Granite Harbour Intrusives and the orthogneisses from Marie Byrd Land.

Trace element variation plots (Figure 8.32) show that the Rb and Sr concentrations of the dacitic clast correlate well with intermediate members of the Read Volcanics but that they are distinctly higher than concentrations displayed by the Glasgow Volcanics. The Liv Volcanics have similar Rb but lower Sr concentrations.

The monzogranitic clast shows some affinities with the Granite Harbour Intrusives and the Liv Volcanics.

A more rigorous geochemical comparison of the two igneous clasts with source provinces is hampered by an often incomplete geochemical data record for these provinces, in particular trace elements.

8.3.3.4 Discrimination of Tectonic Setting

On a discriminant plot (Figure 8.33) of Pearce (1984) all the calc-alkaline, metaluminous to peraluminous source provinces plot predominantly within the field for the volcanic-arc-granites, with only the Liv Volcanics spreading well into the syn-collision-granite field. Both igneous clasts plot within the fields defined by the orthogneisses from Marie Byrd Land and the Benson Volcanics. The monzogranite also correlates with rocks from the Read Volcanics and adakites from the Dry Valleys, whereas the dacite shows similarities with the Granite Harbour Intrusives.

8.3.3.5 Isotopes

The isotope data are from the Read Volcanics (Whitford and Crawford, 1993), the Devil River Volcanics (Münker, 2000), intrusives and extrusives from northern and southern Victoria Land (Borg *et al.*, 1987; Cox *et al.*, 2000), igneous provinces from the central Transantarctic Mountains (Borg *et al.*, 1990; Wareham *et al.*, 2001), and Marie Byrd Land (Pankhurst *et al.*, 1998b).

All $^{87}Sr/^{86}Sr_{(i)}$ and $\varepsilon Nd_{(i)}$ values plotted in Figure 8.34 were recalculated to an approximate common age of 500 Ma. The monzogranitic clast has a high Rb/Sr ratio (4.9) and therefore the $^{87}Sr/^{86}Sr_{(i)}$ ratio is plotted, whereas source rock samples with high Rb/Sr ratios were excluded.

The isotope composition of the dacitic clast ($^{87}Sr/^{86}Sr_{(500)}$ 0.70699 and $\varepsilon Nd_{(500)}$ +0.6) correlates well with members of the Liv and Benson volcanics and shows compositional similarities to the granitoids from Gabbro Hill in the Transantarctic Mountains. The Read and Heath volcanics are isotopically distinctly more primitive, whereas isotope values for the intrusive/extrusive rocks from all other provinces from the Antarctic Gondwana sector indicate various degrees of crustal involvement during magma petrogenesis. The monzogranite has an isotope composition ($^{87}Sr/^{86}Sr_{(i)}$ 0.70405

and $\varepsilon Nd_{(500)}$ -1.9) that is indistinguishable from that of the orthogneisses exposed on Mount Murphy in Marie Byrd Land.

A similar trend is observed when $\varepsilon Nd_{(500)}$ vs. $^{147}Sm/^{144}Nd$ is plotted (Figure 8.35). The monzogranitic clast corresponds well with the Mount Murphy orthogneisses and shows compositional affinities with the Beardmore Glacier granitoids. The dacite from Lake Hill has a generally lower $^{147}Sm/^{144}Nd$ ratio than members of the Liv and Benson volcanics that have similar $\varepsilon Nd_{(500)}$ values.

The depleted mantle model age for the monzogranitic clast (Figure 8.36; T_{DM} = 1.59 Ga) is well within the range displayed by the Mount Murphy orthogneisses (1.29 to 1.93 Ga), the granitoids from the Beardmore Glacier region (1.35 to 2.31 Ga) and the calc-alkaline plutons from the Dry Valleys (1.07 to 1.92 Ga). The adakites from the Dry Valleys, the orthogneisses from Bear Peninsula, and the granites from Gabbro Hill are composed of material too young to be a viable source for the clast, and in the case of the latter two they are isotopically more primitive than the plutonic clast. The materials that make up the Granite Harbour Intrusives and the granitoids from the Miller Glacier region are too old (and too radiogenic) to be a clast source. The Liv and Benson volcanics are the two extrusive provinces that contain members that have similar T_{DM} ages and $\varepsilon Nd_{(500)}$ compositions to those of the dacitic clast from Lake Hill.

8.3.4 Summary and Conclusions

- Available comparative geochronological and geochemical data from the selected Cambrian igneous source provinces indicate that provinces within the Antarctic sector of the pre-break-up Gondwana margin present the most favourable sources for the two igneous clasts (Figure 8.37).

- The calc-alkaline, weakly peraluminous dacitic clast from the Lakehill conglomerate is indistinguishable in age, geochemical and Sr-Nd isotopic composition from the Liv Volcanics (in particular from the Levett Formation). Although the tectonic setting of the Liv Volcanics is uncertain, this igneous province is favoured as a source for the dacitic clast (tectonostratigraphic constrains and detrital contribution from the Transantarctic Mountains to the Rakaia basins are discussed in Section 9.2.2)

- The dacite correlates well in age, major, trace and isotope chemistry with members of the Read Volcanics of Tasmania. However, the distal location from the Rakaia sedimentary basins (see Chapter 9, Figure 9.4) makes the Read Volcanics a less likely source as this detritus would have to bypass the Tasmania sedimentary basin (active in the Permian-Triassic), the Challenger Plateau of the Western Province and the Median Tectonic Zone to reach the Rakaia sedimentary basin.

- Although the dacitic clast shows isotopic similarities with the Benson Volcanics, their intra-oceanic island arc geochemistry differs from that of the igneous clast.

- Although the dacitic clast shows isotopic similarities with plutons from Gabbro Hill, these rocks (and possible extrusive equivalents) are too old to be a suitable clast source.

- Age, geochemistry and isotope data of the calc-alkaline, weakly peraluminous monzogranitic clast from Te Moana correlate well with the orthogneisses exposed at Kay Peak (Mount Murphy) and these rocks are favoured as the provenance for the monzogranite.

- The Bear Peninsula orthogneisses correlate well in age with the monzogranitic clast but are isotopically more primitive and composed of material too young to be a suitable clast source.

- Geochronological and geochemical data for other Cambrian igneous provinces indicate that these provinces are (compared to the two igneous clasts) either too old (Upper Bingara) or too young in age (Dry Valleys adakites), radiogenically too primitive (Read Volcanics) or too radiogenic (Granite Harbour Intrusives, Miller Glacier plutons, Bearmore Glacier plutons, Dry Valleys plutons), or were emplaced in an island arc setting (Devil River Volcanics, Glasgow Volcanics).

8.4 Comparison of Igneous Rakaia Clasts with Rakaia Terrane Sandstones

To evaluate whether the igneous source, represented by the collected igneous clasts, is the sole source providing detritus to the Rakaia terrane sedimentary basins, the geochemistry of igneous clasts from the four Rakaia terrane conglomerates is compared to that of the Rakaia sandstones published by Roser *et al.* (1995).

The depositional ages of the four conglomerates were discussed in Chapter 2 and are also summarised in Figure 2.25. To briefly recapitulate, the salient points are: (1) the sandstone matrix of the Lake Hill conglomerate is part of petrofacies 4 (PF4); (2) the sandstone matrix of the McKenzie Pass conglomerate is part of PF2; (3) the sandstone matrix of the Te Moana conglomerate is part of PF1; and (4) although the depositional age of the Boundary Creek conglomerate is uncertain, a Permian deposition age is assumed that corresponds to PF1.

8.4.1 Major Elements

On the discriminant function plot proposed by Roser and Korsch (1988) the sandstones of PF1 - PF4 plot near the rhyodacitic composition and its plutonic equivalent (Figure 8.38).

The samples from the Boundary Creek conglomerate plot predominantly within the field typical for intermediate rocks, with three clasts plotting within the field of PF1. The majority of the other clasts from Boundary Creek show some PF1 affinities, but as their K_2O (wt%) content decreases they trend further away from the rhyodacitic average, possibly reflecting major element mobility during post-depositional deformation.

Samples from Te Moana are, with the exception of two clasts, confined to the felsic field and plot near the rhyolitic average. Some clasts plot within the field of PF1. In contrast to the Te Moana clasts the samples from McKenzie Pass encompass the whole range of igneous compositions ranging from basaltic to rhyolitic, with most of the clasts plotting near the rhyolitic average and the plutonic clasts being more evolved compared to the extrusive rocks. Some clasts plot within PF1 and close to PF2.

Igneous clasts sampled from Lake Hill are noted for their evolved nature, with most of the clasts plotting near the rhyolitic average and only a few clasts plotting near the field of PF4. Clasts of intermediate composition occur, but overall there is a distinct gap between the rhyolitic and the more mafic clast populations (a similar gap exists in the McKenzie Pass clast population).

Overall the Rakaia terrane igneous clast population is dominated by silicic volcanic and plutonic clasts that show minor overlap with compositions displayed by the Rakaia sandstones.

In order to assess whether the igneous clasts have a suitable bulk composition for producing the Rakaia sandstones, all the clasts were plotted on an A-CN-K plot after Fedo *et al.* (1995). The PF2 to PF3 sandstone fields are defined by a narrow range of K-feldspar - plagioclase ratios and CIA values near an average dacitic composition. The fields for PF2 and PF4 are defined by a similar narrow range of K-feldspar - plagioclase ratios but CIA ratios are more dispersed, particularly in PF4, and trend towards illite and muscovite.

The majority of the clasts from all four Rakaia conglomerate locations plot along a primary source line defined by average igneous rocks (Figure 8.39) and near the plagioclase - K-feldspar join at CIA of around 50. This indicates that the whole spectrum of igneous compositions has been collected. The intermediate and sodic nature of the majority of the clasts from Boundary Creek is apparent with only 4 clasts plotting within or near fields of PF1. Clasts from Te Moana display a wide range of feldspar compositions but the majority plot within or near the PF1 field.

The majority of the clasts from McKenzie Pass trend across all the petrofacies fields, with the more evolved plutonic clasts plotting to the right and the more intermediate clasts to the left of the sandstone fields. A similar trend is observed in the igneous clast population from the Lake Hill conglomerate, again demonstrating that the majority of the clasts are compositionally indistinguishable from the sandstones, with the more evolved samples plotting to the right of the petrofacies fields.

The plotting of nearly all the clasts close to the line of primary igneous source compositions indicates that the igneous clast source and the sandstones collected have undergone very little weathering and that the clasts collected are first cycle.

8.4.2 Trace Elements

Chondrite normalised La_N/Y_N ratios for selected samples are plotted against SiO_2/Al_2O_3 to compare the fractionation of igneous clasts (Figure 8.40). Igneous clasts from all 4 conglomerate locations plot across the fields of PF1 to PF4, with the majority of clasts plotting within the fields, suggesting that these clasts could well represent the source of the sandstones. As mentioned in Chapter 7 there is no clear distinction between metaluminous and peraluminous clasts due to the fact that most of the clasts

are weakly peraluminous and ambiguous with respect to the I/S-type classification scheme.

8.4.3 Isotopes

Sr-Nd data for the Rakaia sandstones and sandstone clasts are listed in Table 7.2 and 7.3 (see Section 7.5.4 for description and depositional ages) and are compared with Sr-Nd data for the Rakaia igneous clasts (Figure 8.41). To compare the various rocks of different ages all the values were recalculated to a Late Triassic depositional age of 220 Ma.

All the sandstones from the Rakaia terrane define a narrow field and range in $Sr_{(220)}$ from 0.70735 to 0.70787 and $\varepsilon Nd_{(220)}$ values from -4.5 to -3.5. The sandstones show good correlation with the most radiogenic igneous clasts from the Rakaia terrane (UC30667, 30668 and 31816). A similar pattern is observed in Figure 8.14 and has been described in Section 8.1.3.5.

Model ages (T_{DM}) for the Rakaia igneous clasts were discussed previously (8.1.3.5) where Permian to Triassic clasts were used for comparison with source provinces (Figure 8.15).

8.4.4 Summary and Conclusions

Major and trace element geochemistry indicates that source plutons were exposed to erosion that could have provided part of the detritus of the Rakaia depositional basins. However, the igneous source is overall too silicic and evolved compared to the Rakaia sandstone compositions. Isotope data show that the igneous source is isotopically too primitive to be the sole supplier of detritus to the Rakaia terrane depositional basins. Only the most radiogenic clasts have suitable compositions to produce sandstones similar to the Rakaia sandstones.

CHAPTER 9

DISCUSSION AND CONCLUSIONS

CHAPTER 9

DISCUSSION AND CONCLUSIONS

Introduction

In this chapter the major observations from this study are summarised and discussed. The longevity of subduction, indicated by the conglomerates, suggests that convergent tectonics dominated along an active continental margin penecontemporaneous with the deposition of the Rakaia and Pahau terrane sediments. On the basis of mineralogical, geochemical, isotope, and geochronological data obtained from igneous and sedimentary clasts, the provenance of both terranes is discussed separately. The present knowledge of the location of the New Zealand microcontinent immediately prior to the separation from Marie Byrd Land (West Antarctica) has been well documented (Mayes *et al.*, 1990; Lawver and Gahagan, 1994; Sutherland, 1999; Mukasa and Dalziel, 2000). Results from this study indicate that the South Island Pahau terrane sedimentation continued almost to the date of fragmentation of this Gondwana sector. Given that the approximate location of the New Zealand block at that time is well constrained, it is reasonable to discuss the provenance of the Pahau terrane first (Section 9.1).

In Section 9.2 data gained from the Rakaia terrane conglomerates and sandstones are used to evaluate proposed provenance models. Combining results from igneous clasts with U-Pb detrital zircon age data from this and other studies, the Rakaia terrane provenance is further constrained and an Antarctic/New Zealand protosource is proposed.

9.1 PAHAU TERRANE PROVENANCE

Based on geochronological, major and trace element, and Sr-Nd isotope data presented in previous chapters the subduction-related MTZ/Amundsen Province Volcanic Belt (MAVB) is proposed as the major source for the Pahau terrane igneous clasts. The clast lithologies preserved in the conglomerates indicate that a spectrum of intrusive levels was exposed at the time of the conglomerate deposition. The

predominantly volcanic and granophyric, hypersolvus clasts indicate that mainly the higher structural levels of the MAVB were being eroded, thus only deeper structural level equivalents of the clast lithologies are now preserved in the sources.

The Late Jurassic to Early Cretaceous calc-alkaline, metaluminous to weakly peraluminous clasts are indistinguishable in age, chemical composition, and petrogenesis from the felsic members of the calc-alkaline I-type granitoids of the Darran Suite and granitoids on Thurston Island. The alkaline rhyolites from Mount Saul and Kekerengu correlate best with the Electric Granite now exposed in the Median Tectonic Zone, whereas clasts with adakitic affinities are similar in composition to the Separation Point Suite rocks. The Early Jurassic calc-alkaline metaluminous clast from Kekerengu may be correlated with the Bounty Island Granite.

Geochronological data from Chapter 3 and geochemical comparison of igneous clasts with published data from Pahau terrane sandstones (Section 7.5) show that igneous activity in the clast source (MAVB) and sedimentation of the Pahau sandstones were penecontemporaneous, but that the igneous clast source cannot be the sole source contributing to the Pahau detritus. Thus, any proposed provenance model for the Pahau terrane sandstones must account for the geochemical compositional differences between the igneous clasts (i.e. source) and the Pahau sandstones.

The time of accretion of the Median Tectonic Zone and all the Eastern Province terranes to the Gondwana margin is a major and ongoing problem in New Zealand basement geology. Therefore, regional tectonostratigraphic constraints have to be considered first in order to better understand the provenance of the Pahau terrane. The position, petrogenesis and tectonic significance of the Median Tectonic Zone are of main interest in this regard and are discussed in the following section.

9.1.1 Median Tectonic Zone

9.1.1.1 Western Boundary

The position of the Median Tectonic Zone with respect to the Gondwana margin (Western Province) during its petrogenesis is poorly understood. Based on field observations and the presence of Carboniferous plutonic rocks in both the Median Tectonic Zone and the Western Province, Mortimer *et al.* (1999b) suggested that Triassic to Cretaceous plutons of the Median Tectonic Zone were intruded along the

autochthonous margin of Gondwana. This model is open to question as the Carboniferous plutons of the Western Province (mainly A-type) differ in composition from that of the MTZ (calc-alkaline I-type, see Section 8.2). Mortimer et al.'s model contradicts the allochthonous model of Muir *et al.* (1995; 1998), who proposed that the Median Tectonic Zone is itself a collided arc, with a back-arc basin between the arc and the Gondwana margin.

The latter model is based on the primitive Sr and Nd isotopic ratios of the Separation Point Suite granitoids and the conspicuous absence of inherited zircons, supposedly suggestive that these magmas have undergone little, if any, interaction with felsic crust and specially Western Province crust. However, the absence of inherited zircons may also indicate: (1) that the crustal component is depleted in zircons, (2) that the zircons were resorbed during petrogenesis, or (3) that the igneous rocks were analysed for their crystallisation age and only euhedral crystals, likely to give such ages, were targeted, thus precluding the recognition of an inherited population. Therefore the model based on the absence of an inherited zircon population is questionable. The Crow Granite is in intrusive contact with Ordovician metasediments (Douglas Formation, Golden Bay Group) of the Buller terrane (Muir *et al.*, 1997) and is therefore not a tectonic slice of the MTZ within the Western Province. It is interesting to note that the Crow Granite, although emplaced into a mature Western Province (Muir *et al.*, 1997), also shows no sign of zircon inheritance.

In their model, Muir *et al.* (1998) demonstrated that the mafic Darran Suite rocks have the appropriate chemical and isotopic compositions to generate the Western Fiordland Orthogneiss (at 125 Ma) and the higher-level Separation Point plutons (at 117±2 Ma). The authors proposed that the appearance of the adakitic magmas was triggered in response to the thrusting of the Median Tectonic Zone arc beneath the Western Province. This model is supported by Hollis *et al.* (2002) who reported 136-129 Ma mafic to intermediate magmatism from the Arthur River Complex (ARC; Milford area in Fiordland, New Zealand). These authors interpreted ARC as a batholith, emplaced at mid-crustal levels and then buried to deeper crustal levels due to the convergence of the MTZ and the continental margin.

The timing and change from calc-alkaline to adakitic magmatism in the Median Tectonic Zone, as noted by Wandres *et al.* (1998), coincided with the emplacement of

the Darran plutons and contemporaneous adakitic sheets at 137 Ma. Magma loading was proposed by these authors as petrogenetic model for the adakites whereby the displacement of the root of the volcanic arc down through the garnet-in zone at depths of >40km and elevated temperatures produced felsic melts in equilibrium with a garnet bearing residue.

The age and composition of the Crow Granite (137 Ma) is very similar to the age and composition of the plutonic rocks that make up the Median Tectonic Zone. The emplacement of the Crow Granite into the Western Province suggests that the Median Tectonic Zone and the Western Province were tectonically linked at 137 Ma (Muir *et al.*, 1997).

A tectonic linkage between the two provinces is also indicated by the isotope data from this study. The relatively radiogenic isotopic ratios of most of the igneous clasts are typical of I-type granitoids (McCulloch and Chappell, 1982). It is now widely accepted that many granitoids consist of at least two isotopically and geochemically distinct components: a depleted mantle and a relatively radiogenic continental crust (e.g., McCulloch and Chappell, 1982; Pickett and Wasserburg, 1989). The igneous clasts plot within the present day mantle array of DePaolo and Wasserburg (1979), suggesting the involvement of an important mantle-derived component (Figure 9.1).

Waight (1995) demonstrated that mixing between a depleted mantle component and the Greenland Group (crustal endmember) cannot account for the isotopic compositions of the Hohonu Batholith, as the amount of Greenland Group sediments (c. 50 %; his Figure 6.56) is too high to retain the I-type characteristics of the Hohonu Batholith. Waight *et al.* (1998b) instead used the Separation Point-type Depleted Mantle (SPDM) of Muir *et al.* (1995) as the lithospheric mantle source.

Geochronological and geochemical data from this study have identified the Darran Suite plutons as the major source for the Pahau terrane igneous clasts, with minor contributions from the Electric Granite. Figure 9.1 shows that the isotopic compositions of clasts from Mount Saul and a single clast from Kekerengu are indistinguishable from those of the Darran Suite plutons and the Electric Granite (which has a $\varepsilon Nd_{(i)}$ value very similar to the Darran Suite, but an exceptional high $^{87}Sr/^{86}Sr_{(i)}$ ratio). For this study the Darran Suite is chosen as the mantle source component, which is very similar to that of the SPDM of Muir et al. (1995). Variation in isotopic

compositions between clasts from the Mount Saul conglomerate (and a single clast from Kekerengu) and the Ethelton/Kekerengu conglomerates is too great to allow for derivation from a single mantle source and indicates the involvement of a crustal component during petrogenesis.

However, there is no evidence of a continental crust within the MTZ that could have been involved during the petrogenesis of magmas similar in composition to the more radiogenic clasts of Ethelton and Kekerengu. The only sedimentary rocks identified within the MTZ are five volcano-sedimentary units (Section 1.3.2) that rest unconformably on plutonic rocks and are Jurassic or earliest Cretaceous in age. However, the contemporaneous emplacement of the Crow Granite - similar in composition to the Darran Suite plutons - into the Western Province justifies the assumption that a Greenland Group type felsic crust was involved. Modelling indicates that the isotopic compositions of the Ethelton and Kekerengu clasts are achievable by the mixing of Darran Suite derived melt and 10-25 % average Greenland Group composition (Figure 9.1). The mixing between the two components is of course a simplification, as the lower continental crust of the Buller terrane (Greenland Group) is more likely to be an extremely complex and heterogeneous mixture of unknown lower crustal and Paleozoic-Mesozoic igneous components (e.g. Muir *et al.*, 1996b).

The crustal contribution required during the petrogenesis of the more radiogenic igneous clasts, together with the contemporaneous emplacements of the Darran Suite plutons and the Crow Granite, lends further support to an autochthonous model for the Median Tectonic Zone as proposed by Mortimer *et al.* (1999b) - i.e., there is no need for a back arc basin between the arc and the Gondwana margin.

9.1.1.2 Eastern Boundary

Based on isotopic compositions and intrusive relationships between Brook Street terrane and Median Tectonic Zone plutons in the Longwood Range, Mortimer et al. (1999a) proposed the accretion of the Brook Street terrane to the Median Tectonic Zone (and Gondwana) to have occurred at 245-230 Ma. Dated granitoid clasts from the Rainy River Conglomerate, which lies within the eastern Median Tectonic Zone in Nelson, and from the Barretts Formation of the Brook Street terrane in Southland, constrain the depositional ages of both units to be no older than c. 170 Ma (Tulloch *et al.*, 1999; Adams *et al.*, 2002). The ages and chemistry of the granitoid clasts are broadly

compatible with derivation from rocks that are now represented by Triassic plutons of the Median Tectonic Zone (Tulloch *et al.*, 1999). Early Jurassic ages as young as 180 Ma have been obtained as well. Based on similarities in stratigraphic age, depositional characteristics, granitoid clast ages and composition between the Rainy River Conglomerate and the Barretts Formation, Tulloch et al. (1999) suggested that they are broadly correlative and that they collectively overlapped a combined Brook Street terrane - MTZ before the Late Jurassic (see also below, Section 9.2).

9.1.2 Recycling of the Rakaia Terrane

The first regional metamorphic event recognised in the Rakaia terrane (Haast Schist, Figure 1.6) is attributed to the Caples-Torlesse terrane collision (e.g., Mortimer, 1993, and references therein). Little *et al.* (1999) noted that the peak of the metamorphism took place in the Middle Jurassic, coinciding broadly with the magmatic lull recognised in the Median Tectonic Zone (see Chart). Whether there is a causal link between the two events is not known and it is not clear whether the schist belt was in a forearc position with respect to the Median Tectonic Zone. Rapid cooling of the Otago Schist between 140-130 Ma has been interpreted by Little *et al.* (1999) as a signal of uplift and erosion. This corresponds to the main conclusions drawn in Chapter 4, where it was argued that continuous uplift of the Rakaia terrane (into the Cretaceous) exposed Permian to early Late Triassic Rakaia rocks, and that these rocks were subsequently recycled into the Pahau depositional basin.

The recycling of the Rakaia rocks is further supported by detrital and igneous zircon data from this and other studies (Figure 3.11). The main zircon age group (250-200 Ma) of the Aptian Ethelton sandstone is indistinguishable from the Triassic Rakaia and Waipapa/Caples detrital zircon age components. The two minor age groups (300-280 Ma; 340-320 Ma) from Ethelton coincide with Permian and Carboniferous Rakaia components. The minor Ordovician, and the rather subdued Cambrian and Precambrian age components in the Ethelton sample broadly resemble those of both the Rakaia and Waipapa/Caples terrane rocks, whereas the Devonian peak in the Ethelton sandstone is absent in the older terranes.

The strong correlation between the Triassic peaks from the Ethelton matrix and the inboard terranes lends further strong support to the conclusions obtained from sandstone clasts in Chapter 4 that there was recycling of older Rakaia and

Waipapa/Caples rocks into the Pahau depositional basin. The Early Jurassic peaks recognised in the Ethelton matrix (and other Pahau sandstones) and the Waipapa/Caples terrane coincide with the dated igneous clast from Kekerengu and the Bounty Island Granite. The peak also broadly coincides with the proposed docking of the Caples/Rakaia terrane in the Jurassic. Trace element compositions shown in Figure 9.2 suggest that both the Pahau and the Waipapa/Caples terranes might have received detritus from a common source of Early Jurassic age.

The conspicuous absence of Triassic (and older) igneous clasts in all the sampled Pahau conglomerates may indicate a distal position of the Pahau basin with respect to the igneous Rakaia source, with only the finer grained detritus reaching the Pahau basin. The compositions of the Rakaia terrane igneous clast zircons and the detrital zircons from the Kurow and Balmaccan Stream sandstones are compared with compositions of zircons from the Ethelton matrix in Figure 9.3. The Triassic to Permian zircon compositions of the two Rakaia sandstones correlate strongly with those of the Rakaia igneous clast zircons and all three populations overlap with the penecontemporaneous zircon composition of the Ethelton matrix. A similar pattern is observed with the Carboniferous and Cambrian zircon compositions. These correlations suggest that the Triassic to Cambrian igneous zircons were either: (1) deposited into Rakaia terrane basins and from there, during Late Jurassic to Early Cretaceous uplift, subsequently recycled into the Pahau depositional basin, or (2) deposited as primary igneous zircons into the Pahau basin in the Late Jurassic to Early Cretaceous, or (3) a combination of both. A protosource origin for the zircons of the Ethelton matrix (second option) implies that the source that contributed detritus to the Rakaia depositional basins was still exposed and eroded at the time of the Pahau sedimentation. However, the time at which the Rakaia and Pahau terranes were amalgamated is not known. An Aptian juxtaposition of all Eastern Province terranes is indicated by the presence of Median Tectonic Zone clasts in the Ethelton conglomerate (youngest dated conglomerate matrix zircon age 112 Ma). The earliest sedimentary units that overlay Eastern Province terranes are Cenomanian non-marine sediments in the Great South Basin (Raine *et al.*, 1993), which is related to the Gondwana break-up.

No detailed analysis of zircon morphology or typology (e.g., Pupin, 1980) was made during the course of this study and the provenance of the Ethelton detrital zircons – i.e., protosource or proximate source – remains speculative.

9.1.3 Regional Tectonic Implications

The tectonic regime in the South Island New Zealand region changed from subduction-related processes to extension at c. 105 Ma (Bradshaw, 1989; Luyendyk, 1995; Spell *et al.*, 2000). The youngest U-Pb dated igneous clast from the Pahau terrane is a subsolvus/hypersolvus monzogranite (UC30743; containing minor granophyric intergrowth) that gave an age of 123.1±2.5 Ma. The youngest detrital zircon dated from the Ethelton matrix gave an age of 111.7±1.4 Ma. This age constrains the minimum age of magmatism in the source region of the Pahau terrane.

An Aptian reconstruction of the New Zealand sector of the Panthalassan Gondwana margin is presented in Figure 9.4 using the tectonostratigraphic constraints discussed above (and below). The reconstruction is adapted from that proposed by Mukasa and Dalziel (2000), with one major modification. The dextral displacement proposed by DiVenere *et al.* (1995) between the eastern and western Marie Byrd Land crustal blocks (Ross and Amundsen Province of Pankhurst *et al.*, 1998b) has been removed based mainly on the following observations:

The LeMay Group of Alexander Island, Antarctic Peninsula, is a Mesozoic accretionary prism that was constructed during subduction of Pacific oceanfloor and Phoenix plate (Tranter, 1992; Doubleday *et al.*, 1993). New assemblages of Radiolaria, including some of the few occurrences of high latitude Jurassic to Cretaceous radiolarian faunas, show that the LeMay Group of Alexander Island ranges in age from the latest Jurassic-earliest Cretaceous to at least the Albian (Holdsworth and Nell, 1992). Sedimentation and deformation in the LeMay was diachronous and younged oceanward, supporting the model of the LeMay Group being an accretionary complex (Holdsworth and Nell, 1992; Tranter, 1992). If sedimentation of the LeMay Group continued at least into the Albian, then the positioning of the Thurston Island block in front of Alexander Island in the Barremian reconstruction of Mukasa and Dalziel (2000, their Figure 9a) is questionable. In the present reconstruction (Figure 9.4) the Thurston Island, eastern Marie Byrd Land and eastern Campbell Plateau blocks (Mukasa and Dalziel terms) have been moved sinistrally, thereby removing the strike slip separation between the Marie Byrd Land and Campbell blocks and closing the 'gap' between the Campbell and Challenger plateaux.

The strike-slip separation proposed by DiVenere (1995) is based on the interpretation of paleomagnetic data collected from granitoids and volcanics along the Ruppert Coast, including areas adjacent to the core complex structure in the Fosdick Mountains of the Ford Ranges (Luyendyk *et al.*, 1996). The proximity of the sampled igneous rocks to a core complex and a zone of continental separation may suggest that plutons and volcanics may have undergone postmagnetisation rotation. This rotation may account for paleopoles that require strike-slip displacement and the placement of the Thurston Island crustal block in front of the accretionary complex while accretion was still taking place.

One of the most striking features on the present day Campbell Plateau is a northeast tending zone of high amplitude positive magnetic anomalies, termed the Campbell Magnetic Anomaly System (CMAS, Davey and Christoffel, 1978). The gravity and the magnetic anomalies clearly suggest a major geological feature in the area of the CMAS, but it has not yet been demonstrated that the associated rocks are correlatives of the Median Tectonic Zone or the Amundsen Province (Sutherland, 1999). If the proposed MTZ allocation of the Bounty Island is correct (Cook *et al.*, 1999), then the CMAS may well represent MTZ (and Western Province?) correlatives intruded into the Campbell Plateau. A similar interpretation of the CMAS has been proposed by Bradshaw *et al.* (1997). For this reason the MTZ in Figure 9.4 has been tentatively extended across the Campbell Plateau to join with the Amundsen Province correlatives, thereby forming the Median Tectonic Zone/Amundsen Province Volcanic Belt (MAVB).

The continuity of the CMAS across the whole central Campbell Plateau also indicates no major strike-slip displacement between the Eastern and Western Campbell plateaux as that proposed by Mukasa and Dalziel (2000), and it lends further support to the crustal block arrangement presented here.

Geochronology, petrography, geochemistry and isotope ratios of the igneous clasts indicate, as previously mentioned, a close spatial proximity of the three Pahau terrane conglomerates during sedimentation. Dean (1993) analysed granitoid clasts from conglomerates within the Early Albian Waihere Formation (Mildenhall, 1977), which unconformably overlies the Rakaia terrane basement on the Chatham Islands. The Bounty Island granites (Section 7.2.3.3) correlate well with the analysed clasts from the

Chatham Islands and may well have contributed to these conglomerates (Dean, 1993). The clasts from the Chatham Island conglomerate compare well with some of the clasts found in all the Pahau terrane conglomerates. In particular, the A-type volcanic clasts from Mount Saul and Kekerengu are very similar in composition to the A-type Chatham Island granitoid clasts.

The attenuation and stretching of thick continental crust in response to extension (e.g., Sutherland, 1999; Mukasa and Dalziel, 2000), prior to the actual separation between New Zealand and West Antarctica, must have resulted in the spatial separation of the Pahau (and Rakaia) and Chatham conglomerates, which probably were considerably closer in the Early Cretaceous. The close proximity of the Aptian conglomerate locations is apparent in Figure 9.4.

Calc-alkaline clasts are geochemically indistinguishable from the Whitsunday Volcanics (Ewart *et al.*, 1992), and Sr/Nd-analysed clasts from Mount Saul and Kekerengu show petrogenetic similarities to this volcanic province. Volcanic activity in the rift-related Whitsunday Volcanic Province (WVP, 125-95 Ma, Ewart *et al.*, 1992; Bryan *et al.*, 2000, see also section 7.2.2) was penecontemporaneous with the sedimentation in the Pahau basins and extension-related magmatism recorded in Marie Byrd Land (105-95 Ma, Storey *et al.*, 1999). The occurrence of WVP derived volcanoclastic sediments in the Otway/Gipsland Basin (Bryan *et al.*, 1997) strongly indicates that the WVP extended into what is now known as the Lord Howe Rise.

That the volcanic/plutonic source of the Pahau igneous conglomerate clasts experienced extension and/or waning magmatism in the Tithonian (latest Late Jurassic), is indicated by the dates obtained from alkaline clasts from Mount Saul (UC30823 = 141.4±2.9 Ma; UC30854 = 145.2 ± 3.4 Ma). Geochemically the alkaline clasts show no affinities with magmas usually associated with hotspots or mantle plumes (Figure 5.30). The clasts show characteristics similar to magmas interpreted as being derived from continental crust, or crust that has been through a cycle of continent collision or island arc magmatism and emplaced in a variety of tectonic settings, including post-collisional and what may be true anorogenic magmatism. If the alkaline clasts are related to the waning stage of a subduction system, then this might suggest that the Pahau source subduction system experienced a first waning stage in the latest Tithonian. The igneous events in the MTZ coincide with the proposed Berriasian to Valanginian uplift of the

Rakaia terrane and the increased cooling rates recorded in the Brook Street terrane (Mortimer *et al.*, 1999a), but whether these tectonic events are connected is not known.

The presence of alkaline rhyolitic clasts may also indicate that the source area of the clasts experienced a previously unrecognised extensional event, coinciding with the similarly Late Jurassic extensional event in the West Antarctic rift system identified by De Santis *et al.* (1994). An earliest Cretaceous extensional event in the New Zealand region has been suggested by Tulloch and Kimbrough (1995). Magmatic activity in the Whitsunday Volcanic Province may have begun as early as 145 Ma (Allen *et al.*, 1998), contemporaneous with whatever tectonic event was experienced in the clast source region. Previous magmatic events associated with crustal extension along the Panthalassan Gondwana margin have been recorded prior to the final break-up of Gondwana (Ferrar Province). The Middle Jurassic Kirwans Dolerite (Western Province) has been correlated with the Ferrar Province (Mortimer *et al.*, 1995). The possible extent of the Whitsunday Volcanic Province into the New Zealand region (Challenger Plateau) is shown on the reconstruction diagram in Figure 9.4.

9.1.4 Pahau Sandstone Provenance

This section uses the isotopic and geochemical provenance characteristics of the Pahau igneous clasts, and the Pahau and Rakaia sandstones to suggest that the components in the Pahau sandstones were derived from an active volcanic arc plus recycled older Rakaia and Caples sandstones.

Th/Sc trace element ratios are effective discriminants for sediments and igneous rocks and have been used elsewhere (McLennan *et al.*, 1990; McLennan and Hemming, 1992; Roser and Korsch, 1999; Wombacher and Münker, 2000) and discussed previously (e.g. Section 4.2.3). If coupled with Nd isotope compositions, they can be used to infer the type (by trace elements) and amount (Nd isotopes) of igneous or crustal input into the Pahau basins. Available Nd isotope and Th/Sc compositions for the SW Pacific igneous provinces are plotted in Figure 9.5 and are compared with compositions of Pahau and Rakaia terrane sandstones and other Eastern Province terranes of New Zealand. Based on the youngest detrital zircons from the Ethelton matrix the depositional age for the Pahau terrane sandstones is taken as 115 Ma and all εNd values were recalculated to this age.

The Darran Suite rocks are separated into granites (Darran 1), granodiorites (Darran 2) and diorites (Darran 3) and are used as the igneous end-members. The Rakaia and Caples terrane sandstones are used as detrital end-members. The 'magmatic gap' between the contemporaneous felsic and mafic members of the Darran Suite, noted by Muir *et al.* (1998), is apparent and may indicate that the 'gap magmas' are: (1) not sampled, or (2) emplaced at different structural levels relative to the sampled rocks, or (3) not generated in a volcanic arc.

The geochemical and isotopic differences between the igneous clast source and the Pahau and Rakaia sandstones and all other Eastern Province terranes is evident. The field for the igneous clasts shows some overlap with the Darran 1 rocks, but generally there is a trend towards a more radiogenic source that reflects the above proposed crustal involvement during petrogenesis of the clast magmas (Section 9.1.1.1, Figure 9.1).

Assuming simple bulk mixing between Rakaia detritus and detritus that is derived from the igneous sources and other Eastern Province terranes, and that no significant trace element fractionation took place, crude and tentative estimates of detritus contributions of the various end-members can be obtained (Figure 9.5).

The combined recycling of Caples and Rakaia sandstone was proposed by Roser and Korsch (1999, using Th/Sc – Al2O3/SiO2), and these authors argued that a mixture of 60-70 % Rakaia and 40-30 % Caples could explain the Pahau sandstone composition. However, results from this study clearly indicate that an active volcanic arc also contributed detritus to the Pahau basin and that at least three or more sources are required to produce the Pahau sandstones.

The Pahau sandstones display a wide range of compositions ranging from intermediate to felsic. Although part of the intermediate Pahau composition can be explained by a simple Rakaia-Caples mixing there is a spread of the Pahau range toward the igneous clast source with a minor overlap between the Pahau sandstone and the igneous clast fields. This indicates that a silicic igneous contribution is more significant in some of the Pahau sandstones. These more felsic compositions could best be explained by mixing 40-60 % Rakaia material and 60-40 % Caples-Darran 2 detritus (Jackson Peak and Mt. Luxmore granodiorites).

The source for the more mafic Pahau detritus is more ambiguous and cannot be explained by the mixing of Rakaia-Caples detritus. The rarity of Pahau terrane intermediate and mafic clasts in the collection of this study, also noted by other workers (Smale, 1978; Dean, 1993; Mortimer, 1995), precludes a direct correlation between mafic clasts and their source. The preservation of only rounded to well rounded, mainly silicic clasts in the Pahau terrane conglomerates may indicate that: either (1) siliceous magmatism dominated in the source area of all three conglomerates; or (2) the catchment of all three conglomerates had no access to mafic rocks; or (3) a selective process during transportation allowed only the more resistant silicic clasts to reach the deposition centre, i.e. mafic clasts disintegrated during transportation and is the favoured option in this study.

Although no mafic igneous clasts have been collected for this study, basaltic clasts were sampled in conglomerates exposed along the Clarence River north of Hanmer Springs (pers. comm. C. Mazengarb). Plagioclase of andesine composition reported from the Pahau sandstone (MacKinnon, 1980b) indicates that detritus of intermediate composition (andesite/dacite, Deer *et al.*, 1992) was shed into the basin and suggests that disintegrated clasts of mafic and intermediate composition are now part of the Pahau sandstone. Kodama (1994a) recognised that the breakdown of particles during fluvial transportation is strongly related to the lithology. He noted that clasts of andesitic composition in his study dominated the clast population close to the volcanic source but disintegrated downstream to give way to particles of more silicic compositions. Evidence of widespread mafic Late Jurassic – Early Cretaceous volcanism within the MTZ is indicated by the Palisade and Big Bush Andesites (Mortimer, pers. comm.) and the Drumduan Group, Rainy river conglomerate and the Patterson Group.

There are other various mafic source rocks that could have contributed detritus by erosion to the Pahau basin, including the Brook Street terrane, the Longwood and Holly Burn Intrusives, and the mafic members of the Darran Suite (Darran 3). If the felsic Darran members contributed detritus to the Pahau basin, then it is reasonable to assume that the contemporaneous mafic Darran member also contributed detritus. The most mafic Pahau sandstones could best be explained by a mixture of 70-80 % Rakaia detritus and 30-20 % Caples-Darran 3 material.

Detritus contribution by the Maitai and Murihiku terranes is a possibility. However, if borehole (Waimamaku-2) interpretations by Isaac *et al.* (1994) are correct (bottom of core interpreted as Murihiku), then the Murihiku terrane is still a depositional basin at the time of the Pahau sandstone deposition and cannot be a major contributor of detritus.

A paleoenvironmental reconstruction, based on the regional tectonostratigraphic constraints discussed above and new geochronological and geochemical data from this and other studies, is shown in Figure 9.6. That the Murihiku basin received detritus not only from the Maitai/Caples terranes to the east, but also from the MAVB to the west is indicated by the presence of MAVB-like igneous clasts in the Murihiku terrane. Furthermore, the detritus shed from the MAVB and the Maitai/Caples terranes is broadly similar in composition (εNd) to that of the Murihiku terrane, as shown in Figure 9.5. The salient points of the paleoenvironmental reconstruction are as follows:

- Initial sediment supply from the MAVB to the Pahau basin was accompanied by the uplift of the combined Rakaia/Caples/Maitai terranes (exposed at c. 130 Ma), giving rivers the opportunity to continuously incise and transect the emerging mountain range.

- Cessation of the Phoenix Plate subduction system occurred first in the South Island region while subduction in the North Island region still continued.

- While large rivers in the South Island region transported MAVB-derived detritus across the slowly uplifting Murihiku basin, the North Island sector was still a depositional basin. The Murihiku basin also received detritus from smaller rivers from the west (MAVB) and the east (mainly Maitai/Caples).

- Rakaia rocks were recycled into the Pahau basin.

- The Hohonu Suite rocks (Western Province) are generally too young and are, together with rocks from the Karamea Batholith, considered to be too distant relative to the Pahau depositional basin (see also Figure 9.4).

9.2 RAKAIA TERRANE PROVENANCE

Rakaia terrane sediments are relatively coarse grained and show overall a marked compositional uniformity from the Permian to the Late Triassic. This indicates that the sediments have been deposited rapidly by large energetic rivers that drained a relatively uniform continental arc source or that there was a very efficient mixing system operating during transport and deposition. Igneous clasts in all the Rakaia terrane conglomerates are first cycle and represent the protosource. Data from these clasts have helped to broadly characterise the igneous source with respect to its age, chemical and isotopic composition, and petrogenesis, and implications for the Rakaia provenance are discussed here.

U-Pb zircon ages for igneous clasts and detrital zircons from the two Rakaia sandstones (Figure 3.11), together with the Rakaia fossil record (Figure 2.25), indicate that igneous activity in the source region and the deposition of the sediments was penecontemporaneous. A continuous replenishment of the magmatic source from the Carboniferous to the earliest Middle Triassic is indicated by the dated igneous clasts, which display a general inboard (Boundary Creek) to outboard (Lake Hill) younging trend (Figure 3.12).

Assuming that the clasts in a conglomerate broadly reflect the lithotypes exposed in the source area, then the petrography of the collected clasts reflects the structural levels of the continental arc source that were exposed at the surface at the time of the deposition of the clasts. As previously noted, the presence or absence of certain lithotypes in a conglomerate might by influenced by the availability and accessibility of these lithotypes in the source area at the time of deposition, or by sorting during transportation, or by the sampling of the conglomerates.

Petrography of the igneous clasts indicates that the clast detritus provided by a predominantly Carboniferous magmatic source to the (Permian?) Boundary Creek conglomerate was mainly by volcanic activity and the erosion of the subvolcanic levels. A similar trend is observed at the Permian Te Moana and the Dorashamian McKenzie Pass conglomerates, where volcanic and hypersolvus clasts dominate over subsolvus clasts. However, at Lake Hill (Carnian) mylonitic and gneissic clasts indicate that deeper levels of the continental arc were exposed and eroded and volcanic activity was minor (see statistical counts Appendix 3). The exposure of gneissic structural levels

indicates that substantial erosion of the upper levels of the source took place before Carnian times. The apparent trend shown by geochronological data and petrographic observations indicates the progressive unroofing of a continental volcanic/plutonic arc source that has experienced continuous magmatism from (at least) the Carboniferous to the latest Middle Triassic.

Although the petrogenesis of the adakitic rocks is not conclusive, the rocks may attest to the presence of a mature crust, given that one petrogenetic model involves the melting of newly underplated mafic magma beneath a thickened continental crust (see Section 6.3.2). The crustal contribution is also reflected in the presence of weakly peraluminous to peraluminous clasts in the Lake Hill conglomerate. In addition, Sr-Nd isotope data from the Carboniferous to the Triassic clast population indicate an increased crustal contribution during petrogenesis as time progressed, with the two youngest clasts (from Lake Hill) being the most radiogenic.

The trend observed in the igneous clast source is paralleled by the progressive evolution of the Rakaia accretionary wedge from the Permian to the Late Triassic. MacKinnon (1983) attributed the gradual and progressive change of Torlesse sandstone compositions through time to the evolution of the source and the gradual unroofing of a continental volcanic/plutonic arc. Roser and Korsch (1999) attributed the chemical evolution of the accretionary wedge to the unroofing of the older Rakaia rocks. Unroofing by cannibalistic recycling of Rakaia sandstones is further supported by data presented in Chapter 4.

Interestingly, the unroofing trends also coincide with trends observed in the Murihiku terrane where Boles (1974) reported an increase in SiO_2 from the Early to the middle Late Triassic and a subsequent reversion to more volcanic detritus from the middle Late Triassic to the Early Jurassic. Boles (1974) ascribed the compositional shift to the change from predominantly andesitic to predominantly dacitic rhyolitic to once again andesitic volcanism in the source.

The presence of a Cambrian igneous clasts in the Kazanian Te Moana and Carnian Lake Hill conglomerates indicate that Cambrian plutons were a protosource and provided actively detritus to the Rakaia depocentres. As described previously, Cambrian magmatism was confined to the Western Province and its Australia and Antarctic correlatives. The presence of the Cambrian clast in the Te Moana

conglomerate therefore implies a linkage between the Rakaia terrane and the Gondwana margin, at least in Kazanian times. The linkage is further supported by the Parapara Peak Group of the Western Province (Section 1.3.1.1). Although the Triassic sediments differ compositionally from the Rakaia terrane, both sequences have a very similar detrital zircon age signature (Figure 3.11), thus providing further evidence that a Gondwana source for the Rakaia sandstones is viable, and indicating a close proximity between the Eastern and Western provinces of New Zealand in Permian to Triassic times.

The value of sampling igneous clasts (and getting information on the protosource) is emphasised here again. As an example, the presence of Cambrian clasts at Te Moana and Lake Hill is also important when interpreting U-Pb detrital zircon age distributions. Most of the detrital U-Pb zircon age distributions from the Rakaia terrane sandstones (see Figure 3.11) display a minor, but distinct Cambrian peak. However, whether these zircon ages represent the age of the protosource or whether they are derived from a proximate source (i.e. recycled sediments, inherited in younger magmatism and transported to the surface) is not clear. These clasts identify Cambrian igneous rocks as a protosource for the Rakaia sediments

The Artinskian/Kungurian (276.8±4.6 Ma, UC31813) volcanic igneous clast in the Te Moana conglomerate is just slightly older than the Kazanian stratigraphic age of the conglomerate. This implies that at the time of deposition the conglomerate (Rakaia terrane) was in close proximity of its igneous source. This is supported by the presence of boulder and cobble sized clasts in the conglomerate, which suggest that detritus was transported 10s to 100s of kilometres rather than 1000s of kilometres (see Section 1.7).

In summary, igneous clast ages and stratigraphic ages discussed above indicate that the Rakaia accretionary wedge was emplaced in an autochthonous setting along the Gondwana margin. Although the provenance of the Rakaia terrane clearly indicates derivation from Gondwana (MacKinnon, 1983), the lateral continuity of rock units along the Panthalassan margin of the super-continent makes definition of the exact location of the source difficult. Combining geochronological, geochemical and isotopic data of the Rakaia igneous clasts an igneous protosource for the clasts can be envisaged as follows:

- A volcanic/plutonic continental arc experienced continuous magmatism into the early Middle Triassic, and had Cambrian and Carboniferous plutons and volcanics exposed at the time of erosion.

- The protosource included a mature crust (at least by the Late Triassic) and, due to continuous uplift (shown by the grain size), had its mid-crustal levels eroded while magmatism continued.

Detrital zircon age distributions from Rakaia sandstones identify a Permian to Triassic arc source as the main contributor of detritus. However, comparison of the igneous conglomerate clasts of these ages with the potential source provinces from the Panthalassan margin is ambiguous and inconclusive. In Section 8.1 both the New England Supersuite and felsic plutons from the Amundsen Province were identified as likely protosources for the Permian to Triassic igneous clasts.

In the following sections these two potential protosources, also proposed by other researchers, are evaluated in the light of tectonostratigraphic and regional constraints.

9.2.1 Australian Source

The detrital zircon age populations of the two Rakaia sandstones analysed for this study are dominated by a distinct 300-200 Ma age group (Figure 3.11). A similar distribution of U-Pb detrital zircon and $^{40}Ar/^{39}Ar$ muscovite mineral ages from similar Rakaia sandstones have been reported by other researchers (Adams, 1996; Wysoczanski *et al.*, 1997; Adams *et al.*, 1998; Adams and Kelley, 1998; Pickard *et al.*, 2000). These age data are remarkable and clearly point to a New England Fold Belt (NEFB) provenance for the Rakaia sandstones. Adams and coworkers proposed a model whereby the depocentres were subsequently tectonically transported, by strike-slip motion >2500 km over 60 Ma, southwards around the Panthalassan margin of Gondwana into a high-latitude Cretaceous position.

This model is also favored by Veevers (2000b, p. 121) who noted, that the detrital zircon age population (and provenance) of the Torlesse sandstones is very similar to that of the Early Triassic Terrigal Formation of the Sydney Basin and modern beach sands in northern New South Wales (Hummock Hill Island, Sircombe, 1999), both of which he considers to be derived from the NEFB. Based on this observation

Veevers (2000) supports the model whereby the Torlesse sandstones were deposited adjacent to the NEFB (Pickard *et al.*, 2000).

However, the Hummock Hill Island beach sand has a pronounced peak between 400-300 Ma (Sircombe, 1999, his Figure 2) and the same age group is the dominant age group in the Terrigal Formation (Sircombe, 1999, his Figure 4). The Carboniferous peak differs markedly from the zircon age distribution observed in the Rakaia sandstones, which have this peak poorly developed (or absent), and thus detrital zircon mineral ages argue against rather than for a NEFB origin for the Torlesse sandstones.

This 400-300 Ma peak is almost completely absent from the Triassic Torlesse muscovite data of Adams and Kelley (1998) and Adams *et al.* (1998). $^{40}Ar/^{39}Ar$ single crystal mineral ages of detrital muscovites from Rakaia sandstones show an age population dominated by a major Permian-Triassic (280-205 Ma) peak and a minor mid-Paleozoic (460-410 Ma) peak. There is a complete absence of peaks in the range 500-460 Ma and 410-330 Ma.

Rb-Sr whole-rock isochron dating of Rakaia sandstones yields initial $^{87}Sr/^{86}Sr$ ratios (at the time of metamorphism) as low as 0.7065 (Adams, 1996; Adams and Graham, 1996). These authors believe that the low $^{87}Sr/^{86}Sr$ initial ratios of the sandstones at the time of their Permo-Triassic deposition indicate that the detritus was derived from a dominantly I-type granitoid terrane, with only subordinate contributions from older and more radiogenic country rock. In combining their $^{40}Ar/^{39}Ar$ detrital mineral age and bulk-rock initial strontium isotope data Adams and coworkers concluded that these characteristics point uniquely to a provenance in the NEFB and immediately adjacent to older terranes of eastern Queensland.

However, according to the classification scheme of White and Chappell (1983) I-type granitoids have a distinct metaluminous mineralogy in which hornblende, biotite and titanite are the common mafic mineral phases and muscovite is conspicuous by its absence. In contrast, S-type granitoids are characterised by a peraluminous mineralogy that is marked by the presence of muscovite, often accompanied by cordierite and/or other aluminosilicates. It is therefore questionable whether peraluminous minerals should or can be used to date metaluminous I-type magmatism.

Muscovite occurs over a wide range of metamorphic grades, from lower greenschist to upper amphibolite and blueschist facies (Deer *et al.*, 1992), but Adams and coworkers do not distinguish between igneous and metamorphic muscovite. S-type magmatism in the NEFB is confined to the latest Carboniferous to earliest Permian (Hillgrove and Bundarra suites), an age group that is poorly represented in the Torlesse sandstones by $^{40}Ar/^{39}Ar$ dated detrital muscovite (n=3) in their study. However, the pronounced Late Permian to Early Triassic muscovite age peak coincides with the Late Permian to earliest Late Triassic I-type magmatism in the NEFB. The S-type granitoids of the NEFB were emplaced close to the backarc basin (Sydney Basin) whereas the I-type magmatism occurred mostly close to the forearc basin (Scheibner and Veevers, 2000, their Figure 192, see also below). If the Rakaia sedimentary basins represent the accretionary wedge to the NEFB, then the detrital muscovite are much more likely to be of metamorphic than of igneous origin, because I-type granitoids (lacking in muscovite) are the predominant source of the forearc-basin detritus. The NEFB provenance model for the Torlesse sandstones, based on combining the $^{87}Sr/^{86}Sr$ initial ratios and $^{39}Ar/^{40}Ar$ muscovite ages, as proposed by Adams and coworkers, is therefore highly questionable.

In the Permian, the Bowen Basin (Figure 8.1) formed behind the arc in a back-arc extensional to foreland-basin setting, between the NEFB and the cratonic block to the west (Roser and Korsch, 1999, and references therein). Deposition continued through the earliest Late Triassic time, and the Bowen Basin fill thus represents the back-arc deposits of the proposed Rakaia source. Petrographic data from the Bowen Basin (Roser and Korsch, 1999, their Figures 16.c) differ significantly from data from the Rakaia sandstones (Figure 4.1). The Permian Bowen Basin sandstones are quartz-poor and volcanolithic, reflecting the input from the volcanic arc to the east which peaked in the Late Permian, with sediment becoming increasingly quartzose in the Permo-Triassic due to an input of mature cratonic sediments from the west (Roser and Korsch, 1999). The compositional contrast between the Rakaia and Bowen sediments is striking and a sorting mechanism must be explained that sheds quartzofeldspathic detritus into the forearc basin and volcanolithic to quartzose detritus into the backarc basin. Roser and Korsch (1999) suggested that the Rakaia and the Bowen sandstones could only have been derived from the same arc if a major contrast in lithotype (volcanic versus granitoid) was present across it.

The Permian to Triassic igneous clast population (Section 8.1) shows a good correlation with New England Supersuite rocks, and a NEFB provenance for the penecontemporaneous Rakaia detritus is therefore feasible. However, Famennian to Visean magmatism (Boundary Creek clasts) in eastern Australia was restricted to the backarc basin of the NEFB (both sides along the Sydney Basin) and to small pockets in north Queensland. Cambrian magmatism was, apart from the Upper Bingara Plagiogranite, restricted to Tasmania and north Queensland (Scheibner and Veevers, 2000, their Figures 219 and 215), i.e., the NEFB clearly lacks the older igneous rocks required to explain the presence of these older igneous clasts in the Rakaia conglomerate.

In addition, Early Jurassic magmatism in eastern Australia is confined mainly to Tasmania and southeast mainland Australia, where magmas have been emplaced as far north as the Sydney Basin. These magmas have been correlated with the Ferrar Dolerites (Scheibner and Veevers, 2000, and references therein). No Early Jurassic (<200 Ma) rocks were reported from within the NEFB that could serve as a suitable source for the single Early Jurassic clast from Kekerengu.

In summary, the conspicuous absence of Cambrian, Carboniferous and Jurassic magmatism along the NEFB sector of the Panthalassan Gondwana margin does not correspond to the volcanic/plutonic continental arc model as proposed in the previous section. In addition, tectonostratigraphic and regional constraints, together with the discrepancy between the detrital mineral age data from the Rakaia sandstones and the NEFB igneous data, do not support a NEFB provenance for the Rakaia sandstones.

9.2.2 New Zealand/Antarctica Source

The Carboniferous to Triassic granitoids from the Median Tectonic Zone/Amundsen Volcanic Belt (MAVB) represent a remnant volcanic/plutonic arc that was active at the time of the Rakaia sandstone deposition. The autochthonous relationship between the Rakaia terrane (including its inboard terranes and the MTZ/Amundsen Province) and the Gondwana margin has been discussed above. This relationship indicates that other Carboniferous igneous rocks (Ross and Western provinces) were in close proximity to the MAVB at the time of Permian to Late Triassic Rakaia sedimentation. In addition, Cambrian orthogneisses, now exposed at Mount Murphy and along the Wallgreen Coast and in the Western Province of New Zealand,

were in the vicinity of the volcanic/plutonic arc source, contributing to the depositional basins.

Other Cambrian rocks in Antarctica are mainly confined to the Transantarctic Mountains that are now separated from West Antarctica (Ross Province) by the West Antarctic rift system (WARS). The rift system consists of the Victoria Land Basin, the Central Trough and the Eastern Basin, which lies beneath the Ross Ice Shelf. The three basins are underlain by highly extended crust and shallow mantle (minimum depth of about 16 km, Trey *et al.*, 1999). Two major extensional phases throughout the Mesozoic and Cenozoic were identified (Hamilton *et al.*, 2001). The first phase of extension is thought to have started with the initiation of the Gondwana break-up in the Late Jurassic (De Santis *et al.*, 1994), followed by a major extensional period beginning at c. 105 Ma (Bradshaw, 1989; Luyendyk, 1995; Luyendyk *et al.*, 1996; Storey *et al.*, 1999). Trey *et al.* (1999) concluded that most extension and basin down-faulting occurred in the Ross Sea during late Mesozoic time, with relatively small extension during Cenozoic time. The rifting post-dates the Permian to Triassic Rakaia terrane sedimentation, implying that at the time of sedimentation West Antarctica must have occupied a position closer or adjacent to the Transantarctic Mountains.

However, at the time of the deposition of the Rakaia sediments (Permian to Late Triassic) the Transantarctic Mountains (TAM) were part of a depositional basin and were covered by the Devonian to Triassic Beacon Supergroup. For a comprehensive summary of the Permian to Triassic Transantarctic Basin the reader is referred to Collinson *et al.* (1994). Before the Beacon deposition, the orogen was eroded to its core with exhumation of 10-20 km in many places (Gleadow and Fitzgerald, 1987; Stump, 1995; Fitzgerald *et al.*, 1996). Based on apatite fission track data from a cross-section in the Dry Valleys Gleadow and Fitzgerald (1987) concluded that the main uplift of the TAM began at c. 50 Ma. Before the Cenozoic uplift the TAM formed the rift shoulder of the West Antarctic rift system.

The Liv Volcanics of the Central Transantarctic Mountains have been suggested as a possible source for the dacitic clast from the Lake Hill conglomerate (Section 8.3). The presence of a TAM derived clast in the Rakaia depocentre therefore indicates, that prior to the opening of the WARS, and at the time of the Rakaia sedimentation, the TAM rocks may have been exposed to erosion along the Panthalassan edge of the

Central Transantarctic Sedimentary Basin (M. Bradshaw, pers. comm.). The edge of the sedimentary basin is now covered by the Ross Ice Shelf and any contribution of Cambrian TAM detritus to the Rakaia basin remains speculative. Given that the TAM were buried by the Devonian to Late Triassic Beacon Group, detrital contribution of the TAM to the Rakaia basin is considered to be minor.

The Cambrian monzogranite from Te Moana correlates best with basement rocks of West Antarctica (Ross Province, Section 8.3), which is favoured as the Cambrian protosource for the Rakaia detritus. The subdued Cambrian detrital zircon age peak in both Rakaia sandstones from this study (and other studies) are ascribed to the detrital contribution of the Amundsen/Ross Province basement.

Magmatism in the source and sedimentation of the Rakaia sandstones was contemporaneous and the sedimentary basins received boulder/cobble/pebble/sand detritus from this source. The presence of boulder and cobble sized clasts suggests a short travel distance for the detritus (see above). Age signatures of detrital zircons from Kurow Hill and Balmacaan Stream correlate well with igneous clast ages, indicating that the depositional basins were positioned adjacent to the volcanic/plutonic arc segment from which the clasts were derived. Thus, the MAVB (including the older provinces) must have comprised plutons and volcanics of appropriate ages to explain the igneous clast population sampled in the Rakaia terrane conglomerates and to account for the detrital zircon age signatures in the Rakaia sandstones.

In stark contrast to eastern Australia, there are very few rocks exposed in West and East Antarctica (<1 % of the total area, Stump, 1995), and interpretations offered in this study are based inevitably on data from a few selected outcrops. Nevertheless, geochronology and geochemistry of the MAVB (and its older inboard provinces) correlate broadly with igneous clasts from the four Rakaia conglomerates. The Amundsen Province and Ross Province are postulated as likely sources for the Permian to Triassic, Carboniferous, and Cambrian igneous clasts respectively (see Chapter 8).

The Permian detrital zircon age peaks for the Kurow Hill and Balmacaan Stream sandstones (and other Rakaia sandstones, Figure 3.11) support the conclusion that granitoids from the Kohler Range were a major source for the Triassic sediments (Figure 8.3). Isotope data presented in Figures 8.14 and 8.15 indicate that the simple erosion of Amundsen Province plutons could produce at least part of the Rakaia terrane

detritus. The minor Carboniferous age component in the Kurow Hill sample resembles that of the Ross Province magmatism. The same peak is present but rather subdued in the Balmacaan Stream sample. The exposure of a Cambrian protosource next to or within the MAVB is also shown in both sandstones, with both having a subdued Cambrian peak.

In Section 9.1.3 the Campbell Magnetic Anomaly System (CMAS) has been tentatively correlated with the Median Tectonic Zone/Western Province magmatism (Figure 9.4). This implies that at least part of the Campbell Plateau was part of the Gondwana margin, with the Rakaia depositional basins nearby. The extent of Rakaia terrane as far as the Chatham Islands has been noted previously. Although no igneous clasts have been sampled from the Campbell Plateau, detrital zircon age distribution of the Chatham Island Torlesse (Matarakau greywacke, Ireland pers. comm.) shows identical peaks to those displayed by the Kurow Hill sandstone (and other Permian to Triassic samples). As noted before, the Artinskian/Kungurian (276.8±4.6 Ma, UC31813) volcanic igneous clast in the Te Moana conglomerate is just slightly older than the Kazanian stratigraphic age of the conglomerate. This implies that at the time of deposition the conglomerate (Rakaia terrane) was in close proximity of its igneous source. It is therefore reasonable to conclude that the sedimentary (Eastern Province) and the igneous (CMAS) components of the Campbell Plateau were in close proximity in the Triassic.

The Early Jurassic clast from Kekerengu has been correlated with the calc-alkaline, weakly peraluminous Bounty Island Granite (Section 7.4). Although no major and trace element geochemical data are available for the Pine Island granitoids, they have characteristics of subduction-related magmas (Weaver pers. comm.). Subduction-related magmatism is also supported by Sr-Nd isotope data from these rocks (Figure 7.31). The resemblance between these two contemporaneous provinces suggests that they shared a similar petrogenetic history, and that the Campbell Plateau was in close proximity (part of?) Thurston Island/Marie Byrd Land in the Early to Middle Jurassic.

Apart from the Early Permian fauna within the Akatarawa terrane (and a few other exotic blocks noted in Section 1.4) the inferred cold-water affinities of the Rakaia faunal assemblages support a deposition of the Rakaia detritus in a high-latitude environment (Shi and Grunt, 2000). The Akatarawa fusulinid formation has

accumulated in a warm-water environment, and Hada and Landis (1995) ascribed the absence of siliciclastic detritus to the accumulation of the formation in an intra-oceanic depositional environment removed from any continental influence (Rakaia accretionary wedge). The formation was initially formed within an exotic low-latitude location near a subduction zone (Hada and Landis, 1995).

Paleomagnetic studies over the past few decades have closely constrained the apparent polar-wander path (APWP) of the Australian continent and its Gondwana neighbours in the Late Paleozoic, Mesozoic and Cenozoic (Schmidt and Clark, 2000, and references therein). The Late Carboniferous-Permian (327-250 Ma) pole path indicates a polar latitude up to the end of the Permian for the Australian part of Gondwana. The Triassic to Early Jurassic group of poles indicates mid to high southern latitudes for Australia before its return to higher latitudes (Schmidt and Clark, 2000), with Antarctica and the Western Province of New Zealand generally depicted as being in the vicinity of the South Pole (Powell and Li, 1994; Mukasa and Dalziel, 2000). This further supports an Antarctic source for the Rakaia terrane as postulated here.

In summary detrital zircon age data from Rakaia sandstones and whole rock geochemistry and geochronology of penecontemporaneous igneous clasts, together with regional tectonostratigraphic constraints, have broadly identified the Antarctic sector of the Panthalassan Gondwana margin as the provenance of the Rakaia terrane igneous clasts. Major and trace element, and Sr-Nd isotope data of Rakaia sandstones indicate that simple erosion of a source segment could account for part of the Rakaia detritus. However, Sr-Nd isotope data also indicate that more radiogenic sources must have contributed detritus to the depocentre. Despite a few good present day outcrop exposures in Antarctica, the complexities of a polylithologic continental arc margin and the paucity of geochemical and isotope data from this sector prevent a more detailed determination of the provenance.

9.3 SUMMARY OF MAIN CONCLUSIONS

A detailed sampling program of igneous clasts from seven Torlesse terrane conglomerates and tectonostratigraphic constraints have helped to broadly characterise the igneous protosources of the Pahau and Rakaia terranes.

Geochronological, major and trace element, and Sr-Nd isotope data from the Pahau terrane igneous clasts indicate that subduction related magmas were intruded into an active continental margin. All the clasts display a general concordance that suggests a similar petrogenesis and derivation from a single suite, except for the alkaline clasts from Mount Saul and Kekerengu. The Late Jurassic to Early Cretaceous calc-alkaline, metaluminous to weakly peraluminous clasts are indistinguishable in age, chemical composition, and petrogenesis from the felsic members of the calc-alkaline I-type granitoids of the Darran Suite, whereas the alkaline rhyolitic clasts from Mount Saul and Kekerengu correlate best with the Electric Granite. The Darran Suite and the Electric Granite are part of the Median Tectonic Zone, and the subduction-related MTZ/Amundsen Province Volcanic Belt (MAVB) is therefore proposed as the source for Pahau terrane igneous clasts.

The clast population from all three Pahau conglomerates are dominated by silicic and highly fractionated volcanic and granophyric, hypersolvus clasts. The presence of these lithotypes is attributed to the stripping and erosion of the upper levels of the MAVB and the subsequent transportation to the place of final deposition.

Most of the igneous clast ages from Ethelton and Kekerengu overlap with the Early Cretaceous detrital zircon age group of the Ethelton conglomerate sandstone matrix, indicating that sedimentation and source magmatism were penecontemporaneous. The youngest detrital zircon dated from the matrix gives an age of 111.7±1.4 Ma that constrains the minimum age of magmatism in the source region of the Pahau terrane.

The Early Jurassic clast from Kekerengu correlates with the calc-alkaline, weakly peraluminous Bounty Island Granite, which shares a similar petrogenetic history with the contemporaneous Pine Island granitoids, suggesting that the Campbell Plateau

was in close proximity to Thurston Island/Marie Byrd Land in the Early to Middle Jurassic.

Sandstone clasts from two Rakaia and two Pahau conglomerates were collected to investigate the recycling of the older Rakaia rocks. Sandstone clast major and trace element chemical data largely support petrographic observations derived from thin section analysis. Data from sandstone clasts from the Pahau terrane suggest that uplift of the Rakaia terrane continued into the Cretaceous. These Pahau terrane clasts indicate that at the time of the Pahau sedimentation Permian to early Late Triassic Rakaia rocks were exposed and recycled into the Pahau basin. Recycling of the Rakaia sediments is supported by the detrital zircon age data from this and other studies. The similarities of petrographic and geochemical data between sandstone clasts from the Rakaia terrane and Rakaia sandstones suggest that clasts in the Te Moana and Lake Hill conglomerates were derived by autocannibalistic reworking of older, consolidated, Rakaia sediments.

Geochronology, geochemistry and Sr-Nd isotopes of igneous clasts from the Pahau terrane identify the MAVB (Darran Suite and Electric Granite) as a detritus contributor to the Pahau depocentre. Based on sandstone and sandstone clast geochronology, geochemistry and Sr-Nd isotopes, the recycling of the older inboard Rakaia and Caples terranes into the Pahau basin was demonstrated. A multi- source model is proposed in which the uplifted Rakaia and Caples terranes as well as an active volcanic arc contributed detritus to the Pahau sedimentary basin.

Geochronology, petrography, geochemistry and Sr-Nd isotopes of igneous clasts from the Rakaia terrane point towards a progressive unroofing of a continental volcanic/plutonic arc source that has experienced continuous magmatism from the Carboniferous to the latest Middle Triassic. The presence of adakitic rocks in the source area may attest to the presence of a mature crust, whereas the exposure of gneissic structural levels at the time of Rakaia terrane sedimentation indicates that extensive erosion of the upper levels of the source took place before Carnian times.

The occurrence of Cambrian igneous clasts in the Kazanian Te Moana and Carnian Lake Hill conglomerates indicates that Cambrian plutons and volcanics were a protosource that provided actively detritus to the Rakaia depocentres. Cambrian magmatism was confined to the New Zealand Western Province and its Australian and Antarctic correlatives as well as the TAM and their Australian correlatives. The

presence of the Cambrian clasts indicates an autochthonous setting for the Rakaia depocentres with respect to the Gondwana margin. The Cambrian clast in the Te Moana conglomerate therefore implies a linkage between the Rakaia terrane and the Gondwana margin in Kazanian times. The close proximity between the Eastern and Western provinces of New Zealand in Permian to Triassic times is indicated by very similar detrital zircon age signatures of the Rakaia sandstones and the Parapara Peak Group, thus providing evidence that a Gondwana source for the Rakaia sandstones is viable.

Source magmatism and deposition of the Rakaia sediments were penecontemporaneous, indicated by the presence of an Artinskian/Kungurian volcanic igneous clast in the Kazanian Te Moana conglomerate and further supported by detrital zircon ages of the sandstones. Some parts of the Otago Schist (Boundary Creek) appear to have a very different provenance from the Permian Rakaia terrane.

Detrital zircon age distributions from Rakaia sandstones identify a Permian to Triassic arc source as the main contributor of detritus to the Rakaia sedimentary basins. Although the lateral continuity of rock units along the Panthalassan margin of the super-continent makes definition of the exact location of the source difficult, geochronology, geochemistry and Sr-Nd isotopes of Rakaia igneous clasts correlate broadly with those of the MAVB and its inboard provinces (Ross/Western Province, TAM). The data presented in this study do not support an eastern Australian provenance for the Torlesse. The Amundsen Province and Ross Province are postulated as likely sources for the Permian to Triassic, Carboniferous, and Cambrian igneous clasts.

ACKNOWLEDGEMENTS

I would like to thank my two supervisors, Associate Professor John Bradshaw and Professor Steve Weaver, for initiating this project and for all their help and illuminating discussions on all things New Zealand geology. Your financial support with the help of a University of Canterbury research grant is greatly appreciated and made this whole study possible. This project was also supported financially by a University of Canterbury Doctoral Scholarship, the Department of Geological Sciences, and the Mason Trust Fund.

This study benefited from valuable comments by Nick Mortimer and Nelson Eby, who enthusiastically read parts of my drafts. Comments by Tod Waight, Barry Roser and Scott Bryan are also much appreciated. Malcolm Laird is thanked for always taking time to discuss aspects of New Zealand geology and always having rare reports, books, and reprints ready at his fingertips.

Special thanks go to Barry Roser, Tod Waight, Bob Pankhurst, Nick Mortimer, Steve Ward and Tony Crawford, who supplied some unpublished data and to Doug Coombs for providing rock samples for geochemical analysis. I would also like to thank Mo Turnbull for suggesting and helping sample the Boundary Creek conglomerate.

Analytical work was undertaken at or by a number of other organisations. Nelson Eby of the University of Massachusetts, Lowell, provided INAA data for igneous clasts. I carried out mineral separation at the University of Waikato and the initiative and help of Peter Kamp is greatly appreciated. Thanks very much to Xu Ganging and Renat Radosinsky for their support and assistance in the lab, and Barbara Hobden and Richard Smith for making my Waikato stay a memorable one. I was fortunate to carry out my SHRIMP work at Stanford University in California under the very helpful guidance of Trev Ireland, who not only showed great enthusiasm for my project, but never objected to late night phone calls when SHRIMP RG 'lost it'. He also made the Kiwi Dollar go a very long way when it came to writing the invoice for the SHRIMP work – thanks Trev. To Jo Wooden, Harold Persing, Marilyn Vogel, Kathleen deGraaff thanks for helping to enliven the long hours spent in the lab. Thanks to Jerry and his friends, who made significant contributions to maintaining my sanity during these long hours. To my flatmates in Palo Alto, who provided marvellous accommodation and to the High Speed Bucks for tremendous entertainment. I carried out radiogenic isotope analysis at La Trobe University in Melbourne. Thanks heaps to Roland Maas, who took the time and had the patience to introduce me to isotope work – and special thanks for your hospitality and company.

Many people at the Department of Geological Sciences at the University of Canterbury have greatly assisted me throughout this study. I would like to thank Dave Shelley, Doug Lewis and Kari Bassett for contributing many stimulating discussions and reading various bits of the manuscript. The technical staff of the Department are also thanked for their many and varied services, in particular: Rob Spiers for all the thin sections, good laughs and company; Steve Brown for running the XRF analyses; Jane Guise for helping me with thin section staining and the use of her HF lab; Cathy Knight for always having the right sampling bag sizes in store and other bits and pieces that are helpful in the field; John Southward for his computer wizardry; Kerry Swanson for photographing hand specimens and advice on photomicroscopy; and last but not least Arthur Nicholas, who I often annoyed and upset, but who always was there when I needed help.

Special thanks go to the secretarial staff of the Department: Julie-Anne Hale for processing all my requests and claims at the speed of light and never questioning my receipts, and to Michele Wright who did.

I was lucky enough to be part of a lively group of postgraduates during my time at the University of Canterbury who must be thanked for their friendship and support over the years, particularly Steelspring–Dave, Robert, Jens, Michael, Spinks, and Johnson.

Special thanks go to Mary and Peter McMorran for their continuous support. And finally, my biggest thank you and hugs go to my partner Anandi. Thank you for your love and understanding, your encouragement and support and fixing my computer problems, helping me in the field, for carrying loads and loads of cobbles and pebbles down from the top of Mount Saul, proof reading my work and always being there and cheering me up whenever I needed it. Without your help and the assistance of Tobi, Nima and Osho – this study would have been much harder to complete – dherai dhanyabaad.

REFERENCES

REFERENCES

Adams, C.J., Harper, C.T. and Laird, M.G., 1975. K-Ar ages of the low grade metasediments of the Greenland and Waiutu Groups in Westland and Buller, New Zealand. *New Zealand Journal of Geology & Geophysics*, 18: 29-48.

Adams, C.J., Bishop, D.G. and Gabites, J.E., 1985. Potassium-aragon age studies of a low-grade, progressively metamorphosed greywacke sequence, Dansey Pass, South Island, New Zealand. *Journal of the Geological Society London*, 142: 339-349.

Adams, C.J., 1987. Geochronology of granite terranes in the Ford Ranges, Marie Byrd Land, West Antarctica. *New Zealand Journal of Geology & Geophysics*, 30: 54-72.

Adams, C.J. and Raine, J.I., 1988. Age of Cretaceous silicic volcanism at Kyeburn, central Otago, and Palmerston, eastern Otago, South Island, New Zealand. *New Zealand Journal of Geology & Geophysics*, 31(4): 471-475.

Adams, C.J., 1996. A Queensland provenance for New Zealand Permo-Triassic Torlesse metagreywacke terranes: a review of the age and isotopic evidence, *Mesozoic Geology of the Eastern Australia Plate Conference*. Geological Society of Australia, Brisbane, p. 1.

Adams, C.J. and Graham, I.J., 1996. Metamorphic and tectonic geochronology of the Torlesse terrane, Wellington, New Zealand. *New Zealand Journal of Geology & Geophysics*, 39(2): 157-180.

Adams, C.J. and Graham, I.J., 1997. Age of metamorphism of Otago schist in eastern Otago and determination of protoliths from initial strontium isotope characteristics. *New Zealand Journal of Geology & Geophysics*, 40(3): 275-286.

Adams, C.J., Barley, M.E., Fletcher, I.R. and Pickard, A.L., 1998. Evidence from U-Pb zircon and $^{40}Ar/^{39}Ar$ muscovite detrital mineral ages in metasandstones for

movement of the Torlesse suspect terrane around the eastern margin of Gondwanaland. *Terra Nova. The European Journal of Geosciences*, 10(4): 183-189.

Adams, C.J. and Kelley, S., 1998. Provenance of Permian-Triassic and Ordovician metagraywacke terranes in New Zealand: Evidence from Ar-40/Ar-39 dating of detrital micas. *Geological Society of America Bulletin*, 110(4): 422-432.

Adams, C.J., Barley, M.E., Maas, R. and Doyle, M.G., 2002. Provenance of Permian-Triassic volcaniclastic sedimentary terranes in New Zealand: evidence from their radiogenic isotope characteristics and detrital mineral age patterns. *New Zealand Journal of Geology & Geophysics*, 45: 221-242.

Aitchison, J.C., Ireland, T.R., Blake Jr, M.C. and Flood, P.G., 1992. 530 Ma zircon age for ophiolite from New England Orogen: oldest rocks known from Eastern Australia. *Geology*, 20: 125-128.

Aitchison, J.C., 1993. Evolution of the eastern margin of Australian Plate: possible correlatives in Australia, New Caledonia and New Zealand. In: P.G. Flood and J.C. Aitchison (Editors), *New England Orogen, Eastern Australia*. Department of Geology and Geophysics, University of New England, Armidale, Australia, pp. 665-669.

Aitchison, J.C., Ireland, T.R., Clarke, G.L., Cluzel, D. and Meffre, S., 1998. Regional implications of U/ Pb SHRIMP age constraints on the tectonic evolution of New Caledonia. *Tectonophysics*, 299(4): 333-343.

Allen, C.M., Williams, I.S., Stephens, C.J. and Fielding, C.R., 1998. Granite genesis and basin formation in an extensional setting: the magmatic history of the northernmost New England Orogen. *Australian Journal of Earth Sciences*, 45(6): 875-888.

Andrews, P.B., Bishop, D.G., Bradshaw, J.D. and Warren, G., 1974. Geology of the Lord Range, central Southern Alps, New Zealand. *New Zealand Journal of Geology & Geophysics*, 17(2): 271-299.

Andrews, P.B., Speden, I.G. and Bradshaw, J.D., 1976. Lithological and paleontological content of the Carboniferous-Jurassic Canterbury Suite, South Island, New Zealand. *New Zealand Journal of Geology & Geophysics*, 19(6): 791-819.

Aronson, J.L., 1965. Reconnaissance rubidium-strontium geochronology of New Zealand plutonic and metamorphic rocks. *New Zealand Journal of Geology & Geophysics*, 8: 401-423.

Atherton, M.P. and Petford, N., 1993. Generation of sodium-rich magmas from newly underplated basaltic crust. *Nature*, 362: 144-146.

Ballance, P.F., Heming, R.F. and Sameshima, T., 1981. Petrography of the youngest known Murihiku Supergroup, New Zealand: latest Jurassic arc volcanism on the southern margin of Gondwana. In: M. Cresswell and P. Vella (Editors), *Gondwana Five; selected papers and abstracts of papers presented at the Fifth International Gondwana Symposium.*, pp. 161-166.

Ballance, P.F. and Campbell, J.D., 1993. The Murihiku arc-related basin of New Zealand (Triassic-Jurassic). In: P.F. Ballance (Editor), *South Pacific sedimentary basins. Sedimentary Basins of the World, 2.* Elsevier Science Publishers B.V., Amsterdam, pp. 21-33.

Barnes, P.M., 1990. Provenance of Cretaceous accretionary wedge sediments: the Mangapokia Formation, Wairarapa, New Zealand. *New Zealand Journal of Geology & Geophysics*, 33(1): 125-135.

Barnes, P.M. and Korsch, R.J., 1991. Melange and related structures in Torlesse accretionary wedge, Wairarapa, New Zealand. *New Zealand Journal of Geology & Geophysics*, 34(4): 517-532.

Bassett, K.N., 2000. Isotopic provenance analysis and terrane tectonics: A warning about sediment transport distances. In: C. Skilbeck and T.C. Hubble (Editors), *Understanding Planet Earth: Searching for a sustainable future. Abstracts of the 15th Australian Geological Convention.* University of Technology, Sydney, NSW, Australia p. 24.

Beggs, J.M., 1980. Sedimentology and paleogeography of some Kaihikuan Torlesse rocks in mid Canterbury. *New Zealand Journal of Geology & Geophysics*, 23: 439-445.

Beggs, J.M., 1981. Phosphorite intraclasts in Torlesse sandstones and conglomerates, South Canterbury: Comment and reply. *New Zealand Journal of Geology & Geophysics*, 24(5-6): 655-656.

Beggs, J.M., 1993. Depositional and tectonic history of the Great South Basin. In: P.F. Ballance (Editor), *South Pacific sedimentary basins. Sedimentary Basins of the World, 2*. Elsevier Science Publishers B.V., Amsterdam, pp. 365-373.

Beresford, S.W., Bradshaw, J.D., Weaver, S.D. and Muir, R.J., 1996. Echinus Granite and Pepin Group of Pepin Island, Northeast Nelson, New Zealand - Drumduan terrane basement or exotic fragment in the Median Tectonic Zone. *New Zealand Journal of Geology & Geophysics*, 39(2): 265-270.

Bhatia, M.R. and Crook, K.A.W., 1986. Trace element characteristics of greywackes and tectonic setting discrimination of sedimentary basins. *Contributions to Mineralogy and Petrology*, 92(2): 181-193.

Bishop, D.G., 1972. Progressive metamorphism from prehnite-pumpellyite to greenschist facies in the Dansey Pass area, Otago, New Zealand. *Geological Society of America Bulletin*, 83(11): 3177-3197.

Bishop, D.G., Bradshaw, J.D., Landis, C.A. and Turnbull, I.M., 1976. Lithostratigraphy and structure of the Caples terrane of the Humboldt Mountains. *New Zealand Journal of Geology & Geophysics*, 19: 827-848.

Bishop, D.G. and Laird, M.G., 1976. Stratigraphy and depositional environment of the Kyeburn Formation (Cretaceous), a wedge of coarse terrestrial sediments in central Otago. *Journal of the Royal Society of New Zealand*, 6(1): 55-71.

Bishop, D.G., Bradshaw, J.D. and Landis, C.A., 1983. Provisional terrane map of South Island, New Zealand. In: G. Howell *et al.* (Editors), *Proceedings of the Circum-Pacific Terrane Conference.* Stanford University Publications. Geological Sciences.

Stanford University, School of Earth Sciences, Stanford, CA, United States, pp. 24-31.

Black, P., 1996a. Mesozoic evolution of the Norfolk Ridge System: evidence from New Caledonia and northern New Zealand, *Mesozoic Geology of the Eastern Australia Plate Conference*. Geological Society of Australia, Brisbane, p. 90.

Black, P., 1996b. Omahuta, Bay of Island and Manaia Hill terranes: Waipapa composite terrane, North Island, New Zealand. *Geological Society of New Zealand Miscellaneous Publication*, 91A: 29.

Black, P.M., Clark, A.S.B. and Hawke, A.A., 1993. Diagenesis and very low-grade metamorphism of volcaniclastic sandstones from contrasting geodynamic environments, North Island, New Zealand; the Murihiku and Waipapa terranes. *Journal of Metamorphic Geology*, 11(3): 429-435.

Boles, J.R., 1974. Structure, stratigraphy and petrology of mainly Triassic rocks, Hokonui Hills, Southland, New Zealand. *New Zealand Journal of Geology & Geophysics*, 17: 337-374.

Borg, S.G., Stump, E. and Holloway, J.R., 1986. Granitoids of Northern Victoria Land Antarctica: a reconnaissance study of field relations, petrography and geochemistry. *Antarctic Research series*, 46: 115-188.

Borg, S.G., Stump, E., Chappell, B.W., McCulloch, M.T., Wyborn, D., Armstrong, R.L. and Holloway, J.R., 1987. Granitoids of northern Victoria Land, Antarctica; implications of chemical and isotopic variations to regional crustal structure and tectonics. *American Journal of Science*, 287(2): 127-169.

Borg, S.G., DePaolo, D.J. and Smith, B.M., 1990. Isotopic structure and tectonics of the Central Transantarctic Mountains. *Journal of Geophysical Research, B, Solid Earth and Planets*, 95 B5: 6647-6667.

Bowen, F.E., 1964. Sheet 15 - Buller. Geological Map of New Zealand 1:250 000.

Bradshaw, J.D., 1972. Stratigraphy and structure of the Torlesse Supergroup (Triassic-Jurassic) in the foothills of the Southern Alps near Hawarden (S60-61), Canterbury. *New Zealand Journal of Geology & Geophysics*, 15(1): 71-87.

Bradshaw, J.D., 1973. Allochthonous Mesozoic fossil localities in melange in the Torlesse Group of North Canterbury. *Journal of the Royal Society of New Zealand*, 3(2): 161-167.

Bradshaw, J.D. and Andrews, P.B., 1973. Geotectonics and the New Zealand Geosyncline. *Nature*, 241(105): 14-16.

Bradshaw, J.D. and Andrews, P.B., 1980. Torlesse terrane excursion. In: S.D. Weaver and D.W. Lewis (Editors), *Geological Society of New Zealand, 1980 Conference, field trip guides.* Geological Society of New Zealand, Christchurch, pp. C1-C12.

Bradshaw, J.D., Adams, C.J. and Andrews, P.B., 1981. Carboniferous to Cretaceous on the Pacific margin of Gondwana; the Rangitata phase of New Zealand. In: M. Cresswell and P. Vella (Editors), *Gondwana Five; selected papers and abstracts of papers presented at the Fifth International Gondwana Symposium.*, pp. 217-221.

Bradshaw, J.D., Weaver, S.D. and Laird, M.G., 1985. Suspect terranes in North Victoria Land, Antarctica. In: G. Howell *et al.* (Editors), *Proceedings of the Circum-Pacific Terrane Conference.* Stanford University Publications. Geological Sciences. Stanford University, School of Earth Sciences, Stanford, CA, United States, pp. 36-39.

Bradshaw, J.D., 1989. Cretaceous geotectonic pattern in the New Zealand Region. *Tectonics*, 8: 803-820.

Bradshaw, J.D., 1993. A review of the Median Tectonic Zone: terrane boundaries and terrane amalgamation near the Median Tectonic Line. *New Zealand Journal of Geology & Geophysics*, 36(1): 117-125.

Bradshaw, J.D., 1994. Brook Street and Murihiku terranes of New Zealand in the context of a mobile South Pacific Gondwana margin. *Tectonics*, 8: 803-820.

Bradshaw, J.D., Pankhurst, R.J., Weaver, S.D., Storey, B.C., Muir, R.J. and Ireland, T.R., 1996. The Mesozoic continental margin: Carboniferous-Mesozoic arc terranes in West Antarctica, New Zealand and Australia. In: G.S. ofAustralia (Editor), *Mesozoic Geology of the Eastern Australia Plate Conference*. Geological Society of Australia, Brisbane p. 114.

Bradshaw, J.D., Weaver, S.D., Pankhurst, R.J., Storey, B.C. and Muir, R.J., 1997. New Zealand superterranes recognized in Marie Byrd Land and Thurston Island. *Terra Antarctica*, 3: 429-436.

Bradshaw, J.Y., 1990. Geology of crystalline rocks of northern Fiordland: details of the granulite facies western Fiordland Orthogneiss and associated rock units. *New Zealand Journal of Geology & Geophysics*, 33(3): 465-484.

Bradshaw, J.Y. and Kimbrough, D.L., 1991. Mid-Paleozoic age of granitoids in enclaves within Early Cretaceous granulites, Fiordland, southwest New Zealand. *New Zealand Journal of Geology & Geophysics*, 34: 455-469.

Brooks, C. and Compston, W., 1965. The age and initial $^{87}Sr/^{86}Sr$ of the Heemskirk granite, western Tasmania. *Journal of Geophysical Research, B, Solid Earth and Planets*, 70(24): 6249-6262.

Brown, G.C., 1982. Calc-alkaline intrusive rocks: their diversity, evolution, and relation to volcanic arcs. In: R.S. Thorpe (Editor), *Andesites*. John Wiley and Sons.

Brown, S.J.A., Burt, R.M., Cole, J.W., Krippner, S.J.P., Price, R.C. and Cartwright, 1998. Plutonic lithics in ignimbrites of Taupo Volcanic Zone, New Zealand: sources and conditions of crystallisation. *Chemical Geology (Isotope Geoscience Section)*, 148: 21-41.

Bryan, S.E., Constantine, A.E., Stephens, C.J., Ewart, A., Schon, R.W. and Parianos, J., 1997. Early Cretaceous volcano-sedimentary successions along the Eastern Australian continental margin: implications for the break-up of Eastern Gondwana. *Earth & Planetary Science Letters*, 153(1-2): 85-102.

Bryan, S.E., Ewart, A., Stephens, C.J., Parianos, J. and Downes, P.J., 2000. The Whitsunday volcanic province, central Queensland, Australia: lithological and

stratigraphic investigations of a silicic-dominated large igneous province. *Journal of Volcanology and Geothermal Research*, 99(1-4): 55-78.

Bryant, C.J., Arculus, R.J. and Chappell, B.W., 1997. Clarence River Supersuite - 250 Ma cordilleran tonalitic I-Type intrusions in Eastern Australia. *Journal of Petrology*, 38(8): 975-1001.

Campbell, H.J., Smale, D., Grapes, R., Hoke, L., Gibson, G.M. and Landis, C.A., 1998. Parapara Group; Permian-Triassic rocks in the Western Province, New Zealand. New Zealand Journal of Geology and Geophysics, 41(3): 281-296.

Campbell, H.J., 2000a. The marine Permian of New Zealand. In: H. Yin *et al.* (Editors), *Permian-Triassic Evolution of Tethys and Western Circum-Pacific*. Elsevier Science Publishers B.V., Amsterdam, pp. 111-125.

Campbell, H.J., 2000b. The Marine Triassic of Australasian and its interregional correlation. In: H. Yin *et al.* (Editors), *Permian-Triassic Evolution of Tethys and Western Circum-Pacific*. Elsevier Science Publishers B.V., Amsterdam, pp. 235-255.

Campbell, H.J., Mortimer, N. and Raine, J.I., 2001. Geology of the Permian Kuriwao Group, Murihiku Terrane, New Zealand. *New Zealand Journal of Geology & Geophysics*, 44(3): 485-498.

Campbell, J.D. and Warren, G., 1965. Fossil localities of the Torlesse group in the South Island. *Transactions of the Royal Society of New Zealand, Geology*, 3(8): 99-137.

Campbell, J.D. and Coombs, D.S., 1966. Murihiku Supergroup (Triassic-Jurassic) of Southland and south Otago. *New Zealand Journal of Geology & Geophysics*, 9(8): 393-398.

Campbell, J.D. and Pringle, I.J., 1982. An association of Torlessia and late Middle-early Upper Triassic fossils at Pudding Hill Stream, Central Canterbury. *Journal of the Royal Society of New Zealand*, 12(5): 5-10.

Caprarelli, G. and Leitch, E.C., 1998. Magmatic changes during the stabilisation of a cordilleran fold belt: The Late Carboniferous-Triassic igneous history of eastern New South Wales, Australia. *Lithos*, 45: 413-430.

Cawood, P.A., Nemchin, A.A., Leverenz, A., Saeed, A. and Ballance, P.F., 1999. U/Pb dating of detrital zircons: Implications for the provenance record of Gondwana margin terranes. *Geological Society of America Bulletin*, 111(8): 1107-1119.

Chappell, B.W. and White, A.J.R., 1974. Two contrasting granite types. *Pacific Geology*, 8: 173-174.

Chappell, B.W. and White, A.J.R., 1992. I- and S-type granites in the Lachlan Fold Belt. *Transactions of the Royal Society of Edinburgh Earth Sciences*, 83: 1-26.

Chappell, B.W., 1994. Lachlan and New England fold belts of contrasting magmatic and tectonic development; discussion. *Journal and Proceedings of the Royal Society of New South Wales*, 127: 47-59.

Cocker, J.D., 1982. Rb-Sr geochronology and Sr isotopic composition of Devonian granitoids, eastern Tasmania. *Journal of the Geological Society of Australia*, 29: 139-158.

Collins, W.J., Beams, S.D., White, A.J.R. and Chappell, B.W., 1982. Nature and origin of A-type granites with particular reference to southeastern Australia. *Contributions to Mineralogy and Petrology*, 80(2): 189-200.

Collinson, J.W., Isbell, J.L., Elliot, D.H., Miller, M.F., Miller, J.M.G. and Veevers, J.J., 1994. Permian-Triassic transantarctic basins. In: J. Veevers and M. Powell (Editors), *Permian-Triassic Pangean basins and foldbelts along the Panthalassan margin of Gondwanaland.* Memoir - Geological Society of America. Geological Society of America (GSA), Boulder, CO, United States, pp. 173-222.

Coney, P.J., Edwards, A., Hine, R., Morrison, F. and Windrim, D., 1990. The regional tectonics of the Tasman orogenic system, eastern Australia. *Journal of Stuctural Geology*, 12: 519-543.

Cook, R.A., Sutherland, R. and Zhu, H., 1999. *Cretaceous-Cenozoic geology and petroleum systems of the Great South Basin, New Zealand.* Institute of Geological and Nuclear Sciences monograph 20, Lower Hut, New Zealand, 188 pp.

Coombs, D.S., Landis, C.A., Norris, R.J., Sinton, J.M., Borns, D.J. and Craw, D., 1976. The Dun Mountain Ophiolite Belt, New Zealand, its tectonic setting, constitution and origin, with special reference to the southern portion. *American Journal of Sciences*, 276: 561-603.

Coombs, D.S., Cook, N.D.J., Kawachi, Y., Johnstone, R.D. and Gibson, I.L., 1996. Park Volcanics, Murihiku Terrane, New Zealand - Petrology, petrochemistry, and tectonic significance. *New Zealand Journal of Geology & Geophysics*, 39(4): 469-492.

Coombs, D.S., Landis, C.A., Hada, S., Ito, M., Roser, B.P., Suzuki, T. and Yoshikura, S., 2000. The Chrystalls Beach-Brighton block, southeast Otago, New Zealand. *New Zealand Journal of Geology & Geophysics*, 43: 355-372.

Cooper, R.A., 1989. Early Paleozoic terranes of New Zealand. *Journal of the Royal Society of New Zealand*, 19(1): 73-112.

Cooper, R.A. and Tulloch, A.J., 1992. Early Palaeozoic terranes in New Zealand and their relationship to the Lachlan fold belt. *Tectonophysics*, 214: 129-144.

Cox, S.C., 1991. The Caples/Aspiring terrane boundary - the translation surface of an early nappe structure in the Otago Schist. *New Zealand Journal of Geology & Geophysics*, 34: 73-82.

Cox, S.C., Parkinson, D.L., Allibone, A.H. and Cooper, A.F., 2000. Isotopic character of Cambro-Ordovician plutonism, southern Victoria Land, Antarctica. *New Zealand Journal of Geology & Geophysics*, 43: 501-520.

Crampton, J.S. and Laird, M.G., 1997. Burnt Creek Formation and Late Cretaceous basin development in Marlborough, New Zealand. *New Zealand Journal of Geology & Geophysics*, 40(2): 199-222.

Crawford, A.J. and Berry, R.F., 1992. Tectonic implications of Late Proterozoic - Early Paleozoic igneous rock associations in western Tasmania. *Tectonophysics*, 214(129-144).

Crawford, A.J., Corbett, K.D. and Everard, J.L., 1992. Geochemistry of the Cambrian volcanic-hosted massive sulfide-rich Mount Read Volcanics, Tasmania, and some tectonic implications. In: Large and Ross (Editors), *A special issue devoted to Australian volcanic-hosted massive sulfide (VHMS) deposits and their volcanic environment.* Economic Geology and the Bulletin of the Society of Economic Geologists. Economic Geology Publishing Company, Lancaster, PA, United States, pp. 597-619.

Cumming, G.L. and Richard, J.R., 1975. Ore lead isotope ratios in a continuously changing Earth. *Earth & Planetary Science Letters*, 28: 155-171.

Davey, F.J. and Christoffel, D.A., 1978. Magnetic anomalies across Campbell Plateau, New Zealand. *Earth and Planetary Science Letters*, 41(1): 14-20.

De Santis, L., Brancolini, G. and Busetti, M., 1994. Structural evolution of the Victoria Land Basin south of the Drygalsky ice tongue (western Ross Sea). In: Ricci *et al.* (Editors), *Proceedings of the 4th meeting on Earth sciences in Antarctica.* Terra Antartica. Universita di Siena. Dipartimento di Scienze della Terra, Siena, Italy, pp. 107-110.

Dean, A.A., 1993. Analysis and correlation of igneous clast geochemistry and petrography from four Mesozoic Conglomerates. Unpublished M.Sc. Thesis, University of Canterbury, Christchurch, New Zealand, 263 pp.

Deer, W.A., Howie, R.A. and Zussman, J., 1992. *An introduction to the rock forming minerals (2nd. ed.).* Addison Wesley Longman Limited, Harlow, Essex, 695 pp.

Defant, M.J. and Drummond, M.S., 1990. Derivation of some modern magmas through melting of young subducted lithosphere. *Nature*, 347: 662-665.

DePaolo, D.J. and Wasserburg, G.J., 1979. Petrogenetic mixing models and Nd-Sr isotopic patterns. *Geochimica et Cosmochimica Acta*, 43: 615-627.

DePaolo, D.J., 1981. Neodymium isotopes in the Colorado Front Range and crustal mantle evolution in the Proterozoic. *Nature*, 291(193-196).

DePaolo, D.J., 1988. *Neodymium isotope geochemistry: An introduction*. Springer Verlag, New York.

Dickin, A.P., 1995. *Radiogenic isotope geology*. Cambridge University Press, Cambridge, UK, 452 pp.

Dickinson, W.R., 1970. Interpreting detrital modes of greywacke and arkose. *Journal of Sedimentary Petrology*, 40: 695-707.

Dickinson, W.R., Beard, L.S., Brakenridge, G.R., Erjavec, J.L., Ferguson, R.J., Inman, K.F., Knepp, R.A., Lindberg, F.A. and Ryberg, P.T., 1983. Provenance of North American Phanerozoic sandstones in relation to tectonic setting. *Geological Society of America Bulletin*, 94: 222-235.

DiVenere, V., Kent, D.V. and Dalziel, I.W.D., 1995. Early Cretaceous paleomagnetic results from Marie Byrd Land, West Antarctica: implications for the Weddellia collage of crustal blocks. *Journal of Geophysical Research, B, Solid Earth and Planets*, 100(5): 8133-8151.

Doubleday, P.A., MacDonald, D.I.M. and Nell, P.A.R., 1993. Sedimentology and structure of the trench-slope to forarc basin transition in the Mesozoic Alexander Island, Antarctica. *Geological Magazine*, 130: 737-754.

Draper, J.J. and Bain, J.H.C., 1997. A brief geological hystory of North Queensland Geology. In: J.H. Bain and J.J. Draper (Editors), *North Queensland Geology, AGSO Bulletin 240, Queensland Geology 9*. Australian Geological Survey Organisation, Canberra, Australia.

Drummond, M.S. and Defant, M.J., 1990. A model for trondhjemite-tonalite-dacite genesis and chrustal growth via slab melting: Archean to modern comparisons. *Journal of Geophysical Research, B, Solid Earth and Planets*, 21: 21503-21521.

Eade, J.V., 1988. The Norfolk Ridge System and its margins. In: A.E. Nairn *et al.* (Editors), *The Oceanic Basins and Margins Volume 7B: The Pacific Ocean*. Plenum Press, New York, pp. 303-324.

Eby, G.N., 1990. The A-type granitoids: A review of their occurrence and chemical characteristics, and speculations on their petrogenesis. *Lithos*, 26: 115-134.

Eby, G.N., 1992. Chemical subdivision of the A-type granitoids: Petrogenetic and tectonic implications. *Geology*, 20: 641-644.

Elvy, J.M., 1999. Tectonic geomorphology and paleoseismic investigations, Mount Hutt district, Canterbury. Unpublished M.Sc. Thesis, University of Canterbury, Christchurch, New Zealand, 153 pp.

Encarnacion, J. and Grunow, A., 1996. Changing magmatic and tectonic styles along the paleo-Pacific margin of Gondwana and the onset of early Paleozoic magmatism in Antarctica. *Tectonics*, 15(6): 1325-1341.

Ewart, A., Schon, R.W. and Chappell, B.W., 1992. The Cretaceous volcanic-plutonic province of the central Queensland (Australia) coast: a rift related "calc-alkaline" province. In: E. Brown and B.W. Chappell (Editors), *The second Hutton symposium on the origin of granites and related rocks; proceedings.* Special Paper - Geological Society of America. Geological Society of America (GSA), Boulder, CO, United States, pp. 327-345.

Fedo, C.M., Nesbitt, H.W. and Young, G.M., 1995. Unraveling the effects of potassium metasomatism in sedimentary rocks and paleosols, with implications for paleoweathering conditions and provenance. *Geology*, 23(10): 921-924.

Ferguson, R., Hoey, T., Wathen, S. and Werritty, A., 1996. Field evidence for rapid downstream fining of river gravels through selective transport. *Geology*, 24: 179-182.

Freund, R., 1971. The Hope Fault. *New Zealand Geological Survey, Bulletin No 86.*

Fioretti, A.M., Capponi, G., Black, L.P., Varne, R. and Visona, D., 2002. Surgeon Island granite crystallisation and inherited zircon ages: Evidence for Lower

Paleozoic basement below the Roberton Bay terrane, northern Victoria Land. (submitted).

Fitzgerald, P.G., Baldwin, S.L., Miller, S.R. and Dingle, G., 1996. Geologic and thermochronologic studies along the front of the Transantarctic Mountains near the Shackleton and Liv glaciers. *Antarctic Journal of the United States*, 31(2): 20-22.

Fleming, C.A., 1970. The Mesozoic of New Zealand: chapters in the history of the Circum-Pacific Mobile Belt. *Quarterly Journal of the Geological Society, London*, 125: 125-170.

Floettmann, T., Gibson, G.M. and Kleinschmidt, G., 1993. Structural continuity of the Ross and Delamerian orogens of Antarctica and Australia along the margin of the paleo-Pacific. *Geology*, 21(4): 319-322.

Flood, P.G. and Shaw, S.E., 1977. Two "S-type" granite suites with low initial $^{87}Sr/^{86}Sr$ ratios from the New England Batholith, Australia. *Contributions to Mineralogy and Petrology*, 61: 163-173.

Force, L.M. and Force, E.R., 1978. Triassic rocks of the Black Forest-Haldon area, Mackenzie Country, South Island, New Zealand. *New Zealand Journal of Geology & Geophysics*, 21(6): 747-760.

Ford, P.B., Lee, D.E. and Fischer, P.J., 1999. Early Permian conodonts from the Torlesse and Caples Terranes, New Zealand. *New Zealand Journal of Geology & Geophysics*, 42(1): 79-90.

Frost, C.D. and Coombs, D.S., 1989. Nd isotope character of New Zealand sediments: implications for terrane concepts and crustal evolution. *American Journal of Science*, 289(June): 744-770.

Fyfe, H.E., 1931. Amuri Subdivision. *New Zealand Geological Survey, Annual Report No 25*: 5-6.

Garbutt, J.M. and Teyssier, C., 1991. Prism <c> slip in the quartzites of the Oakhurst Mylonite Belt, California. *Journal of Structural Geology*, 13: 657-666.

Gibson, G.M., McDougall, I. and Ireland, T.R., 1988. Age constraints on metamorphism and the development of a metamorphic core complex in Fiordland, southern New Zealand. *Geology*, 16(5): 405-408.

Gibson, G.M., McDougall, I. and Ireland, T.R., 1989. Age constraints on metamorphism and the development of a metamorphic core complex in Fiordland, southern New Zealand; reply. *Geology*, 17(4): 381-382.

Gibson, G.M. and Ireland, T.R., 1996. Extension of Delamerian (Ross) orogen into western New Zealand - evidence from zircon ages and implications for crustal growth along the Pacific margin of Gondwana. *Geology*, 24(12): 1087-1090.

Gleadow, A.J.W. and Fitzgerald, P.G., 1987. Uplift history and structure of the Transantarctic Mountains; new evidence from fission track dating of basement apatites in the Dry Valleys area, southern Victoria Land. *Earth and Planetary Science Letters*, 82(1-2): 1-14.

Goldstein, S.L., O'Nions, R.K. and Hamilton, P.J., 1984. A Sm-Nd isotope study of atmospheric dusts and particulates from major river systems. *Earth & Planetary Science Letters*, 70: 221-236.

Graham, I.J. and Korsch, R.J., 1989. Rb-Sr resetting ages and chemical characterization of turbidites in an accretionary wedge: Torlesse Complex, Otaki Gorge, New Zealand. *Geological Society of America Bulletin*, 101: 355-363.

Graham, I.J. and Korsch, R.J., 1990. Age and provenance of granitoid clasts in Moeatoa Conglomerate, Kawhia Syncline, New Zealand. *Journal of the Royal Society of New Zealand*, 20(1): 25-39.

Graham, I.J. and Mortimer, N., 1992. Terrane characterisation and timing of metamorphism in the Otago Schist, New Zealand, using Rb-Sr and K-Ar geochronology. *New Zealand Journal of Geology & Geophysics*, 35(4): 391-401.

Grapes, R.H., Roser, B.P. and Kashai, K., 2001. Composition of monocrystalline detrital and authigenic minerals, metamorphic grade, and provenance of Torlesse and Waipapa greywacke, Central North Island, New Zealand. *Geological Review*: 139-163.

Grindley, G.W., Oliver, P.J. and Sukroo, J.C., 1981. Lower Mesozoic position of southern New Zealand determined from paleomagnetism of the Glenham Porphyry, Murihiku Terrane, eastern Southland. In: M. Cresswell and P. Vella (Editors), *Gondwana Five; selected papers and abstracts of papers presented at the Fifth International Gondwana Symposium.*, pp. 319-326.

Gust, D.A., Stephens, C.J. and Grenfell, A.T., 1993. Granitoids of the northern NEO: Their distribution in time and space and their tectonic implication. In: P.G. Flood and J.C. Aitchison (Editors), *New England Orogen, Eastern Australia.* Department of Geology and Geophysics, University of New England, Armidale, Australia, pp. 565-572.

Hada, S. and Landis, C.A., 1995. Te Akatarawa Formation: an exotic oceanic-continental margin terrane within the Torlesse-Haast Schist transition zone. *New Zealand Journal of Geology & Geophysics*, 38(3): 349-359.

Hamilton, D., 1950. The Geology of the Waikari Valley and its northern ridges, North Canterbury, New Zealand. Unpublished M.Sc. Thesis, University of Canterbury, Christchurch, New Zealand.

Hamilton, R.J., Luyendyk, B.P., Sorlien, C.C. and Bartek, L.R., 2001. Cenozoic tectonics of the Cape Roberts rift basin and Transantarctic Mountain front, southwestern Ross Sea, Antarctica. *Tectonics*, 20: 325-342.

Henderson, R.A., 1986. Geology of the Mount Windsor subprovince - a lower Paleozoic volcano-sedimentary terrane in the northern Tasman orogenic zone. *Australian Journal of Earth Sciences*, 33: 343-364.

Hensel, H.D., McCulloch, M.T. and Chappell, B.W., 1985. The New England Batholith: constraints on its derivation from Nd and Sr isotopic studies of granitoids and country rocks. *Geochimica et Cosmochimica Acta*, 49(2): 369-384.

Hergt, J.M., Chappell, B.W., McCulloch, M.T., McDougall, I. and Chivas, A.R., 1989. Geochemical and isotopic constraints on the origin of the Jurassic dolerites of Tasmania. *Journal of Petrology*, 30(4): 841-883.

Hibbard, M.J., 1995. *Petrography to Petrogenesis*. Prentice Hall, Englewood Cliffs, New Jersey, 573 pp.

Hicks, D.M., 1981. Deep-sea fan sediments in the Torlesse zone, Lake Ohau, South Canterbury, New Zealand. *New Zealand Journal of Geology & Geophysics*, 24: 209-220.

Hitching, K.D., 1979. Torlesse geology of Kakahu, South Canterbury. *New Zealand Journal of Geology & Geophysics*, 22(2): 191-197.

Holdsworth, B.K. and Nell, P.A.R., 1992. Mesozoic radiolarian faunas from the Antarctic Peninsula: age, tectonic and paleo-oceanographic significance. *Journal of the Geological Society, London*, 149(Part 6): 1003-1020.

Hollis, J.A., Clark, G.L., Klepeis, K.A., Daczko, N.R. and Ireland, T.R., 2002. Geochronology and geochemistry of the Arthur River Complex, Fiordland, New Zealand: Cretaceous magmatism and metamorphism on the Paleo-Pacific margin. *Journal of Metamorphic Geology*, in press.

Howell, D.G., 1980. Mesozoic accretion of exotic terranes along the New Zealand segment of Gondwanaland. *Geology*, 8(10): 487-491.

Hurley, P.M., Hughes, H., Pinson, W.H. and Fairbairn, H.W., 1962. Radiogenic aragon and strontium diffusion parameters in biotite at low temperatures obtained from Alpine Fault uplift in New Zealand. *Geochimica et Cosmochimica Acta*, 26: 76-80.

Hutton, L.J., Draper, J.J., Rienks, I.P., Withnall, I.W. and Knutson, J., 1997. Charters Towers Region. In: J.H.C. Bain and J.J. Draper (Editors), *North Queensland Geology, AGSO Bulletin 240, Queensland Geology 9*. Australian Geological Survey Organisation, Canberra, Australia, pp. 599.

Ingersoll, R.V. and Suczek, C.A., 1979. Petrology and provenance of Neogene sand from Nicobar and Bengal Fans, DSDP sites 211 and 218. *Journal of Sedimentary Petrology*, 49: 1217-1228.

Ireland, T.R., 1992. Crustal evolution of New Zealand: Evidence from age distributions of detrital zircons in Western Province paragneisses and Torlesse greywacke. *Geochimica et Cosmochimica Acta*, 56: 911-920.

Ireland, T.R., Floettmann, T., Fanning, C.M., Gibson, G.M. and Preiss, W.V., 1998. Development of the early Paleozoic Pacific margin of Gondwana from detrital-zircon ages across the Delamerian Orogen. *Geology*, 26(3): 243-246.

Isaac, M.J., Herzer, R.H., Brook, F.J. and Hayward, B.W., 1994. *Cretaceous and Cenozoic sedimentary basins of Northland, New Zealand.* Institute of Geological and Nuclear Sciences, Monograph 8. Institute of Geological and Nuclear Sciences Ltd., Lower Hutt, New Zealand, 204 pp.

Ito, M., Yoshiaki, A. and Shigeki, H., 2000. New radiolarian age information for the Chrystalls Beach Complex, southwest of Dunedin, New Zealand. *New Zealand Journal of Geology & Geophysics*, 43: 349-354.

Jacobsen, S.B. and Wasserburg, G.J., 1979. The mean age of mantle and crustal reservoirs. *Journal of Geophysical Research, B, Solid Earth and Planets*, 84(B13): 7411-7429.

Jenkins, D.G. and Jenkins, T.B.H., 1971. First diagnostic Carboniferous fossils from New Zealand. *Nature*, 233: 117-118.

Jones, P.J., 1995. *AGSO Phanerozoic Timescale: Wallchart and explanatory notes.* Oxford University Press, Melbourne, Australia, 32 pp.

Jongens, R., 1997. The Anatoki Fault and structure of the adjacent Buller and Takaka terrane rocks, Northwest Nelson, New Zealand. Unpublished Ph.D. Thesis, University of Canterbury, Christchurch, New Zealand, 384 pp.

Kamp, P.J., 1999. Tracking crustal processes by FT thermochronology in a forearc high (Hikurangi margin, New Zealand) involving Cretaceous subduction termination and mid-Cenozoic subduction initiation. *Tectonophysics*, 307(3-4): 313-343.

Kamp, P.J., 2001. Jurassic age for part of the Rakaia Terrane in Canterbury: Implications for development of the Torlesse accretionary prism. *New Zealand Journal of Geology & Geophysics*, 44: 185-203.

Kear, D., 2001. *The Waipa supergroup - a North Island contribution to the terrane debate*. Kear, D., Whakatane, New Zealand, 14 pp.

Kent, A.J.R., 1994. Geochronology and geochemistry of Palaeozoic intrusive rocks in the Rockvale region, southern New England Orogen, New South Wales. *Australian Journal of Earth Sciences*, 41(4): 365-379.

Kimbrough, D.L. and Tulloch, A.J., 1989. Early Cretaceous age of orthogneiss from the Charleston Metamorphic Group, New Zealand. *Earth and Planetary Science Letters*, 95(1-2): 130-140.

Kimbrough, D.L., Mattinson, J.M., Coombs, D.S., Landis, C.A. and Johnston, M.R., 1992. Uranium-lead ages from the Dun Mountain ophiolite belt and Brook Street Terrane, South Island, New Zealand. *Geological Society of America Bulletin*, 104(4): 429-443.

Kimbrough, D.L., Tulloch, A.J., Geary, E., Coombs, D.S. and Landis, C.A., 1993. Isotopic ages from the Nelson region of South Island, New Zealand: crustal structure and definition of the Median Tectonic Zone. *Tectonophysics*, 225(4): 433-448.

Kimbrough, D.L., Tulloch, A.J., Coombs, D.S., Landis, C.A., Johnston, M.R. and Mattinson, J.M., 1994a. Uranium-lead zircon ages from the Median Tectonic Zone, South Island, New Zealand. *New Zealand Journal of Geology & Geophysics*, 37(4): 393-419.

Kimbrough, D.L., Tulloch, A.J. and Rattenbury, M.S., 1994b. Late Jurassic-Early Cretaceous metamorphic age of Fraser Complex migmatite, Westland, New Zealand. *New Zealand Journal of Geology & Geophysics*, 37(2): 137-142.

Kodama, Y., 1994a. Downstream changes in the lithology and grain size of fluvial gravels, the Watarase River, Japan: Evidence of the role of abrasion in downstream fining. *Journal of Sedimentary Research*, A64: 68-75.

Kodama, Y., 1994b. Experimental study of abrasion and its role in producing downstream fining in gravel-bed rivers. *Journal of Sedimentary Research*, A64: 76-85.

Korsch, R.J. and Wellman, H.W., 1988. The geological evolution of New Zealand and the New Zealand region. In: A.E.M. Nairn *et al.* (Editors), *The Oceanic Basins and Margins Volume 7B: The Pacific Ocean*. Plenum Press, New York, pp. 411-482.

Kreuzer, H., Hoehndorf, A., Vetter, U., Tessensohn, F., Mueller, P., Jordan, H., Harre, W. and Besang, C., 1981. K/ Ar and Rb/ Sr dating of igneous rocks from North Victoria Land, Antarctica. *Geologisches Jahrbuch. Reihe B: Regionale Geologie Ausland*, 41: 267-273.

Kroonenburg, S.B., 1994. Effect of provenance, sorting and weathering on the geochemistry of fluvial sand from different tectonic and climatic environments. *Proceedings of the 29th International Geological Congress*, Part A: 69-81.

Krull, E.S., Retallack, G.J., Campbell, H.J. and Lyon, G.L., 2000. Delta C-13(org) chemostratigraphy of the Permian-Triassic boundary in the Maitai Group, New Zealand: Evidence for high-latitudinal methane release. *New Zealand Journal of Geology & Geophysics*, 43(1): 21-32.

Kuno, H., 1968. Differentiation of basalt magmas. In: H.H. Hess and A. Poldevaart (Editors), *Basalts: The Poldervaart treatise on rocks of basaltic composition, Vol. 2*. Interscience, New York, pp. 623-688.

Laird, M.G., Andrews, P.B. and Kyle, P.R., 1974. Geology of the Northern Evans Névé, Victoria Land, Antarctica. *New Zealand Journal of Geology & Geophysics*, 17: 587-601.

Laird, M.G., Bradshaw, J.D. and Wodzicki, A., 1976. Re-examination of the Bowers Group (Cambrian), northern Victoria Land, Antarctica. *New Zealand Journal of Geology & Geophysics*, 19(2): 275-282.

Landis, C.A. and Coombs, D.S., 1967. Metamorphic belts and orogenesis in southern New Zealand. *Tectonophysics*, 4(4-6): 501-518.

Landis, C.A. and Bishop, D.G., 1972. Plate tectonics and regional stratigraphic-metamorphic relations in the southern part of the New Zealand geosyncline. *Geological Society of America Bulletin*, 83(8): 2267-2284.

Landis, C.A., Campbell, H.J., Aslund, T., Cawood, P.A., Douglas, A., Kimbrough, D.L., Pillai, D.D.L., Raine, J.I. and Willsman, A., 1999. Permian-Jurassic strata at Productus Creek, Southland, New Zealand: implications for terrane dynamics of the eastern Gondwanaland margin. *New Zealand Journal of Geology & Geophysics*, 42(2): 255-278.

Lauder, W.R., 1962. Teschenites from Acheron River, mid-Canterbury, New Zealand, with notes on the geology of the surrounding country. *Transactions of the Royal Society of New Zealand, Geology*, 1(7): 109-127.

Lawver, L.A. and Gahagan, L.M., 1994. Constraints on timing of extension in the Ross Sea region. *Terra Antarctica*, 1(3): 545-552.

Le Maitre, R.W., 1976. The chemical variability of some common igneous rocks. *Journal of Petrology*, 17: 589-637.

Le Maitre, R.W., Bateman, P., Dudek, A., Keller, J., Lamayre, J., Lebas, M.J., Sabine, P.A., Schmid, R., Sorenson, H., Streckeisen, A., WoolleyA.R. and Zanettin, B., 1989. *A classification of igneous rocks and glossary of terms, recommendations of the IUGS subcommission on the systematics of igneous rocks*. Blackwell Scientific Publications, Oxford, 193 pp.

Leat, P.T., Storey, B.C. and Pankhurst, R.J., 1993. Geochemistry of Paleozoic-Mesozoic Pacific rim orogenic magmatism, Thurston Island area, West Antarctica. *Antarctic Science*, 5(3): 281-296.

Leven, E.J. and Campbell, H.J., 1998. Middle Permian (Murgabian) fusuline faunas, Torlesse terrane, New Zealand. *New Zealand Journal of Geology & Geophysics*, 41(2): 149-156.

Lewis, D.W. and McConchie, D., 1994. *Analytical sedimentology*. Chapman & Hall, New York, USA, 179 pp.

Lewis, K., 1999. Distal turbidity currents that flow through a powerful abyssal current: The Hikurangi Channel 2000 Km from Kaikoura. *Geological Society of New Zealand Miscellaneous Publication*, 107A: 87.

Little, T.A., Holcombe, R.J., Gibson, G.M., Offler, R., Gans, P.B. and McWilliams, M.O., 1992. Exhumation of late Paleozoic blueschists in Queensland, Australia, by extensional faulting. *Geology*, 20: 231-234.

Little, T.A., Mortimer, N. and McWilliams, M., 1999. An episodic Cretaceous cooling model for the Otago-Marlborough Schist, New Zealand, based on Ar-40/Ar-39 white mica ages. *New Zealand Journal of Geology & Geophysics*, 42(3): 305-325.

Luyendyk, B., Cisowski, S., Smith, C., Richard, S. and Kimbrough, D., 1996. Paleomagnetic study of the northern Ford Ranges, Western Marie Byrd Land, West Antarctica: motion between West and East Antarctica. *Tectonics*, 15(1): 122-141.

Luyendyk, B.P., 1995. Hypothesis for Cretaceous rifting of east Gondwana caused by subducted slab capture. *Geology*, 23: 373-376.

Maas, R. and McCulloch, M.T., 1991. The provenance of Archean clastic sediments in the Narryer Gneiss Complex, Western Australia: Trace element geochemistry, Nd isotopes, and U-Pb ages from detrital zircons. *Geochimica et Cosmochimica Acta*, 55: 1915-1932.

MacKinnon, T., 1983. Origin of the Torlesse terrane and coeval rocks, South Island, New Zealand. *Geological Society of America Bulletin*, 94: 967-985.

MacKinnon, T.C., 1980a. Geology of Monotis-bearing Torlesse rocks in Temple Basin near Arthur's Pass, South Island, New Zealand. *New Zealand Journal of Geology & Geophysics*, 23(1): 63-81.

MacKinnon, T.C., 1980b. Sedimentologic, petrographic, and tectonic aspects of Torlesse and related rocks. Unpublished Ph.D. Thesis, University of Otago, Dunedin, New Zealand.

Mainprice, D., Bouchez, J., Blumenfeld, P. and Tubia, J.M., 1986. Dominant c-slip in naturally deformed quartz: Implications for dramatic plastic softening at high temperature. *Geology*, 14: 819-822.

Malloch, K.R., 1999. The petrography and geochemistry of the Carboniferous A-Type granites, Western Province, New Zealand. Unpublished M.Sc. Thesis, University of Canterbury, Christchurch, New Zealand, 201 pp.

Mattinson, J.M., Kimbrough, D.L. and Bradshaw, J.Y., 1986. Western Fiordland Orthogneiss; Early Cretaceous arc magmatism and granulite facies metamorphism, New Zealand. *Contributions to Mineralogy and Petrology*, 92(3): 383-392.

Maxwell, P.A., 1964. Structural geology and pre-Quaternary stratigraphy of the Kaiwara District, North Canterbury, New Zealand. Unpublished M.Sc. Thesis, University of Canterbury, Christchurch, New Zealand.

Mayes, C.L., Lawver, L.A. and Sandwell, D.T., 1990. Tectonic history and new isochron chart of the South Pacific. *Journal of Geophysical Research, B, Solid Earth and Planets*, 95(6): 8543-8567.

McClenaghan, M.P., 1984. Granitoids of northeastern Tasmania. *Journal of Australian Geology & Geophysics*, 9: 303-312.

McCulloch, M.T. and Chappell, B.W., 1982. Nd isotopic characteristics of S- and I-type granites. *Earth and Planetary Science Letters*, 58(1): 51-64.

McDonough, W.F., Sun, S.S., Ringwood, A.E., Jagoutz, E. and Hofmann, A.W., 1992. Potassium, rubidium, and cesium in the Earth and Moon and the evolution of the mantle of the Earth. In: M.S. McLennan and R. Rudnick (Editors), *The Taylor Colloquium: Origin and evolution of planetary crusts.* Pergamon, Oxford, pp. 1001-1012.

McDougall, I. and Leggo, P.G., 1965. Isotopic age determinations of granitic rocks from Tasmania. *Journal of the Geological Society of Australia*, 12: 295-332.

McLennan, S.M., Taylor, S.R., McCulloch, M.T. and Maynard, J.B., 1990. Geochemical and Nd-Sr isotopic composition of deep-sea turbidites: crustal

evolution and plate tectonic associations. *Geochimica et Cosmochimica Acta*, 54(7): 2015-2050.

McLennan, S.M. and Hemming, S., 1992. Samarium/neodymium elemental and isotopic systematics in sedimentary rocks. *Geochimica et Cosmochimica Acta*, 56: 887-898.

McLennan, S.M., Hemming, S., McDaniel, D.K. and Hanson, G.N., 1993. Geochemical approaches to sedimentation, provenance, and tectonics. In: M.J. Johnsson and A. Basu (Editors), *Processes controlling the composition of clastic sediments.* Special Paper - Geological Society of America. Geological Society of America (GSA), Boulder, CO, United States, pp. 21-40.

Mildenhall, D.C., 1977. Cretaceous palynomorphs from the Waihere Bay Group and Kahuiatara Tuff, Chatham Island, New Zealand. *New Zealand Journal of Geology & Geophysics*, 20: 655-672.

Millar, I.L., Willan, R.C.R., Wareham, C.D. and Boyce, A.J., 2001. The role of crustal and mantle sources in the genesis of granitoids of the Antarctic Peninsula and adjacent crustal blocks. *Journal of the Geological Society, London*, 158(5): 855-867.

Moore, G.F., Curray, J.R. and Emmel, F.J., 1982a. Sedimentation in the Sunda Trench and forearc region. In: J.K. Leggett (Editor), *Trench-forearc Geology: Sedimentation and tectonics on modern and ancient active plate margins*. Geological Society of London Special Publication 10, pp. 245-258.

Moore, G.W., Drummond, K.J., Chikao, N., Corvalan, J., Doutch, H.F. and Cradock, C., 1982b. *Plate-tectonic map of the circum-Pacific region.* Circum-Pacific Map Project. The American Association of Petroleum Geologists, Tulsa, Oklahoma 74101, U.S.A.

Mortimer, N. and Roser, B.P., 1992. Geochemical evidence for the position of the Caples-Torlesse boundary in the Otago Schist, New Zealand. *Journal of the Geological Society, London*, 149 Part 6: 967-977.

Mortimer, N., 1993. Jurassic tectonic history of the Otago Schist, New Zealand. *Tectonics*, 12(1): 237-244.

Mortimer, N., 1995. Origin of the Torlesse terrane and coeval rocks, North Island, New Zealand. *International Geology Review*, 36: 891-921.

Mortimer, N., Parkinson, D., Raine, J.I., Adams, C.J., Graham, I.J., Oliver, P.J. and Palmer, K., 1995. Ferrar magmatic province rocks discovered in New Zealand: implications for Mesozoic Gondwana geology. *Geology*, 23(2): 185-188.

Mortimer, N. and Parkinson, D., 1996. Hikurangi Plateau - a Cretaceous large igneous province in the Southwest Pacific Ocean. *Journal of Geophysical Research,, B, Solid Earth and Planets*, 101(B1): 687-696.

Mortimer, N. and Smale, D., 1996. Petrology of the Topfer Formation: first Triassic Gondwana sequence from New Zealand. *Australian Journal of Earth Sciences*, 43(4): 467-477.

Mortimer, N., Tulloch, A.J. and Ireland, T.R., 1997. Basement geology of Taranaki and Wanganui Basins, New Zealand. *New Zealand Journal of Geology & Geophysics*, 40(2): 223-236.

Mortimer, N., Herzer, R.H., Gans, P.B., Parkinson, D.L. and Seward, D., 1998. Basement Geology from Three Kings Ridge to West Norfolk Ridge, Southwest Pacific Ocean - Evidence from petrology, geochemistry and isotopic dating of dredge samples. *Marine Geology*, 148(3-4): 135-162.

Mortimer, N., Gans, P., Calvert, A. and Walker, N., 1999a. Geology and thermochronometry of the east edge of the Median Batholith (Median Tectonic Zone): a new perspective on Permian to Cretaceous crustal growth of New Zealand. *Island Arc*, 8(3): 404-425.

Mortimer, N., Tulloch, A.J., Spark, R.N., Walker, N.W., Ladley, E., Allibone, A. and Kimbrough, D.L., 1999b. Overview of the Median Batholith, New Zealand: a new interpretation of the geology of the Median Tectonic Zone and adjacent rocks. *Journal of African Earth Sciences*, 29(1): 257-268.

Muir, R.J., Ireland, T.R., Weaver, S.D. and Bradshaw, J.D., 1994. Ion microprobe U-Pb zircon geochronology of granitic magmatism in the Western Province of the South Island, New Zealand. *Chemical Geology*, 113(1-2): 171-189.

Muir, R.J., Weaver, S.D., Bradshaw, J.D., Eby, G.N. and Evans, J.A., 1995. The Cretaceous Separation Point Batholith, New Zealand: granitoid magmas formed by melting of mafic lithosphere. *Journal of the Geological Society, London*, 152 Part 4: 689-701.

Muir, R.J., Ireland, T.R., Weaver, S.D. and Bradshaw, J.D., 1996a. Ion microprobe dating of Paleozoic granitoids: Devonian magmatism in New Zealand and correlations with Australia and Antarctica. *Chemical Geology*, 127(1-3): 191-210.

Muir, R.J., Weaver, S.D., Bradshaw, J.D., Eby, G.N., Evans, J.A. and Ireland, T.R., 1996b. Geochemistry of the Karamea Batholith, New Zealand and comparisons with the Lachlan Fold Belt granites of southeast Australia. *Lithos*, 39(1-2): 1-20.

Muir, R.J., Ireland, T.R., Weaver, S.D., Bradshaw, J.D., Waight, T.E., Jongens, R. and Eby, G.N., 1997. SHRIMP U-Pb geochronology of Cretaceous magmatism in northwest Nelson-Westland, South Island, New Zealand. *New Zealand Journal of Geology & Geophysics*, 40: 453-463.

Muir, R.J., Ireland, T.R., Weaver, S.D., Bradshaw, J.D., Evans, J.A., Eby, G.N. and Shelley, D., 1998. Geochronology and geochemistry of a Mesozoic magmatic arc system, Fiordland, New Zealand. *Journal of the Geological Society, London*, 155(Part 6): 1037-1052.

Mukasa, S.B. and Dalziel, I.W.D., 2000. Marie Byrd Land, West Antarctica: Evolution of Gondwana's Pacific margin constrained by zircon U-Pb geochronology and feldspar common-Pb isotopic compositions. *Geological Society of America Bulletin*, 112: 611-627.

Münker, C. and Cooper, R.A., 1995. The island arc setting of a New Zealand Cambrian volcano-sedimentary sequence - implications for the evolution of the SW Pacific Gondwana fragments. *Journal of Geology*, 103(6): 687-700.

Münker, C. and Cooper, R.A., 1997. The early Paleozoic Takaka Terrane, New Zealand, as part of the Australian/Antarctic Gondwana margin: New insights from the trace element and isotope geochemistry of Cambrian volcanics. In: J.D. Bradshaw and S.D. Weaver (Editors), *Terrane Dynamics 97, International Conference on Terrane Geology*, Christchurch, New Zealand, pp. 124-127.

Münker, C. and Cooper, R., 1999. The Cambrian arc complex of the Takaka Terrane, New Zealand: an integrated stratigraphical, paleontological and geochemical approach. *New Zealand Journal of Geology & Geophysics*, 42(3): 415-445.

Münker, C., 2000. The isotope and trace element budget of the Cambrian Devil River arc system, New Zealand: Identification of four source components. *Journal of Petrology*, 41(6): 759-788.

Nakamura, N., 1974. Determination of REE, Ba, Fe, Mg, Na, and K in carbonaceous and ordinary meteorites. *Geochimica et Cosmochimica Acta*, 38: 757-775.

Nesbitt, H.W. and Young, G.M., 1982. Early Proterozoic climates and plate motions inferred from major element chemistry of lutites. *Nature (London)*, 299(5885): 715-717.

Nesbitt, H.W. and Young, G.M., 1984. Prediction of some weathering trends of plutonic and volcanic rocks based on thermodynamic and kinetic considerations. *Geochimica et Cosmochimica Acta*, 48(7): 1523-1534.

Orlowski, R.J., 2001. A sedimentological profile of the Pahau terrane type locality. Unpublished M.Sc. Thesis, University of Canterbury, Christchurch, New Zealand, 302 pp.

Palais, D.G., Mukasa, S.B. and Weaver, S.D., 1993. U-Pb and $^{40}Ar/^{39}Ar$ geochronology for plutons along the Ruppert and Hobbs coasts, Marie Byrd Land, West Antarctica: evidence for rapid transition from arc to rift related magmatism. *Abstract of the American Geophysical Union, Spring Meeting*: 123.

Pankhurst, R.J., Millar, I.L., Grunow, A.M. and Storey, B.C., 1993. The pre-Cenozoic magmatic history of the Thurston Island crustal block, West Antarctica. *Journal of Geophysical Research, B, Solid Earth and Planets*, 98(7): 11,835-11,849.

Pankhurst, R.J., Leat, P.T., Sruoga, P., Rapela, C.W., Marquez, M., Storey, B.C. and Riley, T.R., 1998a. The Chon Aike province of Patagonia and related rocks in West Antarctica: a silicic large igneous province. *Journal of Volcanology and Geothermal Research*, 81(1-2): 113-136.

Pankhurst, R.J., Weaver, S.D., Bradshaw, J.D., Storey, B.C. and Ireland, T.R., 1998b. Geochronology and geochemistry of pre-Jurassic superterranes in Marie Byrd Land, Antarctica. *Journal of Geophysical Research, B, Solid Earth and Planets*, 103(B2): 2529-2547.

Pankhurst, R.J., Riley, T.R., Fanning, C.M. and Kelley, S.P., 2000. Episodic silicic volcanism in Patagonia and the Antarctic Peninsula: chronology of magmatism associated with the break-up of Gondwana. *Journal of Petrology*, 41(5): 605-625.

Paterson, O.D., 1941. The geology of the lower Shag Valley. *Transactions of the Royal Society of New Zealand*, 71: 32-58.

Pearce, J.A., Harris, N.B.W. and Tindle, A.G., 1984. Trace element discrimination diagrams for the tectonic interpretation of granitic rocks. *Journal of Petrology*, 25: 956-983.

Peccerillo, A. and Taylor, S.R., 1976. Geochemistry of Eocene calc-alkaline volcanic rocks from the Kastamonu area, northern Turkey. *Contributions to Mineralogy and Petrology*, 58(1): 63-81.

Pell, S.D., Williams, I.S. and Chivas, A.R., 1997. The use of protolith zircon-age fingerprints in determining the protosource areas for some Australian dune sands. *Sedimentary Geology*, 109: 233-260.

Pescini, H.S., 1997. Structure and depositional setting of the Pahau subterrane rocks, Pahau River / Mount Saul Area. Unpublished B.Sc. (Hons) Thesis, University of Canterbury, New Zealand, 87 pp.

Pettijohn, F.J., Potter, P.E. and Siever, R., 1987. *Sand and sandstone*. Springer-Verlag, New York, 553 pp.

Pickard, A.L., Adams, C.J. and Barley, M.E., 2000. Provenance of New Zealand Late Permian to Cretaceous depocentres at the Australian margin of Gondwanaland: evidence from detrital zircon SHRIMP dating. *Australian Journal of Earth Sciences*, 47: 987-1007.

Pickett, D.A. and Wasserburg, G.J., 1989. Neodymium and strontium isotopic characteristics of New Zealand granitoids and related rocks. *Contributions to Mineralogy and Petrology*, 103(2): 131-142.

Powell, C.M. and Li, Z.X., 1994. Reconstruction of the Panthalassan margin of Gondwanaland. In: J. Veevers and M. Powell (Editors), *Permian-Triassic Pangean basins and foldbelts along the Panthalassan margin of Gondwanaland.* Memoir - Geological Society of America. Geological Society of America (GSA), Boulder, CO, United States, pp. 5-9.

Prebble, W.M., 1976. The Geology of the Kekerengu - Waima River district, north-east Marlborough. Unpublished M.Sc. Thesis, Victoria University, Wellington, New Zealand, 123 pp.

Pupin, J.P., 1980. Zircon and granite petrology. *Contributions to Mineralogy and Petrology*, 73: 207-220.

Raine, J.I., Strong, C.P. and Wilson, G.J., 1993. *Biostratigraphic revision of petroleum exploration wells, Great South Basin, New Zealand.* Institute of Geological and Nuclear Sciences, Science Report 93/32, 146 pp.

Reed, J.J., 1957. *The petrology of the lower Mesozoic rocks of the Wellington district.* New Zealand Geological Society Bulletin, 57, 60 pp.

Richard, S.M., Smith, C.H., Kimbrough, D.L., Fitzgerald, P.G., Luyendyk, B.P. and McWilliams, M.O., 1994. Cooling history of the northern Ford Ranges, Marie Byrd Land, West Antarctica. *Tectonics*, 13(4): 837-857.

Richards, J.R. and Singleton, O.P., 1981. Paleozoic Victoria, Australia: Igneous rocks, ages and their interpretation. *Journal of the Geological Society of Australia*, 28: 395-421.

Riley, T.R., Leat, P.T., Pankhurst, R.J. and Harris, C., 2001. Origins of large volume rhyolitic volcanism in the Antarctic Peninsula and Patagonia by crustal melting. *Journal of Petrology*, 42(6): 1043-1065.

Ritchie, D.D., 1986. Stratigraphy, structure and geological history of Mid-Cretaceous sedimentary rocks across the Torlesse-like/non Torlesse boundary in the Sawtooth Range - Coverham area, Marlborough. Unpublished M.Sc. Thesis, University of Canterbury, Christchurch, New Zealand, 173 pp.

Rollinson, H.R., 1993. *Using Geochemical Data: Evaluation, presentation, interpretation.* Longman Scientific & Technical, Harlow, Essex, England, 352 pp.

Roser, B.P. and Korsch, R.J., 1986. Determination of tectonic setting of sandstone-mudstone suites using SiO_2 content and K_2O/Na_20 ratio. *The Journal of Geology*, 94(September): 635-650.

Roser, B.P. and Korsch, R.J., 1988. Provenance signatures of sandstone-mudstone suites determined using discriminant function analysis of major-element data. *Chemical Geology*, 67: 119-139.

Roser, B.P. and Cooper, A.F., 1990. Geochemistry and terrane affiliation of Haast Schist from the western Southern Alps, New Zealand. *New Zealand Journal of Geology & Geophysics*, 33: 1-10.

Roser, B.P., Grapes, R.H. and Palmer, K., 1993a. *Petrofacies and subterrane affiliation of Torlesse sediments, Southern North Island, New Zealand.* Geological Society of New Zealand miscellaneous publication, 79A, 130 pp.

Roser, B.P., Mortimer, N., Turnbull, I.M. and Landis, C.A., 1993b. Geology and geochemistry of the Caples Terrane, Otago, New Zealand: Compositional variations near a Permo-Triassic arc margin. In: P.F. Ballance (Editor), *South Pacific sedimentary basins. Sedimentary Basins of the World, 2.* Elsevier Science Publishers B.V., Amsterdam, pp. 3-19.

Roser, B.P., Grapes, R.H. and Palmer, K., 1995. *XRF analyses of sandstones and argillites from the Torlesse terrane, New Zealand.* Geology Board of Studies Publication, 15. Victoria University of Wellington, Geology Board of Studies, Wellington, New Zealand, 40 pp.

Roser, B.P., Cooper, R.A., Nathan, S. and Tulloch, A.J., 1996. Reconnaissance sandstone geochemistry, provenance, and tectonic setting of the lower Paleozoic

terranes of the West Coast and Nelson, New Zealand. *New Zealand Journal of Geology & Geophysics*, 39(1): 1-16.

Roser, B.P. and Korsch, R.J., 1999. Geochemical characterization, evolution and source of a Mesozoic accretionary wedge: the Torlesse terrane, New Zealand. *Geological Magazine*, 136(5): 493-512.

Sambridge, M.S. and Compston, W., 1994. Mixture modelling of multi-component data sets with application to ion-probe zircon ages. *Earth & Planetary Science Letters*, 128: 373-390.

Saunders, A.D., Norry, M.J. and Tarney, J., 1991. Fluid influence on the trace element compositions of subduction zone magmas. *Philosophical transactions of the Royal Society of London*, 335: 377-392.

Sawka, W.N., Heizler, M.T., Kistler, R.W. and Chappell, B.W., 1990. Geochemistry of highly fractionated I- and S-type granites from the tin-tungsten province of western Tasmania. *Geological Society of America: Special paper*, 246: 161-179.

Scheibner, E. and Veevers, J.J., 2000. Tasman Fold Belt System. In: J.J. Veevers (Editor), *Billion-year earth history of Australia and neighbours in Gondwanaland.* GEMOG Press, Department of Earth and Planetary Sciences, Macquarie University, Macquarie, pp. 154-234.

Schmidt, P.W. and Clark, D.A., 2000. Paleomagnetism, apparent polar-wander path & paleolatitude. In: J.J. Veevers (Editor), *Billion-year earth history of Australia and neighbours in Gondwanaland.* GEMOG Press, Department of Earth and Planetary Sciences, Macquarie University, Macquarie, pp. 12-17.

Shaw, S.E. and Flood, R.H., 1981. The New England Batholith, eastern Australia: geochemical variations in time and space, *Granites and rhyolites.* American Geophysical Union, Washington, DC, United States, pp. 10530-10544.

Shaw, S.E. and Flood, R.H., 1993. Carboniferous magmatic activity in the Lachlan and New England Fold Belts. In: R.H. Flood and J.C. Aitchison (Editors), *New England Orogen, Eastern Australia.* Department of Geology and Geophysics, University of New England, Armidale, Australia, pp. 113-121.

Shaw, S.E., 1994. Age of granitoids. In: J.J. Veevers and C. Powell (Editors), *Permian-Triassic Pangean basins and foldbelts along the Panthalassan margin of Gondwanaland.* Memoir - Geological Society of America. Geological Society of America (GSA), Boulder, CO, United States, pp. 11-171.

Shelley, D., 1985. *Optical mineralogy.* Elsevier Science Publishing Co. Inc., New York, 321 pp.

Shelley, D., 1992. *Igneous and metamorphic rocks under the microscope.* Chapman and Hall, London, 445 pp.

Shi, G.R. and Grunt, T.A., 2000. Permian Gondwana-boreal antitropicality with special reference to brachiopod faunas. *Palaeogeography, Palaeoclimatology, Palaeoecology*, 155(3-4): 239-263.

Silberling, N.J., Nichols, K.M., Bradshaw, J.D. and Blome, C.D., 1988. Limestone and chert in tectonic blocks from the Esk Head subterrane, South Island, New Zealand. *Geological Society of America Bulletin*, 100: 1213-1223.

Sircombe, K.N., 1999. Tracing provenance through the isotope ages of littoral and sedimentary detrital zircons, Eastern Australia. *Sedimentary Geology*, 124: 47-67.

Sivell, W.J. and Rankin, P.C., 1983. Arc-tholeiite and ultramafic cummulate, Brook Street Volcanics, west of D'Uurville Island, New Zealand. *New Zealand Journal of Geology & Geophysics*, 26(3): 239-257.

Sivell, W.J. and McCulloch, M.T., 2000. Reassessment of the origin of the Dun Mountain Ophiolite, New Zealand: Nd-isotopic and geochemical evolution of magma suites. *New Zealand Journal of Geology & Geophysics*, 43(2): 133-146.

Sivell, W.J. and McCulloch, M.T., 2001. Geochemical and Nd-isotopic systematics of the Permo-Triassic Gympie Group, southeastern Queensland. *Australian Journal of Earth Sciences*, 48: 377-393.

Smale, D., 1978. The composition of a Torlesse conglomerate: Ethelton, North Canterbury. *New Zealand Journal of Geology & Geophysics*, 21(6): 699-711.

Smale, D., 1980a. Akatarawa Conglomerate (Permian), Lake Aviemore, South Canterbury. *New Zealand Journal of Geology & Geophysics*, 23(3): 279-292.

Smale, D., 1980b. Phosphorite intraclasts in Torlesse sandstones and conglomerates, South Canterbury (Note). *New Zealand Journal of Geology & Geophysics*, 23(5-6): 273-276.

Smale, D., 1983. The Te Moana Conglomerate (Torlesse), Four Peaks Range, South Canterbury. *New Zealand Journal of Geology & Geophysics*, 26(3): 259-270.

Smale, D., 1997. Heavy minerals in the Torlesse terrane of the Wellington area, New Zealand. *New Zealand Journal of Geology & Geophysics*, 40(4): 499-506.

Speden, I.G., 1974. *Additional fossil localities of the Torlesse rocks of the South Island (including summations of faunal assemblages and lithological information)*. New Zealand Geological Survey Report 69, Lower Hutt, New Zealand, 37 pp.

Speden, I.G., 1976. Fossil localities in Torlesse rocks of the North Island, New Zealand. *Journal of the Royal Society of New Zealand*, 6(1): 73-91.

Speight, R. and Finlayson, A.M., 1909. Physiography and geology of the Auckland, Bounty and Antipodes islands. In: C. Chilton (Editor), *The subantarctic islands of New Zealand; Vol. II.* New Zealand Government Printer, Wellington, New Zealand, pp. 705-744.

Spell, T.L., McDougall, I. and Tulloch, A.J., 2000. Thermochronologic constraints on the breakup of the Pacific Gondwana margin: The Paparoa metamorphic core complex, South Island, New Zealand. *Tectonics*, 19(3): 433-451.

Sporli, K.B., 1978. Mesozoic tectonics, North Island, New Zealand. *Geological Society of America Bulletin*, 89: 415-425.

Steiger, R.H. and Jäger, E., 1977. Subcommission on geochronology: Convention on the use of decay constants in geo- and cosmochronology. *Earth & Planetary Science Letters*, 36: 359-362.

Stevens, G.R., 1978. Paleontology. In: R.P. Suggate *et al.* (Editors), *The geology of New Zealand; Carboniferous-Jurassic; the era of the New Zealand Geosyncline; Torlesse Supergroup.* N.Z. Geol. Surv., Lower Hutt., New Zealand, pp. 255-262.

Storey, B.C., Hole, M.J., Pankhurst, R.J., Miller, I.L. and Vennum, W., 1988. Middle Jurassic within-plate granites in West Antarctica and their bearing on the break-up of Gondwanaland. *Journal of the Geological Society, London*, 145 Part 6: 999-1007.

Storey, B.C. and Kyle, P.R., 1997. An active mantle mechanism for Gondwana breakup. *South African Journal of Geology*, 100(4): 283-290.

Storey, B.C., Leat, P.T., Weaver, S.D., Pankhurst, R.J., Bradshaw, J.D. and Kelley, S., 1999. Mantle plumes and Antarctica-New Zealand rifting; evidence from Mid-Cretaceous mafic dykes. *Journal of the Geological Society, London*, 156(Part 4): 659-671.

Stump, E., White, A.J.R. and Borg, S.G., 1986. Reconstruction of Australia and Antarctica: evidence from granites and recent mapping. *Earth and Planetary Science Letters*, 79(3-4): 348-360.

Stump, E., 1995. *The Ross Orogen of the Transantarctic Mountains.* Cambridge University Press, Cambridge, 284 pp.

Sutherland, R., 1999. Basement geology and tectonic development of the greater New Zealand region: An interpretation from regional magnetic data. *Tectonophysics*, 308(3): 341-362.

Taylor, S.R., 1965. The application of trace-element data to problems in petrology. In: L.H. Ahrens *et al.* (Editors), *Physics and chemistry of the Earth.* Pergamon, Oxford, pp. 133-313.

Taylor, S.R., 1969. Trace element chemistry of andesites and associated calc-alkaline rocks. Oregon Department of Geology and Mineral Industries, Portland, OR, United States, pp. 43-63.

Tera, F. and Wasserburg, G.J., 1972. U-Th-Pb systematics in three Apollo 14 basalts and the problem of initial Pb in lunar rocks. *Earth and Planetary Science Letters*, 14: 281-304.

Tobisch, O.T., Barton, M.D., Vernon, R.H. and Paterson, S.R., 1991. Fluid-enhanced deformation, transformation of granitoids to banded mylonites, western Sierra Nevada, California, and southeastern Australia. *Journal of Structural Geology*, 13: 1137-1156.

Tranter, T.H., 1992. Underplating of an accretionary prism: an example from the LeMay Group of central Alexander Island, Antarctic Peninsula. *Journal of South American Earth Sciences*, 6(1-2): 1-20.

Trey, H., Cooper, A.K., Pellis, G., della Vedova, B., Cochrane, G., Brancolini, G. and Makris, J., 1999. Transect across the West Antarctic rift system in the Ross Sea, Antarctica. *Tectonophysics*, 301: 61-74.

Tulloch, A.J., 1983. Granitoid rocks of New Zealand: a brief review. In: Roddick (Editor), *Circum-Pacific plutonic terranes.* Memoir - Geological Society of America. Geological Society of America (GSA), Boulder, CO, United States, pp. 5-20.

Tulloch, A.J. and Kimbrough, D.L., 1989. The Paparoa metamorphic core complex, New Zealand; Cretaceous extension associated with fragmentation of the Pacific margin of Gondwana. *Tectonics*, 8(6): 1217-1235.

Tulloch, A.J., Kimbrough, D.L. and Waight, T.E., 1994. The French Creek Granite, North Westland, New Zealand: Late Cretaceous A-type plutonism on the Tasman passive margin. In: G.J. van der Lingen *et al.* (Editors), *Evolution of the Tasman Sea basin.* A.A. Balkema, Rotterdam, Netherlands, pp. 65-66.

Tulloch, A.J. and Kimbrough, D.L., 1995. Mesozoic plutonism in western New Zealand: a 50 Ma transition from subduction to continental rifting on the Gondwana margin. In: M. Brown and P.M. Piccoli (Editors), *The origin of granites and related rocks.* U. S. Geological Survey Circular. U. S. Geological Survey, Reston, VA, United States, pp. 153-154.

Tulloch, A.J., Kimbrough, D.L., Landis, C.A., Mortimer, N. and Johnston, M.R., 1999. Relationships between the Brook Street Terrane and Median Tectonic Zone (Median Batholith): evidence from Jurassic conglomerates. *New Zealand Journal of Geology & Geophysics*, 42(2): 279-293.

Turnbull, I.M., 1979a. Stratigraphy and sedimentology of the Caples terrane of the Thomson Mountains, northern Southland, New Zealand. *New Zealand Journal of Geology & Geophysics*, 22(5): 555-574.

Turnbull, I.M., 1979b. Petrography of the Caples terrane of the Thomson Mountains, northern Southland, New Zealand. *New Zealand Journal of Geology & Geophysics*, 22(6): 709-727.

Turnbull, I.M., 2000. *Geology of the Wakatipu area*. QMAP 1:250 000 Geological Map No 18, (in press). Institute of Geological und Nuclear Sciences Limited, Lower Hutt, New Zealand.

Turner, S.P., Foden, J.D., Sandiford, M. and Bruce, D., 1993. Sm-Nd isotopic evidence for the provenance of sediments from the Adelaide Fold Belt and southeastern Australia with implications for episodic crustal addition. *Geochimica et Cosmochimica Acta*, 57: 1837-1856.

Tylor, S.R. and McLennan, S.M., 1985. *The continental crust: Its composition and evolution*. Blackwell Scientific, Oxford, 312 pp.

Van Der Plas, L. and Tobi, A.C., 1965. A chart of judging the reliability of point counting results. *American Journal of Science*, 263: 87-90.

Van Dusschoten, A., 2000. Torlesse stratigraphy and paleontology, Balmacaan Stream, Mid Canterbury. *Geological Society of New Zealand New Letter*, 128: 21-22.

Veevers, J.J., Conaghan, P.J., Powell, C.M., Cowan, E.J., McDonnell, K.L. and Shaw, S.E., 1994a. Eastern Australia. In: J.J. Veevers and C.M. Powell (Editors), *Permian-Triassic Pangean basins and foldbelts along the Panthalassan margin of Gondwanaland.* Memoir - Geological Society of America. Geological Society of America (GSA), Boulder, CO, United States, pp. 11-171.

Veevers, J.J., Powell, C.M. and Collinson, J.W., 1994b. Synthesis. In: J.J. Veevers and C.M. Powell (Editors), *Permian-Triassic Pangean basins and foldbelts along the Panthalassan margin of Gondwanaland.* Geological Society of America (GSA), Boulder, CO, United States, pp. 331-353.

Veevers, J.J., 2000a. *Billion-year earth history of Australia and neighbours in Gondwanaland.* GEMOG Press, Department of Earth and Planetary Sciences, Macquarie University, Macquarie, 388 pp.

Veevers, J.J., 2000b. Antarctic Beadmore-Ross and Mirney provenances saturate Paleozoic-Mesozoic East Gondwanaland with 0.6-0.5 Ga zircons. In: J.J. Veevers (Editor), *Billion-year earth history of Australia and neighbours in Gondwanaland.* GEMOG Press, Department of Earth and Planetary Sciences, Macquarie University, Macquarie, pp. 110-130.

Veevers, J.J., 2000c. Permian-Triassic Pangean basins and foldbelts along the Panthalassan margin of Gondwanaland. In: J.J. Veevers (Editor), *Billion-year earth history of Australia and neighbours in Gondwanaland.* GEMOG Press, Department of Earth and Planetary Sciences, Macquarie University, Macquarie, pp. 292-308.

Vetter, U., Roland, N.W., Kreuzer, H., Hohndorf, A., Lenz, H. and Besang, C., 1983. Geochemistry, petrography, and geochronology of the Cambro-Ordovician and Devonian-Carboniferous granitoids of northern Victoria Land, Antarctica. In: L. Oliver and R. James (Editors), *Antarctic earth science; fourth international symposium.* Cambridge University Press, Cambridge, United Kingdom, pp. 140-143.

Vetter, U. and Tessensohn, K., 1987. S- and i-type granitoids of Northern Victoria Land, Antarctica and their inferred geotectonic setting. *Geologische Rundschau*, 76: 233-243.

von Haast, J., 1871. On the Geology of the Amuri District, in the Provinces of Nelson and Marlborough. *Reports of Geological Exploration for 1870-71*: 25-46.

Waight, T.E., 1995. The geology and geochemistry of the Hohonu Batholith and adjacent rocks, North Westland, New Zealand. Unpublished Ph.D. Thesis, University of Canterbury, Christchurch, New Zealand, 223 pp.

Waight, T.E., Weaver, S.D., Ireland, T.R., Maas, R., Muir, R.J. and Shelley, D., 1997. Field characteristics, petrography, and geochronology of the Hohonu Batholith and the adjacent Granite Hill Complex, North Westland, New Zealand. *New Zealand Journal of Geology & Geophysics*, 40(1): 1-17.

Waight, T.E., Weaver, S.D., Maas, R. and Eby, G.N., 1998a. French Creek Granite and Hohonu dyke swarm, South Island, New Zealand: Late Cretaceous alkaline magmatism and the opening of the Tasman Sea. *Australian Journal of Earth Sciences*, 45(6): 823-835.

Waight, T.E., Weaver, S.D., Muir, R.J., Maas, R. and Eby, G.N., 1998b. The Hohonu Batholith of North Westland, New Zealand; Granitoid compositions controlled by source H_2O contents and generated during tectonic transition. *Contributions to Mineralogy & Petrology*, 130(3-4): 225-239.

Wandres, A.M., Weaver, S.D., Shelley, D. and Bradshaw, J.D., 1998. Change from calc-alkaline to adakitic magmatism recorded in the Early Cretaceous Darran Complex, Fiordland, New Zealand. *New Zealand Journal of Geology & Geophysics*, 41(1): 1-14.

Ward, C.M., 1986. The Fanny and Goodyear terranes of southern Fiordland and their relations with West Nelson. In: Stewart and Mike (Editors), *Abstracts from the Lower Paleozoic Workshop*. Geological Society of New Zealand Miscellaneous Publication. Geological Society of New Zealand, Christchurch, New Zealand, pp. 46-47.

Wareham, C.D., Stump, E., Storey, B.C., Millar, I.L. and Riley, T.R., 2001. Petrogenesis of the Cambrian Liv Group, a bimodal volcanic rock suite from the Ross Orogen, Transantarctic Mountains. *Geological Society of America Bulletin*, 113(3): 360-372.

Weaver, S.D., Bradshaw, J.D. and Laird, M.G., 1984. Geochemistry of Cambrian volcanics of the Bowers Supergroup and implications for the early Palaeozoic tectonic evolution of northern Victoria Land, Antarctica. *Earth and Planetary Science Letters*, 68(1): 128-140.

Weaver, S.D., Smith, I.E.M., Sewell, R.J., Gamble, J.A., Morris, P.A., Duggan, M.B., Gibson, I.L. and Pankhurst, R.J., 1989. New Zealand intraplate volcanism. In: W. Johnson and J. Knutson (Editors), *Intraplate volcanism in eastern Australia and New Zealand.* Cambridge University Press, Cambridge, United Kingdom, pp. 157-188.

Weaver, S.D., Bradshaw, J.D. and Adams, C.J., 1991. Granitoids of the Ford Ranges, Marie Byrd Land, Antarctica. In: M.R. Thomson *et al.* (Editors), *Geological evolution of Antarctica; proceedings of the Fifth International Symposium on Antarctic Earth Sciences.* Cambridge University Press, Cambridge, pp. 345-351.

Weaver, S.D., Adams, C.J., Pankhurst, R.J. and Gibson, I.L., 1992. Granites of Edward VII Peninsula, Marie Byrd Land: anorogenic magmatism related to Antarctic-New Zealand rifting. In: E. Brown and B.W. Chappell (Editors), *The Second Hutton symposium on the origin of granites and related rocks; proceedings.* Special Paper - Geological Society of America. Geological Society of America (GSA), Boulder, CO, United States, pp. 281-290.

Weaver, S.D., Bradshaw, J.D. and Muir, R.J., 1994a. Cretaceous magmatism in Marie Byrd Land and New Zealand: change from subduction to continental rifting. In: H. Neil *et al.* (Editors), *Geological Society of New Zealand 1994 annual conference; programme and abstracts.* Geological Society of New Zealand Miscellaneous Publication. Geological Society of New Zealand, Christchurch, New Zealand, pp. 185.

Weaver, S.D., Storey, B.C., Pankhurst, R.J., Mukasa, S.B., DiVenere, V.J. and Bradshaw, J.D., 1994b. Antarctica-New Zealand rifting and Marie Byrd Land lithospheric magmatism linked to ridge subduction and mantle plume activity. *Geology*, 22(9): 811-814.

Weaver, S.D., Bradshaw, J.D., Pankhurst, R.J., Muir, R.J., Storey, B.C., Waight, T.E. and Ireland, T.R., 1996. Cretaceous Magmatism, make-up and break-up of the SW Pacific Gondwana margin, *Mesozoic Geology of the Eastern Australia Plate Conference*. Geological Society of Australia, Brisbane, p. 548.

Wellman, H.W., 1953. The Geology of the Geraldine subdivision, Department of Scientific and Industrial Research, Wellington.

Whalen, J.B., Kenneth, L.C. and Chappell, B.W., 1987. A-type granites: geochemical characteristics, discrimination and petrogenesis. *Contributions to Mineralogy and Petrology*, 95: 407-419.

White, A.J.R. and Chappell, B.W., 1983. Granitoid types and their distribution in the Lachlan Fold Belt, southeastern Australia. In: Roddick (Editor), *Circum-Pacific plutonic terranes.* Memoir - Geological Society of America. Geological Society of America (GSA), Boulder, CO, United States, pp. 21-34.

Whitford, D., Crawford, T., Korsch, M. and Craven, S., 1990. The Mount Read Volcanics: strontium and neodymium isotope geochemistry. *Exploration Research News / CSIRO Division of Exploration Geoscience*, 4: 10-11.

Whitford, D.J. and Crawford, A.J., 1993. The Mount Read Volcanics, Tasmania; strontium and neodymium isotope geochemistry. In: M.B. Duggan and J. Knutson (Editors), *IAVCEI abstracts; Ancient volcanism & modern analogues.* Australian Geological Survey Organisation, Australia, p. 122.

Williams, I.S., 1966. U-Th-Pb geochronology by Ion microprobe - Applications of microanalytical techniques to understanding mineralisation processes. *SEG Short Course*: 50.

Williams, J.G. and Harper, C.T., 1978. Age and status of the Mackay Intrusives in the Eglinton-upper Hollyford area. *New Zealand Journal of Geology & Geophysics*, 21(6): 733-742.

Williams, N. and Korsch, R., 1996. The Mesozoic geology of the Eastern Australian Plate, *Mesozoic Geology of the Eastern Australia Plate Conference.* Geological Society of Australia, Brisbane, p. 564.

Wilson, M., 1989. *Igneous Petrogenesis.* Harper Collins Academic, London, United Kingdom, 466 pp.

Withnall, I.W., Black, L.P. and Harvey, K.J., 1991. Geology and geochronology of the Balcooma area: part of a Early Paleozoic magmatic belt in North Queensland. *Australian Journal of Earth Sciences*, 38: 15-29.

Withnall, I.W., MacKenzie, D.E., Denaro, T.J., Bain, J.H.C., Oversby, B.S., Knutson, J., Donchak, P.J.T., Champion, D.C., Wellman, P., Cruikshank, B.I., Sun, S.S. and Pain, C.F., 1997. Georgetown Region. In: J.H.C. Bain and J.J. Draper (Editors), *North Queensland Geology, AGSO Bulletin 240, Queensland Geology 9*. Australian Geological Survey Organisation, Canberra, Australia.

Wombacher, F. and Münker, K., 2000. Pb, Nd, and Sr Isotopes and REE systematics of Cambrian sediments from New Zealand: Implications for the reconstruction of the Early Paleozoic Gondwana margin along Australia and Antarctica. *The Journal of Geology*, 108: 663-686.

Wood, R., Andrews, P.B. and Herzer, R.H., 1989. Cretaceous and Cenozoic geology of the Chatham Rise region, South Island, New Zealand, *New Zealand Geological Survey Basin Studies 3*. New Zealand Geological Survey, Lower Hutt, New Zealand.

Wood, R. and Davy, B., 1994. The Hikurangi Plateau. *Marine Geology*, 118(1-2): 153-173.

Wood, R.A. and Herzer, R.H., 1993. The Chatham Rise, New Zealand. In: P.F. Ballance (Editor), *South Pacific sedimentary basins. Sedimentary Basins of the World, 2*. Elsevier Science Publishers B.V., Amsterdam, pp. 329-349.

Wysoczanski, R.J., Gibson, G.M. and Ireland, T.R., 1997. Detrital zircon age patterns and provenance in Late Paleozoic Early Mesozoic New Zealand; Terranes and development of the Paleo-Pacific Gondwana margin. *Geology*, 25(10): 939-942.

Zen, E., 1986. Aluminium enrichment in silicate melts by fractional crystallisation: some mineralogic and petrographic constraints. *Journal of Petrology*, 27: 1095-1118.

IGNEOUS ROCKS

I-Type mainly gabbro/diorite
mainly quartzmonzodiorite/granite
S-Type mainly granitoids
A-Type gabbro to granites
Volcanic mainly volcanics

WESTERN PROVINCE

North-West Nelson

Takaka Terrane

1 Devil River Volcanics (Münker & Cooper 1999)
2 Riwaka Complex (Muir *et al.* 1996)

Buller Terrane

3 Summit Granite (Waight *et al.* 1997)
4 Karamea Batholith: *Whale Creek, O'Sullivans, Dunphy, Karamea granites, Zetland Diorite* (Muir *et al.* 1994)
5 Windy Point & C. Foulwind granitoids (Muir et al. 1994)
6 Paringa Tonalite (Aronson 1965; Hurley 1962; Cooper & Tulloch 1992
7 Toropuihi Granite (Mortimer *et al.* 1997)
8 Kirwans Dolerite (Mortimer *et al.* 1995)
9 Separation Point Suite: *Gouland, Mt. Olympus,Rocky, Pearce, Canaan granitoids; and Crow Granite (137 Ma)* (Muir *et al.* 1997)
10 Rahu Suite: *Hohonu, Buckland, Big Deep granites Berlins Porphyry* (Muir *et al.* 1997; Waight *et al.* 1997)
11 Stitts Tuff (Muir *et al.* 1997)
12 French Creek (Waight *et al.* 1997)
13 Separation Point Granite (Muir *et al.* 1997)

Fiordland

1 Kellard Point Orthogneiss (Gibson & Ireland 1996)
2 Granitoid enclaves in Orthogneiss (Bradshaw & Kimbrough 1991)
3 Hauroko, Kakapo Granites (Muir *et al.* 1998)
4 Western Fiordland Orthogneiss (Mattinson *et al* 1986, Gibson *et al.* 1988)

Campbell Plateau

1 Bounty Island Granite (Ireland, pers. comm.)

MEDIAN TECTONIC ZONE

North-West Nelson

1 Echinus Granite (Kimbrough *et al.* 1993)
2 Buller Diorite *(Kimbrough et al. 1994)*
3 Rotoroa Complex *(Kimbrough et al. 1993)*
4 One Mile Gabbronorite *(Kimbrough et al. 1999)*
5 Cable Granodiorite *(Kimbrough et al. 1993)*

Fiordland

1 Pomona Island Diorite, Roxburgh Tonalite (Muir *et al.* 1998)
2 Poteriteri Pluton (Muir *et al.* 1998)
3 Pomona Island Granite (Muir *et al.* 1998)
4 Manapuri Granite (Muir *et al.* 1998)
5 Longwood Range: *Wakaputu Granite, Oraka Hybrids Pahia Intrusives, Colac Granite, Holly Burn Intrusives* (Kimbrough *et al.* 1994, 1999)
5a Longwood Range: Stitching dikes and plutons (Mortimer *et al.* 1999)
6 Mistake Diorite (Kimbrough *et al.* 1994; Muir *et al.* 1998)
7 Darran Suite granitoids and diorites: *Jackson Peaks, Luxmore, Cleughearn, Mary Island, Calderwood, Beehive, Halfway Peak, Lugar Burn and Darran* (Kimbrough *et al* 1994; Muir *et al.* 1998)
8 Paterson Group, Anglem Complex granitoids (Kimbrough *et al.* 1994)
9 Electric Granite (Muir *et al.* 1998)
10 Separation Point Suite: *Titiroa Granite, North Fiordland Granite, Takahe Granodiorite* (Muir *et al.* 1998)
11 Largs Ignimbrite (Mortimer *et al.* 1999)

BROOK STREET

1 Longwood Range: *Pourakino Trondhjemite, Hekeia Gabbro* (Kimbrough *et al.* 1994; Tulloch *et al.* 1999; Mortimer *et al.* 1999)

SEDIMENTARY ROCKS

mainly low quartz volcanic litharenites
mainly moderate quartz felsarenite
mainly high quartz felsarenite
mainly lime stone

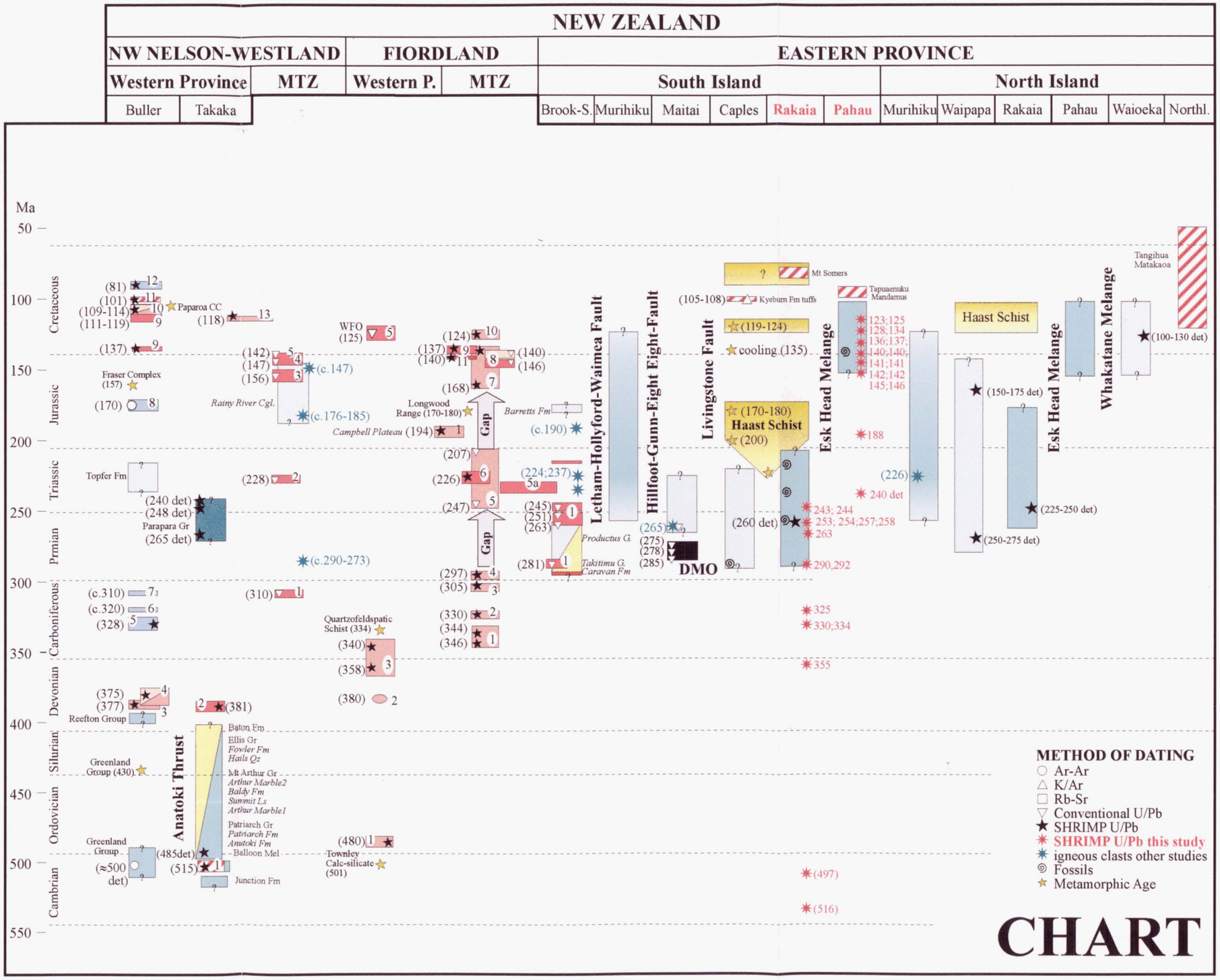

Terrane sequences of New Zealand indicating the main features discussed in the text.